UNIVERSITEIT VAN PRETORIA
UNIVERSITY OF PRETORIA
YUNIBESITHI YA PRETORIA

Interaction of nonstructural protein NS3 of African horsesickness virus with viral and cellular proteins

By

Mia Beyleveld

Submitted in fulfilment of the requirements for the degree

Magister Scientiae

In the Faculty of Natural & Agricultural Science
Department of Genetics
University of Pretoria

March 2007

Declaration

I declare that the thesis/dissertation that I hereby submit for the degree in Magister Scientiae at the University of Pretoria has not previously been submitted by me for degree purposes at any other university

SIGNATURE:..... DATE: 07-06-2007

Acknowledgements

I would like to express my gratitude to the following people:

- Dr. Vida van Staden, for all her help the past three years. Her guidance and leadership proved to be very helpful. I have learnt a great deal from her.

- Prof. Henk Huismans, for making it possible to complete my degree.

- Dr. Christine Maritz-Olivier, for always giving good advice with regards to the yeast two-hybrid system.

- My parents Tom and Marcelle Vorster, they have always believed in me, encouraged me and prayed for me.

- My husband, Paul – who has endured the joy and frustration of my research, always supported me in every way.

- My Lord and Saviour Jesus Christ that made me capable to complete this degree.

Summary

African horsesickness virus (AHSV) is a dsRNA virus that belongs to the *Orbivirus* genus within the *Reoviridae* family. Each of the ten viral dsRNA segments encodes one virus-specific protein. During its life cycle AHSV replicates both in an insect vector and in a mammalian host, but while it has no detrimental effect on insect cells the virus is highly pathogenic to mammalian cells. It is postulated that this relates to different viral release mechanisms. Currently the main candidate for mediating viral release in both insects and mammals is the viral nonstructural protein NS3. In bluetongue virus (BTV), the prototype virus of the *Orbivirus* genus, it has been shown that NS3 interacts with both the viral outer capsid protein VP2 and a cellular exocytosis protein. For AHSV, we investigated whether the same mechanism was involved in viral release. This study aimed to identify and map possible protein-protein interaction between AHSV NS3 and VP2, and AHSV NS3 and unknown insect cellular proteins. For investigating the NS3-VP2 interactions a eukaryotic expression system (yeast two-hybrid), a column binding assay utilising bacterially expressed NS3 and recombinant baculovirus expressed VP2 as well as a membrane flotation assay utilising recombinant baculovirus expressed VP2 and NS3-GFP, were used. A number of problems were encountered and no conclusive results were obtained. For investigating viral-cellular protein interactions the yeast two-hybrid system was also used, utilising NS3 as bait to screen proteins expressed from a *Drosophila* cDNA library. Results showed an interaction between the N-terminal region of AHSV NS3 and ubiquitin, an essential protein for the trafficking and degradation of membrane proteins from the endoplasmic reticulum. It also acts as a sorting signal in both the secretory pathway and in endosomes, where it targets proteins into multivesicular bodies in the lumen of vacuoles/lysosomes. It has been shown that ubiquitin could play a role in the pinching off of budding vesicles. An AHSV infected cell could therefore potentially use ubiquitin in its vesicular budding pathway, therefore giving the opportunity for viruses to use this to release them from the cell. The Hsp70 was another protein identified that interacts with AHSV NS3. This protein plays a role in folding reactions, protein translocation across membranes of organelles and protein assembly. It has been reported in other studies done that both ubiquitin and Hsp70 play roles in regulating the bioavailability of viral proteins, which could explain the different levels of NS3, high in insect cells and low in mammalian cells, which indirectly control the viral exit pathway used, budding versus lytic release. These results lay the foundation for explaining the potential role of NS3 in the AHSV life cycle in insect cells.

Table of contents

Chapter 1: Literature review

Viruses have remarkable characteristics that have shaped the history and the evolution of their hosts. They have become the study material of many scientists, who are working towards ways to understand and control these agents. To understand the way in which viruses interact with the host, and how protein-protein interactions between viral proteins and between viral and host cellular proteins enhance the success of the virus, one must understand what a protein is, how it interacts and how all of this fits into the virus milieu. In this literature review an overview will be given on the importance of protein-protein interactions for virus and host during viral assembly and the lifecycle of the virus, as this will pave the way for understanding the fundamental importance of my project.

1.1 AN OVERVIEW OF PROTEIN-PROTEIN INTERACTIONS IN GENERAL

In any living organism, DNA converted to RNA converted to protein (central dogma of molecular biology) forms the basic pathway for many biological processes. These biological processes are often executed and controlled by proteins. The intrinsic biochemical and/or catalytic activities of proteins are, to a large extent, regulated by dynamic, spatially and temporally confined direct (physical) and indirect (functional) protein-protein interactions (Drewes & Bouwmeester, 2003). Dynamic association and dissociation of protein complexes control most cellular functions, including cell cycle progression, signal transduction, and metabolic pathways. Although complexes of proteins form within the context of a cell, protein-protein interactions regulate signals that govern overall patterns of development, normal physiology, and pathophysiology in living animals (Luker *et al.*, 2003). Protein-protein interactions differ on the basis of protein composition, affinity and whether the association is permanent or transient (Nooren & Thornton, 2003). The whole architecture of cells depends on the formation of various protein complexes to ensure a stable environment for other necessary protein interactions to happen. Overall, without proteins and the interactions they conduct, no life would be possible as it forms part of the basis of life.

To understand proteins and the various interactions they have one must understand where a protein comes from and how it is made. The amino acid sequence, which is the primary structure of a protein, determines its three-dimensional structure, which in turn determines its properties. The correct three-dimensional structure is needed for correct functioning of a protein. Amino acids are linked by covalent peptide bonds to form a polypeptide chain. The secondary structure of proteins is the hydrogen-bonded arrangement of the backbone of the protein in the form of a polypeptide chain. In other words whether e.g. an α-helix or β-pleated sheet folding arrangement will take place. The tertiary structure of a protein is the three-dimensional arrangement of all the atoms in the molecule. The

conformations of the side chains and the positions of any prosthetic groups, together with the arrangement of helical and pleated sheet sections with respect to one another, form part of the tertiary structure.

Two main types of protein conformations are seen namely fibrous proteins and globular proteins. In globular proteins the backbone folds back on itself to produce a more or less spherical shape in comparison to fibrous proteins that are more rod-shaped. Higher-order levels of structure, including secondary and tertiary structure, depend on non-covalent bonds ensuring that the most stable structure for a given protein is the one with the lowest energy (Campbell, 1999). Non-covalent bonds include electrostatic forces, hydrogen bonds and Van der Waals forces. A relatively unfavourable interaction is that found between water and nonpolar molecules/amino acids present in the protein, as these nonpolar molecules cannot participate in hydrogen bonding. But it has been shown that the absence of hydrogen bonding between nonpolar molecules and water and rather the presence of interaction between nonpolar molecules themselves is a major factor in the stability of proteins, nucleic acids and membranes. This type of interactions is known as hydrophobic (Creighton, 1984).

Quaternary structure is a property of proteins that consist of more than one polypeptide chain. The number of chains can range from two to more than a dozen and can be identical or can differ. Therefore, e.g. dimers, trimers and tetramers consisting of two, three and four polypeptide chains respectively can be formed. It is also important to note that as a result of non-covalent interactions, subtle changes in the structure at one site on a protein molecule may cause drastic changes in properties at a distant site. Such proteins are called allosteric (Campbell, 1999).

Post-translational modifications of a protein may take place depending on its function. Some proteins are glycosylated. This entails the addition of one of more carbohydrate units covalently to the protein. Glycosylated proteins play a major role as secretory proteins or as cell receptors where the carbohydrates are involved in cell-to-cell adhesion in the cellular membrane. The iodination, phosphorylation and methylation of proteins are few among many other modifications that can take place as result of property and function of a protein (Creighton, 1984).

A protein is generally found in a crowded environment with many potential binding partners with different surface properties. Most proteins are very specific in their choice of partner while some are multispecific, having multiple competing binding partners on overlapping interfaces. Protein-protein interactions occur between identical or non-identical chains i.e. homo- or hetero-oligomers. When oligomers are identical the protein units can be organized in an isologous or heterologous way with structural symmetry. An isologous association involves the same surface on both monomers;

therefore only dimers can form. In contrast to an isologous protein association, heterologous assemblies use different interfaces that can lead to infinite protein associations. The stability of a protein-protein association also distinguishes protein interactions as either being permanent or transient. All interactions and complexes are driven by the concentration of the components and the free energy of the complex, relative to alternative states. Protein-protein interactions can be controlled either by altering the local concentration of the protein components or by influencing the binding affinity as determined by the physicochemical and geometrical interface properties (Nooren & Thornton, 2003).

1.2 PROTEIN-PROTEIN INTERACTIONS IN ORBIVIRUSES

For a virus, protein-protein interaction between viral proteins and between viral proteins and cellular proteins are of vital importance. As viruses are parasitic, they need the help of the host to replicate and to disperse. During the lifecycle of a virus, different strategies based on the properties of the virus and the host are utilized by the virus to gain entry to the host cell, to replicate, to synthesize its proteins and to exit the host cell. Focus will now be placed on specifically the role of protein-protein interactions in African horsesickness virus (AHSV) and in bluetongue virus (BTV), the prototype virus of the *Orbivirus* genus. As research done on AHSV and BTV is limited in comparison to other more widely known viruses, findings for other viruses relevant to the topic will also be discussed.

1.2.1 Introduction

African horsesickness virus (AHSV), detected in South Africa about three centuries ago, is a member of the *Orbivirus* genus (Fields & Bartel, 2001). The *Orbivirus* genus is one of 12 distinct genera in the *Reoviridae* family recognized by the International Committee for the Taxonomy of Viruses. There are 8 distinct families of dsRNA viruses of which *Reoviridae* is by far the largest. Orbiviruses differ in their structure, physicochemical properties, replication cycle, pathogenesis and epidemiology in comparison to other members of the *Reoviridae* family (Fields & Bartel, 2001, Mertens & Diprose, 2004). AHSV is responsible for causing African horsesickness, an economically important disease in *Equidae.* AHSV infects its host, is non-contagious and is transmitted by the *Culicoides* species (biting midge) (Martin *et al.*, 1998). As BTV is also of major economic importance (it causes bluetongue disease in various ruminants), most analyses over the years have been focused on BTV as the prototype virus of the *Orbivirus* genus. In further discussions I will refer to BTV and state any differences between BTV and AHSV. The relationships between different serogroups such as BTV and AHSV cannot be assessed by cross-hybridization, but phylogenetic relationships can be determined by cDNA and protein sequences of corresponding genes of different orbiviruses. By using this, a close genetic relationship has been shown to occur between BTV and AHSV (Fields & Bartel, 2001).

Understanding the way in which a virus packages all of its dsRNA has given many scientists the chance to investigate the virus's life cycle. The unique way in which the virus hides its contents has interested many – ensuring optimized viral production under the pressure of the host's immune system. In the following paragraphs the structure and packaging of the BTV core will be discussed together with the scaffolding of the outer capsid proteins onto the core domain.

1.2.2 Protein-protein interactions involved in virus assembly and virus packaging

The BTV and AHSV genomes both consists of 10 dsRNA segments, with every segment encoding for the synthesis of one major protein, except for segment S10 that codes for two related proteins NS3 and NS3A (Bremer, 1976, Grubman & Lewis, 1992). The 10 segments can be divided into three groups based on the size of the segments (Figure 1.1), Large (L1 (M_r 2.7 x 10^6) – L3), Medium (M4 - M7) and small (S8 - S10 (M_r 5 x 10^5).

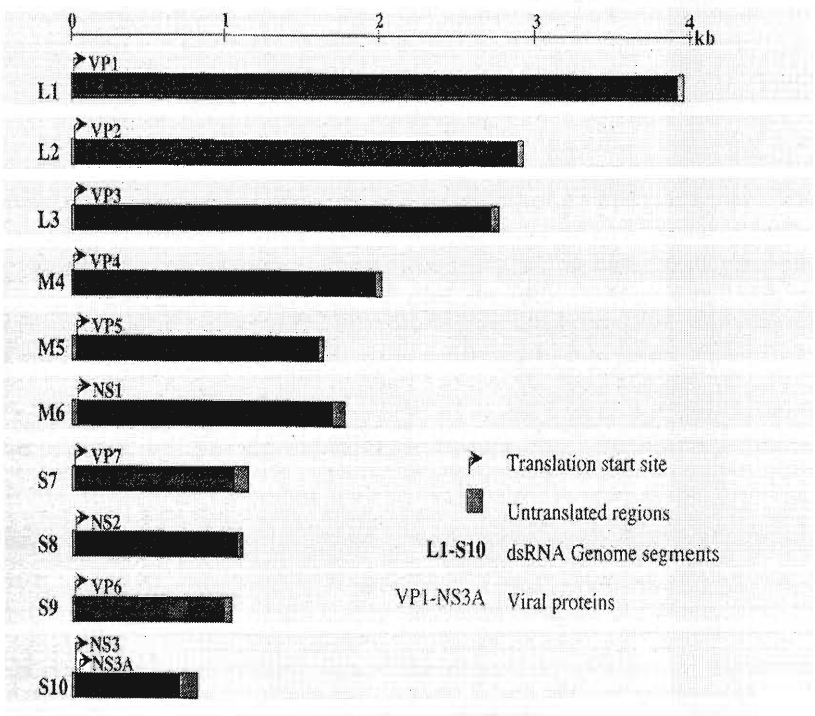

Figure 1.1: Schematic diagrams of the 10 RNA segments of BTV-10 and their relative lengths and other features revealed by sequence analysis. (Diagram taken from Fields *et al.*, 2001)

As all members of the *Reoviridae* family, orbiviruses are nonenveloped viruses that contain two protein shells. The outer shell or outer capsid consists of two major viral proteins, VP2 and VP5. Experiments have shown that the treatment of AHSV and BTV with chymotrypsin and magnesium can

remove the two outer capsid proteins VP2 and VP5, leaving an intact viral core particle (Van Dijk & Huismans, 1982). The inner shell or core consists of the major viral proteins VP3 and VP7.

The inner shell encircles the three minor viral proteins VP1, VP4 and VP6 (Fields & Bartel, 2001, Nason et al., 2004) The current understanding of the topography of the seven structural proteins in the BTV virion is illustrated in Figure 1.2. In Table 1.1, a summary is given of the 10 dsRNA segments of BTV serotype 10, the proteins they encode and their postulated functions (Mertens & Diprose, 2004).

In tissue culture it has been shown that the expression of the outer capsid proteins VP2 and VP5, together with the core proteins VP3 and VP7, leads to the formation of double-shelled virus like particles, which have the same size and appearance as authentic BTV virions (French *et al.*, 1990, Liu *et al.*, 1992). The production of core like particles by the expression of VP3 and VP7 has also been shown in AHSV (Maree *et al.*, 1998) .

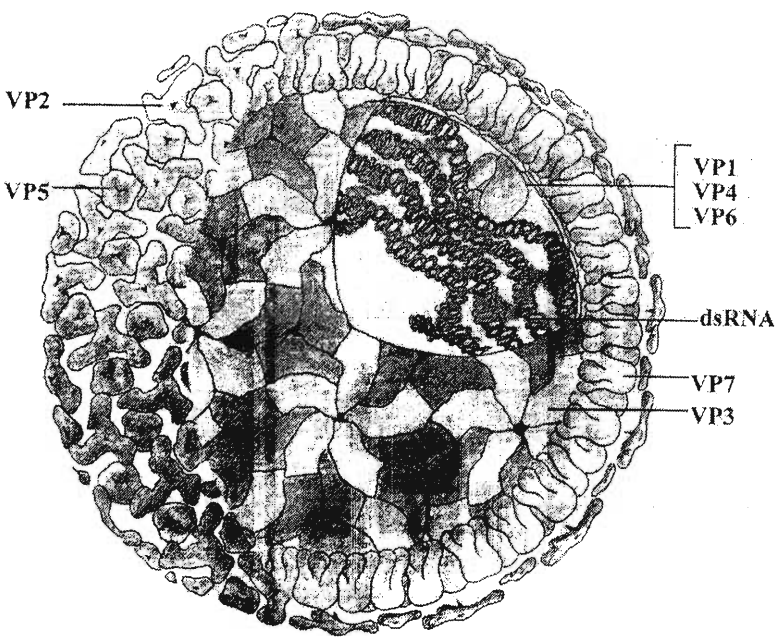

Figure 1.2: Schematic diagram of the bluetongue virus (BTV) particle showing the positions and structures of BTV components. Data for this diagram were obtained from cryoelectron microscopic and X-ray crystallographic analyses and on data obtained from baculovirus recombinant expression systems. See text for description. (Diagram taken from Fields *et al.*, 2001).

Table 1.1: The dsRNA segments and proteins of bluetongue virus serotype 10 (BTV-10)

Genome segment (size, bp)	ORFs (bp)	Proteins	Location	Function and properties
1 (3954)	12-3917	VP1	Inner surface of sub-core	RNA dependent RNA polymerase.
2 (2926)	20-2887	VP2	Outermost capsid protein	Outer layer of the capsid. Controls virus serotype. Cell attachment protein. Involved in determination of virulence, readily cleaved by proteases. Most variable protein. Reacts with neutralizing antibodies. Trimer.
3 (2770)	18-2720	VP3	Sub-core capsid shell	Forms the innermost sub-core capsid shell. Controls overall size and organization of capsid structure. RNA binding. Interacts with minor internal proteins (VP1, VP4 and VP6).
4 (1981)	8-1940	VP4	Inside sub-core	Dimer, transmethylase 1 and 2, guanylyltransferase (capping enzyme), nucleotide phosphohydrolyse. Forms links to NDPs and NTPs.
5 (1769)	35-1690	NS1	Tubules	Forms tubules of unknown function in the cell cytoplasm. These are characteristic of orbivirus replication. Interacts with cytoskeleton.
6 (1638)	30-1607	VP5	Outer capsid	Inner layer of the outer capsid, glycosylated, helps determine virus serotype, variable protein. Trimer. Can mediate cell fusion. Probable role in cell entry.
7 (1156)	18-1064	VP7	Outer core	Trimer, forms outer core surface, which can bind dsRNA. Not exposed on virion surface. In AHSV it can form flat hexagonal crystals. Involved in cell entry and high core particle infectivity in insect cells. Reacts with core neutralizing antibodies. Immuno dominant virus-species specific antigen.
8 (1124)	20-1090	NS2	Viral inclusion body	Viral inclusion body matrix protein, ssRNA binding, phosphorylated. Usually regarded as nonstructural but small amounts may be associated with outer capsid, removed by protease treatment.
9 (1046)	16-1002	VP6	Inside sub-core	ssRNA and dsRNA binding, helicase, NTPase.
10 (822)	20-706 59-706	NS3 NS3A	Viral protein in cell membrane	Glycoproteins, membrane proteins, involved in cell exit. Variable protein. May be involved in determination of virulence and vector competence. Cytotoxic, can disrupt cell membranes.

Table constructed using data provided by Mertens (2004)

1.2.2.1 Role of VP7 and VP3 interactions in virus core assembly

The structure of the BTV core was determined in 1998 by X-ray crystallography at a resolution approaching 3.5Å. The core obeys icosahedral symmetry. The core consists of a lattice of VP7 trimers coating a thin inner shell of VP3 monomers (Grimes *et al.,* 1998). The surface layer of the core is made up of 260 trimers of VP7; underneath this layer VP3 is present as 120 copies organized into 12 flowershaped decamers that are interconnected to form the thin smooth VP3 shell. VP3 forms a scaffold for the deposition of VP7 trimers, but also encapsulates and positions the transcriptase complex of the three minor proteins (VP1, VP4 and VP6) as well as the genomic dsRNA segments (Grimes *et al*., 1998, Hewat *et al*., 1992a, Prasad *et al*., 1992).

To ensure that the capsid follows icosahedral symmetry, the VP3 proteins are arranged into 60 subunits of two distinct types of VP3 (A and B). These monomers (A or B) differ slightly in their final folding ensuring a final large elongated triangular structure, each of which is divided into three distinct domains namely the apical, carapace, and dimerization domains. The structure of the VP3 layer shows that the five VP3 A monomers are arranged like petals of a flower while five VP3 B monomers assemble onto the five VP3 A petals. The connection between these flower shaped VP3 structures (decamers) are achieved mainly via the interactions of the dimerization domains of A and B of the different decamers as well as through subtle changes in the conformational rearrangement of the A and B molecules (Grimes *et al*., 1998) (Figure 1.3). It has been shown that structure-based modification of the VP3 protein by removing the dimerization domain still allows decamer formation but prevents the formation of intact subcores (Mertens & Diprose, 2004). Therefore it is likely that the decamers are the assembly intermediates of the VP3 lattice (Grimes *et al*., 1998, Kar *et al*., 2004).

To determine the role of the N-terminus of VP3 in core assembly and its interaction with the transcription complex, deletion mutants were made in the amino terminal and decamer-decamer interacting region of VP3 (dimerization domain). Deletion of the N-terminal 5 or 10 amino acids did not affect the ability to assemble into core-like particles in the presence of VP7 although cores assembled using the 10 amino acid deficient N-terminal were very unstable. Removal of five amino acids from the N-terminal also did not effect incorporation of the internal VP1 polymerase and VP4 mRNA capping enzyme proteins of the transcription complex. Removal of the VP3-VP3 dimerization domain from the VP3 protein resulted in an inability to assemble into core-like particles, but still retained interaction with VP1 and VP4. Purified dimerization domain mutant proteins still multimerized into dimers, pentamers and decamers although they lost their RNA binding ability. The N-terminal is thus important for binding and encapsulation even though the five amino acid deficient

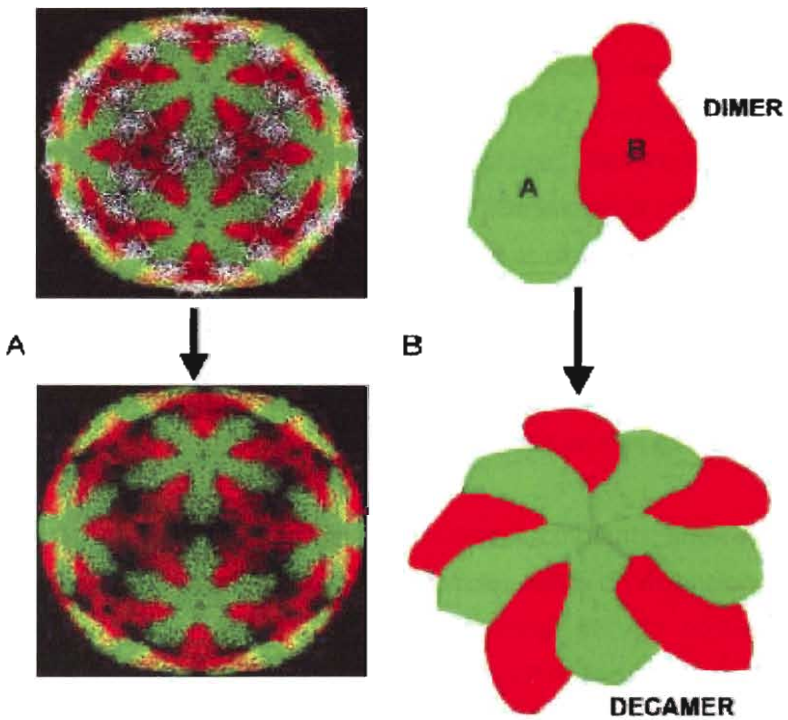

Figure 1.3: Schematics of VP3 shell and VP3 oligomers. The cartoons are adapted from the published report of Grimes *et al.* (1998) and Kar *et al.* (2004). (A) VP3 shell shows the dimerization regions in each molecule in white (upper panel) and deletion of dimerization regions (lower panel). Panel (B) shows a dimer and a decamer of VP3.

mutant could form core-like particles. The dimerization domain is important for subcore assembly and RNA binding (Kar *et al.*, 2004).

As stated previously, the VP7 protein on the outer core is present as 270 trimers. A 23 Å resolution map of the BTV core, determined by cryomicroscopy data, shows that these trimers are organized on a rather precise T=13 icosahedral lattice as expected in accordance with the quasi-equivalence theory. The VP7 protein consists of two domains. One that is largely α-helical (lower domain), and the other that is smaller is a β-barrel with a jelly-roll topology (upper domain). The orientations of these two domains vary in different crystal forms. The β-barrel domains of VP7 are external to the core, projecting outwards to interact with the proteins in the outer layer of the mature virion that consist of VP2 and VP5. The lower α-helical domains of VP7 interact with VP3. VP7 trimer-trimer interactions across the T=13 layer are mediated mainly through well-defined regions in the broader lower domains without any significant conformational changes within the individual trimers (Grimes *et al.*, 1997). In BTV, the VP7 trimers form capsomers, which are visible in negatively stained images of core particles (Basak *et al.*, 1996). When AHSV VP7 proteins are expressed in Sf9 cells they can self-assemble to form disc-shaped crystal structures. These large structures represent a feature

unique to AHSV when compared to other orbiviruses (Chuma *et al.*, 1992). In a VP7 top domain crystal structure study done on AHSV it was revealed that the top domains of both BTV and AHSV are trimeric and structurally very similar. The characteristics of the molecular surface of BTV and AHSV VP7 suggest why AHSV VP7 is much less soluble than BTV VP7. Two amino acid residues namely Ala-167 and Phe-209 makes AHSV VP7 much more hydrophobic. Mutations at these positions have been suggested to increase the solubility of AHSV VP7 (Basak *et al.*, 1996). Two other crystal structures of VP7 have been solved, one a cleavage product at close atomic resolution and the other at lower resolution. The cleavage product forms part of the upper domain, which forms a rigid invariant trimeric fragment. The lower resolution structure of the intact molecule indicates that the α-helical domain (lower domain) can rotate about the linker position to the upper domain to adapt to different orientations with respect to the threefold axis in the intact protein (Basak *et al.*, 1997).

Mutation studies done on VP7, including deletion and extension mutants, showed that the C-terminal of VP7 is very important for the formation of core-like particles, while an extension mutant involving an 11-amino-acid rabies viral sequence added to the N-terminal of VP7 allowed core-like particle formation. Substitution of either of two cysteine residues of VP7 (Cys-15 or Cys-65) by serine also did not prevent core-like particle formation even though this region is highly conserved throughout orbivirus groups. But the substitution of the single lysine residue of VP7 (Lys-255) (the only one present in BTV) by leucine inhibited any formation of core-like particles showing its importance in core assembly (Le Blois & Roy, 1993).

The VP7 and VP3 layers interact through flattish, predominantly hydrophobic surfaces. Because of symmetry mismatch, there are 13 different sets of contacts. It has been seen that VP7 remains virtually undisturbed while making completely different, yet extensive and relatively well fitting contacts with VP3 A and VP3 B molecules (Grimes *et al.*, 1998).

1.2.2.2 Role of VP2 and VP5 in outer capsid assembly

The outer capsid proteins VP2 and VP5 are necessary for mammalian host cell recognition, binding and entry. These two proteins scaffold onto the VP7 lattice. Earlier, three dimensional image reconstruction and cryoelectron microscopic studies showed that one of the two possible outer capsid proteins, VP2 or VP5, looks like a "sail"-shaped spike. The second protein appears to form globular structures that sit neatly on the inner shell of the virion. The "sail"-shaped spikes project 4nm beyond the globular molecules, thus hiding the globular proteins (Hewat *et al.*, 1992a). Because VP2 is the principle antigen responsible for BTV serotype specificity, hemagglutination activity and virus neutralization activity (Cowley & Gorman, 1987, Huismans & Erasmus, 1981, Inumaru & Roy, 1987)

the "sail"-shaped spike would most likely be VP2. For AHSV the same is true (Martinez-Torrecuadrada *et al.*, 1996, Martinez-Torrecuadrada *et al.*, 1994, Martinez-Torrecuadrada *et al.*, 2001, Venter *et al.*, 2000).

Interactions between the outer layer (VP2 and VP5) and the inner VP7 layer are necessary to complete the mature virus structure. VP2 is present as triskelion motifs on the outside capsid of the virus, most probably consisting of VP2 trimers (Hewat *et al.*, 1992b). This motif enables VP2 to bind receptors and enforce its hemagglutinating activity. The other outer capsid protein VP5 is present as globular motifs, made up of two or three VP5 proteins. Studies show that both the VP2 triskelions and VP5 globular motifs interact extensively with the VP7 layer. The VP2 triskelion motifs interact only with the top flat portion of the VP7 trimers, while the VP5 globular motifs interact alongside the VP7 trimers. It is also interesting to notice that the globular VP5 motifs bind to the VP7 platform five times more in comparison to the VP2 motifs that only bind to one VP7 trimer at a time. This probably explains why VP2 is much easier removed from the virion at high salt concentration when compared to VP5. This also supports the model of VP5 assembling to the VP7 scaffold before VP2 (Nason *et al.*, 2004).

1.2.2.3 Proteins that play a role in dsRNA packaging

Electron density maps of the core of both BTV-1 and BTV-10 show layers of density within the central space of the subcore that cannot be modelled as viral proteins. These layers are made up of multiple strands, some of which have a helical structure that is not only highly conserved for the two virus serotypes but are also consistent with layers of packaged genomic viral dsRNA. It is interesting to note that the density of the RNA is very clear especially for the outer layer of RNA that is closest to the inner surface of VP3. This implies that VP3 imposes considerable icosahedral order on the packaged genome. The weakening of the electron density toward the centre of the core suggests that the RNA becomes more disordered the further away it gets from the protein layer (Gouet *et al.*, 1999, Grimes *et al.*, 1998). It has been proposed that the shallow chemically featureless grooves present on the underside of the VP3 protein guides the genomic viral dsRNA to be packaged in a structured way. The model proposed by Gouet *et al.* (1999) states that each dsRNA strand in the outer shell of RNA leaves the transcription complex situated in the middle of the core at the 5-fold axis and spirals around it until at a certain diameter away from the 5-fold axis where it clashes with neighbouring RNA segments. This may redirect the RNA inward to lay down a second discrete layer, spiralling back towards the transcription complex. Further switching will lay down layers three and four. It is noteworthy that the helicase protein of BTV, VP6, unlike the VP1 and VP4 proteins is not readily incorporated within core-like particles. It is believed that VP6 needs to be associated with BTV RNA in

order to be encapsulated. It has been shown that VP1 and VP4 most likely sit as a flower-shaped hetero-dimer just underneath the VP3 layer (Nason *et al.*, 2004).

1.2.3 Protein-protein interaction involved in the virus replication cycle

The lifecycle of a dsRNA virus is complex and structured in such a way that the presence of viral dsRNA cannot be identified by host defensive mechanisms. The remarkable structure of the virus core particle presents a safe shelter where a multitude of biochemical reactions happen, all focused on enhancing the overall efficiency of viral propagation. We will look now at the protein-protein interactions that take place during the lifecycle of the virus as described during viral entry, viral replication and viral exit.

1.2.3.1 Protein-protein interactions present at viral entry

The first obstacle to be bridged is the recognition and binding of the virus to the particular host cell. What makes BTV and AHSV very interesting is the fact that the lifecycle of these viruses happens in both mammalian and *Culicoides* cells (Mellor, 1990). The major difference in host cell attachment between mammalian cells and *Culicoides* cells is the proteins used for host cell recognition and cell attachment. For BTV it has been demonstrated that VP2 is the protein responsible for entry of the virus into a susceptible mammalian cell (Hassan & Roy, 1999). VP2 recognizes and attaches the virion to the outer surface of a susceptible mammalian cell (Figure 1.4). In *Culicoides* cells the outer core protein VP7 plays the role of host cell recognition and binding (Xu *et al.*, 1997). Various studies done have shown that a RGD tripeptide sequence in BTV VP7 (amino acid residues 168 to 170) is used in virus attachment. This RGD motif is recognized by host proteins/ligands from the integrin family. In AHSV this RGD motif is in a slightly different position in the VP7 protein (amino acid residues 178-180) (Basak *et al.*, 1996, Tan *et al.*, 2001).

VP2 play a role in erythrocyte agglutination as it is known that VP2 attaches to the sialoglycophorin A present on erythrocytes showing that VP2 may be responsible for BTV transmission by the *Culicoides* vector to vertebrate hosts during blood feeding (Eaton & Crameri, 1989, Hassan & Roy, 1999). After VP2 has bound to specific cellular receptors, the virion is internalized and clathrin-coated vesicles are formed. After internalization, the clathrin coats of the endocytosed vesicles are rapidly lost. This results in the formation of large endocytic vesicles where VP2 is degraded. After this, the vesicle membrane becomes destabilized, to allow the penetration of the newly uncoated core particles into the cytoplasm. The release of the BTV core from the endosome into the cytoplasm has been shown to be dependent on an acidic pH, although it seems only to be important for the removal of VP2

(Hassan *et al.*, 2001, Nason *et al.*, 2004). It is believed that VP5 acts as a membrane permeabilization protein that mediates release of viral particles from endosomal compartments into the cytoplasm (Nason et al., 2004). The VP5 protein has been shown to be able to permeabilize mammalian and *Culicoides* cells, inducing cytotoxity. The sequence analysis also showed that the VP5 protein possesses characteristic structural features enabling the virus to penetrate the host cell. VP5 forms trimers in solution, expected from proteins involved in membrane penetration. It was also shown that VP5 was able to bind mammalian cells but was not internalized (Hassan *et al.*, 2001). This shows that VP5 is involved in receptor-mediated endocytosis making VP2 the host cell recognition and binding protein. It has been shown that BTV VP2, together with VP5 induces apoptosis in mammalian cells. For insect cells, where a *Culicoides variipennis* cell line was one of the cell lines used, no apoptosis was seen even after seven days of infection (Mortola *et al.*, 2004).

In sequencing studies done on VP2 of all nine serotypes of AHSV the homology between the serotypes varied between 47.6% and 71.4%, indicating that VP2 is the most variable AHSV protein. Possible antigenic regions on VP2 were also suggested based on the amino acid sequence data (Potgieter *et al.*, 2003). In earlier sequencing studies done on BTV, a comparison between 7 different

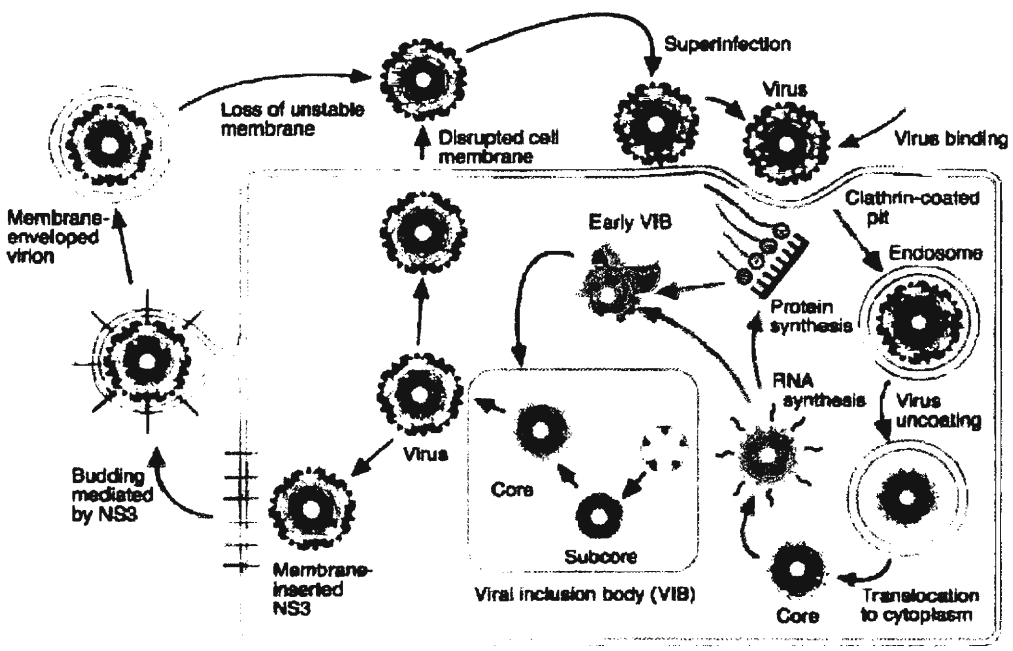

Figure 1.4: Schematic diagram representing the lytic replication cycle of BTV (Diagram taken from Mertens and Diprose, 2004).

BTV serotypes showed a similarity of 22% for VP2. When homologous substitutions were taken, the similarity index climbed to 48% across the 7 serotypes (Jensen et al., 1994).

More is known about the entry process of other dsRNA viruses such as rotavirus and reovirus, both members of the *Reoviridae* family. In reovirus evidence was presented that reovirus intermediate subviral particles (ISVP) (intact virions stripped of outer capsid proteins) gain entry into host L cells primarily by direct penetration of the plasma membrane, although phagocytic vacuoles are also used. Intact virions exclusively use only phagocytic vacuoles (Borsa *et al.*, 1979). Entry of rotaviruses into epithelial cells appears to be a multistep process where at least three contacts between virus and host cell occur. Host proteins $\alpha 2\beta 1$ integrin, $\beta 3$ integrin and/or hsc70 are proposed to be needed for host cell attachment. The rotavirus outer viral spike protein VP4 plays a significant role in the recognition stage of cell entry. The other outer capsid protein VP7 interacts with cell surface molecules at a step subsequent to the initial attachment of the virus through the spike protein. These proteins are associated with cholesterol and glycosphingolipid-enriched lipid microdomains and dissociation of these domains largely inhibits rotavirus infectivity (Arias et al., 2004, Arias et al., 2002). In reovirus, another *Reoviridae* family member, a difference in the binding capacity of the virus attachment protein to distinct cell types in the murine nervous system is seen between different serotypes. The binding of the viral attachment protein $\sigma 1$ to receptors present on the host cell membrane controls these phenotypes. A study showed that reovirus uses junction adhesion molecules as receptors (Barton *et al.*, 2001). These junction adhesion molecules play cellular roles as transmembrane proteins. Whether similar host binding proteins and binding mechanisms are used for BTV or AHSV is not known.

1.2.3.2 Protein-protein interaction present during replication

The second obstacle to be bridged includes the safe transcription and replication of the viral genome without host cell surveillance systems detecting viral activity after host cell entry. All dsRNA viruses face the reality of having their dsRNA contents being attracted by the host's surveillance systems. This happens because mammalian or insect cells do not carry any dsRNA. These virus cores have developed a unique way to provide entry routes and mechanisms to continuously feed the vital cellular NTP's and *S*-adenosyl methionine to the internal viral enzyme complexes. The core must also maintain appropriate levels of certain metal ions and allow by-products such as phosphate groups to escape together with the simultaneous transportation of the nascent mRNA molecules into the infected cell cytoplasm so that translation and packaging can happen (Mertens & Diprose, 2004).

After the virion has been taken up in to the host cell via the endosomal route and uncoated itself in the endosomes to produce cores that lack VP2 and VP5, the transcription machinery is activated (Huismans *et al.*, 1987). The dsRNA segments can be transcribed and capped inside the core in a manner that is dependent on pH, ATP, CTP, UTP and GTP, the methyl donor S-adenosyl–L–methionine (Ado Met) and Mg^{2+} (Mertens *et al.*, 1987, Van Dijk & Huismans, 1980). Between 10-12 copies of transcriptase complexes are present in the BTV core (Stuart *et al.*, 1998) and each complex consists of three structural proteins (VP1, VP4 and VP6).

The VP1 protein is the RNA-directed RNA polymerase responsible for sense strand messenger RNA synthesis (Urakawa *et al.*, 1989) as well as dsRNA synthesis (Boyce *et al.*, 2004). This enables this single protein to firstly transcribe the dsRNA to messenger ssRNA that gets translocated to the ribosomes for translation and secondly to ensure the replication cycle results in ssRNA doubled to dsRNA to be packaged into newly made virions. Because BTV and AHSV are dsRNA viruses, transcription reactions happen inside the core, therefore the post-transcriptional modifications also happen inside the core without any help from cellular proteins. VP4 is a GTP-binding protein (Le Blois *et al.*, 1992). It is important for the virus to create capped ssRNA to protect it when transported to the ribosomes. Cellular methyltransferase proteins typically appear to only encode a single activity, whereas a number of viral methyltranferases have additional functions. BTV maximizes its coding capacity by having VP4 catalyzing all of the capping and methylation steps necessary (Ramadevi *et al.*, 1998); therefore the post-transcriptional modifications also happen inside the core without any help from cellular proteins. VP6 is the helicase, demonstrated to be an RNA-binding protein, unwinding the dsRNA genome prior and subsequent to the initiation of transcription (Roy *et al.*, 1990). The dsRNA genome segments are all transcribed at the same time, although the smaller genome segments are the most frequently transcribed (Huismans & Verwoerd, 1973). All of the transcription and replication reactions happen inside the core to ensure no leaking of dsRNA into the cytoplasm. Only capped ssRNA leave the core to be translated inside the cytoplasm at ribosomal sites.

Another interesting characteristic seen at viral activity sites is the presence of viral inclusion bodies (VIBs) or viral factories. New BTV particles arise from the sequential assembly of subcores to cores to double-shelled BTV particles all within or in association with VIBs. After virus infection these VIBs are present as early as 10h post infection. The NS2 protein is the main component of these VIBs. When NS2 is expressed from a baculovirus recombinant in Sf9 cells, VIB-like structures form in the cytoplasm (Thomas *et al.*, 1990). Other structural proteins, nonstructural proteins and virus particles at different stages of morphogenesis are also associated with these VIBs. It has been reported that the outer capsid protein VP2 is added to the BTV particles at the periphery of VIBs prior to the rapid transport of fully assembled BTV particles into the surrounding cytoplasm (Brookes *et al.*, 1993). An

important characteristic of NS2 is its ssRNA binding ability, this has been shown to play a role in the packaging of ssRNA into newly made BTV or AHSV virions (Theron & Nel, 1997, Thomas *et al.*, 1990). A characteristic of NS2 is the fact that it is phosphorylated in BTV-infected cells or when expressed in insect cells (Devaney *et al.*, 1988, Thomas *et al.*, 1990). It has been found that the phosphorylation of NS2 is necessary for the formation of the VIBs (Modrof *et al.*, 2005). For the recruitment of ssRNAs, three ssRNA-binding domains have been localized on BTV NS2. When these domains are removed it abolishes the ssRNA binding ability of NS2 (Fillmore *et al.*, 2002). It has been shown that NS2 specifically recognizes BTV ssRNA based on different RNA structures present in the different 10 RNA segments transcribed from the BTV genome (Lymperopoulos *et al.*, 2006). It has been shown that NS2 co-localizes with the BTV core proteins that form part of the polymerase complex namely VP1, VP4 and VP6. It is thought that as the phosphorylated form of NS2 is needed to produce VIBs, the unphosphorylated NS2 that is present prior to phosphorylation could play a role in binding VP1 and other core proteins in the cytoplasm and recruit these components to the VIBs when the NS2 is phosphorylated (Modrof *et al.*, 2005, Roy & Noad, 2006).

In rotavirus, also a member of the *Reoviridae* family, viroplasms or VIBs are formed that consists of nonstructural proteins NSP2 and NSP5. It has been confirmed by using siRNA knockdown experiments where the loss of NSP2 or NSP5 has been tied to the lack of viroplasm formation in the infected cells (Eichwald *et al.*, 2004, Patton *et al.*, 2006). These two nonstructural proteins need to interact to produce functional viroplasms. In these viroplasms, rotavirus replication as well as assembly takes place. For rotavirus, mechanisms have been elucidated whereby the virus ensures that both ssRNA necessary for translation and dsRNA necessary for newly made viruses are made. After the virus has entered the cytoplasm, the RNA viral polymerase VP1 that is present inside the viral core synthesizes the primary viral transcripts, which are extruded into the cell's cytoplasm. The RNA transcripts direct the synthesis of the viral proteins and also serve as RNA templates (+ strand) for the synthesis of RNA negative strands (- strand) to form the dsRNA genome segments again (Pesavento *et al.*, 2001).

1.2.4 Protein-protein interactions involved during viral cell exit

The final obstacle for viruses to overcome is the way in which they are released from the host cells. Various methods are used, depending usually whether the virus is naked or enveloped. We will now focus on how orbiviruses are released from the cells and what protein-protein interactions are necessary.

Because non-enveloped viruses usually lack glycosylated proteins known to facilitate both virus entry and exit, orbiviruses are released from infected mammalian cells mainly by cell lysis (Wechsler & McHolland, 1988). However it was shown by immunoelectron microscopy that BTV can either be released in a non-enveloped form by extrusion through the membrane or with a transient membrane envelope through budding at the cell surface (Hyatt *et al.*, 1989). BTV release from vector cells (*Culicoides*) is nonlytic and it is thought that the same mechanism of budding is used by the virus to escape from the infected insect cells (Hyatt *et al.*, 1993).

The candidate protein for mediating viral release in BTV and AHSV is the nonstructural protein NS3, through probable interaction with other viral proteins as well as cellular host proteins. My research will be focusing on aspects related to NS3-mediated virus release. AHSV as well as BTV replicate in both insect and mammalian cells. The virus is vectored to vertebrate species by the *Culicoides* species (biting midges). The cytopathic effect (CPE) caused by viral infection differs between the two hosts (Wechsler & McHolland, 1988). Mammalian cells (foetal tongue cell line) show severe CPE (Castro *et al.*, 1989), most likely due to the mechanism of viral release, where as insect cells show little CPE and appear to release virus without cell lysis (Homan & Yunker, 1988).

It has been shown that nonstructural (NS) proteins NS3 and NS3A are synthesized in low abundance in BTV-infected baby hamster kidney (BHK) cells (French *et al.*, 1989) in contrast to the high level expression of these proteins in invertebrate cells such as in mosquito C6/36 cells in which virus release is nonlytic (Guirakhoo *et al.*, 1995). The difference in expression of the NS3 protein in these infected cell types suggests that NS3 could play a role in the different virus exit pathways employed in different cell types. Sequence analysis of the S10 gene encoding NS3 from different BTV serotypes has indicated the presence of two hydrophobic domains that support its role as an integral membrane protein, as well as the presence of two potential glycosylation sites (Hwang *et al.*, 1992, Lee & Roy, 1986). This has also been noted in other orbivirus species such as AHSV, although the glycosylation sites are not so well conserved in all AHSV NS3 proteins (De Sa *et al.,* 1994, Van Staden & Huismans, 1991, Van Staden *et al.,* 1995).

A few hypotheses have been set on the table on the mechanism whereby NS3 could aid newly packaged virions to escape from the infected host cell. The latest research has shown that NS3 can use the cellular exocytosis pathway via the p11 protein that is part of the Annexin II complex, to traffic itself to the plasma membrane (Beaton *et al.*, 2002). Although the physiological role is not known it is thought that NS3 uses this interaction to direct itself to sites of active cellular exocytosis, or it could be part of the active extrusion process. Another observed interaction that makes the NS3-p11

association significant is the interaction between the C-terminal region of NS3 and VP2, the outer capsid protein of the newly assembled BTV virion (more detailed discussion under 1.2.4.2).

Another interaction that has been observed is the interaction of BTV and AHSV NS3 with the cellular protein Tsg101 (Wirblich *et al.*, 2006). This protein has been implicated in the intracellular trafficking and release of various enveloped viruses. This cellular protein recognizes a highly conserved motif called a L-domain with the amino acid sequence PSAP. Knockdown of Tsg101 with siRNAs resulted in the inhibition of AHSV and BTV release from mammalian cells (more detailed discussion under 1.2.4.3). In Figure 1.5 a summary is seen of how NS3 mediated release is postulated to happen by using protein-protein interaction between NS3 and cellular proteins p11 and Tsg101.

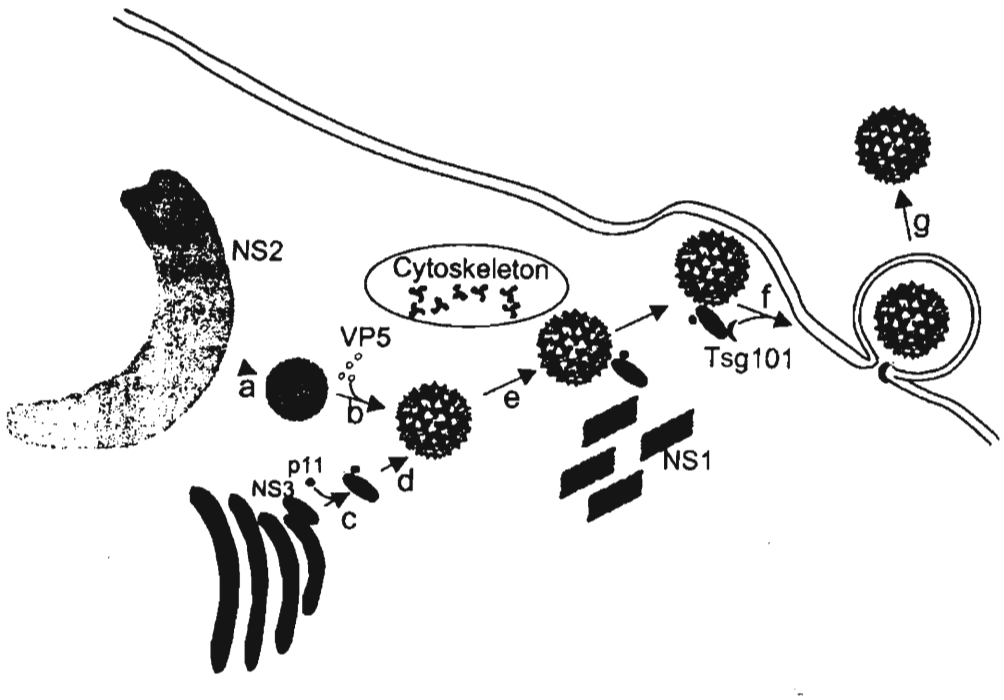

Figure 1.5: Diagram summarizing key interactions in the assembly and release of BTV: cores are released from NS2 inclusion bodies (a) and associate with outer capsid proteins VP5 and VP2 (b). BTV NS3 associates with the intracellular trafficking protein p11 (c) and forms a bridge between this protein and newly assembled virus particles by secondary interaction with VP2 (d). This leads to trafficking of the virus particle to the cell membrane (e) where interaction between the PSAP motif in NS3 and the cellular release factor Tsg101 results in the pinching off of vesicles containing virus particles (f) followed by release of mature virion particles from these vesicles (g) (Image and description taken from Roy and Noad, 2006).

Another interesting observation was made including the role of another nonstructural protein NS1, in the viral egress of BTV. This protein forms the characteristic tubules present in the cytoplasm of BTV infected host cells (Huismans & Els, 1979). Similar tubules are synthesised in AHSV infected cells, except that the absence of a ladder-like structure and the lower sedimentation value of AHSV NS1

tubules clearly distinguished them from those of bluetongue virus (Maree & Huismans, 1997, Van Staden *et al*., 1998). This protein was shown to be associated with cytoskeleton-associated virus-like particles (Eaton *et al*., 1988). It has been suggested that these NS1 tubules can play a role in transport of mature virus particles from the virus inclusion bodies to the cell membrane where NS3 is involved in virus release (Maree & Huismans, 1997). Experiments abolishing the proper function of NS1 resulted in a reduction in cellular pathogenesis and a shift in viral release from cell lysis to budding. It was thought that under deficient NS1 protein conditions, the NS3 protein levels might have been sufficient to shift cell exit from lytic to budding. Further studies are planned to test the hypothesis that the ratio of NS1:NS3 might contribute to BTV pathogenesis and release from host cells (Owens *et al*., 2004).

The latest study done on BTV, with respect to virus assembly and inevitably virus release focuses on the outer capsid protein VP2. It was shown that the intracellular localization of VP2 is dependent on the intermediate filament protein vimentin. VP2 binds via a hydrophobic patch and needs the glycine and valine amino acids present in this patch to bind to vimentin. It has also been shown that disruption of these vimentin filaments in the infected cells inhibited virus egress from these cells. It is suggested that the VP2-vimentin interaction could play a role in virus assembly in infected cells (Bhattacharya & Roy, 2006). This is interesting if it is taken in account that NS3 associates with VP2 to recruit newly assembled viruses for cell exit. Although a number of new interesting findings have emerged recently, it is clear that there are still many unknowns in the orbivirus life cycle.

1.2.4.1 NS3 protein characteristics

As NS3 plays a role in viral egress and forms the focus of my project, one needs to look at the characteristics of this protein. The NS3/NS3A proteins are translated from two conserved in phase overlapping reading frames on the S10 gene and only differ with respect to the presence of 10 additional amino acids at the N-terminal of NS3 (Van Staden & Huismans, 1991). A novel feature of AHSV NS3 is the high CPE seen when it is expressed by the baculovirus system in Sf9 insect cells in comparison to BTV NS3 (Van Staden *et al.,* 1995). These results underlined earlier studies, supporting the role of NS3 in virus pathogenicity. Electron microscopic studies showed that both BTV NS3 proteins (Hyatt *et al*., 1991) and AHSV NS3 proteins (Stoltz *et al*., 1996) are localized in the plasma membranes of infected mammalian cells. The membrane associated state of NS3 in both BTV and AHSV suggests a role in viral release. It has been shown that the addition of BTV NS3 to cells that produce virus like particles (VLP contain VP3, VP7, VP2 and VP5) causes the transport and budding of these non-replicating particles, whereas other nonstructural proteins such as NS1 and NS2 had no such effect (Hyatt *et al*., 1993). Another interesting finding was the role BTV NS3 can play as

a viroporin. Viroporins are a group of small hydrophobic transmembrane proteins that can form hydrophilic pores through lipid bilayers. It has been seen that viroporins play a role in promoting virus release from infected cells and in affecting cellular functions including protein trafficking and membrane permeability. Viroporins have specific properties based on homo-oligomerization capability and presence of transmembrane domains that can associate with the plasma membrane as well as with the Golgi apparatus of an infected cell (Han & Harty, 2004).

An interesting feature of segment 10 from AHSV is the high intra-serogroup variability in its sequence compared to the same gene in BTV and other orbiviruses (Jensen *et al.*, 1994, Moss *et al.*, 1992). NS3 has been identified as the second most variable protein in the AHSV genome, showing variation levels of between 1.8% and 36.3% across different serotypes (Van Niekerk *et al.*, 2001). This is in stark contrast to BTV NS3 that show a 0% - 18% nucleotide sequence variability (Jensen *et al.*, 1994, Pierce *et al.*, 1998). It is thought that this high variation seen among AHSV serotypes with respects to NS3 emphasizes the possible role of NS3 in virus virulence. Although NS3 of AHSV is highly variable across serotypes, a number of highly conserved characteristics are present suggesting important roles in ensuring protein functionality. The N-terminal of NS3 contains a second in-phase methionine codon for initiation of NS3A, a cluster of at least five proline residues are present between amino acid positions 22 to 34 and a stretch of highly conserved amino acids occupy residues 46 to 90 (Van Staden *et al.*, 1995). Phylogenetic analysis of NS3 sequences showed that the strains of the nine serotypes fall into three groups. Group α contains serotypes 4, 5, 6 and 9; group β contains serotype 3 and 7; and group γ contains serotypes 1, 2 and 8 (Martin *et al.*, 1998).

It was thought that these variations seen in NS3 in AHSV could be used to diagnose serotype (Zientara *et al.*, 1995). But these variations can be deceptive as the outer capsid proteins VP2 and VP5 predominantly control viral serotype, to which neutralizing antibodies are raised. In addition, reassortment and exchange of genome segment 10 between viruses of different serotypes is possible and this cannot correlate with specific virus serotype (Zientara *et al.*, 1998). However, it has been shown that reassortment in NS3 can influence virulence (O'Hara *et al.,* 1998). It is been suggested that NS3 influences the virulence of the virus via an effect it has on the rate or timing of virus release from the cell (Martin *et al.*, 1998).

1.2.4.2 Interaction between NS3 and outer capsid protein VP2 and cellular protein p11

As already mentioned in 1.2.4, NS3 associates with the cellular exocytosis pathway as a means to exit an infected cell – more information surrounding this hypothesis will be given in this section. In this study it was shown by using the yeast two-hybrid system that the N-terminal domain of BTV NS3

interacts with a cellular protein p11 (calpactin light chain) that is part of the annexin II complex that is involved in exocytosis. The C-terminal region of NS3 binds to VP2, therefore it is suggested that NS3 forms a bridging molecule that draws an assembled virus into contact with the cellular export machinery of the cell (Figure 1.6). NS3 contains a putative amphipathic helix in its first 13 amino acids that supplies the binding site for p11; this region is also highly conserved among various serotypes in BTV. (Beaton *et al.*, 2002)

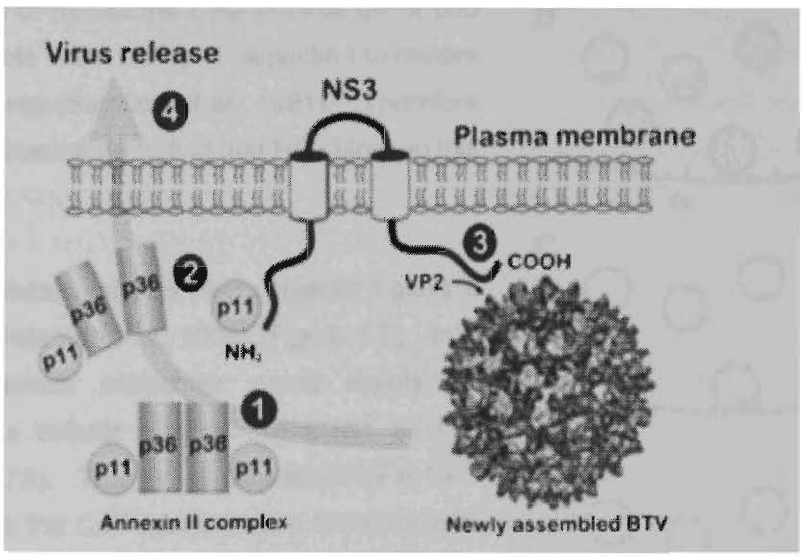

Figure 1.6: A model for the function of NS3 based on its membrane location and known topology. The C-terminal of NS3 binds to the newly assembled virion via VP2. The N-terminal of NS3 binds to p11 with p36, proteins part of annexin complex II involved in cellular exocytosis. By virtue of interactions, the assembled virions are drawn into contact with the p11/annexin II complex and engage the cellular exocytic machinery to affect nonlytic virus release (Diagram and description taken from Beaton *et al.*, 2002).

The annexin protein family consists of at least 18 members. All annexins that have been characterized so far are found in the cytosol and associated with the cytoplasmic face of cellular membranes (Harder *et al.*, 1997). Calpactin I is one of the best characterized components of the annexin family. The calpactin I protein occurs in cells as a 36 kD monomer (heavy chain) and as a 90-kD complex containing two copies of the 36 kD heavy chain and two copies of an 11 kD light chain (Erikson *et al.*, 1984; Gerke *et al.*, 1984; Glenny *et al.*, 1985 as referenced by Sarafian *et al.*, 1991). Most studies done on calpactin I used chromaffin cells present in the adrenal glands. Calpactin I is one of the proteins released by adrenal chromaffin cells by exocytosis in response to micromolar calcium concentrations. It is a phospholipid binding protein known to promote in vitro aggregation of chromaffin granules (Sarafian *et al.*, 1991). Calpactin is dependent on cells that have cytosolic protein kinase C activity. It has been found that the tyrosine and serine phosphorylation sites for protein kinase C are situated in the NH_2-terminal region of the p36 protein (Glenney *et al.*, 1985; Gould *et al.*, 1986 as referenced by Sarafian *et al.*, 1991). This unique NH_2-terminal region also allows binding to

the p11 chain (Glenney *et al.*, 1986; Johnson *et al.*, 1986 as referenced by Sarafian *et al.*, 1991). The observation that annexins interact with membranes in a calcium dependent manner shows that they participate in calcium regulated traffic such as exocytosis (Sarafian *et al.*, 1991). If you take the all the data together it has been suggested that the association of p11 to the NH_2-terminal tail of p36 plays a significant role in the ability of calpactin I to restore the exocytotic pathway (Sarafian *et al.*, 1991). Therefore it is an interesting observation to find that NS3 binds to this cellular p11 protein.

The following hypothesis explains how calpactin I plays a role in exocytosis (Nakata *et al.*, 1990) (Figure 1.7). In a resting state, calpactin molecules would mainly be associated with the cellular plasma membrane as fine globules (Figure 1.7A). The cell is stimulated by a Ca^{2+} influx that increases the Ca^{2+} concentration to micromolar levels in the cell periphery. This increased concentration leads to the activation of the calpactin I complex on the plasma membrane. The cross linking of the vesicles that are in near proximity with the plasma membrane occurs with a conformational change taking place in the connecting calpactin I complex molecules (Figure 1.7B). In this study, it was shown that chromaffin vesicles attach tightly to the plasma membrane by the Ca^{2+} activated calpactin molecules. The association of the vesicles to calpactin I molecules are followed by the fusion of the two membranes (Figure 1.7C). The vesicles can now release their contents (Figure 1.7D).

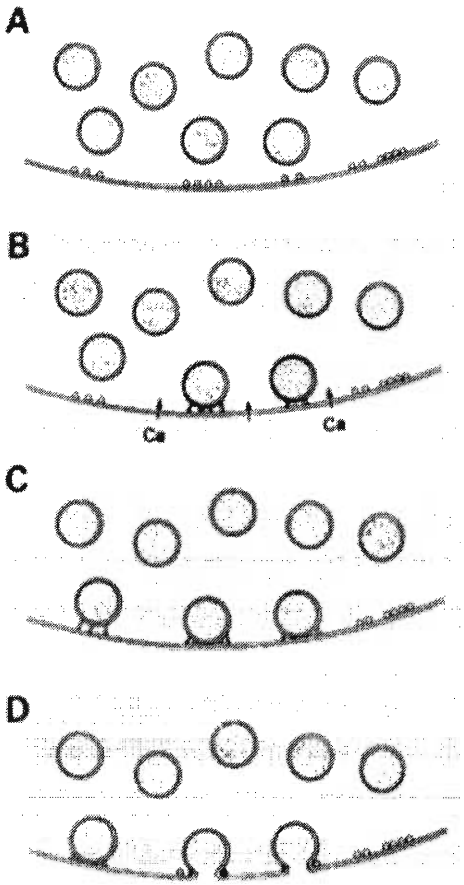

Figure 1.7: A hypotheses of how calpactin I is involved in the exocytosis pathway as studied in chromaffin cells. Activation of the globular calpactin molecules by a Ca^{2+} influx changes its shape to cross-link to nearby vesicles. Fusion of two membranes allows the vesicle contents to be released. (Diagram taken from Nakata *et al.*, 1990)

1.2.4.3 L-domains

The most recent study done on BTV NS3 identified an additional L-domain potentially involved in viral exit as already stated in 1.2.4. Retroviruses such as HIV use the multivesicular bodies (MVB) present in the host cell to bud at the plasma or endosomal membrane (Freed, 2004, Pornillos *et al.*, 2002).

Cellular proteins function in the MVB where they play an important role in protein sorting and degradation. These MVB are formed by the budding of vesicles into the lumen of late endosomal compartments – this then is a process very similar to the formation of an enveloped virus particle (Pornillos *et al.*, 2002, Raiborg *et al.*, 2003). A multitude of cellular proteins functions in a sequential manner in the production of these MVB which include components of the ESCRT-I, -II and –III complexes (Babst, 2005, Babst *et al.*, 2002a, Babst *et al.*, 2002b, Katzmann *et al.*, 2001). Retroviruses bind to different components in these different ESCRT pathways by means of so-called late-domain motifs. These motifs are highly conserved protein-protein interactions motifs that are present at different locations within the Gag protein (Demirov & Freed, 2004, Freed, 2002). The Gag protein forms part of the nucleocapsid shell around the RNA of a retrovirus. Some of these late-domains were identified in BTV and AHSV; this triggered the question whether the same type of viral exit could be utilized by orbiviruses (Wirblich *et al.*, 2006).

For the Gag protein, three classes of late-domain motifs have been identified namely P(S/T)AP, YPXL/LXXLF, and PPXY. The PSAP motif recruits the cellular protein Tsg101. This protein forms part of the ESCRT-I complex (Garrus *et al.*, 2001, Martin-Serrano *et al.*, 2001, Martin-Serrano *et al.*, 2003b). The YPXL/LXXLF motifs bind to the AIP-1/Alix protein which acts downstream of Tsg101. This protein appears to form a bridge between the ESCRT-I and ESCRT-III complexes (Martin-Serrano *et al.*, 2003a, Strack *et al.*, 2003). The PPXY motif plays a role in recruiting host ubiquitin ligases (Blot et al., 2004, Bouamr et al., 2003, Kikonyogo et al., 2001, von Schwedler et al., 2003). At this stage it is known that the cellular ubiquination machinery plays a role in the budding of many animal viruses, but the mechanism whereby ubiquitin ligases interact and target the components of the budding machinery is still unknown (Blot *et al.*, 2004, Martin-Serrano *et al.*, 2004, Patnaik *et al.*, 2000). The PTAP and PPXY domains have also been identified in other proteins such as the VP40 protein of Ebola virus, the matrix protein of vesicular stomatitis virus and the Z protein of Lassa virus. It appears that these domains have similar function to the late-domains present in retroviruses (Craven *et al.*, 1999, Harty *et al.*, 2000, Perez *et al.*, 2003).

In Figure 1.8 a cartoon is seen representing BTV NS3 and the late-domains present in orbivirus NS3 proteins. Late-domains were previously identified in BTV NS3 (Strack *et al.*, 2000), but Wirblich *et al.* (2006) looked at a number of orbiviruses namely BTV, AHSV, epizootic hemorrhagic disease virus (EHDV), Chuzan virus and Broadhaven virus to see whether late-domains were encoded in general in these orbiviruses. In Figure 1.8 a summary is seen that shows the late-domains present as well as their positions in the NS3 protein of each orbivirus. All the NS3 sequences contained the most common late-domains i.e. PPXY and P(S/T)AP. In the NS3 proteins, the PPRY domain is followed by one or two amino acids which then are followed by the P(S/T)AP domain. For the Broadhaven virus

the PTAP precedes and partly overlaps the PPXY domain (Wirblich *et al.*, 2006). L-domains are in the same area as that what is called a "proline-rich" region in NS3 and therefore already been identified as a putative important interaction domain for AHSV NS3 (Van Niekerk *et al.*, 2001).

Another interesting observation was that the BTV late-domain sequences were fully conserved across 10 serotypes while much more variation was seen in these late-domain sequences in AHSV. We know that in AHSV, the NS3 protein is the second most variable protein after the outer capsid protein VP2 (Van Niekerk *et al.*, 2001). This is in stark contrast to the high sequence conservation seen in NS3 of BTV (Jensen *et al.*, 1994, Moss *et al.*, 1992). This high variation in AHSV NS3 has clustered the NS3 sequences of the 9 serotypes into three different phylogenetic groups (Martin *et al.*, 1998). Representatives of these three phylogenetic groups differ in their pathogenesis towards the host cell (Tracy Meiring, unpublished results). AHSV-2 (from phylogenetic group γ) has the most severe CPE on mammalian cells, followed by AHSV-3 (group β) and then AHSV-4 (group α) which causes the least CPE. This same effect was mimicked by expressing only the NS3 proteins of each of these viruses in insect cells, and then adding the NS3 containing lysate exogenously to mammalian cells. Therefore the variation seen in the late-domain sequences in AHSV could be a further key in understanding the difference in pathogenesis between the different serotypes that are based on the NS3 phylogenetic groups.

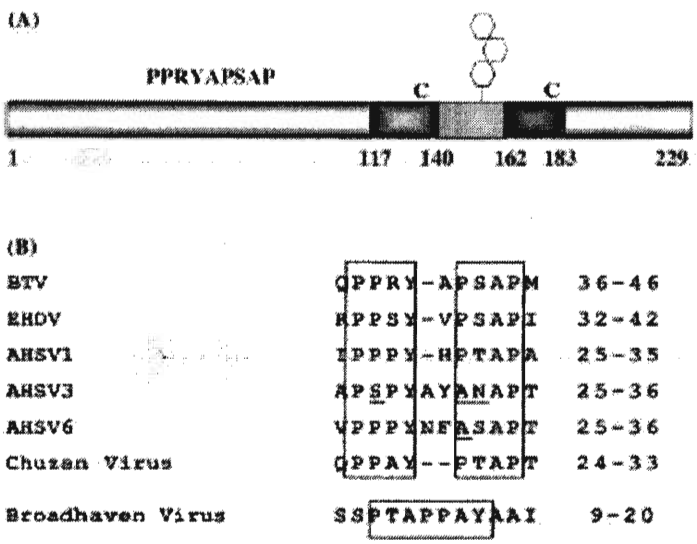

Figure 1.8: Cartoon of BTV NS3 and late-domain motifs in orbivirus NS3 proteins. (A) Cartoon showing the domain structure of NS3 and the location and sequence of the late-domain motifs. Transmembrane domains are indicated by dark gray boxes, and the extracellular domain is shown in light gray. The N- and C-terminal intracellular domains extend from amino acids 1 to 117 and 183 to 229, respectively. Hexagons indicate the single glycosylation site, which is encoded by all BTV strains, and "C" indicates the two conserved cysteine residues. The late-domain motifs extend from amino acids 37 to 45. NS3A is generated by initiation at an in-frame ATG at codon 14 of the NS3 open reading frame. (B) Alignment of late-domain motifs in orbivirus NS3 proteins. Numbers to the right indicate the amino acid positions of the aligned sequences within NS3. Cartoon and description taken from Wirblich *et al.* (2006).

Wirblich *et al.* (2006) showed that the BTV NS3 late domain PSAP and AHSV6 NS3 late domain ASAP could bind to the Tsg101 protein that forms part of the ESCRT-I complex. They also discovered that the *Drosophila* homologue of the Tsg101 protein bound to the BTV and AHSV late-domains although the interaction was weaker. They also showed that the PPXY domain present in BTV did indeed bind to cellular ubiquitin ligases such as NEDD4.1, WWP1 and Itch. An interesting observation was that depletion of Tsg101 from cells inhibited BTV release much more than it did AHSV release. As budding is the way of cell exit when Tsg101 is associated with NS3, the result that Tsg101 not having such a big effect on AHSV release is consistent with the fact that AHSV display a much stronger cytopathic effect at early times of infection if compared to BTV infection that indicates a lytic cell release. In conclusion, Wirblich *et al.* (2006) stated that the use of late-domains in orbiviruses could play a bigger role in insect cell release where non-lytic cell release is observed in comparison to mammalian cell release, where lytic cell release is observed (Hyatt *et al.*, 1989, Hyatt *et al.*, 1993, Wechsler & McHolland, 1988)

1.2.4.4 Lipid rafts

Recent research has indicated a role for lipid rafts in virus entry, virus assembly and virus exit. Lipid rafts are small, mobile and unstable molecules that form partly mobile platforms that carry specific proteins from the *trans*-Golgi network (TGN) to the cell surface, along the plane of the plasma membrane, and from the plasma membrane to the internal membrane (Nichols & Lippincott-Schwartz, 2001). Viruses can use these micro lipid domains to move around in the cell and to assist itself in entering the host cell and exiting the host cell (Chazal & Gerlier, 2003). Most research done in the *Reoviridae* family has focused on rotaviruses that actively use these lipid rafts to exit an infected cell. Rotavirus differs in the way it releases itself from cells in comparison to BTV and AHSV. During maturation, rotavirus double-layer particles bud into the endoplasmic reticulum by using the virally encoded nonstructural protein NSP4 and acquire an ER-derived lipid membrane that is eventually lost and replaced by two outer capsid proteins VP7 and VP4 (Pesavento *et al.*, 2006). In a recent study done, it was shown by using siRNA knockdown assays that only one of its outer capsid proteins, VP4 and not VP7 plays a direct role in associating with rafts. As expected inhibition of the NSP4 protein also inhibited any viral association with the rafts. The virus uses this association with rafts via its outer capsid protein and the NSP4 protein to exit the infected cell via a cellular exocytic pathway (Cuadras *et al.*, 2006).

1.3 METHODS USED TO INVESTIGATE PROTEIN-PROTEIN INTERACTIONS

There are a number of methods available to study protein-protein interaction. In Table 1.2 a summary is given of the methods used in the majority of studies (Uetz & Hughes, 2000). The yeast two-hybrid system is a powerful and widely used way to assay whether proteins interact. It was first described 1989 by S. Fields and O-K. Song (Fields & Song, 1989). The yeast two-hybrid assay is based on the fact that many eukaryotic *trans*-acting transcription factors can be separated from each other. These regulators often contain a DNA-binding domain (DNA-BD) that binds to a specific upstream activation site of a target gene. The transcription of this gene can only happen when one or more activation domains (AD) direct the RNA polymerase II complex to transcribe the target gene downstream of the upstream activation site where the DNA-BD binds. These two domains cannot activate the target gene unless they are brought in close physical proximity in the promoter region. This can be done by using different cloning vectors to generate fusions of these domains to genes that encode proteins that potentially can interact with each other. Therefore an interaction between a bait protein and a prey protein creates a novel transcription factor that can activate the target gene, which is under control of the GAL4-responsive upstream activation site. This factor then activates reporter genes, which then give rise to phenotypically detectable protein-protein interactions (Notes taken from CLONTECH Matchmaker user manual).

Table 1.2: Methods employed to study protein-protein interactions

Method	Major properties
Yeast two-hybrid	Inexpensive; *in vivo* conditions; yields binary interactions; uses living cells; requires protein fusions; requires localization to the nucleus; simple
Pull-down (*in vitro* assays)	*In vitro* conditions; semi-quantitative
Immuno-precipitation	Allows study of native complexes; requires antibodies
Confocal-microscopy using Fluorescence resonance energy transfer (FRET)	Allows study *in vivo,* gives information on intracellular localization of interactions
Mass spectrometry	Allows study of native complexes; requires purification of complex; expensive; technically difficult

Table compiled from Uetz and Hughes (2000) and Snippe *et al.* (2005)

The yeast two-hybrid system has various advantages in the sense that protein-protein interactions can be assayed *in vivo* using the yeast cell as a living test tube. It brings the higher eukaryotic reality closer than most *in vitro* approaches or techniques that are based on bacterial expression. Another feature is the minimal requirements the system needs to initiate a screening as either cDNA or full length or even partial gene sequence can be used. This is in contrast to the sometimes high quantities of purified or good quality antibodies that are needed in classical biochemical approaches. The yeast two-hybrid system has the capacity to recognize weak and transient interactions – but it must be kept in mind that there is usually a trade-off between the identification of weak interactions and the number of false positives encountered when performing a screening procedure (Van Criekinge & Beyaert, 1999). It is therefore pertinent that any protein-protein interactions detected by using the yeast two-hybrid system should undergo confirmatory analysis by doing independent re-screenings of the interactions detected and even using a second or third independent functional assay.

The yeast two-hybrid system has been used to investigate protein-protein interaction in BTV as already discussed in 1.2.4.2 and 1.2.4.3. This system was also used in a similar study done on rotavirus, another dsRNA virus part of the *Reoviridae* family to investigate binding of a nonstructural viral protein to a cellular protein (Vitour *et al.*, 2004). The mRNAs of rotavirus are capped but not polyadenylated, and the viral proteins are translated by cellular translation machinery. The viral nonstructural protein NSP3 binds specifically to the 3' consensus sequence of the viral mRNAs and interacts with the eukaryotic translation initiation factor eIF4G I. To further understand the role of NSP3 in rotavirus replication, the yeast two-hybrid system was used to determine whether NSP3 interacted with other cellular proteins. A 110-kDa cellular protein, named RoXaN (rotavirus X protein associated with NSP3) was identified that contains a minimum of three regions suggested to be involved in protein-protein or nucleic acid-protein interactions. Domains of interaction were mapped and these domains correspond to the dimerization domain of NSP3 (amino acids 244 to 341). The association of NSP3 with RoXaN does not impair the interaction of NSP3 with eIF4G I. Further it has been found that rotavirus infected cells contains ternary complexes made of NSP3, RoXaN and eIF4G, implicating RoXaN as part of translation regulation (Vitour *et al.*, 2004).

As a confirmatory assay is needed when the yeast two-hybrid system is used, a separate assay such as column binding (Dimitrova *et al.*, 2003, Xu *et al.*, 2000) or co-immunoprecipitation (Eichwald *et al.*, 2004, Khu *et al.*, 2004, Surjit *et al.*, 2004) are used. Co-immunoprecipitation is a classical method of detecting protein interactions and has been used in literally thousands of experiments. The basis of this experiment is simple, and is most commonly used to test whether two proteins of interest are associated *in vivo*. A cell lysate must be generated, antibody must be added and the antigen must be

precipitated and washed. Bound proteins are eluted and analyzed. The antigen used to make the antibody can be purified protein gained either from natural tissue or purified after expression in another organism. Epitope tags (e.g. C-myc) or protein tags (GST) can also be used. Several criteria are used to substantiate the authenticity of a co-immunoprecipitation experiment. Firstly, it has to be established that the co-precipitated protein is precipitated by the antibody itself and not by a contaminating antibody. This problem can be avoided by the use of monoclonal antibodies. Secondly, it has to be established that the antibody does not itself recognize the co-precipitated protein. This can be done by demonstrating persistence of co-precipitation with independently derived antibodies, ideally with specificities toward different parts of the protein. Third, one would like to determine if the interaction is direct or proceeds through another protein that contacts both the antigen and the co-precipitated protein. This is usually addressed by using purified proteins and immunological techniques. Fourth and most difficult is determining whether the interaction takes place in the cell and not as a consequence of cell lysis. Even though co-immunoprecipitation is not as sensitive as other methods because of the smaller concentration of antigen used, this can be overcome by deliberately adding excess of antigen to drive complex formation (Phizicky & Fields, 1995).

Column binding or GST pull-down assays make use of chimeric proteins comprised of gluthione-S-transferase (GST) linked in frame to a protein of interest. It has been shown that the fusion of this GST tag to a protein can enhance the solubility of the protein in question. The GST pull-down assay technique (column binding) can be used to determine hetero- and homo-oligomerization of viral proteins (Sambrook & Russel, 2001). This technique analyses the binding of a labelled, in-vitro-translated prey protein to a purified GST-bait protein bound to glutathione-sepharose beads. Expression vectors are available for the easy expression of GST-fusions in both bacterial and mammalian cells. GST-fusion proteins are used to study protein-protein interaction because of the strong affinity between GST and glutathione. This interaction can be used to couple the fused protein to an immobilized glutathione matrix. The advantage of this system is the robustness of it and the resistance of the interaction formed to stringent buffer conditions. Proteins can also be studied most of the times in their native form without any influence on the protein structure by the GST tag (Vikis & Guan, 2004).

The latest type of technology is the technique of fluorescence resonance energy transfer (FRET). This technology holds a unique niche in modern fluorescence microscopy because it provides the means by which one can probe inter- and intra-molecular interactions in the 1 – 10nm range. FRET microscopy yields quantitative information that portrays the precise protein-protein interactions as seen in a living cell – giving it the edge above other more used *in vitro* assays (Herman *et al.*, 2004).

The two protein of interest are fused to different coloured fluorophores. The one is seen as the donor fluorescent protein and the other as the acceptor fluorescent protein. FRET will only take place if the two proteins fused to the individual fluorophores interact. This will allow a decrease in the donor fluorescence as well as an increase in acceptor fluorescence as seen through a confocal laser microscope. This protein-protein binding assay not only gives information on protein-protein interactions, but at the same time it gives a good idea on the localization of this interaction in the cell (Snippe *et al.*, 2005).

To quantify protein interactions from different samples, mass spectrometry can be used. This system is based on the stable isotope dilution approach. Proteins or peptides are labelled with identical tags that differ in mass based on stable isotope content. In a quantification experiment, proteins or peptides derived from the protein in one sample are labelled with an isotopically heavy mass tag, whereas the light isotope tag is used to label the sample to be compared. All these labelled peptides are combined, purified, or separated into fractions and analyzed by mass spectrometry, which measures the mass and ion abundance of the peptides. It is the difference in measured ion abundance between heavy- and light-labelled peptides that give the actual abundance ratio of this peptide from the two different samples (Xu et al., 1997).

1.4 CONCLUSION

To date, much more research has focused on viral release patterns in enveloped viruses due to their danger as human pathogens. For non-enveloped arboviruses such as bluetongue virus (BTV), only recently results have shown remarkable characteristics in the release mechanisms these viruses use. For the first time a few hypotheses have been formed on how specifically the NS3 protein of BTV uses cellular proteins to release mature virions from infected cells. We would like to investigate these mechanisms in AHSV. One of the main focus areas of the orbivirus research program in the Department of Genetics is to study the role of AHSV proteins in pathogenicity, virulence and disease. Therefore, to study the release patterns of AHSV in regards to the role of specific viral proteins as well as the influence it has on the pathogenicity of its vector or host will offer a big opportunity to expand our knowledge.

We know that BTV NS3 presumably forms a bridging molecule across the cell membrane to bind to the outer capsid protein VP2 on the one side and to the cellular annexin complex protein p11 on the other side to establish an exit route. Because of the relatedness between AHSV and BTV the same type of mechanism is expected for AHSV. We would like to investigate whether in AHSV; the C-terminal of NS3 also binds to VP2. We would also like to expand on this knowledge by determining

the domain on VP2 (N-terminal or C-terminal) were this interaction between NS3 and VP2 takes place. Conclusions drawn from sequencing studies done on the nine serotypes of AHSV shows that the C-terminal of VP2 contains a much more conserved region in comparison to the N-terminal (Potgieter *et al.*, 2003). This would probably be the most likely site of NS3-VP2 interaction.

The viral exit route used by AHSV in its insect vector is not known. We would therefore also like to research possible cellular interactions between NS3 of AHSV and proteins expressed from a *Drosophila melanogaster* cDNA library. It is expected to find proof of budding as the means of viral exit in insect cells as no severe CPE is seen when BTV infects insect cells in cell culture (Homan & Yunker, 1988). Also it has been shown that NS3 is synthesized in a higher abundance in mosquito cells (insect), which relates to budding, if compared to that which has been found in BHK cells (mammalian) (French *et al.*, 1989, Guirakhoo *et al.*, 1995). We are planning to use the yeast two-hybrid system together with other protein-protein interaction systems such as the column binding pull-down assay to ensure reliable results.

Long Term Aim:

Investigate the role of AHSV NS3 in the viral life cycle and morphogenesis, focusing on its contribution to release, pathogenesis and virulence by identifying and mapping protein-protein interactions between different viral and/or cellular proteins that plays a role in the AHSV life cycle, specifically with respect to viral release in both mammalian host cells and insect vector cells. This then in the end can shed more light on how the virulence of a virus is determined.

Specific Aims

- Investigating protein-protein interaction between membrane protein NS3 and outer capsid protein VP2 in AHSV.

- Investigating protein-protein interactions between AHSV NS3 and insect cellular proteins by using a *Drosophila melanogaster* cDNA library.

Chapter 2: Investigating protein-protein interaction between nonstructural membrane protein NS3 and outer capsid protein VP2 in AHSV

2.1 INTRODUCTION

During the orbivirus life cycle, mature virions are produced in viral inclusion bodies (VIBs) in the cytoplasm of infected cells. These virions then need to be transported to the cell surface to be released. In BTV it has been shown that this process involves the membrane protein NS3, which can interact with both a cellular exocytosis protein (p11) and the viral capsid protein, VP2 (Beaton *et al.*, 2002). We asked whether the same mechanism could be at work in African horsesickness virus (AHSV), and decided to investigate if AHSV NS3 binds to VP2. For this project, three different approaches were used to investigate interaction between AHSV VP2 and NS3 namely the yeast two-hybrid system, a GST-pulldown assay and a density gradient assay. We did not investigate whether AHSV NS3 interacts with the p11 protein as shown with BTV in this study. The first 13 N-terminal amino acids of AHSV NS3 can also form an amphipathic helix, which is the structure proposed to mediate interaction with p11. AHSV NS3 therefore probably also binds to p11 to fulfil the same role in trafficking, but this remains to be confirmed experimentally.

The AHSV3 NS3 protein consists of 217 amino acids encoded by nucleotides 20 - 673 of the 758 base pair S10 gene. NS3 contains two hydrophobic domains that are present from amino acids 116 – 137 and 154 – 176 and prescribed to be transmembrane regions. The N-terminal domain (amino acids 1 – 118 encoded by nucleotides 20 – 374) contains a amphipathic helix (amino acids 1 – 13), a proline rich region/L-domain (amino acids 25 – 36) and a region predicted to have a high potential for coiled-coil structure (amino acids 95 – 118). It is thought that this coiled-coil region could mediate protein stability and multimerization (Van Niekerk *et al.*, 2001, Wirblich *et al.*, 2006) (See Figure 2.1). The N-terminal domain in BTV is postulated to bind to cellular proteins such as p11 and Tsg101 (Beaton *et*

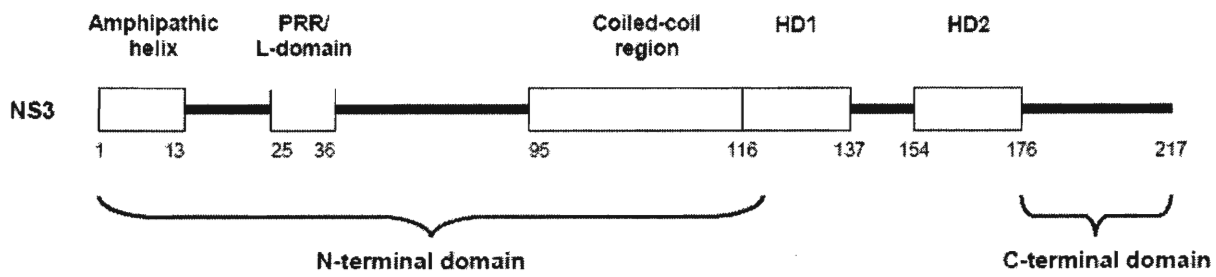

Figure 2.1: A schematic representation of the AHSV NS3 protein. The amphipathic helices, the proline rich region (PRR)/L-domain, coiled-coil region and hydrophobic domains are indicated.

al., 2002, Wirblich *et al.*, 2006). The C-terminal region of AHSV3 NS3 contains 40 amino acids encoded by nucleotides 551 – 671 of the S10 gene. It is postulated that the C-terminal of AHSV NS3 binds to the outer capsid protein VP2, analogous to the situation in BTV (Beaton *et al.*, 2002). The C-terminal region of NS3 was used in the yeast two-hybrid screen to investigate VP2 – NS3 interaction. The N-terminal of NS3 of AHSV2 was used to further investigate homo-dimerization of NS3.

The other protein used in this study was the AHSV VP2. The full-length VP2 protein consists of 1057 amino acids encoded by nucleotides 13 - 3186 of the 3221 base pair L2 gene. In a virion, this protein associates into trimers and forms the outer capsid of the virus in conjunction with VP5 (Hassan & Roy, 1999, Mertens & Diprose, 2004). It is not known which part of VP2 interacts with NS3, thus as a preliminary screening, two truncated versions of VP2 were made. We decided to divide the VP2 protein in half therefore nucleotides 13 - 1618 encoding amino acids 1 – 535 were prepared as the N-terminal region and nucleotides 1588 - 3184 encoding amino acids 525 - 1057 were prepared as the C-terminal region of VP2. The structure of VP2 is not known for BTV or AHSV, therefore the decision for "halving" the VP2 gene were decided upon randomly. It should be noted that this could have an effect on the possibility of interaction with the NS3 mutants, thus the full-length VP2 protein was also included in the experiments.

The yeast two-hybrid system is based on the Gal4 transcription factor that consists of a DNA-binding domain and an activation domain. These two domains need to interact to result in a functional transcription factor that can activate reporter genes such as histidine via an upstream activation site present in the reporter gene. In the yeast two-hybrid system the DNA-binding domain is fused to a bait protein, usually of known function and the activation domain is fused to the prey, usually a protein of unknown function. If the bait and prey proteins interact when transformed into yeast, the DNA-binding domain and activation domain is brought into close proximity and a functional transcription factor can be formed. Thus the interaction between the bait and prey protein allows the DNA-binding and activation domains to interact and initiate expression of the reporter genes. The yeast two-hybrid screen requires nuclear targeting of the two fusion proteins to activate expression of the reporter genes (CLONTECH Matchmaker user manual). As NS3 is a membrane protein, expression of the full-length protein would result in its localization to the cytoplasmic membrane components via its hydrophobic domains. This would prevent the assay from working, therefore only truncated versions of NS3 excluding its hydrophobic domains were used. In total 12 constructs were used for the yeast two-hybrid screen, where full length or truncated VP2 or NS3 genes of AHSV2 and AHSV3 were cloned into the pAS2-1 and pACT2 yeast vectors (Table 2.1). These constructs were used to assay interaction between VP2 – NS3, as well as homo-dimerizations between NS3 - NS3 and VP2 - VP2.

Another method used in investigating NS3 - VP2 protein-protein interaction was the column binding assay or GST-pulldown assay. VP2 was produced from recombinant baculovirus infected Sf9 insect cells. The NS3 N-terminal and NS3 C-terminal domains were bacterially expressed via the pET system as GST fusion proteins. The GST-NS3 fusion proteins were bound to the glutathione beads via the GST protein and the VP2 protein was added to the glutathione slurry to allow for protein-protein interaction, any protein interacting with NS3 would then be captured.

Due to the membrane association of the AHSV NS3 protein, it was decided to use this characteristic in a membrane flotation assay. In this assay, proteins are separated based on density, but specifically then on their association with lipids. As NS3 is associated with the lipid bilayer of the cell membrane of infected cells (Van Staden *et al.*, 1995), it floats upwards in the gradient (unpublished results, Tracey-Leigh Hatherell). We decided to investigate the effect of VP2 on NS3 when co-expressed in the baculovirus expression system. Interaction between VP2 and NS3 should shift VP2 (not associated with lipids) into the fractions containing NS3 (associated with lipids).

2.2 MATERIALS AND METHODS

2.2.1 Plasmids

The following plasmids containing genes of interest were available:

Table 2.1: List of available plasmids and their genes of interest used

Plasmid vector	Clone	Clone construction
pAS2-1	AHSV2 NS3 20 - 374	Nucleotides 20 - 374 of AHSV2 segment 10 encoding NS3 N-terminal (amino acids 1 – 118), cloned into the NdeI and EcoRI sites of pAS2-1 (Dr. Michelle van Niekerk, Department of Genetics, University of Pretoria)
pACT2	AHSV2 NS3 20 - 374	Nucleotides 20 - 374 of AHSV2 segment 10 encoding NS3 N-terminal (amino acids 1 – 118), cloned into the NdeI and EcoRI sites of pACT2 (Dr. Michelle van Niekerk, Department of Genetics, University of Pretoria)
pAS2-1	AHSV3 VP2	Nucleotides 1-3221 (Open reading frame, nucleotides :13 - 3186) of AHSV3 L2 encoding VP2, cloned into the NcoI and BamHI sites of pAS2-1 (Dr. Michelle van Niekerk, Department of Genetics, University of Pretoria)
pACT2	AHSV3 VP2	Nucleotides 1-3221 (Open reading frame, nucleotides:13 -

		3186) of AHSV3 L2 encoding VP2, cloned into the NcoI and BamHI sites of pACT2 (Dr. Michelle van Niekerk, Department of Genetics, University of Pretoria)
pAS2-1	AHSV3 NS3 546 - 758	Nucleotides 546 – 758 (last 129 bp of S10 ORF) of AHSV3 segment 10 encoding NS3 C-terminal (amino acids 176 – 217), cloned into the NcoI and EcoRI sites of pAS2-1 (Dr. Michelle van Niekerk, Department of Genetics, University of Pretoria)
pACT2	AHSV3 NS3 546 - 758	Nucleotides 546 – 758 (last 129 bp of S10 ORF) of AHSV3 segment 10 encoding NS3 C-terminal (amino acids 176 – 217), cloned into the NcoI and EcoRI sites of pACT2 (Dr. Michelle van Niekerk, Department of Genetics, University of Pretoria)
pVA3	murine p53 gene	pVA3 is a positive control plasmid that encodes a fusion of the murine p53 protein (a.a. 72–390) and the GAL4 DNA-BD (a.a. 1–147).
pTD1	SV40 large T-antigen gene	pTD1 is a positive control plasmid that encodes a fusion of the SV40 large T-antigen (a.a. 86–708) and the GAL4 AD (a.a. 768–881).
pFastbac1	pFastbac-VP2	Nucleotides 1 – 3221 (ORF:13 - 3186) of AHSV2 L2 encoding VP2, cloned into the pFastbac plasmid via XmaI (Dr. C. Potgieter, Onderstepoort Veterinary Institute, Pretoria)
pET41c(+)	pETs2NS3 Nterm	Nucleotides 20 – 374 encoding amino acids 1 – 118 of AHSV2 NS3 cloned into the pET41c vector via BamHI and EcoRI (Tracy Meiring, Department of Genetics, University of Pretoria)
pET41c(+)	pETs2NS3 Cterm	Nucleotides 546 – 761 encoding amino acids 176 – 218 of AHSV2 NS3 cloned into the pET41c vector via BamHI and EcoRI (Tracy Meiring, Department of Genetics, University of Pretoria)
pET41c(+)	Native plasmid	
TOPO®	Native plasmid	Plasmid obtained with the TOPO® XL PCR cloning kit (Life Technologies)
pACT2	Activation domain	Plasmid obtained with the Matchmaker Gal4 two-hybrid

	plasmid	system that contains the activation domain (Clontech Laboratories, Inc)
pAS2-1	DNA-binding domain plasmid	Plasmid obtained with the Matchmaker Gal4 two-hybrid system that contains the DNA-binding domain vector (Clontech Laboratories, Inc)

2.2.2 Antisera

Following antisera were used:

Table 2.2: List of antisera used

Antisera	Specificity
α-β-gal-NS3 serotype 3	Polyclonal antibodies raised in rabbits against a β-galactosidase NS3 fusion protein expressed in *E. coli*. (Vida van Staden, Department of Genetics, University of Pretoria)
α-DNA-Binding domain	Antibodies specific to the full length yeast Gal4 protein (Calbiochem®)
α-Activation domain	Antibodies specific to the full length human Gal4 protein (Calbiochem®)

2.2.3 Primers

The following primers were used:

Table 2.3: List of primers used to prepare and sequence constructs

Primer	Sequence	Additional information
AHSV3.2NtermBamF	5' CGGGATCCCCATGGCTTC GGAATTCGGG '3	Primers were used to amplify the 5' region of the L2 gene (nucleotides 1 – 1605) that encodes for the N-terminal region of the AHSV3 VP2 protein (amino acids 1 – 535). Manufactured by Inqaba Biotechnical Industries, South Africa. Terminal sequences (underlined) of the primers added restriction enzyme sites to the ends of the PCR products to facilitate cloning.
AHSV3.2NtermXhoR	5' GCGCTCGAGTCTTCAC GAATAATTCATC '3	

AHSV3.2CtermBamF	5'CGGGATCCCGGTGTCAG GAATCAG '3	Primers were used to amplify the 3' region of the L2 gene (nucleotides 1575 – 3171) that encodes for the C-terminal region of the AHSV3 VP2 protein (amino acids 525 – 1057). Manufactured by Inqaba Biotechnical Industries, South Africa. Terminal sequences (underlined) of the primers added restriction enzyme sites to the ends of the PCR products to facilitate cloning.
AHSV3.2CtermXhoR	5' GCGCTCGAGTTC AGTTTTCGCAAGCAGC '3	
DNA-binding domain sequencing primer	5' AGTAGCCTTCTCTCATC '3	Specific to Gal4 DNA-binding domain in pAS2-1 plasmid (nucleotides 5895 – 5912)
Activation domain sequencing primer	5' TATGGTGATGTTACCTA '3	Specific to Gal4 Activation domain in pACT2 plasmid (nucleotides 5138 – 5154)

2.2.4 Viruses

Bac S2 NS3-GFP: Recombinant baculovirus expressing an AHSV2 NS3-eGFP fusion protein (Tracy Meiring, Dept. of Genetics, University of Pretoria)

Bac eGFP: Recombinant baculovirus expressing eGFP (Tracey-Leigh Hatherell, Dept. of Genetics, University of Pretoria)

2.2.5 Cells

Bacterial strains used were the *Escherichia coli* strain DH5α (obtained from Dr. M. Van Niekerk, University of Pretoria), BL21 (pET expression system - Novagen) or Top10 (TOPO® XL PCR Cloning Kit - Life technologies). The yeast strain used was AH109 grown on minimal SD medium according to standard protocols as provided by the manufacturer (Clontech Laboratories, Inc). Amino acid deficient medium lacking leucine, tryptophan, histidine or a combination of above mentioned amino acids were made according to standard protocols as given by Clontech Laboratories, Inc.

The GIBRO BRL BAC-to-BAC™ baculovirus expression system (Life Technologies) was used for expression of recombinant baculoviruses. All viral work was carried out in *Spodoptera frugiperda* (Sf9) insect cells maintained as suspension cultures in spinner flasks at 27℃ in TC-100 insect medium (Highveld biological (PTY) Ltd) containing 10% foetal calf serum, antibiotics (Penicillin – 100 U/ml, Streptomycin – 0.1 mg/ml and fungizone – 2.4 µg/ml) and 1% pluronic (Sigma). Cell culture techniques were essentially as described in the BAC-to-BAC™ baculovirus expression system (Life Technologies) manual.

2.2.6 Polymerase chain reaction

Briefly, 50 µl PCR reaction mixtures were set up using ± 100 ng template DNA, 100 pmol of each primer, 0.2 mM dNTPs, 1.5 mM $MgCl_2$, 1x Taq polymerase specific buffer and 1 U Taq polymerase. A hotstart was performed on all reactions where polymerase was added after the first denaturing step of cycle 1. The template was denatured at 94℃ for 1 minute, primers annealed at 55℃ for 5 minutes (first five cycles) / 58℃ for 30 seconds and elong ated at 72℃ for 1 minute for the rest of the 30 cycles. The Perkin-Elmer 9600 GeneAmp PCR system was used.

The PCR products were purified by using the High Pure PCR product purification kit (Roche diagnostics) for subsequent cloning or sequencing purposes.

2.2.7 Restriction enzyme digestion and dephosphorylation of DNA

All restriction enzyme reactions were carried out in the enzyme's recommended buffer, at its optimal pH and temperature. For the single digestions, 5 U of enzyme was made up in a reaction mixture of 10 µl containing 1 µl appropriate 10x buffer. Restriction enzyme reactions were briefly centrifuged and incubated for ± 2 hours at 37℃ depending on th e enzyme.

Vectors that were used for non-directional cloning purposes were dephosphorylated. After the vector was prepared by restriction digest the enzyme was heat inactivated at 65℃ for 15 minutes. 1 U shrimp alkaline phosphatase (Roche diagnostics) was used with the correct dephosphorylation buffer. The reaction was incubated for 10 minutes at 37℃.

2.2.8 Plasmid preparation from *E. coli* cells

Plasmid and bacmid DNA isolations were done according to the alkaline-lysis method as described in Sambrook & Russel (2001). Overnight bacterial cultures grown in the correct medium were collected and resuspended in lysis buffer. By adding the alkaline-SDS buffer, residual spheroplasts were lysed. The addition of sodium acetate precipitated the chromosomal DNA and proteins. For the isolation of

bacmid DNA, Potassium Acetate (pH 5.5) instead of Sodium acetate was used as indicated in the GIBRO BRL BAC-to-BAC™ baculovirus expression system (Life Technologies) manual. Plasmid DNA was precipitated by adding 96% ethanol. Bacmid DNA was precipitated by using iso-propanol as indicated in the GIBRO BRL BAC-to-BAC™ baculovirus expression system (Life Technologies) manual. Plasmid DNA was purified by using the Roche High Pure purification kit (Roche diagnostics) for use in subsequent procedures.

2.2.9 Recovery of DNA fragments from agarose gel

The geneclean® kit III (Q-biogene) was used for subsequent purification of DNA from agarose gels. The glassmilk or silica powder method was used. The DNA band that needed to be recovered was excised from the agarose gel, weighed and transferred to an eppendorf tube. Three volumes of NaI (volume not more than 4 molar) was added and mixed to dissolve the agarose. The insoluble silica matrix stock (glassmilk) was vortexed and 5 µl of the glassmilk suspension was added to the DNA (5 µl or less per 5 µg DNA). Glassmilk and DNA were allowed to bind, after which the glassmilk containing bound DNA was washed with the NEW wash solution. The pure DNA was eluted twice with 7 µl ultra high quality water.

2.2.10 Agarose gel electrophoresis

For general purposes 1% agarose gels were used. A solution of molten agarose was prepared by adding 40 ml 1x TAE buffer (40 mM Tris-acetate, 1 mM EDTA) to the appropriate amount of agarose powder (0.40 g). The solution was boiled and ultra high quality water was added to compensate for any evaporation. After that, 2.5 µl Ethidium Bromide/40 ml was added to the gel just before casting. The gel was cast after agarose had cooled down to about 60℃. After the gel had set, it was placed in the electrophoresis tank with enough 1x TAE buffer to cover the gel properly. The gel was run at ± 95 V until the bromophenol blue marker reached to about two thirds from the top. All gels were visualized on a UV transilluminator.

2.2.11 Ligation of insert and vector

Purified restriction fragments were ligated to the linearised vector at a 3:1 ratio using 10x ligase buffer (66 mM Tris-HCL, pH 7.5, 5 mM $MgCl_2$, 1 mM ATP) and 1 U of T4 DNA ligase (Roche diagnostics) in a reaction volume of 20 µl. The reaction was incubated for 16 - 18 hours at 16℃ (sticky-end ligation).

2.2.12 Preparation of *E. coli* competent cells

Competent cells were prepared by the standard $CaCl_2$ method as given in Sambrook & Russel (2001). An overnight culture (1 ml) was used to inoculate 100 ml LB-broth, and the cells were allowed to grow

to log phase ($O.D._{600}$ of 0.5) by shaking at 37℃. Cells were then harve sted by centrifugation at 5000 rpm for 5 minutes at 4℃. Cells were then resuspen ded in half the original volume of ice-cold 50mM $CaCl_2$. After centrifuging for 5 minutes at 5000 rpm at 4°C, supernatant was discarded and cells again were resuspended in 1/20 of the original volume in $CaCl_2$. Cells were left overnight at 4℃ and stored at -70℃ in 15% glycerol.

2.2.13 Preparation of DH10 bac competent cells for baculovirus expression system

The DMSO method was used according to Chung and Miller (1988). An overnight incubated inoculum of 5 ml was prepared with DH10Bac™ cells. This was added to a 100 ml volume of appropriate medium and grown to early log phase (O.D. ≈ 0.6). Cells were collected via centrifugation at 5000 rpm for 5 minutes at 4℃. Cells were then resuspen ded in 1/10 of the culture volume in ice-cold TSB and incubated for 20 minutes on ice. TSB (100 ml) consists out of 1.6 g Peptone (w/v), 1.0 g Yeast extract (w/v), 0.5 g NaCl (w/v), 10% PEG (MW 3350) (w/v), 5% DMSO (v/v), 10 mM $MgCl_2$ and 10 mM $MgSO_4$. The reagents were made up to 100 ml with ultra high quality water. Competent cells were stored in 15% glycerol at -70℃.

2.2.14 Transformation

The PCR products were cloned into the TOPO® vector and transformed into Top10 cells by using manufacturer instructions as given in the TOPO® XL PCR Cloning Kit manual (Life technologies). The TOPO® cloning kit was used as it incorporates PCR products without any restriction and ligation reactions as required with normal cloning procedures. This enables efficient PCR product cloning. Transformed Top10 cells were selected by antibiotic resistance and the TOPO® vector isolated as by use of the alkaline-lysis method as indicated in 2.2.8.

Subsequent subclonings of PCR products or cloning of prepared DNA fragments were done by using the cloning procedure as given by Sambrook and Russel (2001). Ligation mixtures were transformed via the heat-shock method (42℃ for 90 seconds) as described by Sambrook and Russel (2001). The ligation mixtures were transformed into $CaCl_2$ competent cells (2.2.12). Recombinants were selected based on plasmids providing antibiotic resistance as needed. TOPO® clones were plated out on Luria Broth-agar containing kanamycin, yeast plasmid clones were selected for on LB-agar containing ampicillin.

Recombinant baculoviruses were prepared according to the GIBRO BRL BAC-to-BAC™ baculovirus expression system (Life Technologies) manual. The pFastbac plasmid containing the correct insert was mixed with 100 µl DH10Bac™ competent cells that were prepared as described in 2.2.13.

Transformation mixture was incubated on ice for 30 minutes and a heat shock of 45 seconds at 42℃ allowed for the transformation of the DNA into the cells. After this, 900 µl TSB + 20 mM Glucose was added and the mixture was incubated for 4 hours at 37℃. A dilution series was carried out and dilutions were plated out on agar plates containing 50 µg/ml kanamycin, 7 µg/ml gentamycin, 10 µg/ml tetracycline, 100 µg/ml X-gal and 40 µg/ml IPTG and incubated at 37℃ until colonies appeared. Recombinant colonies where white and untransformed colonies where blue. White colonies were re-plated on the same medium to ensure that they were recombinant composite bacmid containing cells. These cells were grown for 2 days in Luria-Bertani (LB) broth containing above mentioned antibiotics and the recombinant bacmid DNA was isolated as in 2.2.8.

2.2.15 DNA Sequencing

All plasmid constructs were sequenced by using primers provided with the TOPO® XL PCR product cloning kit (Life Technologies) and Matchmaker Gal4 two-hybrid system (Clontech Laboratory, Inc). Internal primers for AHSV-3 L2 segment encoding VP2 were kindly provided by Daria Rutkouska (University of Pretoria). Primers specific to the Gal4-activation domain in the pACT2 plasmid and Gal4-DNA binding domain in the pAS2-1 were used to sequence the AHSV-2 fragment that encodes VP2. The ABI Prism Big Dye Terminator Cycle Sequencing Ready Reaction Kit, version 3.0 (Perkin Elmer, Applied Bioscience) was used as indicated by manufacturers instructions to carry out the sequencing reactions on the 3100 Applied Biosystems Genetic Analyzer. Sequences were analyzed by use of computer software including DNAssist, Chromas and VectorNTI.

2.2.16 Protein extraction from yeast cells

Two different methods were used to isolate protein from the yeast cells. In contrast to the second method, the first method does not use yeast cells that have grown to mid-log phase, therefore the experimental procedure is shortened drastically.

Method 1:

Yeast cells containing recombinant pACT2 or pAS2-1 plasmids were grown overnight in appropriate medium from where the cells were harvested by centrifugation at 2000 rpm for 5 minutes at 4℃. Proteins were isolated by using 200 µl Complete Cracking buffer. This was prepared by mixing 1000 µl cracking buffer (8 M Urea, 5% SDS w/v, 40 mM Tris-HCl pH 6.8, 0.1 mM EDTA and 0.4 ng ml^{-1} Bromophenol blue) with 10 µl β-mercapto ethanol and 100 µl protease inhibitor (1 ng ml^{-1} Pepstatin and 20 ng $µl^{-1}$ Pefabloc). Glass beads (80 µl) were added, the cocktail was heated for 10 minutes at --70℃ after which the samples were mixed by vortexi ng for 1 minute. Samples was centrifuged (14 000 rpm for 5 minutes). The supernatant was harvested and the remaining pellet was boiled for 3 – 5 minutes with the addition of ≈ 25 µl Complete Cracking Buffer to ensure optimal protein extraction.

Method 2:

Protocol as given in the Yeast Protocols Handbook (Clontech Laboratories, Inc) was used. Briefly, yeast cells that contained recombinant pACT2 or pAS2-1 plasmids were grown to mid-log phase ($O.D_{600}$= 0.4 – 0.6) at 30℃ in the correct SD medium. Cells were washed with ultra high quality water and were collected at 1000 rpm for 5 minutes at 5℃. Cells were immediately frozen by placing the tube in liquid nitrogen and the cells were stored at -70℃. Subsequently, protein was extracted by adding ≈ 300 µl pre-warmed Complete Cracking Buffer (same as for method 1, except for protease inhibitors – Pepstatin (0.7 µg ml^{-1}) and Pefabloc (10 mg ml^{-1}). Because Pefabloc was used, 100X PMSF was not used in subsequent reactions as recommended in the protocol.

2.2.17 Protein gel electrophoresis

Protein samples were separated by SDS-PAGE using a 10% or 12% polyacrylamide gel as indicated by Sambrook and Russel (2001). The separating (10% or 12% polyacrylamide, 0.375M Tris-HCl, pH 8.8, 0.1% SDS, 0.008% TEMED and 0.08% Ammonium persulphate) and 5% stacking (5% polyacrylamide, 0.125 M Tris-HCl, pH 6.8, 0.1% SDS, 0.008% TEMED and 0.08% ammonium persulphate) polyacrylamide gels were used and cast between 7 x 10 cm glass plates.

For loading the samples on the gel, 10 µl of the sample was added to an equal volume of 2x Protein Solvent Buffer (0.125 M Tris, pH 8; 4% SDS; 20% glycerol; 10% mercaptoethanol) and boiled at 96℃ for 5 minutes to denature the protein. For samples obtained from the membrane floatation gradient, 3x Protein Solvent Buffer (0.1875 M Tris, pH 8; 6% SDS and 15% mercaptoethanol) was added without any glycerol as the samples contained sucrose. For the protein extracted from the yeast cells, the protein obtained was loaded directly without adding 2x Protein Solvent Buffer. The denatured samples were then electrophoresed at 120 V in 1x TGS (0.3% Tris; 1.44% Glycine; 0.1% SDS) until the bromophenol blue marker reached the bottom of the separating gel.

The SDS-PAGE gels were stained by totally immersing the gel with gentle agitation in 0.125% Coomassie Blue, 50% methanol, and 10% acetic acid for 20 minutes. The gel was destained in 5% acetic acid and 5% methanol with gentle agitation.

2.2.18 Western blot

A Western blot was performed when the separated proteins on the acrylamide gel were transferred to Hybond-C+ membranes (Life Technologies) for about 2 hours. The Hybond-C+ membrane was washed in 1x PBS for 5 minutes and non-specific binding sites were blocked by washing the membrane with 1% blocking solution (1% milk powder in 1x PBS) for 30 minutes. The membrane was

incubated overnight in the correct primary antibodies depending on the protein to be detected. The antiserum or primary antibodies were removed and the membrane was washed three times in wash buffer (0.05% Tween in 1x PBS) for 5 minutes each. A secondary antibody solution (1:250 dilution of protein A conjugated to horseradish peroxidase in 1% blocking solution) was then incubated with the membrane for 1 hour. Unbound antibody was washed off by doing three washing steps in wash buffer and lastly in 1x PBS for 5 minutes each. Antibody binding was visualized by the addition of an enzyme substrate (60 mg 4-chloro-1-naphtol in 20 ml methanol and 60 µl hydrogen peroxide in 100 ml 1x PBS). The reaction was allowed to proceed until bands became visible.

2.2.19 Chemiluminescence

Chemiluminescence, a more sensitive protein expression detection assay, was also used. The Supersignal® West Pico Chemiluminescent Substrate for Western Blotting (Pierce) was used. Briefly the working solution as indicated by the manufacturer was prepared and membrane was sufficiently wetted with the solution containing the substrate for 5 minutes. Working solution was removed and membrane was placed in a plastic bag and sealed after air bubbles were removed. Membrane blot was placed against the film and exposed for 5 minutes.

2.2.20 Transformation of yeast plasmids encoding fusion proteins into AH109 yeast cells

The yeast two-hybrid system contains two vectors; the DNA-binding domain (DNA-BD) vector pAS2-1 that enables the AH109 yeast stain to grow on tryptophan deficient medium and the activation domain (AD) vector pACT2 that enables the AH109 yeast strain to grow on leucine deficient medium. Two domains, expressed from these vectors need to interact to produce a functional transcription factor that can activate the reporter gene which enables the AH109 yeast strain to grow on histidine deficient medium. The strength of the interaction can be assayed by the expression of the β-galactosidase gene that makes yeast colonies turn blue in the presence of Lac Z enriched medium. DNA fragments encoding potential interacting proteins (bait and prey) are cloned and expressed as DNA-binding domain or activation domain fusion proteins. When the bait and prey proteins interact, it brings the DNA-binding domain and activation domain into close proximity, forming an activated functional transcriptional factor. This transcription factor binds to the upstream activation site (UAS) element in the promoter region and this activates the expression of the reporter genes (histidine or β-galactosidase) (Notes taken from CLONTECH Matchmaker user manual).

The yeast vectors containing genes of interest were co-transformed into competent AH109 yeast cells by use of the PEG transformation method (personal communication, Dr Christine Maritz-Olivier, Department of Biochemistry, University of Pretoria). This quick mini-scale yeast transformation

entailed the resuspension of 1-2 day old AH109 yeast colonies in 1 ml of ultra high quality water. The cells were washed in ultra high quality water and collected at 3000 rpm for 3 minutes. Pelleted cells were resuspended in 1 ml of 100 mM Lithium acetate (LiAc) and incubated at 30℃ for 5 minutes without any shaking. Cells were collected and the following reagents added to the yeast cell pellet in the specified order: 240 µl 50% PEG (MW 3350), 36 µl 1M LiAc, 25 µl 2 $mg.ml^{-1}$ sperm DNA (Deoxyribonucleic acid sodium salt type III from salmon testes, Sigma D1626) (boiled for 2 minutes and kept on ice for another 2 minutes before use) and the plasmid DNA to be transformed made up to 50 µl with UHQ. The transformation mix was mixed by vortexing for at least 1 minute and incubated at 42℃ for 25 minutes (30 minutes should not be excee ded). Transformed cells were collected at 3000 rpm for 3 minutes and resuspended in 200 µl of UHQ and plated out on one correct amino acid medium-deficient agar plate. The double transformation mixtures were plated out on SD/-Leu/-Trp and replica plated on SD/-Leu-Trp/-His. Plates were typically incubated for 2-5 days at 30℃.

All SD/-Leu/-Trp/-His plates contained 10 mM 3-amino-1,2,4-triazol (3-AT) that acted as a competitive His3 inhibitor that eliminated the formation of background colonies as a result of Histidine production by the host yeast cells.

2.2.21 β-galactosidase assay

A colony-lift filter assay was done as indicated in the Yeast Protocols Handbook (Clontech). Briefly, a Whatman filter was placed over 2-4 day old yeast colonies to be assayed. The colonies that stuck to the filter were lysed by frosting cycles in liquid nitrogen. Colonies were frozen for 10 seconds in liquid nitrogen and defrosted 3 times. Another filter was pre-soaked in a Z-buffer (16.1 g/l $Na_2HPO_4.7H_20$, 5.50 g/l $NaH_2PO_4.H_20$, 0.75 g/l KCl and 0.246 g/l $MgSO_4.7H_20$, pH 7 and autoclaved) containing 1.67 ml X-gal (20 mg/ml) and 0.27 ml β-mercaptoethanol. The Whatman filter paper containing the lysed colonies was placed colony side up on the Z-buffer pre-soaked Whatman filter and allowed to incubate at 30℃ until blue colour was detected. The assay was terminated after 3 hours until negative control started to turn blue as any further colour development happened due to background.

2.2.21 Transfection of Sf9 cells with recombinant bacmid DNA

Six well (35 mm) tissue culture plates were seeded at 1 x 10^6 cells/well in 2 ml TC-100 insect medium with 10% foetal calf serum and antibiotics and allowed to attach for 1 hour. Fresh isolated recombinant Bacmid DNA was transfected into insect cells by lipofection. Six µl of the Bacmid DNA was diluted in 100 µl insect medium without antibiotics. Six µl CELLFECTIN™ (BRL) reagent was mixed with 100 µl insect medium without antibiotics in a separate centrifuge tube. The solution containing diluted Bacmid DNA and CELLFECTIN™ was then mixed and incubated at room

temperature for 30 minutes. A volume of 0.8 ml insect medium without antibiotics or serum was then added to the lipid DNA complexes and the total sample was added to the insect cells. The cells and DNA were incubated together at 27℃ for 5 hours aft er which the DNA was removed and replaced with 2 ml insect medium containing antibiotics and serum. The transfected cells were incubated for a further 96 hours at 27℃. Recombinant viruses harv ested in the supernatant were stored at 4℃ for later use.

Two rounds of amplification were done to make sufficient virus stocks. Insect cell monolayer in 25 cm^3 flasks were infected with 300 µl of recombinant virus obtained from the transfection. A further round of amplification included insect cell monolayer in 75 cm^3 flasks infected again with 300 µl virus from the first amplification round. Both rounds of amplification were carried out for 72 hours at 27℃ after w hich the medium containing the virus was clarified by centrifugation at 2000 rpm for 5 minutes and filter sterilization. Virus stocks were stored at 4℃.

2.2.22 Infection of insect cells with recombinant baculoviruses and harvesting of protein

Sf9 cell monolayers were seeded at 1 x 10^7 cells in 75 cm^3 flasks or 3 x 10^6 cells in 25 cm^3 flasks or 1 x 10^6 cells per well (6-well plate) and incubated at 27°C to allow the cells to attach for 1 hour. After the incubation, cells were washed with TC-100 insect medium without foetal calf serum but containing antibiotics (Penicillin – 100 U/ml, Streptomycin – 0.1 mg/ml and fungizone – 2.4 µg/ml) and infected with wild type baculovirus or with the recombinant baculovirus at a multiplicity of infection (MOI) of ± 2 or 5 plaque forming units (pfu)/cell. Infections were done in just enough medium to cover the cells and left for 2-3 hours at 27℃ before adding TC-100 ins ect medium containing 10% foetal calf serum and antibiotics to provide sufficient nutrients for the cells. The cells were harvested between 42 - 45 hours post infection (h.p.i.), collected by centrifugation at 3000 rpm for 3 minutes and resuspended in one of three alternative buffers. Lysis buffer 1: 0.15 M STE containing 1mg/ml Pefabloc and 0.7 µg/ml Pepstatin), Lysis buffer 2: 0.02 M Tris pH8, 0.001 M EDTA pH 8, 0.2 M NaCl, 0.5% Nonidet-P40, 1 mg/ml Pefabloc and 0.7µg/ml Pepstatin (Sambrook and Russel, 2001). Hypotonic buffer 3 (pH 7.4): 10 mM Tris and 0.2 mM $MgCl_2$. Lysis buffer 2 was used for the GST pull-down assay and the hypotonic buffer was used for the membrane flotation assay. Cells were mechanically lysed with a dounce for 20 times or passed through a 15G needle and 1 ml syringe 5 times.

Cell lysates prepared for the GST pull-down assay were centrifuged for 5 minutes at 2000 rpm to separate the nuclei from other cellular components. The post-nuclear supernatant was again centrifuged at 10 000 rpm for 1 hour to obtain all soluble protein in the supernatant fraction and collect the insoluble or particulate fraction in the pellet. The pellets were resuspended in 1x PBS or in Lysis buffer 2 depending on the application.

Cell lysates prepared for the membrane flotation assay were resuspended in 135 µl hypotonic buffer and incubated on ice for 30 minutes after which the cells where mechanically broken by resuspension with a needle as stated above.

2.2.23 Labelling with [S^{35}]-methionine

After baculovirus infected Sf9 cells were incubated for 39 - 42 h.p.i. at 27℃, cells were washed and starved for 30 minutes in minimal essential medium lacking methionine. A total of 7 µl NEG 709A EASYTAG™ Methionine L-[S^{35}] (Perkin Elmer, Life Sciences) was added per 75 cm^3 flask, 4 µl was added per 25 cm^3 flask and 2 µl was added per well (6-well plate) and left for 3 hours at 27℃ before harvesting the cells.

2.2.24 Preparation of *E. coli* cell lysates containing NS3

This optimized protocol for obtaining GST fusion proteins was obtained from Tracy Meiring (Department of Genetics, University of Pretoria) as modified from Sambrook & Russel (2001). BL21 cells (pET expression system – Novagen) containing the pET41c (+) vector were incubated overnight at 37℃ in Luria bertani (LB) broth. Overnight cultures were diluted 1:100 and grown to an O.D. reading of ± 0.8. Fresh IPTG was added to a concentration of 1 mM and incubation continued overnight on a benchtop shaker at 18 – 20℃ to induce expression of GST or GST-fusion proteins. Cells were collected at 4000 rpm for 15 minutes and frozen at –20℃ (cells to be used the next day) or flash frozen in liquid nitrogen and defrosted (cells to be used the same day). The cell pellets were resuspended in lysis buffer (0.05% Tween 20, 50 mM EDTA, 1 mg/ml Lysozyme, 0.7 µg/ml Pepstatin and 1mg/ml Pefabloc in 1x PBS) and kept on ice for 3 – 4 hours. The lysate was sonicated 5 times with a 50% 3 output for 10 seconds and left on ice for 10 sec between cycles. Lysate was centrifuged at 4000 rpm for 20 minutes and the supernatant was added to 50% glutathione-agarose slurry (2 ml for each 100 ml original culture) together with dithiothreitol (DTT) at a final concentration of 1 mM.

The 50% glutathione-agarose slurry (Sigma Aldrich) was prepared by adding 140 mg glutathione-agarose to 30 ml ultra high quality water and left to swell overnight at 4℃. Glutathione-agarose beads were collected at 1000 rpm at 4℃ for 5 minutes and stored in 1M NaCl at 4℃ (beads to be used the next day) or washed in 10 volumes of 1x PBS (beads to be used the same day). The glutathione-agarose beads were again pelleted and resuspended in an equal volume of 1x PBS immediately prior to use.

The GST or GST fusion proteins were allowed to bind to the glutathione-agarose beads by shaking the slurry at room temperature for ± 1 hour. The glutathione-agarose beads were collected at 1000

rpm for 5 minutes and washed two times with 1x PBS and 1% Triton-X and one time with 1x PBS. Glutathione-agarose beads were stored at 4℃ in 1x PBS and 0.05% sodium azide for not longer than 2 weeks.

2.2.25 GST-pulldown assay

The GST-pulldown assay was done according to Sambrook & Russel (2001) with a few modifications. The cell lysate containing the baculovirus expressed proteins obtained from the Sf9 cells was pre-cleared by incubation with the glutathione-agarose beads slurry that only contained the GST protein for 1 hour at 4℃ on a benchtop shaker. The mixture was centrifuged at maximum speed for 2 minutes at room temperature in a microcentrifuge. The supernatant was divided equally depending on the number of binding assays done into fresh eppendorf tubes. The cleared supernatant was probed by adding separately the glutathione-agarose beads slurry that either contained the GST fusion protein or the GST protein. The tubes were incubated for up to 18 hours at 4℃ on a benchtop shaker. The samples were centrifuged at maximum speed for 2 minutes at room temperature. The supernatants were kept at 4℃ to be analyzed the same day or kept at - 20℃ for later use. The beads were washed 3 times with 1 ml ice-cold lysis buffer 2 (0.02 M Tris pH 8, 0.001 M EDTA pH 8, 0.2 M NaCl, 0.5% Nonidet-P40, 1 mg/ml Pefabloc and 0.7 µg/ml Pepstatin). Beads were mixed with an equal volume of 2x SDS-PAGE gel-loading buffer (0.125 M Tris pH 8, 4% SDS, 20% glycerol and 10% 2-mercaptoethanol) or stored in 1x PBS at –20℃ for later use.

2.2.26 Membrane flotation assay

Flotation assays were done as described by Briggs *et al.* (2003) and Brignati *et al.* (2003). After the cell lysate prepared in 2.2.23 was incubated on ice for 30 minutes and the cells mechanically broken, 125 µl of the prepared cell lysate was resuspended in 670 µl 85% sucrose. The sucrose was dissolved in a gradient buffer (100 mM NaCl, 10 mM Tris and 1 mM EDTA at a pH of 7.4). Two other fractions were prepared as follow: 2920 µl 65% sucrose and 1290 µl 10% sucrose. The 5 ml centrifuge tube was loaded from the lowest to the highest density sucrose i.e. 10% was loaded first, 65% was loaded beneath it and finally the 85% sucrose containing the cell lysate was loaded last. This was done by using a 5 ml syringe with a needle and injecting the higher density sucrose underneath the lower density sucrose thereby pushing the lower density fraction to the top of the centrifuge tube. The Beckman ultra centrifuge SW55Ti rotor was pre-chilled to 4℃. Gradients were centrifuged overnight at 38 000 rpm for 18 hours at 4℃. Fractions were tapped by pushing a needle through the bottom of the centrifuge tube and collecting 11 drops of sucrose per tube resulting in a total of ± 20 fractions containing ± 200 µl per fraction. Levels of fluorescence in each fraction were

quantified by taking fluorescence readings at an excitation of 485 and emission of 538 nm and analyzed on 10% SDS-PAGE gels as described in 2.2.17.

2.3 RESULTS

Three different approaches were used to investigate protein-protein interaction between AHSV NS3 and VP2, namely the yeast two-hybrid system, a GST-pulldown assay and a density gradient assay.

2.3.1 Yeast two-hybrid assay

To do the yeast two-hybrid screen, a total of 12 constructs containing full-length or truncated VP2 or NS3 genes of AHSV2 or AHSV3 were required. These would enable us to assay VP2 – NS3 interactions between proteins of the same viral serotype, between VP2 and NS3 of different serotypes, as well as homo-dimerization of VP2 and NS3 respectively. Some of these constructs had been prepared previously (Table 2.1), however six constructs still had to be made that were not already available in our library. This included the AHSV3 VP2 N- and C-terminal domains in both the pAS2-1 and pACT2 vector and AHSV2 full length VP2 in both the pAS2-1 and pACT2 vectors. The VP2 N- and C-terminal constructs were made to determine which domain of VP2 possibly binds to NS3. The AHSV2 full length VP2 constructs were made to investigate the possible serotype dependent or independent binding between AHSV2 VP2 and AHSV3 NS3.

2.3.1.1 Cloning of AHSV3 VP2 N- and C-terminal domains into the TOPO vector

The sequences encoding the N-terminal and C-terminal AHSV3 VP2 domains were prepared as PCR products. The PCR products were generated from the full length AHSV3 VP2 template by amplification with the correct primers to gain constructs ready for cloning into the TOPO® plasmid vector. The TOPO® cloning kit was used as it incorporates PCR products without any restriction and ligation reactions as with normal cloning procedures, which enables efficient PCR product cloning. As indicated in 2.2.3, primers AHSV3.2NtermBamF and AHSV3.2NtermXhoR were used to amplify nucleotides 11 – 1678 of L2 that encode the N-terminal domain (amino acids 1-535) of VP2, and primers AHSV3.2CtermBamF and AHSV3.2CtermXhoR were used to amplify nucleotides 1583 – 3186 of L2 that encode the C-terminal domain (amino acids 525-1057) of VP2. The two PCR products were purified and ligated to the TOPO® vector and transformed into the TOP10 competent cells obtained from the TOPO® PCR kit. Twenty putative recombinants were selected. Plasmid DNA was isolated from the putative recombinants and the plasmid DNA was screened for the insert by EcoRI digestions, as the TOPO® vector has EcoRI sites flanking the cloning site. In Figure 2.2 a 1% agarose gel can be seen that shows EcoRI digests done on putative recombinants. In lane 1 the linearised TOPO® vector is seen as a size standard. In lane 4 and 5, two N-terminal recombinants (N2 and N6)

are seen that show the expected band if compared to lane 2 that contains the N-terminal PCR product. In lane 8, a C-terminal recombinant (C19) is seen that shows the expected band if compared to lane 6 that contains the C-terminal PCR product. Lanes 3 and 7 show non-recombinant vector plasmids (N1 and C11) that linearised without excising an EcoRI fragment. Therefore the PCR products representing the N-terminal and C-terminal domains of VP2 of AHSV-3 were successfully cloned into the TOPO® vector.

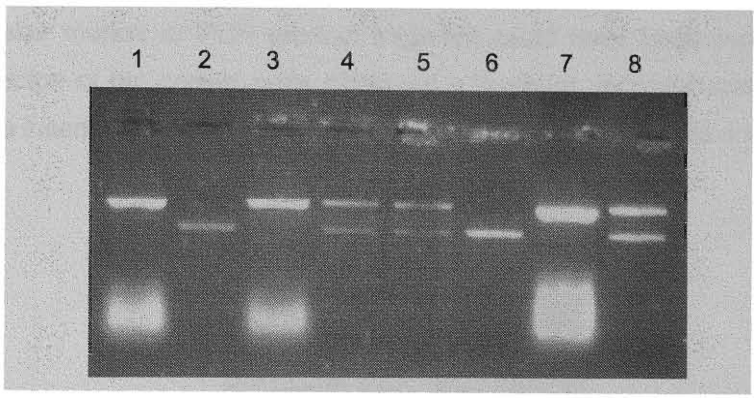

Figure 2.2: A 1 % agarose gel to identify recombinant TOPO® plasmids. Controls are linearised TOPO® vector (lane 1), and PCR amplification products of VP2 N-terminal (lane 2) and VP2 C-terminal (lane 6). Putative N-terminal recombinants TOPO® N1 (lane 3), N2 (lane 4) and N6 (lane 5) and the C-terminal recombinants C11 (lane 7) and C19 (lane 8) were digested by EcoRI prior to electrophoresis.

2.3.1.2 Cloning of AHSV3 VP2 N- and C-terminal domains from the TOPO® vector into the yeast vectors

The N-terminal and C-terminal domains of VP2 present in the TOPO® vector were subsequently cloned into the yeast vectors, pACT2 and pAS2-1. The PCR primers used in 2.3.1.1 were designed to incorporate BamHI and XhoI sites at the 5' and 3' ends of the amplified fragments respectively, to facilitate directional cloning into the correct reading frame of the yeast activation domain vector pACT2. Cloning of the PCR products from the TOPO® clones into the yeast DNA-binding domain vector, pAS2-1 would be done non-directionally using the BamHI site present in the multiple cloning site in the pAS2-1 vector. The multiple cloning site of the TOPO® vector also contains a BamHI site adjacent to the EcoRI site in to which the PCR products were cloned. Therefore, the N- and C-terminal fragments could be excised from the TOPO® vector by using the BamHI site at the 5' end of the fragment (incorporated via PCR primer) and the BamHI site present in the vector and cloned into the BamHI site of the pAS2-1 vector. This could be done providing that the fragments in the TOPO® vector were present in such a way that the 3' end of the fragment was closest to the TOPO® BamHI site. Therefore the orientations of the inserts in the recombinant TOPO® plasmid vectors (N2, N6 and C19) were determined by doing a BamHI digest. A linearised recombinant TOPO® plasmid vector

containing the insert was expected for an insert that was in the incorrect orientation. Two bands, one representing the TOPO® plasmid vector and the other representing the insert were expected if the insert was in the desired orientation.

In Figure 2.3, lane 1 is a TOPO® N-terminal recombinant (N2) that carries its insert in the desired orientation. Lane 2 shows a TOPO® N-terminal recombinant that carries its insert in the incorrect orientation (N6). The TOPO® C-terminal recombinant (C19) also carries its insert also in the desired orientation. A size marker or PCR product fragment could have been included, that would have enabled confirmation of the correct sizes observed. Therefore recombinants N2 and C19 could be used to clone the inserts non-directionally via a BamHI digest into the pAS2-1 vector.

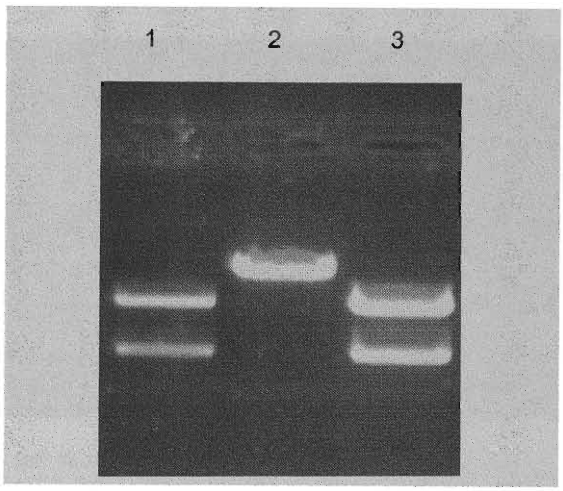

Figure 2.3: A 1 % agarose gel indicating restriction digests done with BamHI to determine the orientation of the N-terminal and C-terminal AHSV-3 VP2 insert in the recombinant TOPO® clones. N2 (lane 1), N6 (lane 2) and C19 (lane 3)

The pACT2 and pAS2-1 vectors were prepared for cloning by digesting the pACT2 vector with BamHI and XhoI and the pAS2-1 vector with only BamHI. The pAS2-1 vector was also dephosphorylated to ensure that ends could not re-anneal. The digested vectors were purified from agarose gels and the PCR products were excised from the TOPO® vector via BamHI/XhoI or BamHI. These fragments were then ligated to the pACT2 and pAS2-1 vectors and transformed into DH5α cells.

The pACT2 recombinants could only be in the correct orientation due to the directional BamHI/XhoI cloning. In Figure 2.4 a 1% agarose gel can be seen that shows the success of the subcloning of the N- and C-terminal fragments into the pACT2 yeast plasmid. In lanes 8 and 9, the N-terminal and C-terminal PCR products are seen as controls for the size insert expected. In lane 1 linearised pACT-2 plasmid vector can be seen as another control. Undigested N-terminal and C-terminal recombinants are seen in lanes 2 and 5 respectfully. Putative pACT2 recombinants were digested with BamHI and

XhoI, in lane 3 and 4, two N-terminal recombinants can be seen as the correct size fragments are seen if compared to the controls. The same is true for the two C-terminal recombinants shown in lane 6 and 7. The slight size difference seen between the smaller fragments in lanes 3, 4, 6, 7 when compared to the PCR products seen in lanes 8 and 9 can be explained by the difference in DNA concentration and presence of RNA in the sample.

For the pAS2-1 cloning, C- and N-terminal recombinants were identified by a BamHI digest. For all the recombinants, BamHI excised a band the size of the C-terminal and N-terminal insert respectively (results are not shown).

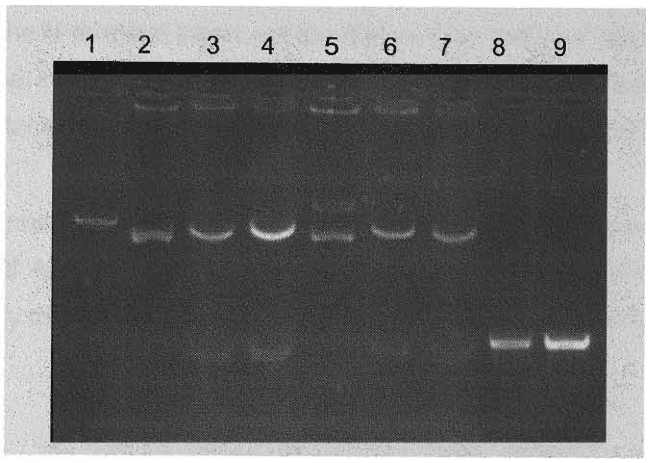

Figure 2.4: A 1 % agarose gel to determine the presence of the inserts in the pACT2 activation domain yeast vector. Linearised pACT2 plasmid vector (lane 1), undigested pACT2 + N-terminal VP2 (lane 2), undigested pACT2 + C-terminal VP2 (lane 5), N-terminal PCR product (lane 8) and C-terminal PCR product (lane 9) served as controls. pACT2 recombinants N4 (lane3), N10 (lane 4), C6 (lane 6) and C9 (lane 7) were digested with BamHI and XhoI.

2.3.1.3 Determining the orientation of the N- and C-terminal VP2 domains in the pAS2-1 vector

It was necessary to screen the pAS2-1 recombinants for orientation due to the non-directional BamHI cloning. The orientation of the insert in the C-terminal recombinants that were cloned into pAS2-1 was determined by an EcoRI digest. The C-terminal insert contains an EcoRI site incorporated at its 3' end that originated from the TOPO vector. The pAS2-1 vector contains an EcoRI site upstream from the BamHI site in which the insert was cloned (see Appendix with plasmid maps). Recombinants with the insert in the correct orientation would have the 5' end of the insert closest to the EcoRI site situated in the pAS2-1 vector. An EcoRI digest done on recombinants with the insert in the correct orientation would result in two bands: one representing the insert and the other the linearised pAS2-1 vector. Following this approach, seven C-terminal pAS2-1 recombinants were identified with the insert in the correct orientation (results not shown).

Orientation for the N-terminal recombinants was determined by a NcoI digest. The part of the VP2 gene encoding the N-terminal domain contains a NcoI restriction site at nucleotide position 11. The pAS2-1 vector contains a NcoI restriction site upstream from the BamHI cloning site (see Appendix). Recombinants with the insert in the correct orientation would have their NcoI site closest to the pAS2-1 NcoI restriction site, resulting in a linear fragment of ± 9992 nucleotides (8400 bp plasmid + 1592 insert) after digestion with NcoI. In Figure 2.5 a 1% agarose gel show that clones pAS2-1-N10 (lane 5), pAS2-1-N14 (lane 6) and pAS2-1-N19 (lane 7) contains inserts in the correct orientation as the recombinants linearised on digestion with NcoI yielding a band of the expected size of ± 9992 bp. The linearised recombinant bands are larger than the linearised pAS2-1 (8400 bp) band that is present in lane 1 as a control. Clones pAS2-1-N2 and pAS2-1-N5 have inserts in the wrong orientation, as the NcoI restriction site in the N-terminal insert are the distant from the NcoI site in the vector – therefore a NcoI digest excises the insert as seen in lanes 3 and 4. The linearised pAS2-1 (lane 1) and N-terminal PCR product (lane 2) serve as confirmation for the bands shown in lanes 3 and 4.

In summary, four recombinant yeast vectors were successfully constructed. Both the N-terminal and C-terminal fragments of AHSV-3 VP2 were cloned into pACT2 and pAS2-1. All recombinants were also sequenced to verify the presence of a correct reading frame and absence of mutations.

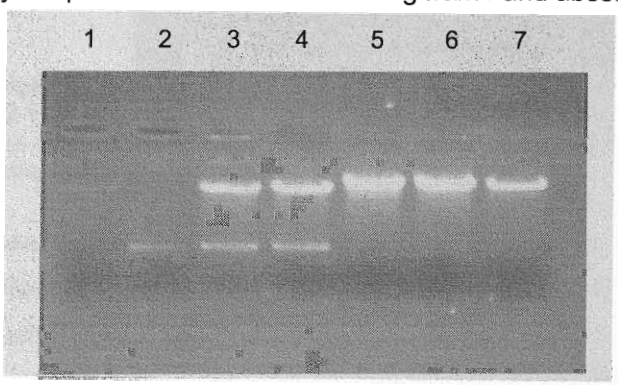

Figure 2.5: A 1% agarose gel used to determine the orientation of the insert in five pAS2-1 N-terminal recombinants. Linearised pAS2-1 vector (lane 1) and N-terminal PCR product (lane 2) as controls. Recombinants with insert in the wrong orientation in lane 3 (pAS2-1-N2) and 4 (pAS2-1-N5). Recombinants with the insert in the desired orientation in lane 5 (pAS2-1-N10), lane 6 (pAS2-1-N14) and lane 7 (pAS2-1-N16).

2.3.1.4 Cloning of AHSV2 VP2 into both the pAS2-1 and pACT2 vectors

Another two constructs were needed to complete all the constructs needed for the yeast two-hybrid study. We wanted to investigate protein-protein interaction between NS3 and VP2 of different AHSV serotypes. We therefore still needed the VP2 gene of AHSV serotype 2 to be cloned into the yeast vectors. The VP2 gene of AHSV serotype 3 was already available in both yeast vectors. To obtain the AHSV VP2 serotype 2 construct (3221 nucleotides), the VP2 gene was excised from a

recombinant pFastbac plasmid by digestion with XmaI. The VP2 gene was originally cloned into the pFastbac vector as a PCR product that contained XmaI sites at the 5' and 3 ' ends that originated from the primers. After XmaI digestion, the VP2 gene fragment was purified form the agarose gel and ligated separately to XmaI digested pAS2-1 and pACT2 vectors. These vectors were first dephosporylated before ligation to ensure that vector ends could not re-anneal. Ligation mixtures were transformed into DH5α cells and putative recombinant colonies were characterized. First the colonies were screened for the presence of the VP2 gene by XmaI digestion (Figure 2.6). A 1% agarose gel shows the linearised pAS2-1 plasmid in lane 1. In lane 2 the VP2 insert is seen as a further size standard. As expected, recombinant plasmids excised the VP2 gene when digested with XmaI. Four pACT2 recombinants are seen in lanes 3 – 6 and two pAS2-1 recombinants are seen in lanes 7 – 8.

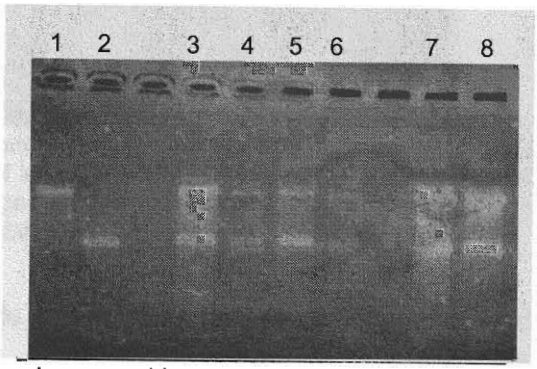

Figure 2.6: A 1% agarose gel showing recombinant screening done by using the XmaI enzyme. Lane 1 contains linearised pAS2-1 plasmid and lane 2 the full length VP2 insert prepared from pFastbac as size standard. Lanes 3-6 show results of XmaI digests done on the pACT2 recombinants. Lanes 7-8 show results of XmaI digests done on the pAS2-1 recombinants.

The orientation of the inserts was determined by using the SacI enzyme. SacI has a recognition site in the VP2 gene at position 434 and in the multiple cloning site of the pACT2 vector just downstream of the XmaI site into which the VP2 gene was cloned. If the VP2 gene is in the correct orientation in the pACT2 vector, 2 bands will be present of ± 2800 and ± 8800 nucleotides. If the insert is in the incorrect orientation, once again two bands (11600 + 400 nucleotides) will be seen. In Figure 2.7 (lanes 3-6), the results of the SacI digests done on the pACT2 recombinants are shown. Recombinants in lanes 3 + 4 are in the correct orientation (2 bands of ± 2800 bp and ± 8800 bp) while recombinants in lanes 5 + 6 are in the incorrect orientation (only 1 band of ± 11600 is seen, 400 bp band not visible). For the pAS2-1 plasmid, SacI is present as a unique restriction site, but outside the multiple cloning site at position 3298 in the plasmid. For the VP2 gene in the correct orientation, digestion with SacI will result in 2 bands of 2671 and 8940 bp. In the case of incorrect orientation, two bands of 5882 and 5729 bp are expected. On a 1% agarose gel, these two bands will co-migrate so that one would only see a single band. In Figure 2.7 (lanes 7 + 8) the results of the SacI digest done on the pAS2-1 recombinants are shown. Two bands are seen in these lanes of approximate size

2671 and 8940 nucleotides if compared to pAS2-1 and VP2 gene size standards in lanes 1 + 2. Therefore both clones have the insert in the correct orientation.

Thus, we had successfully cloned the full length AHSV2 VP2 gene into both the pAS2-1 and pACT2 vectors. Both these constructs were sequenced to ensure the presence of the correct reading frame and absence of mutations.

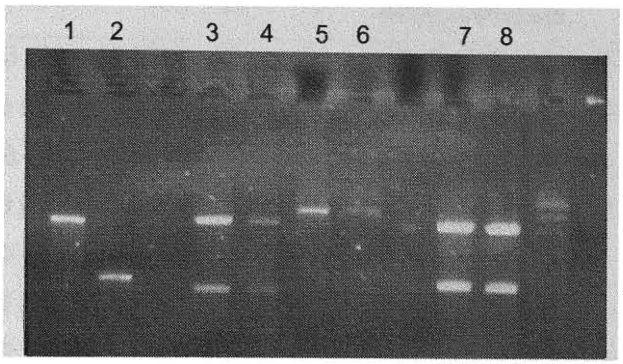

Figure 2.7: A 1% agarose gel showing orientation screening done by using the SacI enzyme. Lane 1 shows the linearised pAS2-1 plasmid and lane 2 the VP2 insert as prepared form the pFastbac as size standard. Lanes 3-6 show results of SacI digests done on the pACT2 recombinants. Lanes 7-8 show results of SacI digests done on the pAS2-1 recombinants.

Therefore as summarized in Table 2.4, a total of 12 constructs were available for analysing the VP2 – NS3 interactions. Six of these were made as described above; the other 6 had been constructed previously. Table 2.4 gives the plasmid construct name, as well as the fusion protein expected to be expressed from the construct in yeast. The two positive control plasmids provided with the Matchmaker yeast two-hybrid system, pVA3 and pTD1 are also shown in Table 2.4.

2.3.1.5 Protein expression of fusion proteins

To establish whether the fusion proteins as indicated in Table 2.4 were expressed correctly, protein expression was tested by using the methods as described in 2.2.16. The fusion proteins AD-S3VP2 and BD-S3NS3Cterm43 were used. As a further control, the activation domain (AD) and DNA-binding (BD) domain proteins obtained from the pACT2 and pAS2-1 plasmids respectively were also used. Method 1 in the Materials and methods was used initially, but as it was a shortened protocol, it was decided that it might influence the quantity of proteins extracted as a 15% SDS-PAGE gel showed very poor protein expression (results not shown). Method 2 as described in 2.2.16 was used subsequently. Here cells were harvested when the cell density reached an O.D. reading of ~ 0.6.

Western blots were done with 5 µg/ml antibodies (α-DNA-Binding domain and α-Activation domain) to detect the AD, BD, AD-S3VP2 and BD-S3NS3Cterm43 proteins. After several attempts no protein

could be detected on the membrane (results not shown). Two plasmids provided with the yeast two-hybrid system were used as further controls. pVA3 encodes for a fusion of the murine p53 protein (a.a. 72–390) with the GAL4 DNA-BD (a.a. 1–147). pTD1 encodes for a fusion of the SV40 large T-antigen

Table 2.4: Summary of Yeast two-hybrid plasmid constructs, together with the fusion proteins encoded by each construct to be used in the yeast two-hybrid assay.

Plasmid construct	Fusion Protein
pAS2-1 AHSV2 NS3 (20 – 374 bp)	BD-S2NS3Nterm118
pACT2 AHSV2 NS3 (20 – 374 bp)	AD-S2NS3Nterm118
pAS2-1 AHSV3 NS3 (546 – 758 bp)	BD-S3NS3Cterm43
pACT2 AHSV3 NS3 (546 – 758 bp)	AD-S3NS3Cterm43
pAS2-1 AHSV3 VP2 (1-3221 bp)	BD-S3VP2
pACT2 AHSV3 VP2 (1-3221bp)	AD-S3VP2
pAS2-1 AHSV2 VP2 (1-3221bp)*	BD-S2VP2
pACT2 AHSV2 VP2 (1-3221 bp)*	AD-S2VP2
pAS2-1 AHSV3 VP2 (11 - 1618 bp)*	BD-S3VP2Nterm535
pACT2 AHSV3 VP2 (11 – 1618 bp) *	AD-S3VP2Nterm535
pAS2-1 AHSV3 VP2 (1588 - 3184 bp)*	BD-S3VP2Cterm532
pACT AHSV3 VP2 (1588 - 3184 bp)*	AD-S3VP2Cterm532
pTD1 - SV40 large T-antigen gene (+ control)	AD-SV40 large T-antigen
pVA3 - murine p53 gene (+ control)	BD-murine p53 protein

*** Constructs made during this project**

(a.a. 86–708) with the GAL4 AD (a.a. 768–881). The expression of these control proteins was also analyzed via SDS-PAGE gel and Western blots, still no protein could be detected. Subsequently a more sensitive detection method, namely chemiluminescence was used (personal communication, Dr. Christine Maritz-Olivier). As an additional control, the AHSV3 β-gal-NS3 protein was included. This is an *E. coli* expressed β-galactosidase NS3 fusion protein, which reacts with the α-β-gal-NS3 antisera. The chemiluminescence detected the β-galactosidase NS3 fusion protein with the α-β-gal-NS3 antiserum, but no other yeast expressed fusion proteins were detected with the α-DNA-Binding domain and α-Activation domain antibodies (results not shown). It was concluded that the protein expression in the yeast was very low, or that the protein yield from the protein extraction protocols used was insufficient for protein detection.

2.3.1.6 Co-transformation of plasmids encoding fusion proteins into the AH109 yeast strain to assay for protein interactions

As protein expression could not be verified via Western blotting or chemiluminescence, we decided to transform the plasmids into the yeast and determined whether the plasmids that carry the fusion proteins were present or not based on their growth on selective media. The plasmids expressing the fusion proteins as indicated in Table 2.5 were simultaneously transformed (co-transformed) and transformation mixes were plated out on SD/-Leu/-Trp medium. Co-transformations were done in both directions i.e. if the bait protein was fused to the DNA-binding domain when used in the co-transformation, the same bait fused to the activation domain was also used in another co-transformation to ensure that important putative interaction sites on the bait protein were not hidden by the protein folding of the fused DNA-binding or activation domain proteins. For example, AD-S3VP2 was co-transformed with BD-S3NS3Cterm43, and BD-S3VP2 was co-transformed with AD-S3NS3Cterm43. The positive control plasmids pVA3 and pTD1 were included to verify the assay system.

Table 2.5: Summary of co-transformations of recombinant plasmids expressing different DNA-Binding domain and Activation domain fusion proteins in the yeast strain AH109. The shaded blocks indicate the interactions that were investigated.

		DNA-Binding domain fusion proteins					
		BD murine p53 protein	BD-S3VP2	BD-S3VP2 Nterm535	BD-S3VP2 Cterm532	BD-S2NS3 Nterm118	BD-S3NS3 Cterm43
Activation domain fusion proteins	AD SV40 large T-antigen	▲					
	AD-S3VP2		◊				●
	AD-S3VP2 Nterm535			◊	●		●
	A-DS3VP2 Cterm532			●	◊		●
	AD-S2NS3 Nterm118					◊	
	AD-S3NS3 Cterm43		●	●	●		◊

▲: Positive control. ◊: Homo-dimerizations ●: Hetero-dimerizations

The co-transformations done can be divided into two groups namely homo-dimerizations and hetero-dimerizations. The homo-dimerizations include the same protein or protein domain that is allowed to interact with itself. Hetero-dimerizations are when different proteins or protein domains are allowed to interact. All the fusion proteins used were tested for homo-dimerization except the positive control proteins. As VP2 forms trimers in the BTV particle (Hassan & Roy, 1999, Hewat *et al.*, 1992b, Nason *et al.*, 2004) and BTV NS3 has been shown to homo-oligomerise (Han & Harty, 2004), it was expected that these proteins would show interaction with themselves in the yeast two-hybrid system.

Quick mini-scale yeast co-transformations were done as described in 2.2.20. Following the co-transformation, mixtures were plated out on SD/-Leu/-Trp agar plates and left for 2-3 days. Colonies were restreaked on SD/-Leu/-Trp, and from there on SD/-Leu/-Trp/-His plates. Histidine is the reporter gene that is activated when there is an interaction between the bait and prey proteins resulting in the DNA-binding and activation domain becoming a functional transcription factor. Some plates were supplemented with 10 mM 3-amino-1,2,4-triazol (3-AT) to investigate whether it had any effect on the histidine production of the yeast. 3-AT is an inhibitor of leaky histidine expression in the yeast. This proved to be unnecessary, as the AH109 strain is known to inhibit any leaky expression of histidine. When colonies appeared on the SD/-Leu/-Trp/-His plates, they were restreaked on the same freshly prepared medium to verify growth. On average 27 colonies per co-transformation were screened for interaction on the SD/-Leu/-Trp/-His medium.

In Table 2.6 a summary is given of the results obtained with the co-transformations. All the co-transformations colonies grew successfully when restreaked on SD/-Leu/-Trp medium (21 – 50 colonies assayed per co-transformation) indicating that both the pACT2 and pAS2-1 plasmids expressing the leucine and tryptophan selection amino acids respectively were present in the yeast cells. As these same plasmids also contain the DNA sequence encoding the fusion proteins under investigation, it can be assumed that these proteins were also present in the yeast even though protein expression could not be verified previously.

A number of colonies from each co-transformation were streaked onto SD/-Leu/-Trp/-His. For some of the co-transformations as indicated in Table 2.6, colonies grew initially on SD/-Leu/-Trp/-His plates but died off when re-streaked. This indicated false positives and most likely in these cases the yeast could still grow due to histidine that was present in the colony after it was taken from the SD/-Leu/-Trp plates. When the colony was streaked again on SD/-Leu/-Trp/-His medium, no histidine was present in the yeast cell anymore causing the yeast to die. Thus, none of the fusion proteins investigated for interaction grew successfully on SD/-Leu/-Trp/-His medium, indicating that the proteins of interest did not interact. In all instances positive controls were included to confirm the proper working of the yeast

two-hybrid system. Although none of the AHSV proteins under investigation gave positive results, the assay clearly worked as the co-transformed positive control plasmids grew on SD/-Leu/-Trp/-His indicating that the murine p53 and large T-antigen protein did indeed interact with one another.

As a final test, the β-galactosidase colony-lift assay was performed on the interacting murine p53 and large T-antigen proteins. In Figure 2.8A a SD/-Leu/-Trp/-His agar plate is seen with 4 copies of the yeast colonies that contain the interacting murine p53 and large T-antigen proteins. In Figure 2.8B a replica is seen of Figure 2.8A, but after the colony-lift assay was done as indicated in 2.2.21. After only a 30 minute incubation period, a clear change in colour to blue was seen indicating the protein-protein interactions between murine p53 and large T-antigen.

Table 2.6: Summary of the number of colonies obtained from co-transformations that were screened for protein-protein interactions on SD/-Leu/-Trp and SD/-Leu/-Trp/-His medium.

Type co-transformation	SD/-Leu/-Trp	Status	SD/-Leu/-Trp/-His	Status
Positive control				
AD SV40 large T-antigen and BD murine p53	50	✔	8	✔
Heterodimerizations				
BD-S3VP2 and ADS3NS3Cterm43	40	✔	40	x
AD-S3VP2 and BDS3NS3Cterm43	21	✔	21	x
BD-S3VP2Nterm535 and ADS3NS3Cterm43	40	✔	32	x
AD-S3VP2Nterm535 and BDS3NS3Cterm43	30	✔	28	x
BD-S3VP2Cterm532 and ADS3NS3Cterm43	50	✔	37	x
AD-S3VP2Cterm532 and BDS3NS3Cterm43	30	✔	25	x
Homo-dimerizations and other co-transformations				
BD-S3NS3Cterm43 and ADS3NS3Cterm43	30	✔	28	±
BD-S2NS3Nterm118 and ADS2NS3Nterm118	25	✔	24	±
BD-S3VP2Nterm535 and ADS3VP2Nterm535	35	✔	30	±
BD-S3VP2Cterm532 and ADS3VP2Cterm532	25	✔	22	±
BD-S3VP2 and ADS3VP2	30	✔	27	±

✔: indicates that yeast colonies grew after they where restreaked on the same medium tested.
X: indicate that the yeast colonies did not grow.
±: indicates that the colonies grew initially on the specific medium, but died when restreaked (indicating false positives).

One of the initial aims was to investigate whether protein-protein interactions can take place between proteins from different AHSV serotypes, in this case, specifically between NS3 C-terminal (AHSV3) and wild type VP2 (AHSV2). These assays were however not conducted, as the NS3 - VP2 protein-protein interaction results obtained from studies done for AHSV serotype 3 were negative.

To conclude, the yeast two-hybrid assay was used to test for interaction between the C-terminal domain of AHSV3 NS3 and either the AHSV3 full length VP2 or N-terminal VP2 or C-terminal VP2. Homo-dimerizations were also assayed. No interactions investigated could be detected (i.e. yeast did not grow on SD/-Leu/-Trp/-His medium). As protein could not be detected via Western blot or chemiluminescence no concise explanation could be formulated except for the fact that the protein yield could have been too low. It could also be that not enough fusion protein was produced by the yeast hampering any chance of successful protein-protein interaction. The yeast two-hybrid assay did work, as the positive control obtained with the system gave the expected results.

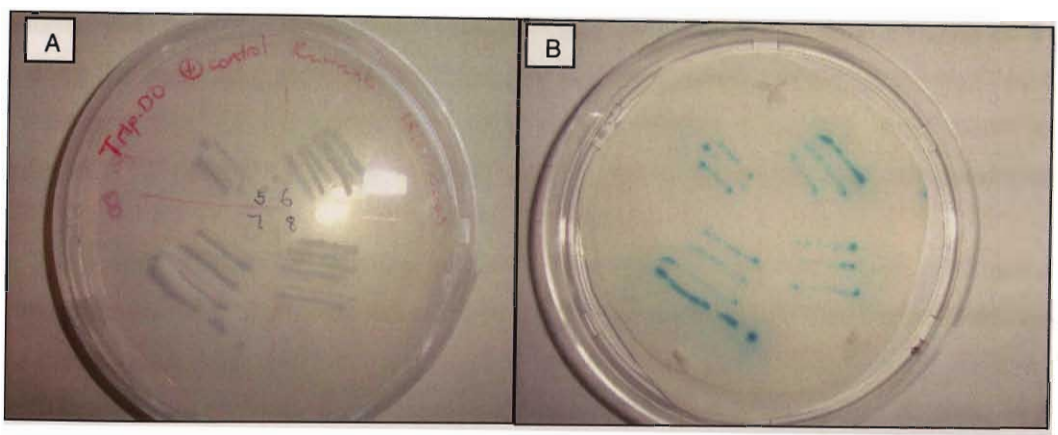

Figure 2.8A + B: A. Yeast strain AH109 co-transformed with pVA3 and pTD1 plasmids and streaked onto SD/-Leu/-Trp/-His plates. B. Results of the β-galactosidase assay done on the plate in A. Within 30 minutes the colonies turned blue, indicating protein-protein interaction.

2.3.2 GST pull-down experiment

As the yeast two-hybrid system did not give the expected results, it was decided to do a GST pull-down experiment. This experiment is usually used as a secondary confirmatory experiment to confirm results obtained from a yeast two-hybrid screen. It is based on a GST-fusion protein that binds to glutathione agarose beads via the GST protein. A cell lysate containing the protein of interest that needs to be screened against the GST-fusion protein is made. For our experiment the N-terminal NS3 of AHSV2 (amino acids 1 – 118) and C-terminal NS3 of AHSV2 (amino acids 176 – 218) fused to GST in the pET41c vector were used. The N-terminal in this case was used as a negative control, as the NS3 C-terminal domain was expected to bind to VP2. The native GST protein was also used as a control to allow all non-specific protein-protein interaction with the GST protein and not the protein

fused to the GST protein, to be eliminated. As no antibodies were available against the VP2 protein, radio-labelling with [^{35}S]-Methionine was used to identify VP2. The GST-N-term NS3 and GST-C-term NS3 constructs present in the pET41c vector were available in our laboratory (Tracy Meiring). The full length VP2 gene was obtained in the pFastbac vector from Onderstepoort Veterinary Institute, Pretoria (Dr. C. Potgieter). It was necessary to express soluble GST-NS3 proteins from bacterially induced cells. It was also necessary to generate recombinant baculoviruses expressing VP2 in infected Sf9 insect cells.

2.3.2.1 Preparation of recombinant VP2 baculovirus

The pFastbac-VP2 plasmid containing the wild type AHSV2 VP2 gene was transposed into the Bacmid genome as indicated in 2.2.14. Recombinants were selected based on their white phenotype. Recombinants were grown overnight and recombinant bacmid DNA was isolated from the white colonies as described in 2.2.14. Bacmid DNA was transfected into insect cells (1x 10^6 cells) and recombinant VP2 baculoviruses were harvested from the supernatant to be used for subsequent virus amplifications. Wild type non-recombinant baculoviruses were also prepared to be used as a control. This was done the same way as for the VP2 recombinant baculovirus, except for the fact that the blue colonies were selected. After amplification, 1 ml of the supernatant containing recombinant virus was used to infect 1 x 10^7 cells to determine whether the VP2 protein expression was being expressed.

In Figure 2.9 a 10% SDS-PAGE gel can be seen showing the expression of the VP2 protein from recombinant baculovirus that was amplified. The cells were harvested 42 hours post infection and the cells were collected at 2000 rpm for 3 minutes and resuspended in 1 x PBS buffer. In lane 2 mock infected Sf9 insect cells are seen and in lane 3 non-recombinant or wild type baculovirus. In lane 4 a unique band of the expected size of 111 kDa is seen representing the expressed VP2 protein (indicated by the arrow). The virus titre for the recombinant wild type VP2 baculovirus was determined to be 1.8 x 10^7 virus.ml^{-1}. Subsequent infections were done at a multiplicity of infection (MOI) of 2 as indicated in 2.2.23. Therefore the VP2 protein was successfully expressed via the recombinant baculovirus expression system.

2.3.2.2 Solubility assays of VP2 protein

It was known from previous work in our laboratory that baculovirus expressed VP2 could form into insoluble aggregates (Filter, 2000). Solubility assays were therefore done on the VP2 protein to ensure that soluble protein was obtained to be used in the GST pull-down assay. A 75 cm^3 flask containing 1 x 10^7 cells was infected at a MOI = ± 2 and labelled with [^{35}S]-Methionine 39 hours post

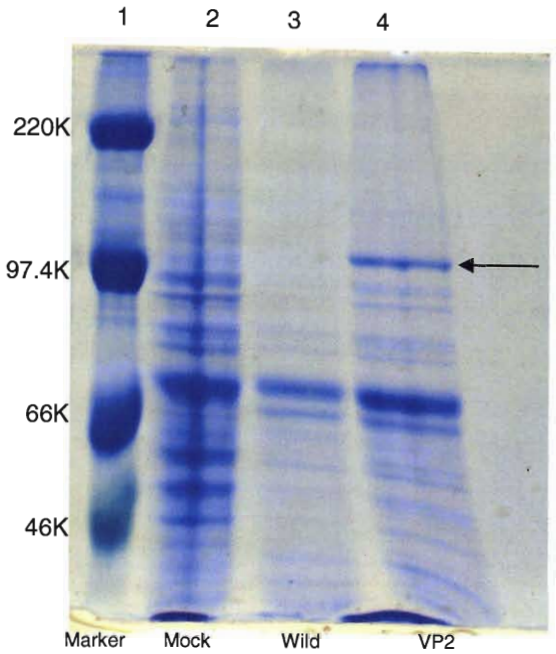

Figure 2.9: Coomassie blue stained 10% SDS-PAGE gel showing expression of AHSV2 VP2 by a recombinant bavulovirus in lane 4 (indicated by arrow). Marker in lane 1, Mock infected cells in lane 2 and Wild type baculovirus infected cells in lane 3

infection for 3 hours as described in Materials and methods to verify the presence of the VP2 protein. The cells were harvested at 42 hours post infection as this was the time shown previously when the most soluble VP2 was obtained (Filter, 2000). Cells were harvested as indicated in 2.2.23 by using Lysis buffer 1. Nuclei were collected and the supernatant separated into soluble and particulate (insoluble) fractions as detailed in 2.2.23. The different fractions were then analysed. Figure 2.10 shows a 10% SDS-PAGE gel together with its autoradiography image. The soluble fraction of VP2 is shown in lanes 6 + 7 and the insoluble fraction of VP2 in lanes 4 + 5. From this it is clearly seen that the VP2 protein is soluble with almost no protein in the particulate or pellet fraction which contradicted our beliefs that VP2 is highly insoluble.

A further experiment was done to determine whether the soluble form of VP2 could be stored over a longer period without losing its solubility. A 6-well plate was used where a well containing 1 x 10^6 cells was infected at a MOI = ± 2 with VP2 recombinant baculovirus and wild type virus respectively. A mock infection was also done. Cells were harvested as stated in 2.2.23 using Lysis buffer 1. Proteins were separated based on solubility and soluble fractions were instantly frozen using liquid nitrogen and stored at -20℃ and -70℃ for 3 days. Protein lysates were defrosted on ice and centrifuged for

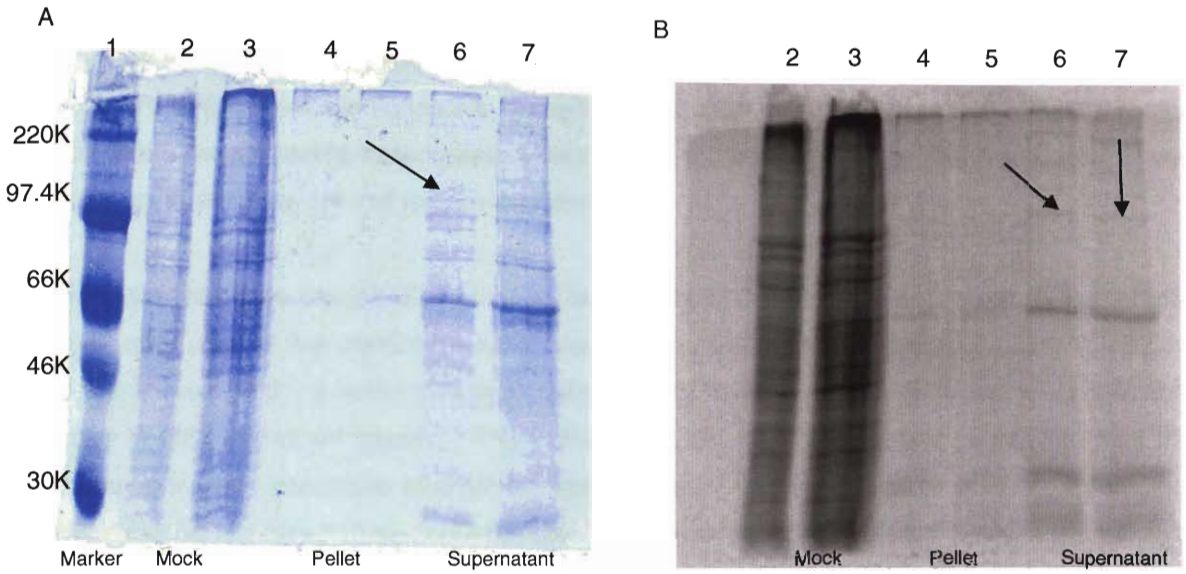

Figure 2.10: 10% SDS-PAGE gel and autoradiography image showing the results of the solubility assay done on the VP2 protein. In Lanes 2 + 3, mock infected cells are seen as a control. In lanes 4+5 the pellet fraction of the cell lysate is seen and in lanes 6+7 the supernatant fraction containing the soluble proteins are seen. VP2 is indicated by the arrows

another 60 minutes at 10 000 rpm to separate soluble and insoluble components from one another again. Insoluble pellet fractions were resuspended in 1 x PBS buffer. In Figure 2.11 a 12% SDS-PAGE gel is seen showing the total cell lysate containing VP2 obtained from the cells before centrifugation in lane 4. In lanes 5 – 8 the pellet fraction (-20℃), the supernatant fraction (-20℃), the pellet fraction (-70℃) and the supernatant fractio n (-70℃) is seen. In lane 2, mock infected cells are seen and in lane 3, wild type baculovirus infected cells. VP2 is indicated with an arrow. A distinct

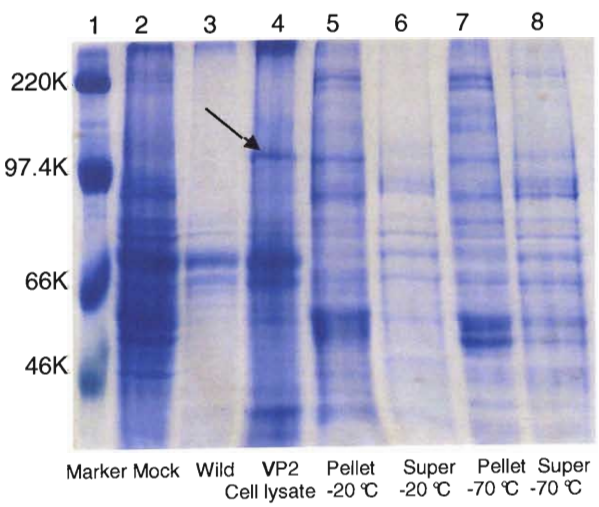

Figure 2.11: 12% SDS-PAGE gel showing the effect of storage on the solubility of VP2. Lane 2 contains mock infected cells, lane 3 contains wild type baculovirus infected cells. Lane 4 contains the whole cell lysate from VP2 recombinant baculovirus infection before any long centrifugation. Lanes 5 – 8 represent pellet and supernatant fractions of VP2 cell lysates stored at -20 ℃ and -70℃ for 3 days.

conversion of soluble protein to insoluble protein is seen when VP2 is stored over longer periods. More VP2 is seen in its insoluble form when stored at -20 ℃ than when stored at -70℃. If compared to lane 4, more VP2 is insoluble (lanes 5 + 7) than soluble which lessens the amount of native soluble VP2 to be used in subsequent experiments. We decided to use VP2 directly after harvesting for the binding assays to ensuring optimal levels of soluble VP2.

We decided to investigate which buffer would be best to use in the GST pull-down assay. Lysis buffer 1 was the buffer used in the previous solubility assays and was known to generate soluble VP2. In Sambrook & Russel (2001) a buffer was given (named Lysis buffer 2) which was specifically described for the use in GST pull-down assays. This buffer was optimized to generate an environment that would favour increased interaction strength between proteins. The only problem was that it contained a detergent named Nonidet-P40 that could influence the solubility of the VP2 protein. As the solubility of VP2 is a problem we investigated the effect this buffer could have on the solubility of VP2. In Figure 2.12 a 10% SDS-PAGE gel is seen showing the effect of the lysis buffer 1 and lysis buffer 2 on the solubility of the VP2 protein. Lysis buffer 1 contains 0.15 M STE together with 1mg/ml Pefabloc and 0.7 µg/ml Pepstatin. Lysis buffer 2 contains 0.02 M Tris pH8, 0.01 M EDTA pH 8, 0.2 M NaCl, 0.5% Nonidet-P40, 1 mg/ml Pefabloc and 0.7 µg/ml Pepstatin. Lane 2 contains cells infected with the recombinant VP2 baculovirus. Lane 3 contains the pellet fraction of cells treated with lysis buffer 1; lane 5 contains the pellet fraction of cells treated with lysis buffer 2. Lanes 4 and 6 contain respectively the supernatant fractions of cells treated with lysis buffer 1 (lane 4) and lysis buffer 2 (lane 6). Lane 6 shows that in the presence of lysis buffer 2 that contains a detergent, VP2 is still found in a

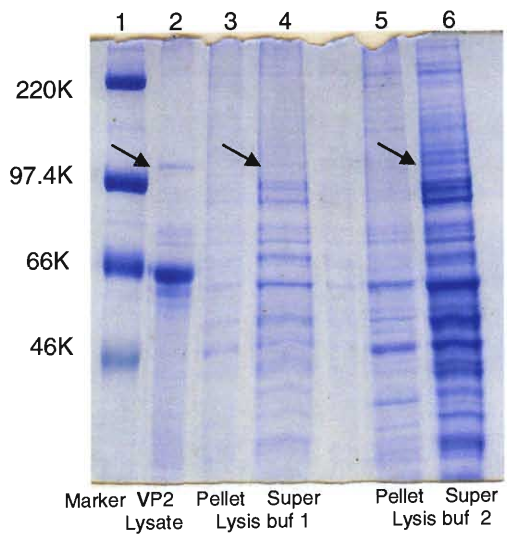

Figure 2.12: 10% SDS-PAGE gel showing the effect of different lysis buffers on VP2 solubility. Lane 2 contains a VP2 size standard. Cells were disrupted in Lysis buffer 1 (lanes 3 + 4) or Lysis buffer 2 (lanes 5 + 6) and separated into pellet and supernatant fractions respectively. VP2 indicated by an arrow

soluble state (VP2 indicated by arrows). We concluded that we can use this buffer in preparing VP2 and as a binding buffer during the GST pull-down assay.

2.3.2.3 Preparation of GST-NS3 N-terminal fusion, GST-NS3 C-terminal GST fusion and GST proteins

As the VP2 protein necessary for the GST pull-down assay was available in a soluble form, the next step was to express NS3 N-terminal and C-terminal GST fusion proteins from the IPTG induced recombinant pET41c plasmids present in bacterial cells. The native GST protein was also prepared from the pET41c plasmid. The proteins were harvested as indicated in 2.2.25 and stored at 4℃. The protocol for harvesting these GST-fusion proteins was obtained from Tracy Meiring, who already optimized it to produce soluble GST-fusion proteins. As required by the protocol given in Sambrook and Russel (2001) the approximate protein concentration of the GST-fusion proteins was determined as needed for the GST pull-down assay. The protein concentration was judged by the eye when compared to a protein marker of known concentration. A 1 µl aliquot of marker is equal to 1 µg protein. The NS3 N-terminal and NS3 C-terminal GST fusion proteins and the GST protein were allowed to bind to glutathione-agarose beads and a sample was visualized on a SDS-PAGE gel. In Figure 2.13 a 10% SDS-PAGE gel is seen showing the presence of the GST protein in lane 2, the presence of the GST-NS3 C-terminal protein in lane 3 and the presence of the GST-NS3 N-terminal

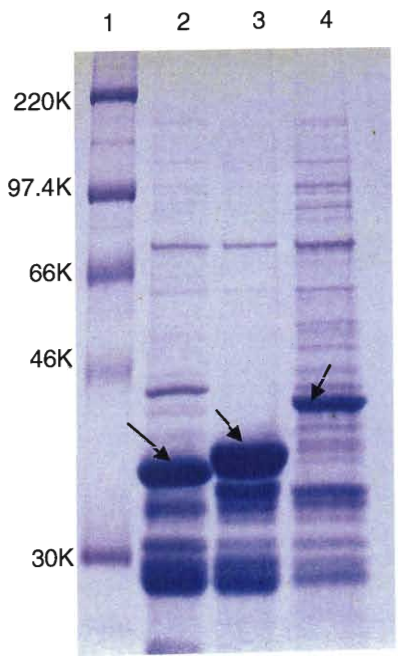

Figure 2.13: 10% SDS-PAGE gel showing protein expression of GST-fusion proteins from bacterial cells. Lane 1 shows rainbow marker at 1 $\mu g.\mu l^{-1}$. Lane 2 contain the GST protein, lane 3 the GST-NS3 C-terminal protein and lane 4 the GST-NS3 N-terminal protein. Proteins of interest indicated by arrows.

protein in lane 4. The protein concentration for these proteins was estimated to be at least as follow: GST protein = 3 $\mu g.\mu l^{-1}$, GST-NS3 C-terminal protein = 4 $\mu g.\mu l^{-1}$ and GST-NS3 N-terminal protein = 1 $\mu g.\mu l^{-1}$.

2.3.2.4 GST-pull down experiment

The GST-NS3 N-terminal, GST-NS3 C-terminal and GST proteins were prepared one day in advance and stored at 4℃ in the presence of 1 x PBS with 0 .05% sodium azide as detailed in 2.2.25. On the day of the pull down assay, the Sf9 cells infected with recombinant expressed VP2 or with wild type baculovirus were radiolabelled with [^{35}S]-Methionine. The cells were harvested up to 3 hours after addition of [^{35}S]-Methionine as indicated in 2.2.24. Lysis buffer 2 was used as soluble VP2 protein was obtained by using it as shown in previous results. The cell lysates were pre-cleared by incubation with the GST protein as indicated in 2.2.26. This step should remove all proteins that bind non-specifically to GST. The pellet fractions containing the GST protein from the pre-clearing step were kept for later analysis. The supernatants containing cleared lysate were transferred to a new eppendorf tube and combined with the GST protein (further negative control), or the GST-NS3 N-terminal protein (another negative control) or the GST-NS3 C-terminal protein and allowed to bind for 18 hours (overnight) as indicated in 2.2.26. This incubation time was shortened in subsequent experiments to only 3 hours to ensure that the conversion of soluble to insoluble protein was kept to a minimum.

After protein-protein interaction took place between the cell lysate contents and the GST fusion proteins, the slurry was centrifuged and the supernatant containing all unbound protein was retained to be visualized on a SDS-PAGE gel. The beads present in the pellet fraction containing the GST NS3 N-terminal or GST NS3 C-terminal or GST proteins with any bound protein from the cell lysate (VP2) were washed as indicated in 2.2.26 to rid the beads from any unbound protein from the cell lysate.

The results of the GST-pulldown are shown in Figure 2.14 A + B. Two 10% SDS-PAGE gels are seen with their respective autoradiography images after [^{35}S]-Methionine labelled VP2 and [^{35}S]-Methionine labelled wild type baculovirus proteins were allowed to bind for 3 hours to the GST, GST-NS3 N-term and GST-NS3 C-term proteins present on the glutathione beads. In lane 2 of Figure 2.14A, a fraction of the cell lysate is seen that was not included in the binding assay. VP2 is clearly present as indicated with the arrow. No VP2 protein is present in lanes 4 - 6 where the pellet fractions are present. If the GST-NS3 C-term fusion protein present on the beads in the pellet fraction interacted with VP2, VP2 would also have been present in the pellet fraction as expected. In these results obtained, VP2 also did not bind to GST NS3 N-term fusion protein or to the GST protein on its own.

All of the VP2 protein seems to be present in lanes 7 - 9. These are the supernatant fractions obtained after pelleting the GST-containing beads and represent all unbound protein. Clearly it is seen that VP2 is present in the supernatant fractions indicating soluble unbound VP2.

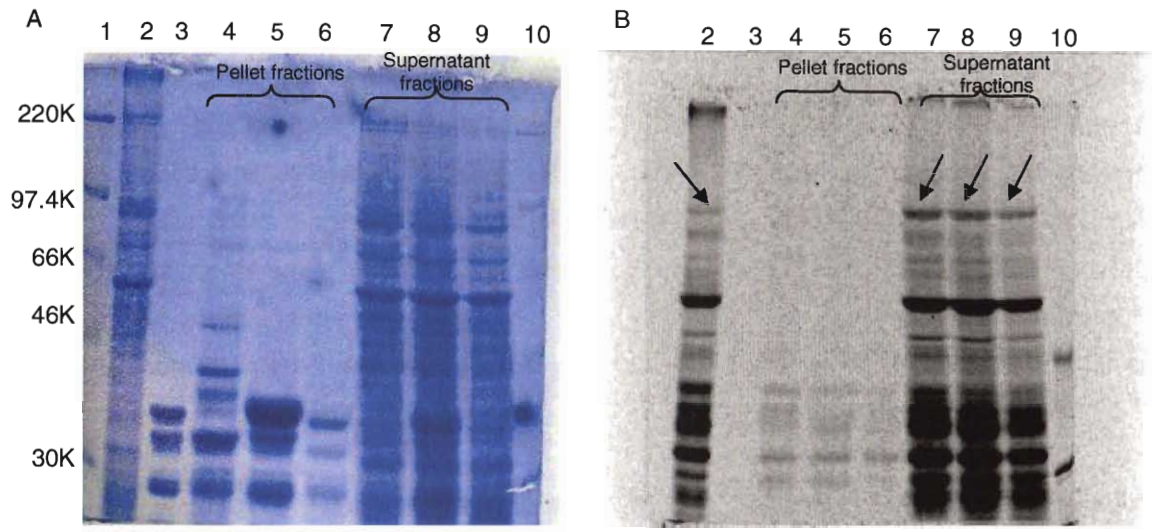

Figure 2.14A: 10% Coomassie blue stained SDS-PAGE gel (A) and its autoradiography image (B) showing GST pull-down results for the pellet and supernatant fractions of VP2 and NS3 N-terminal (lanes 4 and 7), VP2 and NS3 C-terminal (lanes 5 and 8) and VP2 and GST (lanes 6 and 9). Lane 2 contains VP2 cell lysate and lane 3 NS3-Cterm as size standards. Lane 1 and 10 contains rainbow marker. VP2 is indicated with an arrow.

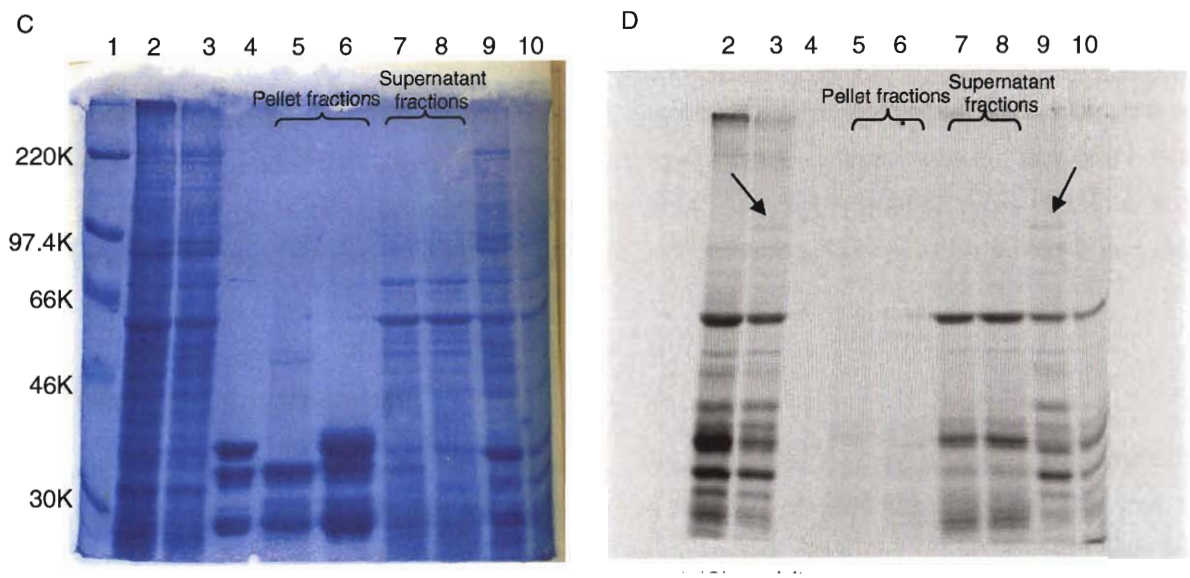

Figure 2.14B: 10% Coomassie blue stained SDS-PAGE gel (C) and its autoradiography image (D) showing GST pull-down results for the pellet and supernatant fractions of wild type baculovirus proteins and NS3 N-terminal (lanes 5 and 7), wild type and NS3 C-terminal (lanes 6 and 8). Lane 2 contains wild type baculovirus protein cell lysate and lane 3 the VP2 cell lysate. Lane 1 contains the rainbow marker. Lane 9 contains the pellet fraction from the pre-clearing of the VP2 cell lysate and lane 10 contains the pellet fraction from the pre-clearing of the wild type baculovirus lysate. VP2 is indicated by an arrow

The wild type baculovirus proteins were included as seen if Figure 2.14B to show that nothing originating form the virus influenced the GST pull-down assay. It was also included to clearly identify the VP2 protein when wild type recombinant virus infected cells were compared to VP2 recombinant virus infected cells. Two additional samples present in lanes 9 + 10 of Figure 2.14B represent the pellet fractions obtained from pre-clearing the two lysates (VP2 and Wild type) with unfused GST. We wanted to establish whether VP2 became insoluble after a 60 minute pre-clearing step. As seen in lane 9 of Figure 2.14B, a small amount of VP2 is present in the pellet (GST bound to glutathione beads) fraction. It is important to note that the pellet fraction obtained after the pre-clearing step was not washed, but the pellet fractions obtained after the actual interaction steps were vigorously washed. The VP2 present could represent a fraction of protein that bound non-specifically to GST, but more probably it represents some VP2 that had been converted to an insoluble form, and therefore was pelleted by the centrifugation step. However, still a relatively large portion of VP2 remained soluble and was present to interact with NS3 (Soluble VP2 present in supernatant fractions). GST-NS3 C-term could have interacted with VP2, but it did not.

An additional factor to consider was the solubility of the GST-NS3 C-terminal protein. The addition of the GST tag to NS3 C-term enhances solubility and this fusion protein was used less then 24 hours after preparation. Results have shown that the native NS3 protein is highly insoluble when expressed as a full-length NS3 GST fusion protein in the pET system. When the hydrophobic domains are removed as seen in our NS3 constructs (truncated N-terminal or C-terminal NS3 fused to GST), the proteins become soluble (unpublished results, Tracy Meiring). Experiments were done to verify solubility of the fusion protein after 24 hours thus it can be concluded that solubility in this case was not a factor that influenced the results of the GST pull-down. One drawback was the lack of a positive control for the GST pull-down assay. It would have made the results obtained more absolute. It can be concluded that the GST pull-down assay did not indicate interaction between the VP2 and GST-NS3 C-term proteins.

2.3.3 Membrane flotation assay

The membrane flotation assay is based on density. Three different sucrose densities are loaded in a 5 ml centrifuge tube and centrifuged for 18 hours at 38 000 rpm at 4℃. Only proteins that are associated with lipids float to the upper fractions of the gradient. Proteins not associated with lipids will stay in the bottom fractions (Briggs *et al.*, 2003, Brignati *et al.*, 2003, Simons & Ehehalt, 2002, Simons & Ikonen, 1997).

Proteins were prepared from Sf9 cells infected with recombinant baculovirus that expressed GFP (enhanced green fluorescent protein), NS3-GFP or VP2 of AHSV2 in Sf9 cells. We established the

flotation profile of NS3-GFP and GFP to ensure that the flotation worked, from where we co-expressed VP2 with NS3-GFP and GFP respectively and monitored the effect of VP2 could have NS3 and GFP. We hypothesized that NS3-GFP (membrane associated) might shift VP2 (not membrane associated) up into the upper fractions, demonstrating protein-protein interaction. VP2 co-expressed with GFP (negative control) would stay in the bottom fractions of the gradient.

Therefore, the cell lysates were prepared as indicated in 2.2.22 and loaded onto the gradient as depicted in 2.2.27 and centrifuged at 38 000 rpm for 18 hours. The fractions were collected as described in 2.2.27 and the amount of NS3-GFP or GFP present in each fraction was quantitated by using an Fluoroskan Ascent FL fluorescence spectrophotometer (Thermo Labsystems) with the excitation filter set at 485 nm and the emission filter set at 538 nm. This was done by loading 50 µl of each fraction into a well of a 96-well plate. The percentage of fluorescence in each fraction was calculated by dividing the fluorescence value in each fraction by the sum of the values in all the fractions. In addition, 25 µl samples of fractions 2 - 4 and 11 - 14 (fractions with peak fluorescence values) were analysed by 10% SDS-PAGE.

It is shown in Figure 2.15 that expressed NS3 fused to the GFP protein in the baculovirus system, when loaded on the membrane flotation gradient, floated to the upper fractions (14 - 15) as expected of the membrane associated NS3 protein. Expression of only GFP in the baculovirus system resulted

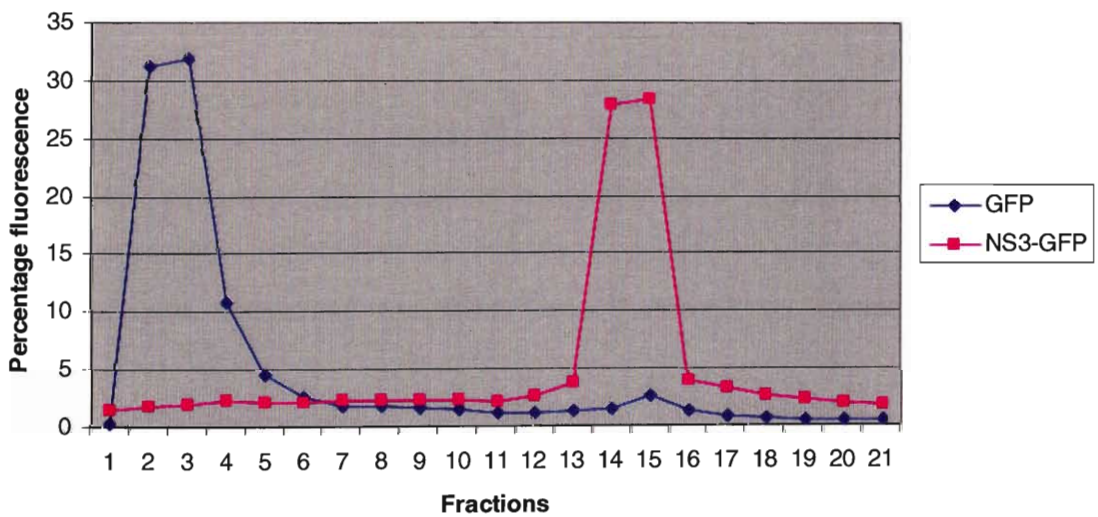

Bottom.....Top

Figure 2.15: The membrane flotation profile of recombinant baculovirus expressed GFP (—◆—) and NS3-GFP (—■—). Infected cells were lysed and subjected to centrifugation as described in 2.2.17. Fractions were collected and fluorescence monitored.

in the GFP protein remaining in the bottom fractions (2 - 3) of the membrane flotation gradient. It was decided to investigate the effect AHSV2 VP2 would have when co-expressed with AHSV2 NS3-GFP. It was hypothesized that as VP2 was not membrane associated, it would remain in the bottom fractions of the membrane flotation assay or pellet as an insoluble protein aggregate. If protein-protein interaction was present between VP2 and NS3-GFP, it was postulated that the NS3-GFP - VP2 complex would still float into the upper fractions of the gradient.

Therefore it was decided to infect 1 x 10^7 insect cells with recombinant baculovirus at a multiplicity of infection (MOI) of 5. VP2 and GFP were co-expressed by dually infecting the insect cells with two recombinant viruses, each at a MOI of 5. The same was done for VP2 and NS3-GFP. VP2 was also expressed on its own. Cells were starved and labelled with [^{35}S]-Methionine as indicated in 2.2.24 at 42 h.p.i. and prepared as described in 2.2.23.

In Figure 2.16 the effect of VP2 can be seen on the position of the GFP and NS3-GFP protein in the gradient. VP2 had no effect on the position of GFP in the gradient. The distribution pattern of NS3-GFP however differs from that seen in Figure 2.15 in the sense that the relative amount of NS3-GFP in the upper fractions (11 - 14) is much smaller (34.4% of total fluorescence) if compared to the equivalent fractions in Figure 2.15 (± 56%). Also a shift is seen in the position of NS3-GFP in the upper fractions. The position of NS3-GFP moved from fractions 14 - 15 (Figure 2.15) to fractions 11 - 14 (Figure 2.16). This could be due to the range in which the fractions were collected or to the effect

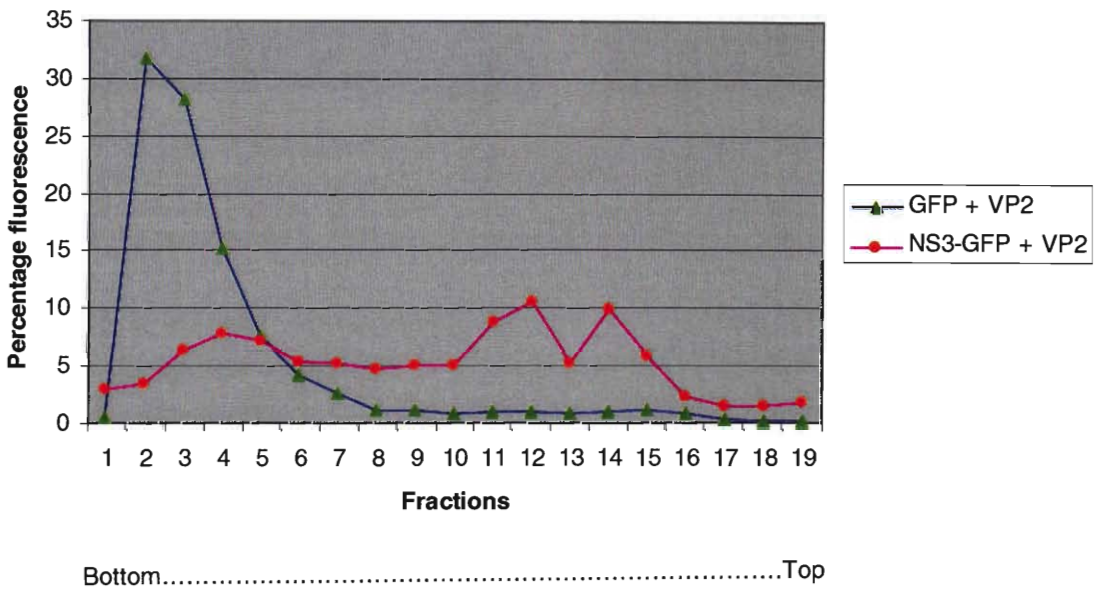

Figure 2.16: The membrane flotation profile of recombinant baculovirus co-expressed GFP + VP2 (—▲—) and NS3-GFP + VP2 (—◆—). Infected cells were lysed and subject to centrifugation as described in 2.2.17. Fractions were collected and fluorescence monitored.

of VP2 redistributing NS3-GFP towards a lower gradient position. In Figure 2.15, 21 fractions were collected and in Figure 2.16, only 19 fractions were collected. In Figure 2.16, two peaks are seen in the upper fractions of NS3-GFP. This is also interesting as it again could be due to the effect of VP2 on NS3-GFP. Also, approximately 27% of the total NS3-GFP co-expressed with VP2 is present in the lower fractions 3 - 6 indicating a soluble protein component, which is not the case if NS3-GFP is expressed on its own.

The next step was to determine the position of VP2 in the different gradient fractions. As already stated previously, 25 µl samples of fractions 2 - 4 and 11 - 14 were loaded onto a 10% SDS-PAGE gel. In Figure 2.17 a 10% SDS-PAGE gel is seen together with its autoradiography image showing

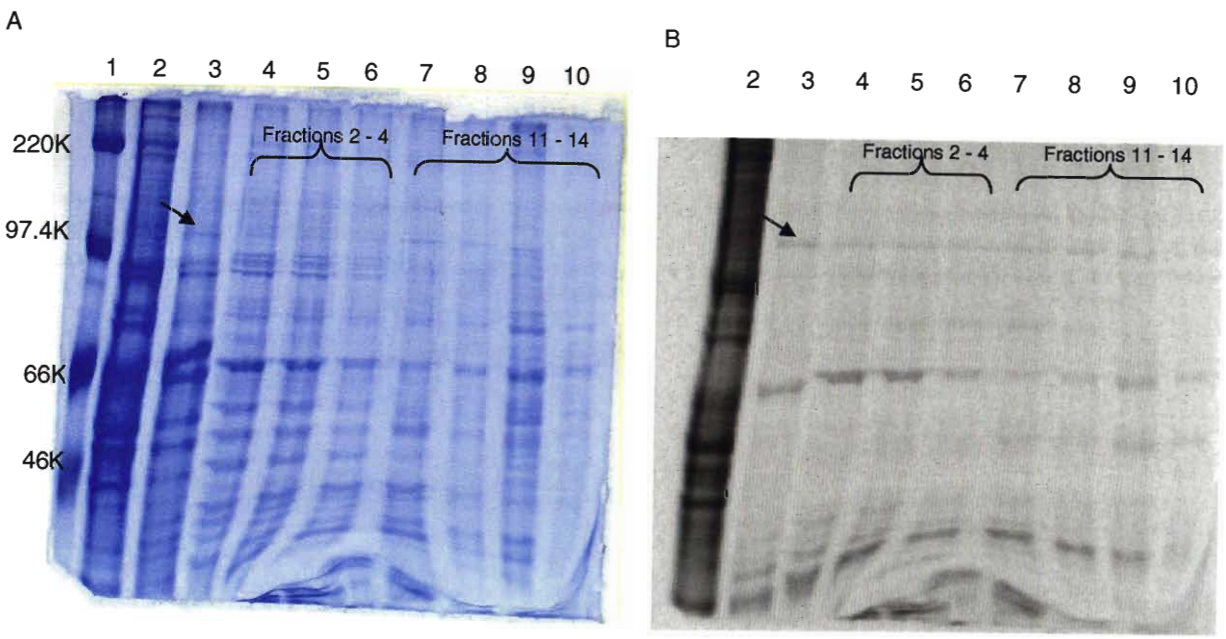

Figure 2.17: Membrane floatation assay of co-expressed recombinant baculovirus VP2 and NS3-GFP. (A) 10% SDS-PAGE gel and (B) Autoradiography image of A. In lane 1 the marker is seen and in lane 2 the wild type baculovirus infected cell lysate. Lane 3 represents a sample of the cell lysate containing co-expressed VP2 and NS3-GFP. Fractions 2 – 4 and 11 – 14 are seen in lanes 4 – 10. VP2 is indicated by an arrow.

fractions containing NS3-GFP co-expressed with VP2. VP2 is seen throughout fractions 2 - 4 as expected but is also present in fractions 11 – 14. This could indicate NS3-GFP/VP2 interaction. But in Figure 2.18, the same profile is seen when GFP is co-expressed with VP2. VP2 is also present in fractions 2 - 4 and 11 - 14. In the membrane flotation experiment done with only VP2, VP2 was also found to be in fractions 2 - 4 and 11 - 14 (Figure 2.19). After several attempts, we concluded that VP2 is not only present in the lower fractions as expected, but is also present in the upper fractions that are associated with lipids. Therefore, the membrane floatation assay could not be used to show conclusively interaction between NS3-GFP and VP2.

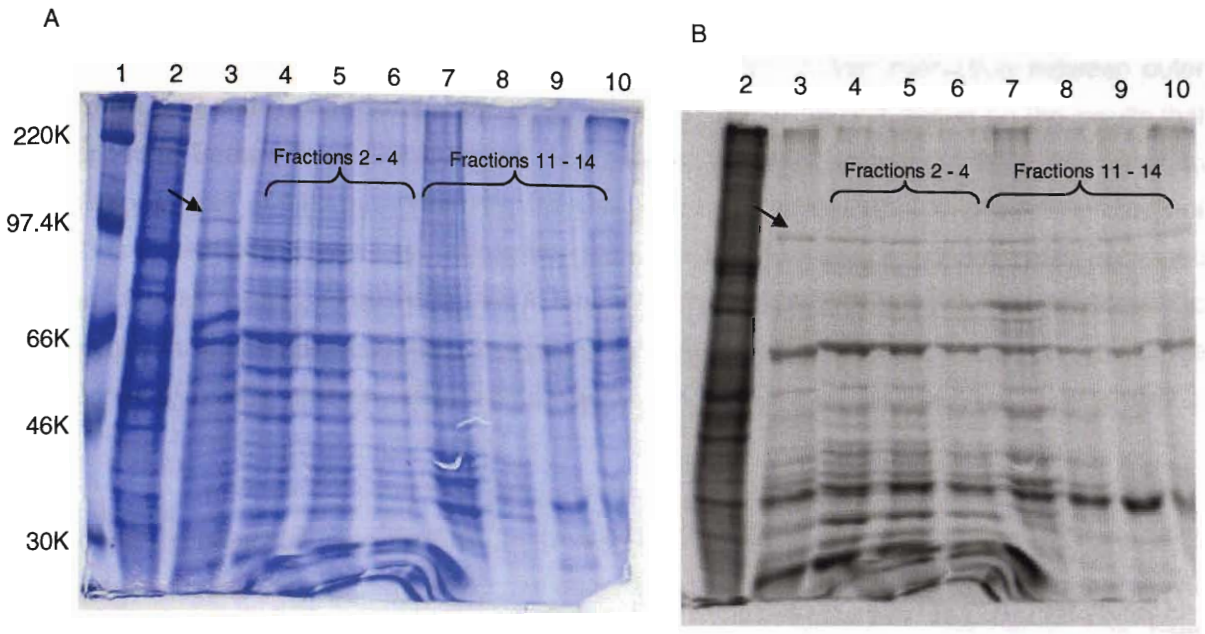

Figure 2.18: Membrane flotation assay of co-expressed recombinant baculovirus VP2 and GFP. (A) 10% SDS-PAGE gel and (B) Autoradiography image of A. In lane 1 the marker is seen and in lane 2 the wild type baculovirus infected cell lysate. Lane 3 represents a sample of the cell lysate containing co-expressed VP2 and GFP. Fractions 2 – 4 and 11 – 14 are seen in lanes 4 – 10. VP2 is indicated by an arrow.

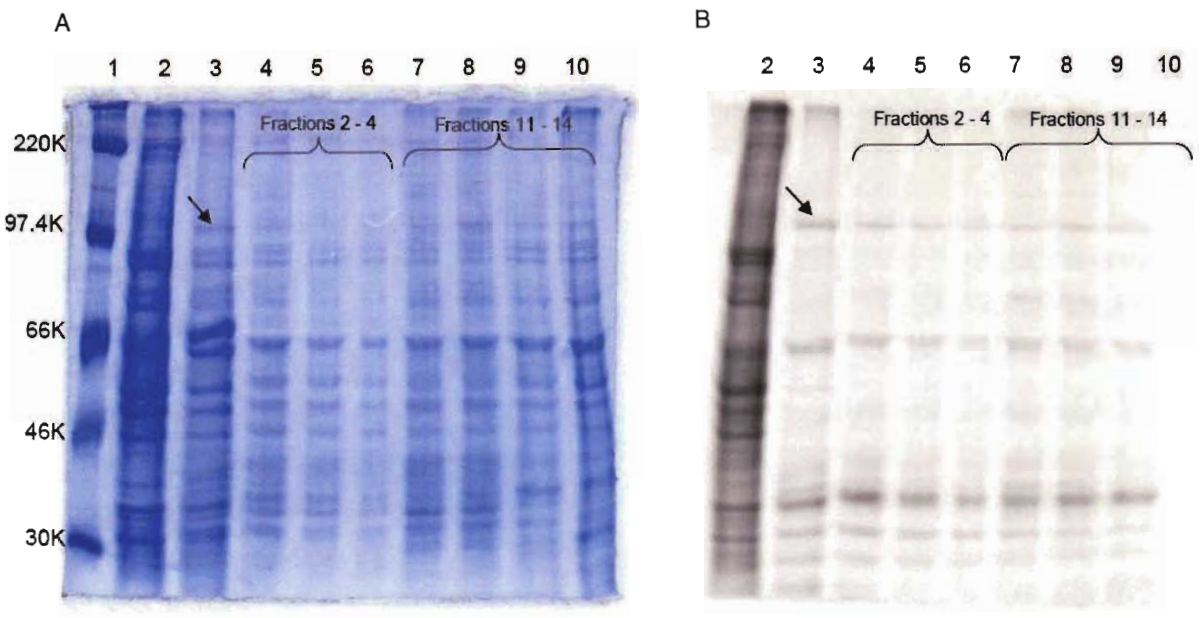

Figure 2.19: Membrane flotation assay of expressed recombinant baculovirus VP2. (A) 10% SDS-PAGE gel and (B) Autoradiography image of A. In lane 1 the marker is seen and in lane 2 the wild type baculovirus infected cell lysate. Lane 3 represents a sample of the cell lysate containing expressed VP2. Fractions 2 – 4 and 11 – 14 are seen in lanes 4 – 10. VP2 is indicated by an arrow.

2.4 DISCUSSION

The aim for this part of the study was to investigate viral protein-protein interaction between outer capsid protein VP2 and nonstructural proteins NS3 of AHSV. This study was based on the results that were obtained in Beaton *et al.* (2002) where they showed that the C-terminal of BTV NS3 binds to VP2. This forms part of their hypothesis that after virus infection and production of all 11 proteins of BTV, NS3 is localized to intracellular membrane components from where it recruits newly packaged virions via the outer capsid protein VP2. From here it seems that NS3 uses its N-terminal domain to recruit the cellular protein p11 that forms part of the exocytosis pathway, to allow the virus to exit the cell (Beaton *et al.*, 2002). We wanted to investigate whether this same mechanism could be at work in AHSV.

Three different approaches were undertaken to study the interaction between AHSV NS3 and VP2. The first of which was the yeast two-hybrid assay. This assay has been used widely to investigate protein-protein interaction in the *Reoviridae* family. Viral protein-protein interaction has been investigated in rotavirus between the NSP2-NSP5 proteins (Eichwald *et al.*, 2004) and in reovirus between the σNS and μNS proteins by using the yeast two-hybrid system (Becker *et al.*, 2003). This assay was also used to study viral protein-protein interaction between BTV membrane protein NS3 and outer capsid protein VP2 (Beaton *et al.*, 2002).

Our results showed that no protein-protein interaction could be detected between AHSV VP2 and NS3 by using the yeast two-hybrid system. The experiment was done in such a way to eliminate any intervention the activation domain or the DNA-binding domain could have on the proper folding of VP2 and NS3. This was done by cloning the DNA sequences of interest in both the pAS2-1 (contains DNA-binding domain) and the pACT2 (contains activation domain) plasmids and transforming the prey protein in experiment 1 as a bait protein in experiment 2. This technique of switching or "swapping" of the activation domain with the DNA-binding domain and vice versa has been used quite often to eliminate any influence these domains might have on the protein of interest (Van Criekinge & Beyaert, 1999). The NS3 protein could not be expressed in its native form due to the presence of two hydrophobic domains that target the protein to the cellular membrane (Stoltz *et al.*, 1996, Van Staden *et al.*, 1995). Because the yeast two-hybrid system needs the expressed proteins to be targeted to the nucleus, NS3 mutants were made including either the N-terminal (region before two hydrophobic domains) or the C-terminal (region after the hydrophobic domains).

It could be that the changing of the 3-dimensional structure of the native NS3 due to the absence of the hydrophobic domains, could influence its binding efficiency to VP2 (Van Criekinge & Beyaert,

1999, Vollert & Uetz, 2003). As the structure of VP2 is not known, the two mutants used could lack important minimal regions used for di/multimerization that could have influenced the ability of binding although the native VP2 protein also did not show any interaction. If the interaction we assayed for was dependent on the correct NS3 conformation, it could be that the interaction would not work at all, unless only a linear conformation was needed. An enormous drawback was the fact that no protein expression of the fusion proteins (NS3 or VP2 fused to either activation domain or DNA-binding domain) could be detected. There could be various reasons such as the quality and/or quantity of protein harvested from the yeast. It is known that the harvesting of protein from yeast is a difficult process with factors such as the efficiency with which yeast cell walls are broken and the amount of endogenous yeast proteases that are released when the cell walls are broken, that need to be dealt with (notes taken from Clontech's yeast protocol handbook). The inability to detect protein expression could also reflect the low level of transcription and translation of these genes in the yeast cell.

Despite the fact that protein expression could not be confirmed, the interaction between VP2 and NS3 was investigated by co-transforming the proteins into the yeast. A positive control was included that worked, showing that the system was functioning properly although none of the interactions assayed for showed interaction. Another thought that needs to be kept in mind is the fact that it has been shown that VP2 is a highly insoluble protein, especially when expressed in large amounts (du Plessis et al., 1998, Venter et al., 2000). It could be that when the VP2 fusion protein is expressed from the plasmid, it aggregates causing any interaction domain that could be recognized by NS3 to be hidden. Also in the absence of the other outercapsid protein VP5, the correct conformation of the VP2 protein could be influenced, inhibiting any NS3 recognition. It could therefore be that because both VP2 and NS3 are not in their native configuration or environment when expressed as Gal4 fusion proteins, protein-protein interaction could not be shown for these AHSV proteins.

We wanted to investigate the homo-dimerization or oligomerization probability of AHSV NS3 as it has been shown that BTV NS3 can oligomerise (Han & Harty, 2004). This is a characteristic of a typical viroporin, together with other specific properties that include the presence of hydrophobic domains and the association of these proteins with the plasma membrane as well as with the Golgi apparatus of an infected cell as described by Han & Harty (2004). VP2-VP2 multimerization was another homo-dimerization we investigated as it is known that VP2 forms trimers when packaged as the outer capsid in BTV (Hewat *et al.*, 1992b). We thought that the yeast two-hybrid system could be used to investigate whether the N-terminal domain or C-terminal domain of AHSV NS3 were responsible for oligomerization, also if AHSV VP2 did oligomerize, although without any success. This system has been used to study homo-dimerization in the P3 structural protein of rice dwarf phytoreovirus (Uyeda *et al.*, 1999).

With the second approach, the GST pull-down assay was used to investigate interaction between AHSV2 NS3 C-terminal and full length VP2. This *in vitro* method is usually used to confirm results obtained in the yeast two-hybrid system as done by Beaton *et al.* (2002) as well as others (Dimitrova *et al.*, 2003, Wirblich *et al.*, 2006, Xu *et al.*, 2000). This experiment clearly showed that traceable amounts of VP2 were still in a soluble form after being harvested from the insect cells and therefore available to interact with GST-NS3 C-terminal or GST-NS3 N-terminal or GST. The results obtained here clearly indicated that soluble VP2 did not interact with any of the GST fusion proteins or even GST. A drawback of this experiment done was the lack of any positive control. It would have been good to confirm the proper working of the system to substantiate the results obtained as mentioned above.

Due to the membrane association of NS3, we decided to use this characteristic in a membrane flotation assay as a third approach. Unpublished data from our laboratory (Tracey-Leigh Hatherell) has shown that when NS3 is placed at the bottom of a density gradient, it floats to the upper fractions when centrifuged at 38 000 rpm for 18 hours. This is because NS3 is associated with lipids. This technique has been used in various viruses such as HIV, Ebola and Sendai virus where characteristics of viral proteins were investigated in regards to whether the protein was membrane associated or not (Gosselin-Grenet *et al.*, 2006, Ono & Freed, 2001, Scianimanico *et al.*, 2000).

We thought we could investigate the effect NS3 would have on the position of VP2 as a cytoplasmic protein in a membrane flotation gradient. No conclusive result could be obtained from the experiment as VP2 was present in the lower fractions (where expected) as well as in the upper fractions (not expected) when expressed on its own in the baculovirus expression system. An interesting observation was the fact that VP2 indeed had some effect on the position of NS3 in the gradient. NS3 was still present in the upper fractions as expected, but NS3 was also present in a shifted position two fractions lower in the gradient. As both the full length NS3 and VP2 proteins were used in a eukaryotic system for this experiment and not any truncated forms as for the yeast two-hybrid and GST-pulldown assay, it could possibly show preliminary evidence for protein-protein interaction between VP2 and NS3. Another consideration would be the influence of GFP. The N-terminal of GFP was fused to the C-terminal of NS3; it could be that the presence of GFP at the C-terminal of NS3 could inhibit efficient protein-protein interaction as the C-terminal domain of NS3 is the region for VP2 interaction in BTV. A study should perhaps be done that include confocal microscopy done on AHSV infected cells with VP2 and NS3 monospecific antibodies – co-localization should prove further confirmation for VP2 – NS3 interaction.

The presence of a non membrane protein in the upper fractions of a membrane flotation gradient is an observation difficult to answer. There is no evidence in the literature that the outer capsid protein of AHSV or BTV is associated with lipids within the cell, especially in Sf9 cells. VP2 is the protein responsible for viral entry of BTV in mammalian cells (Hassan & Roy, 1999). It has been thought that VP2 recognizes and binds to cellular receptors and mediates endocytosis of the viral particle. It has been shown that VP5, another outer capsid protein, is responsible for membrane destabilization to ensure the release of the virion from the endosome (Hassan *et al.*, 2001, Roy & Noad, 2006) It has been shown for the infectious bursal disease virus, also an non enveloped virus that its outer capsid protein VP2 plays a role in cell entry as for AHSV and BTV and that this protein induces large structural rearrangements in liposomes and destabilize target membranes present in a host cell (Chevalier *et al.*, 2005). As the research done on the role VP2 plays in viral entry included BTV and not AHSV, we do not know whether the VP2 protein of AHSV might have additional characteristics which include lipid association.

We could not conclusively show protein-protein interaction between AHSV NS3 and VP2. Three different approaches were used to gain answers to the question posed, but with no success. One should maybe look at other hypothesis where an interaction between NS3 and VP2 might not contribute at all to help AHSV to exit infected host cells. Time will only tell whether any truth is present in such ventures.

Chapter 3: Investigating protein-protein interactions between AHSV NS3 and insect cellular proteins by using a *Drosophila melanogaster* cDNA library

3.1 INTRODUCTION

The yeast two-hybrid system has been developed for the screening of protein-protein interactions. It is based on the Gal4 transcription factor that consists of 2 domains, namely the DNA-binding domain (DNA-BD) that binds to a specific upstream activation site of a target gene and the activation domain (AD). The transcription of a gene can only happen when one or more activation domains direct the RNA polymerase II complex to transcribe the target gene downstream of the upstream activation site where the DNA-BD binds. These two domains cannot activate the target gene unless it is brought in close physical proximity in the promoter region.

To understand this system better, one needs to understand the origin of the yeast two-hybrid system as present in native yeast. In wild type yeast, two regulatory proteins i.e. GAL4 and GAL80 are needed to control galactose metabolism. When galactose is present, the GAL4 protein binds to GAL4-responsive elements present within the upstream activation site (UAS) of several genes that is involved in galactose metabolism and activates transcription. When galactose is absent in yeast, the GAL80 regulatory protein binds to GAL4 and blocks transcriptional activation of galactose metabolism genes. The galactose responsive genes all contain UAS's that are detected by GAL4. There are 20 known UAS's that all contain one or more conserved palindromic sequence that are grouped into the GAL1, GAL2 and MEL1 UASs. This tight regulation of the GAL UAS's by GAL4 is used in the Yeast two-hybrid system to manipulate the expression of reporter genes that are depended on the GAL4 DNA-BD. However, it must be noted that yeast host strains that are used for these studies usually carry mutations in the gal4 and gal80 genes to avoid interference by endogenous GAL4 and GAL80. Therefore no significant glucose repression is observed in these strains and no induction is seen unless a two-hybrid interaction occurs. In the GAL4-based MATCHMAKER Two-hybrid system used in this study, the GAL1, GAL2 and MEL1 UASs are used in conjunction with the regulation of the reporter genes. In the AH109 yeast strain used in this study, three reporter genes are present i.e. HIS3 (contains GAL1 UAS), ADE2 (contains GAL2 UAS) and lacZ (contains MEL1 UAS).

Therefore, the GAL4 regulatory protein is divided into its two domains, the DNA-BD that recognizes the UAS present upstream of the reporter gene and the AD (activation domain) that directs the RNA polymerase II complex to the reporter gene via the DNA-BD to start transcription. The reporter gene can only be switched on if the DNA-BD and AD are brought together. As these proteins are fused to

proteins that are investigated for interaction, only proteins that interact will bring the DNA-BD and AD together, activating transcription of the reporter gene (Notes taken from CLONTECH Matchmaker user manual).

The biggest problem with the yeast two-hybrid system has been its lack of specificity in identifying true protein-protein interactions. In the AH109 strain used in this study, three reporter genes already increase the sensitivity of the assay, as the protein-protein interaction must allow expression of all three reporter genes which are governed by three different UAS's. Non-specific interactions should be sifted out by using the three reporter genes, but it is also important to test the bait protein and prey proteins investigated for protein-protein interaction for non-specific activation of the reporter genes (i.e. DNA-BD bait fusion protein or AD prey fusion protein activating the reporter genes on their own).

Wide genome screens can be done based on proteins originating from random RNA transcripts being converted to complementary cDNA fragments. These fragments are cloned into a yeast two-hybrid vector creating activation domain fusion proteins. These activation domain fusion proteins can be screened with a DNA-binding domain fusion protein, which is usually a protein with a known function. Therefore, a single bait protein (DNA-binding domain fusion protein) is used to scan for protein-protein interactions with multiple prey proteins (activation domain fusion proteins).

For our study, we used the yeast two-hybrid system to investigate possible viral-cellular protein-protein interaction by using the NS3 protein of AHSV as bait and proteins expressed from a *Drosophila* cDNA library as putative prey proteins. AHSV NS3 is a membrane associated protein, with two membrane-spanning hydrophobic domains. Both the N- and C-termini are located in the cytoplasm, with the short spacer region between the two hydrophobic domains exposed extracellularly. In the previous chapter we investigated a possible interaction between the viral outer capsid protein VP2, and the C-terminal region of NS3. This was based on results obtained for bluetongue virus (prototype of *Orbivirus* genus), where it was shown that the VP2 outer capsid protein present on newly formed viruses interacts with the C-terminal cytoplasmic region of NS3 to help these viruses exit the cell (Beaton *et al.*, 2001). It was also shown in the same study that the N-terminal region of NS3 interacts with a cellular p11 protein, which forms part of the exocytotic pathway present in host cells. Therefore, the hypothesis is that NS3 forms a bridging molecule in the cellular membrane, recruiting newly formed viruses via VP2 on its C-terminal side and using the cellular exocytotic pathway via its N-terminal region to help the virus escape the cell via budding to infect other cells. Another recent study showed that BTV NS3 also interacts with the cellular Tsg101 protein via a late-domain present in the N-terminal of NS3. The Tsg101 protein that has been implicated in the intracellular trafficking and release of various enveloped viruses via budding.

An interesting observation was made including the role of another nonstructural protein NS1, in the viral egress of BTV. This protein was shown to be associated with cytoskeleton-associated virus-like particles, with viruses present in the cytoplasm and those released from infected cells (Eaton *et al.*, 1988). It has been suggested that these NS1 tubules can play a role in transport of mature virus particles from the virus inclusion bodies to the cell membrane where NS3 is involved in virus release (Maree & Huismans, 1997). Studies where the NS1 function was disrupted showed a reduction in cellular pathogenesis and a shift in viral release from cell lysis to budding. It was thought that under deficient NS1 protein conditions, the NS3 protein levels might have been sufficient to shift cell exit from lytic to budding (Owens *et al.*, 2004).

AHSV and BTV infect mammalian cells as well as insect cells. For these viruses a difference is seen in the way the virus exits insect cells (vector) in comparison to mammalian cells (host). Immunoelectron microscopy images have shown that BTV can either be released in a nonenveloped form by extrusion through the membrane or with a transient membrane envelope through budding at the cell surface (Hyatt *et al.*, 1989). Differences are also seen in the cytopathic effect (CPE) caused by viral infection in mammalian versus insect cells (Wechsler & McHolland, 1988). A high CPE is present in mammalian cells (foetal tongue cell line) (Castro *et al.*, 1989) where little CPE is seen in insect cells, most likely due to release without cell lysis (Homan & Yunker, 1988) . A difference is also seen in the expression levels of NS3 and NS3A proteins. In BTV-infected baby hamster kidney (BHK) cells (French *et al.*, 1989), these proteins are synthesized in low abundance where as in invertebrate cells such as in mosquito C6/36 cells in which release in nonlytic, a high level of expression is seen (Guirakhoo *et al.*, 1995). The difference in expression of the NS3 protein in these infected cell types suggests that NS3 could play a role in the different virus exit pathways employed in different cell types.

For AHSV no studies have been done on the mechanisms used for viral exit, although it is known that NS3 is present at the sites where viral release takes place (Stoltz *et al.,* 1996). As we have already looked at the NS3 - VP2 interaction in AHSV in chapter 2, we wanted to investigate possible cellular binding partners for the NS3 N-terminal region. As the BTV study used a human cDNA library to detect p11, we decided to utilize a *Drosophila* cDNA library for our screen as barely anything is known about cellular-viral protein-protein interaction in the insect vector of AHSV. The vector is a small biting midge of the genus *Culicoides*, with *C. imicola* and *C. bolitinos* the most important species in SA (Meiswinkel *et al.*, 2000, Meiswinkel & Paweska, 2003). No *Culicoides* cDNA library was available, and both *Drosophila melanogaster* and *Culicoides* belong to the order *Diptera* (common name: flies). It was therefore decided to utilise a commercially available *Drosophila* cDNA library, assuming there would be sufficient conservation of protein structure or function to identify significant protein

interactions. The analogous genes can then subsequently be cloned from *Culicoides* and the interactions verified.

It is expected to find evidence supporting the hypothesis that the virus would most probably use budding to exit insect cells as no severe CPE is seen in infected cells. Therefore, this study entails the use of the yeast two-hybrid system to identify putative protein-protein interactions between AHSV3 NS3 N-term and proteins expressed from a *Drosophila melanogaster* cDNA library.

3.2 MATERIALS AND METHODS

3.2.1 Plasmids

The following plasmids containing genes of interest were available:

Table 3.1: List of available plasmids and their genes of interest used

Plasmid	Clone	Clone construction
pAS2-1	AHSV2 NS3 20-296	Nucleotides 20 – 296 of AHSV2 segment 10 encoding NS3 N-terminal (amino acids 1 - 92), cloned into the NdeI and EcoRI sites of the pAS2-1 plasmid (Dr. Michelle van Niekerk, Department of Genetics, University of Pretoria)
pAS2-1	AHSV2 NS3 20 - 374	Nucleotides 20 - 374 of AHSV2 segment 10 encoding NS3 N-terminal (amino acids 1 – 118), cloned into the NdeI and EcoRI sites of the pAS2-1 plasmid (Dr. Michelle van Niekerk, Department of Genetics, University of Pretoria)
pAS2-1	AHSV2 NS3 544 – 764	Nucleotides 544 – 764 (last 129 nt of ORF) of AHSV2 segment 10 encoding amino acids 175 – 218 (43 in total) of NS3, cloned into the pAS2-1 plasmid via NcoI and EcoRI (Dr. Michelle van Niekerk, Department of Genetics, University of Pretoria)
pACT2	Activation domain plasmid	Plasmid obtained with the Matchmaker Gal4 two-hybrid system that contains the activation domain (Clontech laboratories, Inc)
pAS2-1	DNA-binding domain plasmid	Plasmid obtained with the Matchmaker Gal4 two-hybrid system that contains the DNA-binding domain vector (Clontech laboratories, Inc)
pVA3	murine p53 gene	pVA3 is a positive control plasmid that encodes a fusion of the murine p53 protein (a.a. 72–390) and the GAL4 DNA-

		BD (a.a. 1–147).
pTD1	SV40 large T-antigen gene	pTD1 is a positive control plasmid that encodes a fusion of the SV40 large T-antigen (a.a. 86–708) and the GAL4 AD (a.a. 768–881).

3.2.2 Primers

The following primers were used:

Table 3.2: List of primers used to sequence pACT2 constructs

Primer	Sequence	Additional information
pACT2 LRev	5' GTGAACTGCGGGTTTT TCAGTATCTACGAT '3	pACT2 specific primers obtained from Invitrogen™ and used to screen cDNA library clones
pACT2 LFwd	5' CTATTCGATGATGAGAT ACCCCACCAAACCC '3	
pACT2NRev	5' GGGTTTTTCAGTATCTAC GATTCATAG '3	Nested pACT2 specific primers obtained from Invitrogen™ and used to screen cDNA library clones
pACT2NFwd	5' TGTATGGCTTACCCATAC GATGTTCC '3	
DNA-binding domain sequencing primer	5' AGTAGCCTTCTCTCATC '3	Specific to Gal4 DNA-binding domain in pAS2-1 plasmid (nucleotides 5895 – 5912)

3.2.3 Cells and cDNA library

All bacterial work was carried out in the *Escherichia coli* strain KC8 (Obtained from Dr. Christine Maritz-Olivier, Department of Biochemistry, University of Pretoria). All yeast work was carried out in the yeast strain AH109 grown on minimal SD medium, according to standard protocols as provided by the manufacturer (Clontech Laboratories, Inc). Amino acid deficient medium lacking Leucine,

Tryptophan, Histidine, Adenine or a combination of these amino acids were prepared according to standard protocols as given by Clontech Laboratories, Inc. A matchmaker *Drosophila melanogaster* cDNA library was purchased from BD Biosciences, Clontech Laboratories, Inc. It contained 2 x 1.0 ml library culture in the *E. coli* strain BNN132. The titre was determined by manufacturers to be $\geq 10^8$ colony forming units per ml and the restriction enzyme sites XhoI/EcoRI were used to clone cDNA inserts. The number of independent clones was estimated at 3.5 x 10^6 and the average cDNA size was 1.9 kb. The cDNA fragment sizes ranged between 0.4 – 3.8 kb.

3.2.4 Amplification of premade cDNA library

The purchased cDNA library was received in 2 x 1 ml bacterial culture vials. One vial was used and resuspended in 100 ml of Luria Bertani broth (LB broth) without any antibiotics. The 100 ml of culture was streaked out on agar plates (1 ml per plate) containing the antibiotic Ampicillin (100 µg/ml final concentration). Plates were first dried for 5 – 10 minutes before they were turned upside down and incubated for 2 days at 30℃. Colonies on plates were harvested by scraping them from the plates in 5 ml of LB broth containing Ampicillin with 50% glycerol. All the collected colonies (5 ml per plate) were combined and mixed well. These glycerol stocks were aliquoted in 1.5 ml eppendorf tubes and stored at -70℃.

3.2.5 Titering of cDNA library

The cDNA library was titered by using the protocol as described in the MATCHMAKER GAL4 Two-Hybrid System 3 & Libraries User Manual appendix B (Clontech Laboratories, Inc). An aliquot of the amplified cDNA library was thawed on ice. Two dilutions were made, dilution A ($1:10^3$) and dilution B ($1:10^6$). Dilution A was plated out on one agar plate (Luria Broth agar + ampicillin) as stated in the protocol and 50 µl and 100 µl dilution B aliquots were plated out on agar plates. Plates were incubated at 30℃ for 2 days, the number of colonies counted by the eye and the titre determined as indicated using the calculation in the protocol.

3.2.6 Screening of library to validate cDNA insert presence and approximate size

Twenty colonies were selected at random during the amplification step (3.2.4) before the colonies were frozen away as glycerol stocks and restreaked on LB broth containing ampicillin (100 µg/ml final concentration) and incubated at 30℃ for 2 days. A colony-PCR was performed on these colonies to determine whether the pACT2 plasmids contained an insert. The size of these inserts was also determined. A toothpick was used to pick a small amount of *E. coli* (BNN132) that was diluted in 10 µl ultra high quality water. 25 µl PCR reaction mixtures were set up using template DNA present in colony picked, 5 pmol of each primer, 0.2 mM dNTPs, 1.5 mM $MgCl_2$, 1x Taq polymerase specific

buffer and 1 U Taq polymerase. The template was first denatured for 5 minutes initially to lyse *E. coli* cells (BNN132) and from there denatured at 94℃ for 1 minute, annealed at 54℃ and elongated at 72℃ for 8 minute for 30 cycles. The extended elon gation time was used to ensure that large fragments were amplified optimally. The PxE 0.2 Thermal cycler (Thermo Electron Corporation) was used.

3.2.7 Megapreparation of pACT2 plasmids containing cDNA library from BNN132 cells

Aliquots from the amplified cDNA library were defrosted and resuspended in LB-broth containing ampicillin (100µg/ml final concentration). The bacterial culture was grown until it reached an O.D reading of ≈ 0.6. Plasmid purification was done by using the Nucleobond® PC2000 system (Machery-Nagel) and the low-copy plasmid purification (Maxi/Bac-Mega) method as set out in the user manual was strictly followed. Briefly the bacterial culture was collected and the bacterial cell walls were lysed with buffer S1 that contains RNase A. Buffers S2 and S3 were added as indicated and then two options were given in the user manual on how to clarify the cell lysate. Option 1 was used where the suspension was filtered by using the Nucleobond® folded filter. The cleared lysate collected in two x 50ml tubes was allowed to bind onto the Nucleobond® column as described in the user manual. After washing the column, the plasmid DNA was collected in different fractions as it was eluted from the column. Thus, the 25 ml added to the column was collected as 25 x 1 ml fractions. Immediately after the plasmid DNA was added to each tube, 800 µl of isopropanol was added per tube and centrifuged on a benchtop centrifuge at 14 000 rpm at 4℃ to pr ecipitate the plasmid DNA. The supernatant was removed and the DNA pellets were washed with 500 µl 70% ethanol and allowed to dry. Each DNA pellet was resuspended in 50 µl ultra high quality water and stored at -20℃.

3.2.8 Sequential transformation of bait and library prey into AH109 yeast cells

The bait plasmid was first transformed into AH109 cells by using the quick mini-scale transformation obtained from Dr. Christine Maritz-Olivier (personal communication) (Department of Biochemistry, University of Pretoria). This method entails the resuspension of 1-2 day old AH109 yeast colonies in 1 ml of ultra high quality water. The cells were washed in ultra high quality water and collected at 3000 rpm for 3 minutes. Pelleted cells were resuspended in 1 ml of 100 mM Lithium acetate (LiAc) and incubated at 30℃ for 5 minutes without any shaking . Cells were collected and the following reagents were added in the specified order to the yeast cell pellet: 240 µl 50% PEG, 36 µl 1M LiAc, 25 µl 2 $mg.ml^{-1}$ herring sperm DNA (boiled for 2 minutes and kept on ice for another 2 minutes before use) and the plasmid DNA (minimum 450 ng) to be transformed made up to 50 µl with UHQ. The transformation mix was mixed by vortexing for at least 1 minute and incubated at 42℃ for 25 minutes

(30 minutes should not be exceeded). Transformed cells were collected at 3000 rpm for 3 minutes and resuspended in 200 µl of UHQ and plated out on one correct amino acid medium-deficient agar plate. AH109 cells that had been transformed with the bait were then prepared for transformation of the prey cDNA library plasmids. The two-hybrid system TRAFO protocol obtained from http://www.umanitoba.ca/faculties/medicine/biochem/gietz/2HS.html was used for the high efficient transformation of the cDNA library plasmid into the AH109 yeast strain that already contained the bait construct. This protocol entails the inoculation of the AH109 cells that contain the bait plasmid in tryptophan deficient medium (SD/-Trp). This was incubated overnight at 30℃. A TRAFO protocol can be done at different scales depending on the size of the transformation done. According to the 10x scale, the overnight culture containing the bait transformed AH109 strain was done in 25 ml SD/-Trp medium.

The cell titre was determined and the volume of cell culture that yielded 2.5 x 10^8 cells was used to inoculate 50 ml of YPD medium (yeast extract, peptone and dextrose). The cells were collected at 3000 rpm for 5 minutes before the YPD medium was inoculated. The YPD cell culture was incubated at 30℃ shaking at 200 rpm for 3 to 4 hours until t he cell titre reached 2 x 10^7 cells/ml (OD_{600nm} reading of ≈ 1.040). Cells were harvested at 3000 rpm for 5 minutes and washed via resuspension with ½ the volume of ultra high quality water and collected again as indicated above. The pellet was then resuspended in 3 ml of sterile 100 mM Lithium acetate (pH between 8.4 and 8.9) and incubated without shaking at 30℃ for 15 minutes. Cells were collected again and the supernatant was removed.

In a separate tube the following was added together and mixed: 2.4 ml 50% PEG (MW 3350), 360 µl 1.0 M Lithium acetate (pH between 8.4 and 8.9) and 500 µl 2 $mg.ml^{-1}$ single-stranded carrier DNA (Deoxyribonucleic acid sodium salt type III from salmon testes, Sigma D1626). This mixture was added to the cell pellet and then the cDNA plasmid DNA was added at a concentration of 20 – 100 µg. Ultra high quality water was added at a volume of 340 µl minus the volume of the plasmid DNA added. The transformation mixture was vigorously mixed by vortexing until the cell pellet was totally resuspended. The transformation mix was incubated at 30℃ for 30 minutes without any shaking. The cells were then heat shocked at 42℃ for 30 min utes with mixing by inversion for 15 seconds after every 5 – 10 minutes. The cells were finally collected at 300 rpm for 5 minutes and resuspended in 10 ml of ultra high quality water. The transformation mix was plated out 1ml per tryptophan and leucine deficient plate (SD/-Trp/-Leu). Plates were incubated for 3 – 5 days at 30℃ or until colonies appeared. All colonies on the 10 plates were harvested by adding 4 ml of SD/-Trp/-Leu medium with 50% glycerol per plate and scraping off the colonies into one big container. These glycerol stocks were then aliquoted in 1.5 ml fractions and stored at -70℃.

3.2.9 Screening of protein-protein interaction via colony streaking on amino acid deficient medium

AH109 yeast colonies containing a bait and prey plasmid were screened for protein-protein interaction between the bait and prey by streaking the colonies on the correct amino acid deficient medium. One tube containing co-transformed AH109 cells as prepared in the method above was centrifuged at 3000 rpm for 2 minutes and the cells were washed in 1 ml of ultra high quality water. The cells were resuspended in 2 ml of ultra high quality water and 400 µl was streaked out per plate. The first round of screening was done on plates lacking tryptophan, leucine and histidine (SD/-Trp/-Leu/-His). Plates were left for 2-3 days at 30℃. Colonies that grew on these plates were restreaked on plates lacking tryptophan, leucine, histidine and adenine (SD/-Trp/-Leu/-His/-Ade). These plates were also incubated for 2-3 days at 30℃. Colonies that grew on these plates were screened via PCR and/or restriction digests to determine size and presence of cDNA insert.

3.2.10 Restriction enzyme digests

All restriction enzyme reactions were carried out in the enzyme's recommended buffer, at its optimal pH and temperature as described in 2.2.7. For the double digestions (BamHI and HindIII) done, 5 U of enzyme was made up in a reaction mixture of 10 µl containing 1 µl appropriate 10x buffer. All restriction enzyme reactions were briefly centrifuged and incubated for 1.5 hours at 37℃.

3.2.11 Preparation of genomic and plasmid DNA from yeast to transform into KC8 cells

Colonies that grew on SD/-Trp/-Leu/-His/-Ade plates were inoculated in SD/-Trp/-Leu/-His/-Ade medium and incubated for 2 days at 30℃ with shaking. The cells were harvested at 3000 rpm for 5 minutes and resuspended in 4 ml of YPD medium. The cell culture was grown for ± 4 hours at 30℃ until the yeast medium was saturated. The cells were again harvested at 3000 rpm for 5 minutes and resuspended in 200 µl smash and grab buffer (1% SDS, 2% Triton-X, 100 mM NaCl, 10 mM Tris (pH=8) and 1mM EDTA). At a ratio of 25:24:1, 200 µl chloroform, phenol and isoamylalcohol (propanol) was added. Glass beads, acid washed – G8772-50G (Sigma) and lysate was mixed by vortexing at maximum speed for 3 minutes. Protein was collected at 13 000 rpm for 5 minutes. The supernatant was removed and the volume of the supernatant was determined (≈ 300 µl). The DNA was precipitated with 0.5 volumes 7.5 M ammonium acetate (≈ 150 µl) and 2 volumes absolute ethanol (≈ 600 µl). The lysate was centrifuged at 13 000 rpm for 30 minutes. The DNA pellet was washed with 70% ethanol and dried. The DNA pellet was resuspended in 11 µl ultra high quality water and stored at -20℃.

3.2.12 Preparation of electrocompetent KC8 cells

A single colony of bacterial strain KC8 was inoculated into 15 ml of Luria Bertani broth and grown overnight at 37℃ with moderate shaking. 5 ml of the overnight culture was used to inoculate each of the 2 x pre-warmed flasks containing 500 ml Luria Bertani broth. This was left to incubate at 37℃ with vigorous shaking until OD_{600nm} reached ≈ 0.5 - 0.6. The culture was transferred to four pre-chilled 250 ml centrifuge bottles and cooled on ice for 20 minutes. It is important to note that the cells should be kept ice-cold for all subsequent steps. After the cells were cooled, they were harvested at 5000 rpm for 10 minutes at 4℃. The supernatant was poured off while pellets were kept on ice. Each cell pellet was resuspended in 10 ml ice cold distilled water with swirling and no pipetting. Another 240 ml ice cold distilled water was added and mixed gently.

The cells were collected at 5000 rpm for 10 minutes at 4℃. The supernatant was poured off immediately (pellets are very loose) and the pellets were resuspended in the remaining water by swirling the cells. This wash step was repeated and after the supernatant was removed after the second wash, as much as possible supernatant was removed without loosing too much of the cell pellet. The cell pellets were resuspended in 10 ml 10% glycerol and the cell pellets of two centrifuge tubes were combined in a 50 ml centrifuge tube, thus 2x 50 ml centrifuge tubes were present. These tubes were incubated on ice for 30-60 minutes and the cells were collected again at 5000 rpm for 10 minutes at 4℃. The supernatant was removed and the final cell pellets were resuspended in 0.5 ml 10% glycerol. Both the pellets from the 50 ml tubes were combined together to give a total volume of 1 ml. The cells were aliquoted in 90 µl fractions in sterile eppendorf tubes and immediately placed and stored at -70℃

3.2.13 Transformation of cDNA library plasmid into KC8 cells

Transformation of yeast genomic and plasmid DNA into KC8 cells was done via electroporation. The cuvettes used must be ice cold. The 10 µl yeast DNA as prepared in section 3.2.11 was added to 90 µl defrosted electrocompetent KC8 cells and transferred to pre-cooled cuvettes. The 100 µl transformation mixture was electroporated at 2000 V with the electroporator 2510 (Merck). In a 2 ml centrifuge tube, 1 ml of Luria Bertani broth with 10 µl 2 M glucose was prepared and 100 µl of this was added to the cuvette after electroporation, mixed with the cells, and transferred back to the centrifuge tube that contained the rest of the broth. These tubes were incubated at 37℃ for 45-60 minutes with shaking and plated out on M9 salt minimal medium plates with ampicillin that lacked the correct amino acid as specified by the plasmid that was selected i.e. if was pACT2 selected, all amino acids except leucine were added. Plates were incubated for 1 - 2 days at 37℃.

M9 salt minimal medium is prepared as shown in Table 3.3.

Table 3.3: Preparation of M9 salt minimal medium for KC8 cells

Chemicals	Amount of medium		
	1L	500ml	250ml
10x Dropout –Leu	100ml	50ml	25ml
5x M9 salts	200ml	100ml	50ml
Glucose/Dextrose	20g	10g	5g
Agar	20g	10g	5g
Distilled H_2O	700ml	350ml	175ml
Autoclave for 10 minutes and add ampicillin at a final concentration of 100 µg/ml			

The 10x Dropout –Leu is made according to manufacturers protocol (Clontech Laboratories, Inc) in the yeast two-hybrid protocols handbook. The M9 salt minimal solution is made as shown in Table 3.4.

Table 3.4: Preparation of M9 salt minimal solution to be added to M9 salt medium

Chemicals	Amount of solution
	500ml
$Na_2HPO_4.2H_20$	32g
KH_2PO_4	7.5g
NaCl	1.25g
NH_4Cl	2.5g
Autoclave for 15 minutes and store at 4℃	

Before the M9 salt minimal solution is added to the medium as shown in Table 3.3, the following reagents as shown in Table 3.5 must be added to the M9 salt minimal solution.

Table 3.5: Reagents that need to be added to the M9 salt minimal solution before used

5x M9 salt minimal solution	100ml	50ml
1 M $MgSO_4$	1ml	500µl
20% Glucose	10ml	5ml
1 M $CaCl_2$	50µl	25µl
All reagents are stored at 4℃		

3.2.14 Plasmid preparation from KC8 cells

KC8 colonies were inoculated in 3 - 4 ml of Luria Bertani broth containing ampicillin (100 µg/ml final concentration) and incubated overnight at 37℃ shak ing. The Roche High Pure purification kit (Roche diagnostics) was used to prepare plasmid from these KC8 cells.

3.2.15 PCR

A nested PCR was performed on AH109 yeast colonies that grew on selective medium and thus potentially contained plasmids encoding proteins that showed interaction. A small sample of 2-3 day old colonies was combined with 15 pmol of each primer (pACT2 LFwd and pACT2 LRev), 0.2mM dNTPs, 1.5 mM $MgCl_2$ and 1x buffer. The volume was made up to 20 µl with ultra high quality water. A hotstart was performed where the yeast cells were denatured at 94℃ for 7 minutes and 1.25 U Taq polymerase, together with 1x buffer made up to 5 µl of ultra high quality water was added before the reaction completed stage one at 80 ℃ for 2 minutes. The second stage of the PCR reaction was repeated for 30 cycles with the following steps: 94℃ for 30 sec, 55℃ for 30 sec and 72℃ for 2 minutes. Reactions were kept at 4℃ if necessary.

The second PCR done on the product of the previous amplification was done in the same way, except that 1 µl of the previous PCR reaction was added to the PCR cocktail containing the same reagents and the denaturing step (94℃) of stage one was onl y done for 3 minutes instead of the 7 minutes as seen previously. A different set of primers (pACT2NFwd and pACT2NRev) were used where the primers annealed within the PCR product of the previous amplification.

For amplification of the pACT2 plasmids harvested from the KC8 bacterial clones, a single PCR reaction was done with 1 µl plasmid DNA that was combined with the same cocktail as above using the pACT2LFwd and pACT2LRev primers. A hotstart was also performed with a denaturing step (94℃) of 3 minutes after which the 30 cycles were done under the same conditions as above.

3.2.16 Sequencing

The cDNA library prey plasmids obtained from yeast and transformed into bacterial KC8 cells were sequenced by using the pACT2 LRev and pACT2 LFwd primers respectively. The ABI Prism Big Dye Terminator Cycle Sequencing Ready Reaction Kit, version 3.0 (Perkin Elmer, Applied Bioscience) was used as indicated by manufacturers instructions to carry out the sequencing reactions on the 3100 genetic analyzer (Applied Biosystems). Sequences were analysed by use of computer software including DNAssist, Chromas and VectorNTI. The NCBI blast utility

http://www.ncbi.nlm.nih.gov/BLAST/ was used to recognize the protein related to the protein expressed from the cDNA library sequence.

3.2.17 β-galactosidase assay

See section 2.2.21

3.3 RESULTS

In order to identify *Drosophila* proteins that interact with the AHSV NS3 proteins, the following was planned: The purchased cDNA library had to be amplified and titered to confirm its specifications as given by the manufacturer. The plasmid DNA had to be prepared from both the bacterial cells that contained the cDNA library as well as from the bacterial cells that contained the bait plasmid. By doing a sequential transformation, the bait DNA was added to the yeast cells followed by the transformation of the cDNA library plasmid DNA into the same yeast cells. Yeast colonies containing both the bait and cDNA library proteins had to be tested for protein-protein interaction by streaking the yeast colonies on the correct SD deficient medium. The cDNA library plasmids that encoded for the putative interacting cDNA library proteins were selected, harvested and transformed into KC8 bacterial cells. Selected cDNA library plasmid DNA was sequenced to determine the identity of the putative interacting cDNA library protein. Subsequently, these plasmids had to be co-transformed together with the initial bait used, and other positive or negative bait partners, to confirm whether the protein interaction identified was true or a false positive.

3.3.1 Amplification and titering of premade cDNA library

The matchmaker *Drosophila melanogaster* cDNA library was purchased from BD Biosciences, Clontech Laboratories, Inc and the library was amplified as described in 3.2.4. The library was also titered after the amplification to ensure that the library adhered to the specifications as given by die manufacturers. The number of colony forming units (cfu) detected per plate varied from 1.32×10^9 – 3.65×10^9 cfu/ml. According to the manufacturer's manual, a 3-fold difference is acceptable between the counts per plate. We were satisfied with our titre as it was greater than 10^8 cfu, the specified titre as stated by the manufacturer.

3.3.2 Screening of library to validate cDNA inserts presence and approximate size

To verify the sizes of the library inserts, 20 colonies were picked at random from the library after it was streaked out for the first time. A colony-PCR was performed to determine library insert sizes, which varied from 0.3 – 1 Kb (results not shown). After the library was amplified and 181 1.5 ml centrifuge

tubes were stored at – 70℃, one tube was selected and the contents streaked out on LB-agar plates containing ampicillin. Again 20 colonies were selected at random from the plates that contained the amplified library and screened via colony-PCR. This was done to verify that the yeast colonies carrying the library plasmids were successfully amplified. Library inserts were seen that varied in size from 0.4 – 0.6 Kb.

3.3.3 Megapreparation of cDNA library plasmid from *E. coli* strain BNN132

From the amplified cDNA library stock, 10 ml culture was added to two separate 500 ml liquid luria broth flasks that contained ampicillin. These flasks were incubated for only 60 minutes, as the OD_{600nm} was already beyond 1.0. According to protocol, cells should be harvested when the OD_{600nm} reaches 0.6. We continued with the experiment according to the protocol as indicated in 3.2.7. The eluate containing the plasmid DNA (pACT2 + cDNA library inserts) was collected in 25 fractions of 1 ml each. In Figure 3.1A a 1% agarose gel shows the DNA present in fractions 9 - 18. The smears seen indicate the different sized pACT2 plasmids containing different sized cDNA library inserts although the lanes could have been overloaded as well. In Figure 3.1B is a graph showing the elution kinetics of the 25 fractions based on DNA concentration eluted per fraction. The highest concentration of DNA eluted was in fraction 15 (2426.7 ng/µl) resulting in a total of 121.34 µg DNA in the 50 µl fraction.

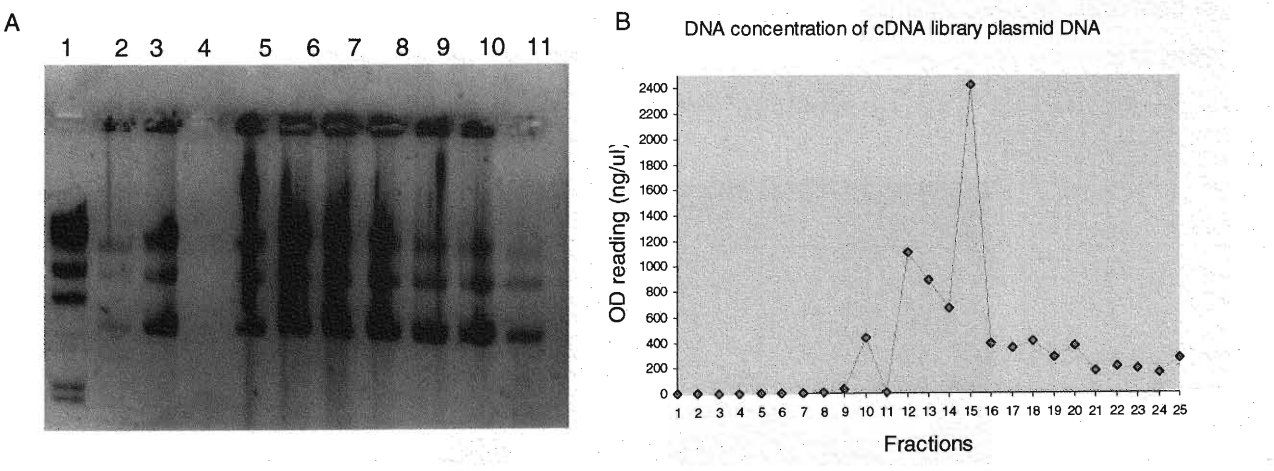

Figure 3.1: Isolation of cDNA library plasmid DNA. A. Agarose gel electrophoresis of plasmid DNA prepared from the *E. coli* strain BNN132. Lane 1 contains a molecular weight marker, lane 2 – 11 contains fractions 9 – 18 of the 25 fractions. B. Graph of the elution kinetics of the 25 fractions collected during the megapreparation of the cDNA library plasmids from *E. coli* strain BNN132. The y-axis represents the DNA concentration and the x-axis the fraction number

3.3.4 Sequential transformation of bait and library prey into AH109 yeast cells

The pAS2-1 AHSV2 NS3 20 - 374 (amino acids 1-118) was used as the bait protein as it is postulated that this terminal region of NS3 present in the cytoplasm recruits cellular proteins to assist in the virus egress. Before transformation, it was important to screen the phenotype of the AH109 yeast strain to ensure that reporter genes were not switched on non-specifically by the yeast itself. This was done by streaking a single colony on 6 different plates that lacked different components i.e. leucine, tryptophan, uracil, methionine, histidine and adenine. The AH109 yeast strain should grow on medium that lacks either methionine or uracil, but should not grow on medium that lacks leucine, tryptophan, histidine or adenine. In Figure 3.2 six plates are seen with a single AH109 yeast colony streaked on all of them. Clearly it was seen that the single colony used had the correct phenotype and this colony could be amplified and used for further transformations. It was necessary to screen the yeast strain phenotype before any experiment was done.

The pAS2-1 plasmid containing the DNA-binding domain fused to NS3-N-terminal (20 - 374 bp) was transformed into the AH109 yeast strain as indicated in 3.2.8. Transformed NS3-N-terminal yeast was prepared for the transformation of the cDNA library pACT2 plasmid DNA. The eluted plasmid DNA from fraction 12 (1110.7 ng/µl) was used as it contained a total of 55 µg DNA. According to the TRAFO protocol scale, a 10x transformation reaction needs between 20 – 100 µg DNA and therefore 55 µg was sufficient. The transformation of the cDNA library plasmid DNA was done as described in 3.2.8. After 3 days, the yeast colonies containing the bait (NS3-N-terminal 20-374 bp) and prey (cDNA library) were harvested and stored in ± 27 1.5 ml centrifuge tubes.

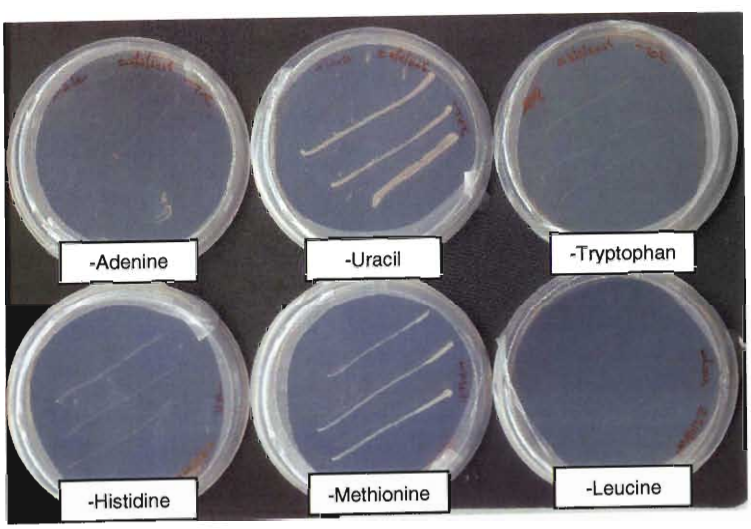

Figure 3.2: Testing the phenotype of the AH109 yeast strain. A single yeast colony was streaked on 6 different mediums that lacked adenine, uracil, tryptophan, histidine, methionine or leucine.

3.3.4 Identification of yeast colonies containing proteins of interest

Three independent screenings were done, in each case yeast from one 1.5 ml tube containing bait and prey transformed yeast was washed and streaked out on tryptophan, leucine and histidine deficient medium (SD/-Trp/-Leu/-His). After 2 - 3 days at 30℃, the plates were full of single colonies, indicating protein-protein interaction present in the colonies where the histidine reporter gene was activated, enabling the yeast to grow on SD/-Trp/-Leu/-His medium (Triple dropout colonies – TDO) (Figure 3.3A). In the three independent screenings done, a total of 850 TDO colonies were restreaked on tryptophan, leucine, histidine and adenine deficient plates (SD/-Trp/-Leu/-His/-Ade) (Quadruple dropout – QDO) to verify protein-protein interaction of the proteins by the activation of the adenine reporter gene together with the histidine reporter gene (Figure 3.3B).

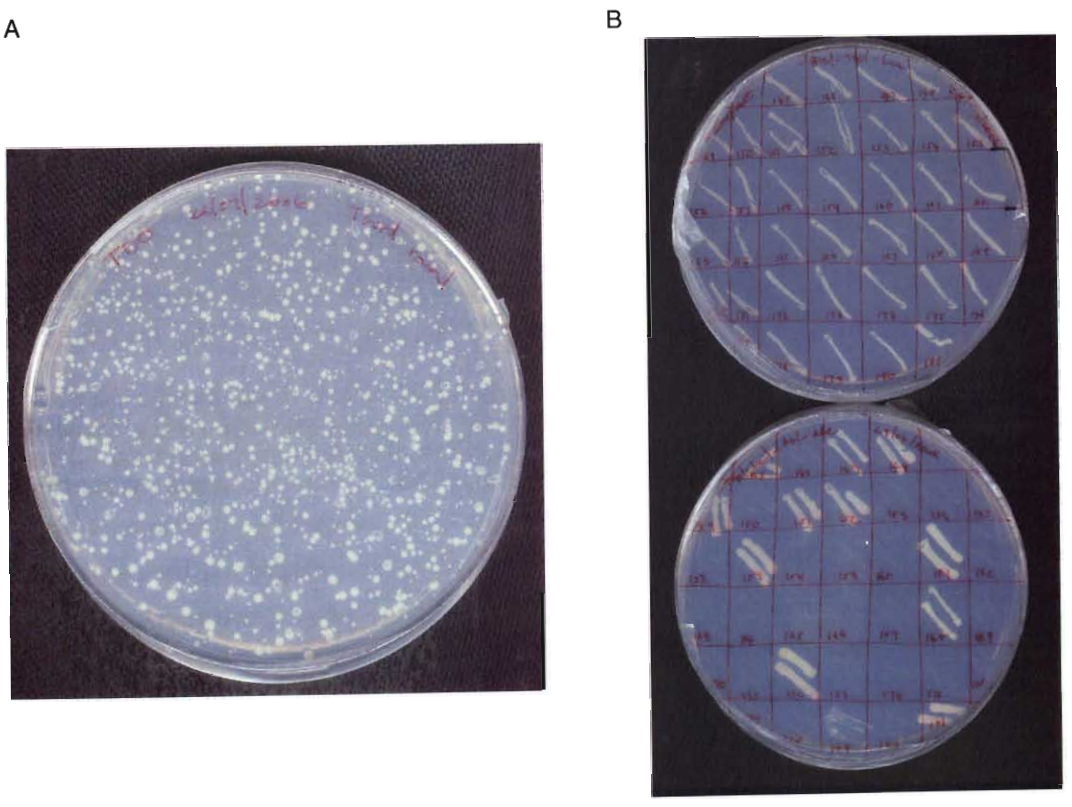

Figure 3.3: Screenings done to identify yeast colonies that displayed putative protein-protein interactions between the bait (NS3 N-term) and prey (cDNA library) proteins. A. SD/-Trp/-Leu/-His plate with yeast that was streaked from -70℃ stocks. Colonies present indicate that the histidine reporter gene is switched on. B. Colonies were picked at random from plate A and restreaked onto SD/-Trp/-Leu/-His (top) and SD/-Trp/-Leu/-His/-Ade (bottom) plates to select for colonies where the adenine together with the histidine reporter genes are turned on.

A total of 130 QDO colonies were selected and screened via polymerase chain reaction (PCR) to visualize the insert size encoding the interacting protein. A small amount of yeast DNA was used for amplification and re-amplification via a nested PCR as indicated in 3.2.15 and a 1.5% agarose gel was used to visualize the amplified insert region of the pACT2 plasmid. Figure 3.4 shows the results of the colony PCR done on 24 of the 130 colonies screened during the project. Many of the yeast colonies contained more than two, even up to four, pACT2 plasmids as seen by the presence of multiple bands following the PCR – e.g. colony 346 in lane 7. This is normal as yeast can maintain more that one different plasmid.

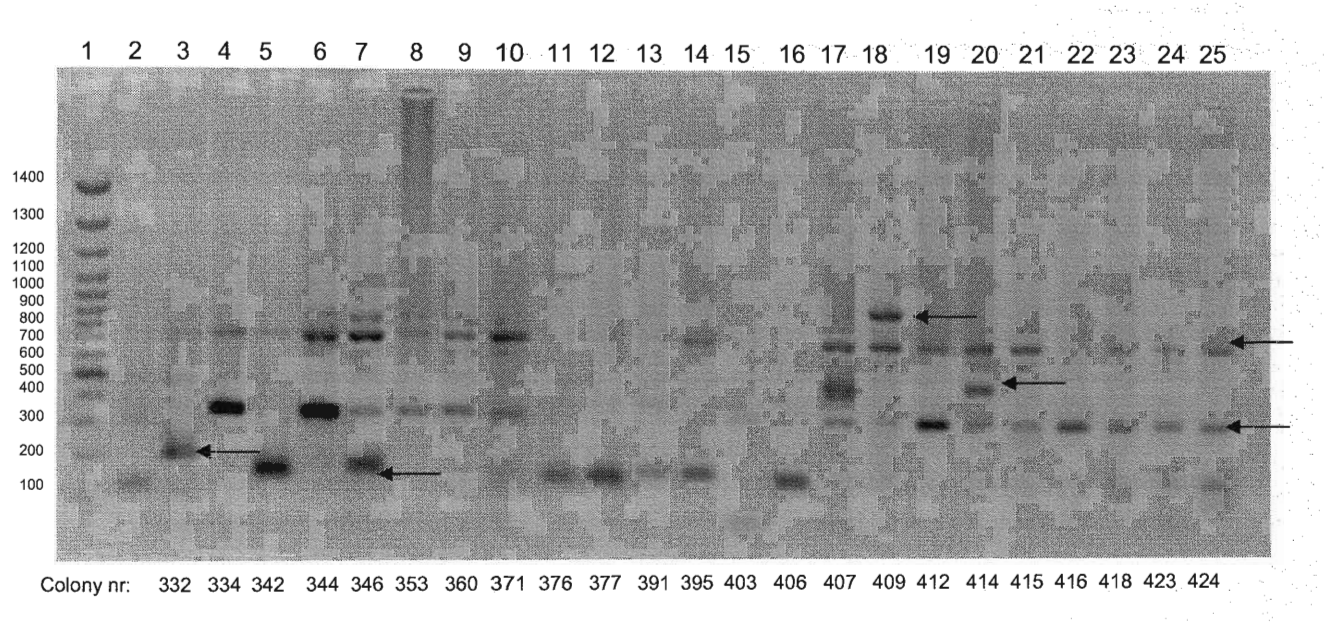

Figure 3.4: A 1.5% agarose gel showing the results of a colony PCR done on 24 of the 130 QDO colonies screened. In lane 1 a DNA ladder is shown and in lanes 3 – 25 the PCR products of the colonies screened. In lane 2 is the PCR product obtained from the pACT2 vector, representing the ≈ 150 bp amplicon of the multiple cloning site without any insert. Arrows indicate different sized fragments observed.

The colonies screened are labelled according to the number given to the TDO colony before it was restreaked on QDO medium to verify interaction. The numbers absent in the QDO colonies in Figure 3.4 implicate that the specific TDO colony died on the QDO medium, indicating that the interaction on the TDO plate was not a true interaction. The band in lane 16 (clone 406) represents the size of the PCR product of the multiple cloning site of the pACT2 plasmid. The presence of these PCR products the size of the multiple cloning site is an artefact of this system, and is present quite often. This is usually lost when the plasmid DNA prepared from the yeast is transformed into the bacterial KC8 cells as will be seen later.

For the 130 QDO colonies analyzed, 6 different size classes of inserts were identified that were present throughout the study as indicated by the arrows in Figure 3.4. Only 66 colonies in total gave single PCR bands indicating yeast containing only one pACT2 plasmid, the rest contained two or more bands.

The next step was to determine whether the observed fragments in each colony that had the same size across different colonies, was indeed the same fragment or whether they represented different clones from the library. This was done by a restriction enzyme digest on the PCR products with two random cutters to compare the profiles of the restriction digest results between the different colonies. In the first screening done, this approach was used as the PCR results showed only single bands per yeast colony. As described in 3.2.10, BamHI and HindIII were used. In the results obtained from this, all the same sized PCR fragments from different yeast colonies gave the same restriction enzyme profile (results not shown). These results could not be trusted as BamHI and HindIII are not truly frequent cutters and the PCR product sizes are too small (150 – 800 bp) to statistically show any difference between two same sized products.

As most yeast colonies contained more than one plasmid, it seemed impossible to screen it properly to distinguish between same size fragments, so another approach was used as will be explained in the next section.

3.3.5 Transformation of cDNA library plasmids from yeast cells into KC8 bacterial cells

We decided to distinguish between multiple pACT2 library plasmids in a yeast cell by extracting the yeast chromosomal and plasmid DNA and transforming it into bacterial KC8 cells that were grown on leucine deficient M9 salt medium to select for pACT2 library plasmids. KC8 *E. coli* cells can be used to selectively rescue the activation domain (library plasmid) or the DNA-binding domain (bait plasmids) from positive yeast cotransformants that have been identified in a GAL4-based two-hybrid library screen. KC8 cells carry *trp*C, *leu*B, and *his*B mutations that can be complemented by the yeast *TRP*1, *LEU*2, and *HIS*3 wild-type genes—the selectable markers present on the pACT2 or pAS2-1 cloning vectors (http://www.clontech.com/products). We hoped that by transforming the pACT2 plasmid that contained the cDNA library insert into KC8 bacterial cells, it would help in determining which of the multiple plasmids present in the specific yeast colony enabled the yeast to grow on QDO deficient medium. As the yeast colonies contain more than one plasmid, it would be a random event that determined which plasmid present in the yeast would be transformed into the bacterial cells, although plasmid DNA at a higher concentration than others in the yeast cell would have an advantage. By harvesting the library plasmid from the bacterial clones, one can determine by PCR and sequencing the identity of the clone and by re-screening it with the bait whether it is a true interaction or not.

DNA was isolated from the yeast cells containing the cDNA library plasmids by using the method as indicated in 3.2.11. The total yeast DNA extract was transformed into electrocompetent KC8 cells as indicated in 3.2.12. Before transformation into KC8 cells, 1 µl of the 11 µl DNA prepared was used as a template for a PCR reaction to see whether the same fragments were present if compared to the colony PCRs done on the intact yeast. In Figure 3.5 a 1.5% agarose gel is seen showing the results of a PCR done on the yeast DNA extracted from the yeast cells. If you compare clone 332 from Figure 3.4 with clone 332 in Figure 3.5, the same sized band of ± 200 bp is seen. If you look at clone 414, in Figure 3.4, 4 bands are seen (± 300 bp, ± 400 bp, ± 550 bp and ± 700 bp). In Figure 3.5, lane 9 only 2 bands are seen, one band of ± 120 bp and another band of ± 300 bp, the latter being the same size as the one band seen in Figure 3.4. It seems as though the 120 bp fragment present in lane 9 of Figure 3.5 could represent the multiple cloning site of the pACT2 vector i.e. plasmid without any insert. As stated previously, this is an artefact and one should monitor whether the fragment is lost when transformed into the KC8 bacterial cells. As different bands are sometimes seen in the yeast DNA purified from the yeast when compared to the PCR done on intact yeast, it shows that the PCR done in Figure 3.5 was either not optimized or some of the fragments got lost when the DNA was prepared from the yeast.

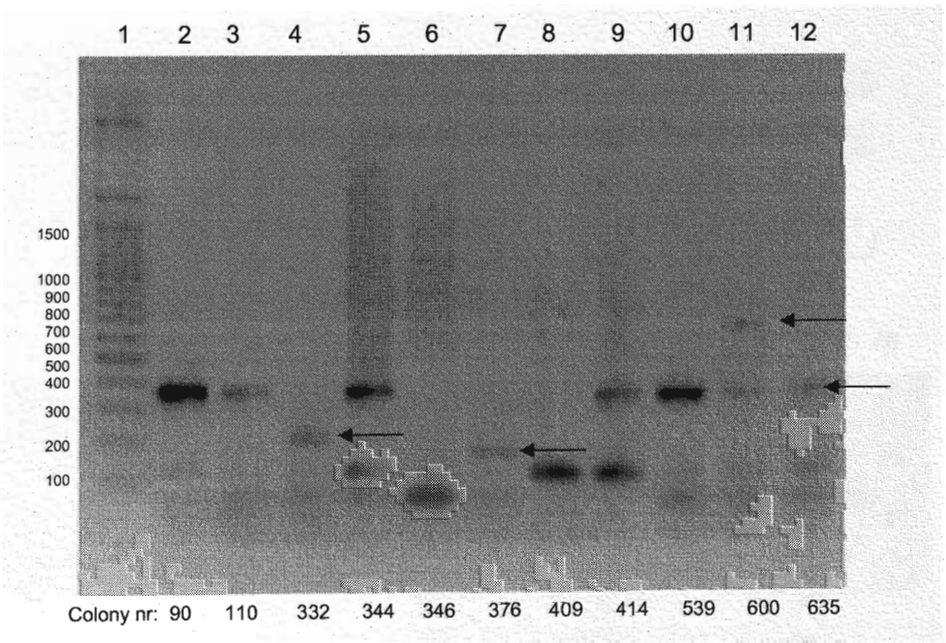

Figure 3.5: A 1.5% agarose gel showing results of PCR done on the DNA prepared from the yeast colonies. Lane 1 contains the DNA ladder and lanes 2 – 12 contains the PCR products of the colony yeast DNA collected from the yeast to be transformed into KC8 bacterial cells. Arrows indicate different fragment sizes observed.

After the DNA was isolated from the yeast colonies, it was transformed into the KC8 cells as indicated in 3.2.13 and the transformation mixtures were plated out on M9 minimum salt plates that contained all the amino acids except leucine as well as the antibiotic ampicillin. This was done so that only cells containing pACT2 or pAS2-1 plasmid DNA (ampicillin resistance) and then specifically only the pACT2 plasmid that contains the cDNA library insert (can produce leucine) would be selected. About 4 – 6 colonies were selected per transformation done and the plasmid DNA was collected from these bacterial cells as indicated in 3.2.14. In Figure 3.6, a 1% agarose gel shows the plasmid DNA that was collected from the KC8 bacterial cells. In lane 1 the pACT2 vector without any insert is seen as a size control. The plasmid prepared from each KC8 clone is also indicated. We decided to do a PCR on all of the plasmids as it would be more sensitive to determine whether the plasmids indeed had a cDNA library insert and also whether all the colonies picked from the same plate contained the same size insert. This then could also be compared to the PCRs done before the KC8 transformation (Figure 3.5) and with the initial colony-PCRs done on the yeast (Figure 3.4).

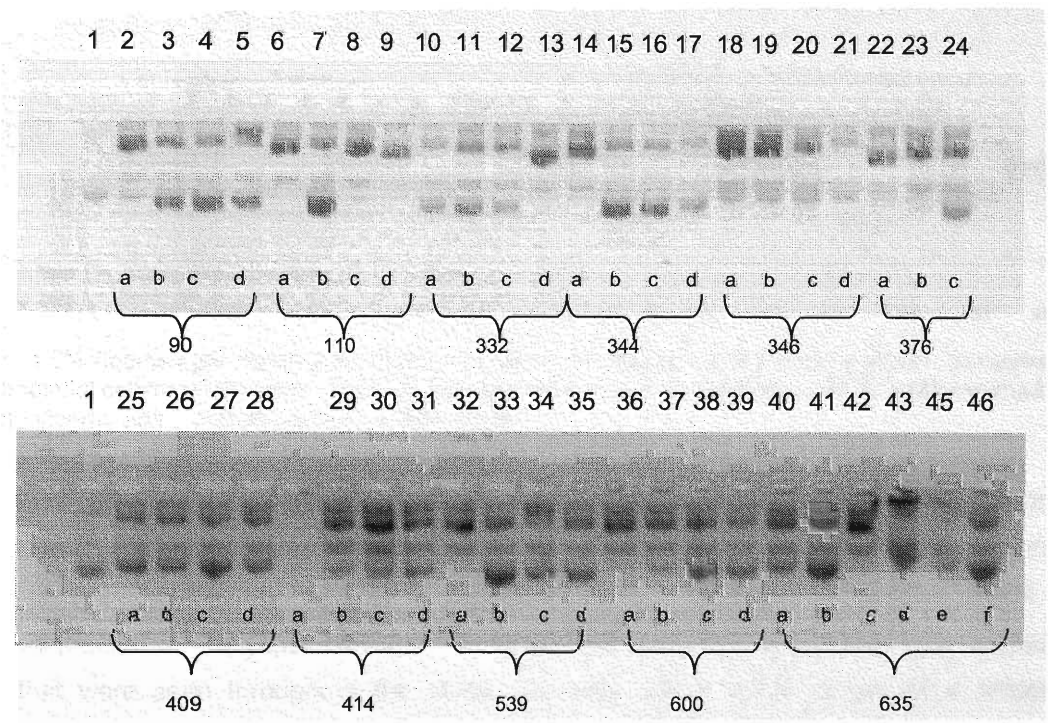

Figure 3.6: Agarose gel electrophoresis of plasmid DNA prepared from KC8 bacterial colonies. Lane 1 contains pACT2 plasmid. Lanes 2 – 46 contain the plasmid from selected KC8 clones as indicated by the number, a-f represent different colonies from one transformation.

The 19 cDNA library plasmids were amplified via PCR. These 19 plasmids represented clones containing the different sized fragments seen throughout the study. Only 4 – 8 KC8 colonies per transformation were screened. Where some of the QDO yeast colonies contained more than one pACT2 plasmid, we wanted to see if different bacterial clones from one transformation all contained the same or different plasmids. In Figure 3.7 a 1.5% agarose gel is seen that shows the results of the PCR products. All the clones from a single transformation produced PCR products of the same size, indicating the identified plasmid. Therefore when more than one pACT2 plasmid was present in the yeast, only one was probably transformed into the KC8 cells, the others were lost. Based on these results, only 1 or 2 plasmids representing each of the 19 selected clones (Figure 3.7) were used to sequence. If clones 332, 344, 346, 376, 409 and 414 present in Figure 3.7 are compared to the initial colony-PCR done on the QDO clones (Figure 3.4), all the bands present in Figure 3.7 can be seen in Figure 3.4. One can also see that some of the pACT2 library fragments that were present in Figure 3.4 were lost after the DNA extracted from these clones was transformed into the KC8 cells.

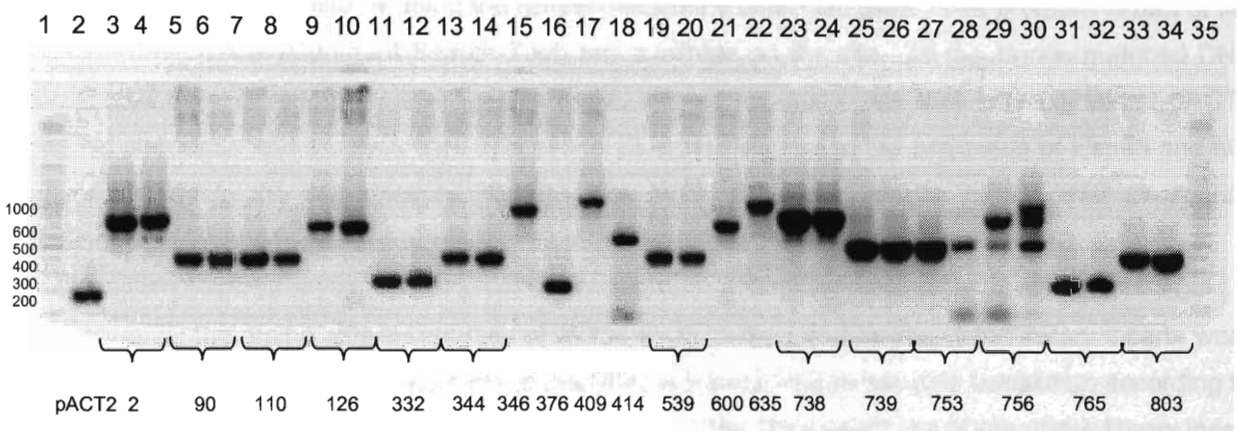

Figure 3.7: 1.5% Agarose gel showing the PCR products of 19 different QDO clones (lanes 2 – 34) screened after KC8 bacterial cell transformation. The pACT2 fragment in lane 2 represents a pACT2 vector without any cDNA library insert. Lane 1 and 35 contains a DNA ladder.

To summarize, 850 yeast colonies that grew on tryptophan, leucine and histidine deficient medium were restreaked on medium that lacked tryptophan, leucine, histidine and adenine. Only 130 colonies that grew on SD/-Leu/-Trp/-His/-Ade were screened via PCR to determine whether cDNA library inserts were present in the yeast colonies. In these 130 colonies, six different size classes were identified that were seen throughout the study. In total, 19 of these clones were selected for sequencing. This would enable us to identify proteins or protein domains that putatively interact with NS3 N-terminal (20-374 bp).

3.3.6 DNA sequencing

The 19 clones selected for sequencing contained cDNA library inserts cloned into the EcoRI and XhoI sites of the pACT2 yeast vector. The pACT2 LFwd primer was used in the sequencing reactions as indicated in 3.2.16. This ensured that the sequence obtained contained both vector and cDNA library insert information. On the 5' end of the sequence, the GGG ATC C**GA ATT C** sequence containing an EcoRI site (bold) showed the start point of the library insert. On the 3' end the **CT CGA G**AG GAG sequence containing the XhoI site (bold) showed the 3' end of the cDNA library insert. The reverse sequences using the pACT2 LRev primer were also done, but these were often unsuccessful as some of the cDNA library inserts contained a poly-A tail at the 3' end.

After the sequences of the clones selected were obtained, the position of the insert as well as the correct reading frame was identified. All the sequences contained *Drosophila* DNA when the nucleotide sequences were searched on the NCBI – National Centre for Biotechnology Information (www.ncbi.nlm.nih.gov) site by using the nBlast (nucleotide blast) program. This program is part of the BLAST (Basic Local Alignment Search Tool) tool available on the site. All the clones matched DNA sequences from *Drosophila melanogaster* origin, except for clone 765 that only contained pACT2 plasmid sequence and a poly-A tail. Five of the 19 clones aligned to the sequence of Hsp68 and two others aligned to the sequence of Hsp70. The other 11 clones aligned to 11 other *Drosophila melanogaster* sequences. These results are summarised in Table 3.6.

Subsequently the amino acid sequences of all the proteins encoded by the cDNA library inserts were determined. In Figure 3.8, one example of the DNA sequence and amino acid translation according to the pACT2 plasmid reading frame is shown for clone 2. The DNA sequence of the cDNA library insert is highlighted in blue with the 5' and 3' restriction enzyme cloning sites indicated in red blocks. The first in-frame stop codon present in the insert is encircled in green and the poly-A tail is underlined in purple. The pACT2 plasmid sequence is underlined in yellow.

The amino acid sequences were compared to other protein sequences on the NCBI website by using the pBlast and psiBlast programs. The pBlast program searches the protein database available on the NCBI website for direct protein sequence matches. The psiBlast program is used for finding distant relatives of a protein. First, a list of all closely related proteins is created. Then these proteins are combined into a "profile" that forms a "consensus" sequence. A query against the protein database is then run using this profile, and a larger group of proteins found. This larger group is used to construct another profile, and the process is repeated (www.en.wikipedia.org/wike/BLAST).

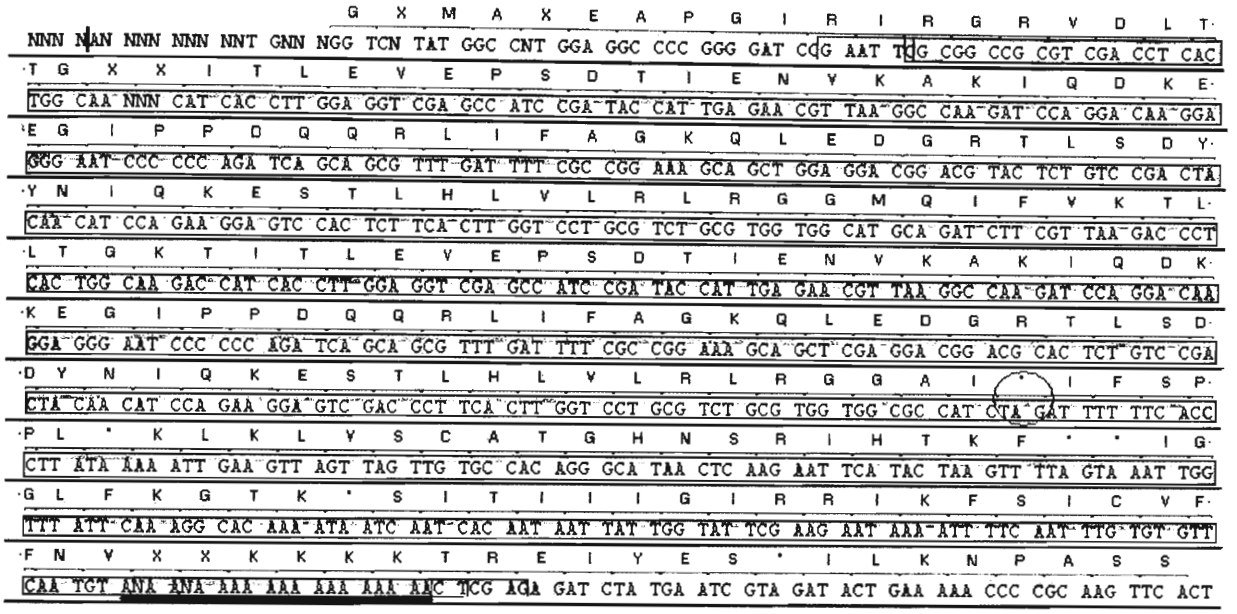

Figure 3.8: The DNA sequence and amino acid translation of clone 2. The cDNA library insert is highlighted in blue with the EcoRI and XhoI restriction cloning sites indicated with red blocks. The pACT2 plasmid sequence is underlined in yellow and the poly-A tail originating from the mRNA is underlined in purple. The first in frame stop codon is encircled in green.

Thus the reading frames of the DNA sequences translated were compared to known proteins in the NCBI database. Twelve of the inserts encoded known protein sequences; these included a multiubiquitin fusion protein, 5 proteins from the heat shock 70 family, and the yolk 1 protein. Seven of the 19 clones did not encode any known protein sequences – this could be due to unidentified polypeptides that have not been described in the *Drosophila* genome or an incorrect reading frame. Also some unexplained recombination happened in some clones i.e. 126 where pACT2 plasmid sequence was inserted into the sequence of the insert. The inserts that did not encode any protein sequences were also due to some inserts that were very small i.e. clone 376. In Table 3.6 a summary is given of these results.

Table 3.6: Summary of the DNA sequence information obtained from the 19* Drosophila *cDNA library fragments that showed interaction with AHSV2 NS3 N-terminal.

Clone	Length of insert in bp	nBlast	pBlast	psiBlast	Putative function
2	626	*Drosophila melanogaster* GH17513 full insert cDNA.	GH17513p	P125	Multiubiquitin protein, protein binding, protein modification
90, 110, 344, 539, 803	271	*Drosophila melanogaster* Heat shock protein 68 CG5436-RA (Hsp68), mRNA	Heat shock protein 68 (431 - 508)	RE48592p (Hsp 68)	Belongs to heat-shock 70 family, determination of adult life span
346, 635	> 700	*Drosophila melanogaster* strain 3CPA61 heat shock protein Hsp70Bc gene, complete cds	Major heat shock 70 kDa protein Ab	Heat shock 70 kDa protein Ab	Belongs to heat shock 70 family, protein binding, response to heat, response to unfolded protein
409	> 714	*Drosophila melanogaster* Yolk protein 1 CG2985-RA (Yp1), mRNA Length=1890	Vitellogenin -1 [Precursor]	Yolk protein 1 CG2985-PA	Belongs to the AB hydrolase superfamily. Lipase family. Catalytic activity and lipid metabolism
414	> 300	*Drosophila melanogaster* CG7182-RA (CG7182), mRNA	CG7182-PA	none	Belongs to heat shock 70 family, protein binding
738	> 673	*Drosophila melanogaster* heat shock protein 68 (hsp68) gene, hsp68d allele, complete cds	Heat shock protein 68 (overlap 356 - 510)	CG5436-PA (Hsp 68)	Belongs to heat shock 70 family, determination of adult life span
756	> 673	*Drosophila melanogaster* strain AUS heat shock protein Hsp70Bb gene, complete cds	Hsp70Bb [Fragment]	heat shock protein Hsp70Bc	Belongs to heat shock 70 family, ATP binding, nucleotide binding
126	533	*Drosophila melanogaster* CG7182-RA (CG7182), mRNA	No putative conserved domains were detected. Contains pACT2 vector sequence in the insert position		
332	Small piece of ± 52 bp	*Drosophila melanogaster* histone deacetylase dHDAC3 mRNA, complete	No putative conserved domains were detected		
376	65	*Drosophila melanogaster* Small ribonucleoprotein Sm D3 CG8427-RA			
600	501	*Drosophila melanogaster* 3L BAC RP98-13E21 complete sequence			
739, 753	330	*Drosophila melanogaster* clone BACR01B21, complete sequence			
765			Only poly-A tail present + pACT2 sequence		

3.3.8 Verification of cDNA library clones interaction with NS3 N-terminal

The library plasmids that encoded proteins present in the NCBI database were co-transformed with pAS2-1 AHSV2 NS3 20 – 374 to confirm whether the interactions detected were true. As further controls, the library plasmids were also co-transformed with pAS2-1 AHSV2 NS3 20-296 and pAS2-1 AHSV2 NS3 544–764. The pAS2-1 AHSV NS3 20-296 plasmid expresses a truncated N-terminal domain that lacks a coiled-coiled region present in the last 26 amino acids of the N-terminal region of NS3. The pAS2-1 AHSV2 NS3 544-764 encodes the C-terminal region of NS3. These two plasmids were included to determine the specificity of the protein-protein interaction. The library plasmids that did not encode any functional protein product were also co-transformed with pAS2-1 AHSV2 NS3 20 – 374 to determine whether these false positives would fail to grow when re-screened. This would also prove the specificity of the yeast two-hybrid system.

Four colonies were selected from each co-transformation and re-streaked on SD/-Leu/-Trp/-His and SD/-Leu/-Trp/-His/-Ade respectively. Clones that still grew when re-screened also underwent a β-galactosidase assay to determine the strength of the interaction as described in 3.2.17. The colour reaction was allowed to proceed for 3 hours or until the negative control started to turn blue. The intensity of the blue colour indicates the strength of the protein-protein interaction. In all cases a positive and negative control were added to validate the assay. The colour intensity was judged by the eye and a rating between 0 (no blue seen) – 5 (high blue intensity) was given. In Table 3.7 a summary is given of all the co-transformations done and the results obtained. The number of colonies out of the 4 tested that grew on SD/-Leu/-Trp/-His/-Ade for each co-transformation is shown under "Colonies that grew on QDO medium".

Table 3.7: Summary of results obtained from cDNA library clones that were re-screened for true protein-protein interaction by co-transforming the clones with pAS2-1 bait proteins as shown

Clone	Co-transformed with	Colonies that grew on QDO medium	β-galactosidase assay rating
	Library clones that encode functional *Drosophila melanogaster* protein products		
Positive control	pACT2 SV40 large T-antigen and pAS2-1 murine p53	4/4	5
2 (Ubiquitin fusion protein)	pAS2-1 AHSV2 NS3 20-374	4/4	2
	pAS2-1 AHSV NS3 20-296	0/4	-
	pAS2-1 AHSV2 NS3 544-764	0/4	-

539 (Hsp68)	pAS2-1 AHSV2 NS3 20-374	4/4	3
	pAS2-1 AHSV NS3 20-296	1/4	1
	pAS2-1 AHSV2 NS3 544-764	0/4	-
635 (Hsp70Ab)	pAS2-1 AHSV2 NS3 20-374	4/4	2
	pAS2-1 AHSV NS3 20-296	0/4	-
	pAS2-1 AHSV2 NS3 544-764	0/4	-
409 (Yolk 1 protein)	pAS2-1 AHSV2 NS3 20-374	2/4	3
	pAS2-1 AHSV NS3 20-296	0/4	-
	pAS2-1 AHSV2 NS3 544-764	4/4	3
414 (Belongs to Hsp70 family)	pAS2-1 AHSV2 NS3 20-374	0/4	-
	pAS2-1 AHSV NS3 20-296	0/4	-
	pAS2-1 AHSV2 NS3 544-764	0/4	-
738 (Hsp68-another region)	pAS2-1 AHSV2 NS3 20-374	0/4	-
	pAS2-1 AHSV NS3 20-296	0/4	-
	pAS2-1 AHSV2 NS3 544-764	0/4	-
756 (Belongs to Hsp70 family)	pAS2-1 AHSV2 NS3 20-374	0/4	-
	pAS2-1 AHSV NS3 20-296	0/4	-
	pAS2-1 AHSV2 NS3 544-764	0/4	-
Library proteins that do not encode functional *Drosophila melanogaster* protein products			
126	pAS2-1 AHSV2 NS3 20 – 374	2/4	1
332	pAS2-1 AHSV2 NS3 20 – 374	1/4	1
376	pAS2-1 AHSV2 NS3 20 – 374	3/4	2
600	pAS2-1 AHSV2 NS3 20 – 374	4/4	2
753	pAS2-1 AHSV2 NS3 20 – 374	0/4	-
765	pAS2-1 AHSV2 NS3 20 – 374	2/4	3

β-Galactosidase assay rating: 5 (high blue intensity) – 0 (no blue seen)

The clones that encode for functional protein products that seem to show true and specific interaction with the NS3 N-terminal 20 – 374 include the ubiquitin fusion protein and the Hsp70 protein. These proteins only interact with the original bait used and not with the truncated version of NS3 N-terminal or with the NS3 C-terminal. The interaction of both clone 2 and clone 635 with only the full length NS3

N-terminal and not the truncated version could hint to the importance of the last 26 amino acids of the N-terminal domain for these interactions. The other proteins interacted with either the truncated version of NS3 N-terminal (clone 539 encoding Hsp68) or with the NS3 C-terminal (clone 409 encoding Yolk 1 protein). The interaction of clone 539 with both the N-terminal proteins assayed for indicates that the interacting domain could be outside of or overlapping with the 26 amino acid region unique to the NS3 N-terminal 20 – 296 bait. For clone 409 that encodes the yolk-1 protein it could be that this protein interacts with more than one domain present in the NS3 protein, although it would be highly unlikely. In unpublished data obtained from Rencia Appelgryn (Department of Genetics, University of Pretoria), it was found by using the PRATT analysis program that AHSV NS3 contains two patterns, one present in the N-terminal region and the other one present in the C-terminal region, that are similar. This could explain why the yolk-1 protein interacts with both the N- and C-terminal domain of NS3. The PRATT program was designed to find flexible patterns in a set of unaligned protein sequences. The program finds common sequence patterns or motifs in a group of functionally related proteins, often indicating important conserved residues in functionally important parts of the protein.

In the β-galactosidase assay done, the blue intensity of the ubiquitin protein was relatively low, with a rating of 2 as it was in the case of the Hsp70 protein. This should reflect the strength of the interaction, which in this case is not very strong. But the fact that these proteins showed specific interaction with our bait, and grew on SD/-Leu/-Trp/-His/-Ade medium repeatedly should underline the accuracy of these interactions. It seems that both the Hsp68 and yolk 1 protein performed better, having a higher blue intensity when compared to the Hsp70 and ubiquitin.

The clones that do not encode functional protein products seemed to circumvent the specificity of the yeast two-hybrid system. Most of these clones still grew on SD/-Leu/-Trp/-His/-Ade medium when re-screened with NS3 N-terminal 20 – 374. The only clone that fell out was clone 753. This clone contains *Drosophila melanogaster* DNA sequence although in the wrong orientation with respect to the orientation of the pACT2 plasmid reading frame. Therefore no functional product is possible from such an insert. It was therefore reassuring that this clone was eliminated.

3.3.9 Alignment and description of important clones identified

The four proteins that showed interaction with our bait, NS3 N-terminal amino acids 1 – 118, after being re-screened for true interactions were ubiquitin, Hsp70, Hsp68 and the yolk-1 protein. The pBlast or psiBlast alignment data will be given for these four clones together with a short description of their functions. Information on these four proteins was also obtained from www.expasy.org. The

```
>gi|21428336|gb|AAM49828.1|  GH17513p [Drosophila melanogaster]
Length=306

 Score =  283 bits (724),  Expect = 1e-75
 Identities = 145/147 (98%), Positives = 145/147 (98%), Gaps = 0/147 (0%)

Query  7    LTGXXITLEVEPSDTIENVKAKIQDKEGIPPDQQRLIFAGKQLEDGRTLSDYNIQKESTL  66
            LTG  ITLEVEPSDTIENVKAKIQDKEGIPPDQQRLIFAGKQLEDGRTLSDYNIQKESTL
Sbjct  160  LTGKTITLEVEPSDTIENVKAKIQDKEGIPPDQQRLIFAGKQLEDGRTLSDYNIQKESTL  219

Query  67   HLVLRLRGGMQIFVKTLTGKTITLEVEPSDTIENVKAKIQDKEGIPPDQQRLIFAGKQLE  126
            HLVLRLRGGMQIFVKTLTGKTITLEVEPSDTIENVKAKIQDKEGIPPDQQRLIFAGKQLE
Sbjct  220  HLVLRLRGGMQIFVKTLTGKTITLEVEPSDTIENVKAKIQDKEGIPPDQQRLIFAGKQLE  279

Query  127  DGRTLSDYNIQKESTLHLVLRLRGGAI  153
            DGRTLSDYNIQKESTLHLVLRLRGGAI
Sbjct  280  DGRTLSDYNIQKESTLHLVLRLRGGAI  306
```

Figure 3.9: Using pBlast from NCBI, clone 2 (query) was found to encode the GH17513p protein (Sbjct) from *Drosophila melanogaster*. This is a multiubiquitin fusion protein with a total length of 305 amino acids.

ExPASy (**Ex**pert **P**rotein **A**nalysis **Sy**stem) is a proteomics server of the Swiss Institute of Bioinformatics (SIB) that is dedicated to the analysis of protein sequences and structures as well as 2-D PAGE. Therefore the primary accession number for each protein searched on this database is given in brackets. In Figure 3.9 the alignment between the subject (multiubiquitin fusion protein) and the query (clone 2) is seen with a 98% similarity. The 2% discrepancy is due to a sequencing error present in the sequence of clone 2. The multiubiquitin fusion protein consists of 305 amino acids. The insert of clone 2 encodes 153 amino acids; this aligns with the last 153 amino acids of the full length multiubiquitin fusion protein. This fusion protein consists of 3 tandem copies of the ubiquitin protein. The protein expressed from the cDNA library clone 2 aligns to almost two complete copies of ubiquitin (first ubiquitin protein lacks 7 amino acids at the 5' end). An interesting finding was that the full length copy of the ubiquitin protein present in our insert also matches 98% to the ubiquitin protein of *Culicoides sonorensis* (AAV84266.1), the insect vector for BTV and AHSV. Ubiquitin binds target proteins to modify them post-translationally to function in particular cellular responses (UniProtKB/TrEMBL entry Q8MT02).

In Figure 3.10 the pBlast alignment data is seen for clone 539 that encodes Hsp68. Hsp68 is a 635 amino acid protein of which 75 amino acids (431 – 506) are represented in clone 539. This protein belongs to the heat shock 70 family and mutant studies have shown it to play a role in determining the lifespan of an adult fly (UniProtKB/Swiss-Prot entry O97125). As a very small portion of Hsp68 is represented in clone 539, interaction with NS3 most probably will occur via a linear protein structure.

```
>gb|AAM11231.1| RE48592p [Drosophila melanogaster]
 ref|NP_524474.1| Heat shock protein 68 CG5436-PA [Drosophila melanogaster]
 gb|AAD16140.1| heat shock protein 68 [Drosophila melanogaster]
 gb|AAF56230.1| CG5436-PA [Drosophila melanogaster]
 sp|O97125|HSP68_DROME Heat shock protein 68
Length=635

 Score =  143 bits (360),  Expect = 2e-33
 Identities = 71/78 (91%), Positives = 71/78 (91%), Gaps = 0/78 (0%)

Query  9    DNQXXXTIQVFEGERALTKDNNVLGTFDLTGVPPAPRGXPKIDVTFDLDANGILNVTAKE  68
            DNQ   TIQVFEGERALTKDNNVLGTFDLTGVPPAPRG PKIDVTFDLDANGILNVTAKE
Sbjct  431  DNQPAVTIQVFEGERALTKDNNVLGTFDLTGVPPAPRGVPKIDVTFDLDANGILNVTAKE  490

Query  69   QGXGNAXNITIKNDKGDL  86
            QG GNA NITIKNDKG L
Sbjct  491  QGTGNAKNITIKNDKGRL  508
```

Figure 3.10: Using pBlast from NCBI, clone 539 (query) was found to encode the heat shock protein 68 (Sbjct) from *Drosophila melanogaster*. The total length of this protein is 635 amino acids.

In Figure 3.11 the pBlast alignment data is seen for clone 635. This clone encodes amino acids 429 – 601 (172 in total) of the 642 amino acid major Hsp70 protein Ab. This protein also belongs to the heat shock 70 family and plays a role in protein binding and has a response to heat and unfolded protein (UniProtKB/Swiss-Prot entry P02825). Once again the full length Hsp70 is not represented by the

```
 gb|AAN13535.1| CG31366-PA [Drosophila melanogaster]
 sp|P02825|HSP71_DROME Major heat shock 70 kDa protein Ab (Heat shock protein 70Ab)
(HSP70-87A7)
Length=642

 Score =  337 bits (864),  Expect = 1e-91
 Identities = 168/175 (96%), Positives = 169/175 (96%), Gaps = 0/175 (0%)

Query  8    YADNQPGVSIQVYEGERAMTKDNNALGTFDLSGIPPAPRGVPXIEVTFDLDANGILNVSA  67
            YADNQPGVSIQVYEGERAMTKDNNALGTFDLSGIPPAPRGVP IEVTFDLDANGILNVSA
Sbjct  429  YADNQPGVSIQVYEGERAMTKDNNALGTFDLSGIPPAPRGVPQIEVTFDLDANGILNVSA  488

Query  68   KEMSTGKAKNITIKNDKGRLSQAEIDRMVNEAEKYAXXDXKHRQRITSRNAXESYVFNVK  127
            KEMSTGKAKNITIKNDKGRLSQAEIDRMVNEAEKYA  D KHRQRITSRNA ESYVFNVK
Sbjct  489  KEMSTGKAKNITIKNDKGRLSQAEIDRMVNEAEKYADEDEKHRQRITSRNALESYVFNVK  548

Query  128  QAVEQAPAGKLDEADKNSVLDKCNDTIRWLDSNTTAEKEEFDHKLEELTRHCSQL  182
            QAVEQAPAGKLDEADKNSVLDKCNDTIRWLDSNTTAEKEEFDHKLEELTRHCS +
Sbjct  549  QAVEQAPAGKLDEADKNSVLDKCNDTIRWLDSNTTAEKEEFDHKLEELTRHCSPI  603
```

Figure 3.11: Using pBlast from NCBI, clone 635 (query) was found to encode the major heat shock protein 70 Ab (Sbjct) from *Drosophila melanogaster*. The total length of this protein is 642 amino acids.

library clone, and interaction would probably not be dependent on correct protein folding.

In Figure 3.12 the psiBlast alignment data is seen for clone 409 that encodes the Vitellogin-1 precursor or yolk-1 protein. Vitellogenin is the major yolk protein of eggs where it is used as a food source during embryogenesis. It is only expressed in female flies and is synthesized in the fat body and ovarian follicle cells and accumulates in the oocyte. The protein belongs to the lipase family in the AB hydrolase superfamily (UniProtKB/Swiss-Prot entry P02843). Clone 409 encodes amino acids 215 – 439 (224 in total) of the 439 amino acid yolk-1 protein.

```
>ref|NP_511103.1| Yolk protein 1 CG2985-PA [Drosophila melanogaster]
 gb|AAF46548.1| CG2985-PA [Drosophila melanogaster]
 sp|P02843|VIT1_DROME Vitellogenin-1 precursor (Vitellogenin I) (Yolk protein 1)
 emb|CAA23502.1| unnamed protein product [Drosophila melanogaster]
Length=439

 Score =  447 bits (1150),  Expect = 2e-124
 Identities = 219/225 (97%), Positives = 219/225 (97%), Gaps = 0/225 (0%)

Query  8    TYERYAMLDIEKTGAKIGKWIVQMVNELDMPFDTIHLIGQNXGAHVAGAAAQEFXRLTGH  67
            TYERYAMLDIEKTGAKIGKWIVQMVNELDMPFDTIHLIGQN GAHVAGAAAQEF RLTGH
Sbjct  215  TYERYAMLDIEKTGAKIGKWIVQMVNELDMPFDTIHLIGQNVGAHVAGAAAQEFTRLTGH  274

Query  68   KLRRVTGLDPSKIVAXSKNTLTGLARGDAEFVDAIHTSVYGMGTPIRSGDVDFYPNGPAA  127
            KLRRVTGLDPSKIVA SKNTLTGLARGDAEFVDAIHTSVYGMGTPIRSGDVDFYPNGPAA
Sbjct  275  KLRRVTGLDPSKIVAKSKNTLTGLARGDAEFVDAIHTSVYGMGTPIRSGDVDFYPNGPAA  334

Query  128  GVPGASNVVEAAMRATRYFAXSVRPXNERSFPAVPANSLQQYKQNDGFGKRAYMGIDTAH  187
            GVPGASNVVEAAMRATRYFA SVRP NERSFPAVPANSLQQYKQNDGFGKRAYMGIDTAH
Sbjct  335  GVPGASNVVEAAMRATRYFAESVRPGNERSFPAVPANSLQQYKQNDGFGKRAYMGIDTAH  394

Query  188  DLEGDYFLQVNPKSPFGRNAPAQKQSSYHGVHQAWNTNQDSKDYQ  232
            DLEGDY LQVNPKSPFGRNAPAQKQSSYHGVHQAWNTNQDSKDYQ
Sbjct  395  DLEGDYILQVNPKSPFGRNAPAQKQSSYHGVHQAWNTNQDSKDYQ  439
```

Figure 3.12: Using psiBlast from NCBI, clone 409 (query) was found to encode the Yolk-1 protein (Sbjct) from *Drosophila melanogaster*. The total length of this protein is 439 amino acids. Clone 409 consists of 224 amino acids and aligns with amino acids 215 - 439 of the full length Yolk-1 protein.

3.4 Discussion

The aim of this part of the study was to identify putative binding partners encoded from a *Drosophila melanogaster* cDNA library that interact with AHSV2 NS3 N-terminal amino acids 1 - 118. This study was undertaken based on the lack of knowledge in cellular-viral interactions present in assisting the AHSV to exit insect cells. Both BTV and AHSV are vectored by a small biting midge of the genus *Culicoides* and replicate in both insect and mammalian cells. We know from cell culture studies done that BTV is released from insect cells with no cytopathic effect (CPE) (Homan & Yunker, 1988) while release from mammalian cells is highly cytopathic (Castro *et al*., 1989). BTV and AHSV are released

from infected mammalian cells mainly by cell lysis (Wechsler & McHolland, 1988). BTV release from vector cells (*Culicoides*) is nonlytic and it is postulated that this might be the result of viral budding being used by the virus to escape from the infected insect cells (Hyatt *et al.*, 1989, Hyatt *et al.*, 1993).

We know from studies done on BTV using proteins expressed from mammalian cDNA libraries that NS3 interacts with the p11 protein, part of the Annexin II complex (Beaton *et al.*, 2002) as well as with Tsg101 and Nedd4-like ubiquitin ligases (Wirblich *et al.*, 2006). It has also been shown that AHSV NS3 binds Tsg101 and that both BTV and AHSV NS3 bind to the *Drosophila* homologue of Tsg101. It is thought that the virus buds from an infected cell as follow: Newly assembled viral cores are released from NS2 inclusion bodies and associate with outer capsid proteins VP5 and VP2. NS3 associates with the intracellular trafficking protein p11 and forms a bridge between this protein and newly assembled virus particles by secondary interaction with VP2. This leads to trafficking of the virus particle to the cell membrane where interaction between the PSAP motif in NS3 and the cellular release factor Tsg101 results in the pinching off of vesicles containing virus particles followed by release of mature virion particles from these vesicles (Roy & Noad, 2006).

With this knowledge we set out to identify other insect specific cellular binding partners that could assist the AHSV via its NS3 protein to exit insect cells. We hoped it would shed some light on how the virus might employ different strategies that would enable one to understand why the virus is released lytically from mammalian cells but nonlytically from insect cells. A *Drosophila melanogaster* cDNA library was purchased from Clontech Laboratories, Inc. The library's inserts were cloned as activation domain fusions to be used in the yeast two-hybrid system. The AHSV2 NS3 N-terminal 20 – 274 was used as bait and cloned as a DNA-binding domain fusion. After 850 SD/-Leu/-Trp/-His colonies were screened on SD/-Leu/-Trp/-His/-Ade plates, 19 of the clones that survived were prepared for sequencing. Twelve of the inserts encoded known *Drosophila* protein sequences; these included a ubiquitin protein (matches the *Culicoides* (vector) ubiquitin sequence), 5 proteins from the heat shock 70 family, and the yolk 1 protein. Seven of the 19 clones did not encode any known protein sequences.

The clones that encoded functional protein products were re-screened with NS3 N-terminal 20 - 374 to verify whether they indeed were true interactions. We also included a truncated version of NS3 N-terminal that lacked the coiled-coiled domain at the end of the NS3 N-terminal domain as well as the C-terminal domain of NS3. This was done to investigate the specificity of the interaction. More conclusive results could have been obtained if the *Drosophila* proteins were also tested for interaction with the GAL4 DNA-binding domain (empty pAS2-1 vector) as this could have eliminated false positives such as the yolk protein that showed interaction with both the NS3 N-term (20-374) and NS3

C-term (544-764). Only two clones showed interaction specific to the NS3 N-terminal (amino acids 1 - 118) and not to the truncated NS3 N-terminal of C-terminal domains, namely ubiquitin and Hsp70. The yolk-1 protein showed interaction to both NS3 N-terminal (amino acids 1 - 118) and NS3 C-terminal domains. The Hsp68 protein showed interaction with NS3 N-terminal (amino acids 1 - 118) and to a lesser extent to NS3 N-terminal (amino acids 1 - 92). According to the website (http://www.fccc.edu/research/labs/golemis/Table2.html), heat shock proteins and ubiquitin are commonly found as false positives in cDNA library screens. We decided to continue to investigate the Hsp70 and ubiquitin proteins as literature showed possible roles for these proteins in virus lifecycles.

The clones that did not encode functional protein products were also re-screened with only NS3 N-terminal 20 – 374 to determine the specificity of the yeast two-hybrid system. Only one clone fell out, with 5 others that showed interaction although it must be observed that for some only 1 out of the 4 colonies screened grew most probably indicating non-specific interactions or mutations that took place in those colonies.

The fact that only two positive protein-protein interactions were detected could be explained by the lack of an exhaustive screen. Replica plating yeast colonies from TDO to QDO to β-galactosidase plates would have allowed the screening of all colonies present and not only the colonies picked manually as described. This would definitely have allowed a better representation of the proteins available from the library, and we might therefore still have missed relevant interactors.

As indicated previously, late domains have been found in BTV and AHSV NS3 (Strack *et al.*, 2000, Wirblich *et al.*, 2006). Two of the three classes of late-domain motifs have been identified namely P(T/S)AP and PPXY. The PSAP motif recruits the cellular protein Tsg101. This protein forms part of the ESCRT-I complex (Garrus *et al.*, 2001, Martin-Serrano *et al.*, 2001, Martin-Serrano *et al.*, 2003b). The PPXY motif plays a role in recruiting host ubiquitin ligases (Blot et al., 2004, Bouamr et al., 2003, Kikonyogo et al., 2001, von Schwedler et al., 2003). The identification of a Drosophila ubiquitin protein that interacts specifically with the N-terminal of AHSV was very interesting. The PPXY motif, which has been shown in retroviruses to recruit host ubiquitin ligases, is present in the N-terminal of BTV and AHSV NS3, although not highly conserved throughout the different AHSV serotypes. In AHSV2 NS3 the motif is present as PPPY between amino acids 25 – 28. Wirblich *et al.,* (2006) showed that BTV NS3 (PPRY) showed interaction with GST-tagged WW domains of NEDD4.1, WWP1, and Itch. These are three different ubiquitin ligases shown to be recruited by retroviruses needed for the budding process. It has been shown that the Gag protein (nuclear capsid protein) of HIV-1, human T-cell leukemia virus type 1 and Rous sarcoma virus bind via their PPXY motif to various ubiquitin

ligases (Bouamr et al., 2003, Kikonyogo et al., 2001, Martin-Serrano et al., 2004, Strack et al., 2000, von Schwedler et al., 2003).

Not only ubiquitin ligases, but also ubiquitin was found to interact with the Gag protein. Ubiquitin is a small, highly abundant protein that can be covalently attached to certain Lys residues in target proteins (Hershko & Ciechanover, 1998). AHSV NS3 serotype 2 contains 8 Lysine residues (spaced out in protein) in the N-terminal situated more to the end of the N-terminal domain (amino acids 65 – 114). Four of these lysines are present in the 26 amino acids that are truncated from NS3 N-terminal amino acids 1 – 92 protein. It could be that the four lysines present in the last 26 amino acids of the NS3 N-terminal domain could play a significant role in binding ubiquitin. Ubiquitin binds target proteins to modify them post-translationally to function in particular cellular responses that include degradation (Driscoll & Goldberg, 1990, McGuire *et al.*, 1988), protein trafficking and transcription activation (Babst *et al.*, 2000, Hicke & Riezman, 1996, Salghetti *et al.*, 2001). It has been shown that ubiquitination in itself also has an effect on viral release. Several retroviruses contain free, virion-associated ubiquitin (Putterman *et al.*, 1990) and a small amount of mono-ubiquitylated Gag. It has been found that poly-ubiquitylated proteins are known to be associated with their degradation through the proteasome (Haglund & Dikic, 2005). More recently is has been proposed that the mono-ubiquitination of proteins may result in their targeting to the endosomal/lysosomal compartment where either degradation or further processing may occur (Hoeller *et al.*, 2006). It is also thought that mono-ubiquitination tags membrane-associated proteins for internalization and/or sorting into the endosomal pathway (Demirov & Freed, 2004).

It has been postulated that by depleting the intracellular pools of free ubiquitin, proteasome inhibitors limit the extent to which Gag is ubiquitylated, therefore resulting in a disruption in viral budding (Demirov & Freed, 2004). The importance of ubiquitin associated Gag was supported by a study that showed that virus like particles generated with Gag-Ubiquitin fusion proteins were partially resistant to proteasome inhibitors (Patnaik *et al.*, 2000). Another study also showed that cumulative mutations of ubiquitin acceptor sites in HIV-1 Gag caused a late budding defect. These results indicated that ubiquitination of lysine residues in Gag in the vicinity of the viral late domain is important for HIV-1 budding (Gottwein *et al.*, 2006).

The role that ubiquitination and association of the ubiquitin ligases have on viral budding can be summarized as seen in Figure 3.13 (Putterman et al., 1990). After the newly assembled virus has reached the host plasma membrane and prepared for exiting by forming a spherical particle ready to pinch off, some ubiquitin molecules both free and conjugated to Gag, are present in the virus. A ubiquitin ligase is recruited to the site of budding by the PXXY late domain present in the Gag protein.

This ligase forms a bridge, binding ubiquitin to some of the Gag molecules and perhaps to cellular proteins. These ubiquitin conjugates may interact with other cellular proteins that will set up the machinery to pinch off the virus bud (Putterman et al., 1990). The machinery that catalyzes Gag ubiquitination has not been identified and ongoing research is focusing on this aspect.

The role the ubiquitin protein could play in orbivirus release is another study on itself – one difference being that orbiviruses do not contain a lipid envelope that in itself allows viruses such as HIV to bud. Also, enveloped viruses such as HIV contain a nuclear capsid protein, Gag that allows interaction with the multivesicular body machinery via the presence of late domains. For orbiviruses such as BTV and AHSV, the nonstructural protein NS3 contains similar late domains that could possibly help these viruses to bud from host cells. A functional study possibly including cells lacking ubiquitin could shed some light on whether this cellular protein indeed has any real effect on the virus exit. Also, whether the late domains present in AHSV NS3 interact with ubiquitin or ubiquitin ligase. Another factor would also be how NS3 is ubiquitylated, whether mono-ubiquitylated or poly-ubiquitylated NS3 is needed.

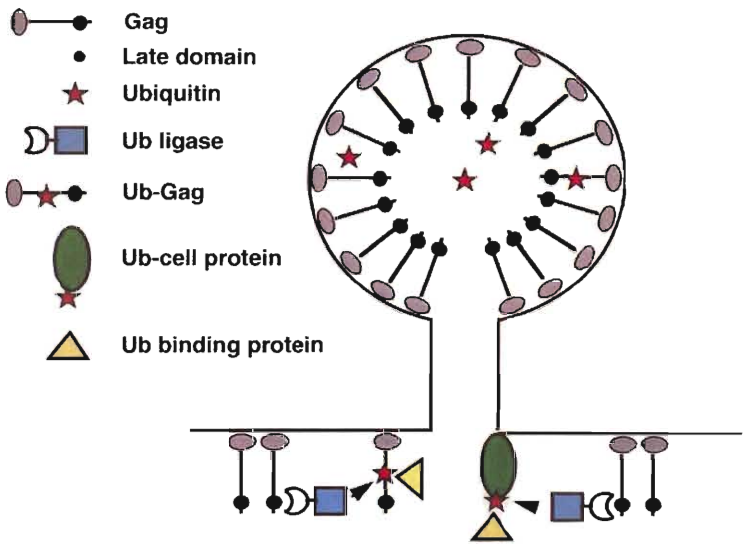

Figure 3.13: Speculative representation of late stage in retroviral budding. The Gag molecules have formed a spherical particle ready to pinch off from the plasma membrane. Some ubiquitin molecules (red star), both free and conjugated to Gag, are present in the nascent virus. A ubiquitin ligase (blue rectangle) is recruited to the site of budding by the Gag late domain, and it conjugates ubiquitin to some of the Gag molecules and perhaps to cellular proteins (green oval). Other cellular proteins (yellow triangle) may bind to these ubiquitin conjugates, setting up the machinery to pinch off the virus bud (Image and description taken from Vogt, 2000).

In a very recent study done in hepatitis C virus (HCV), the authors investigated the role of ubiquitination in the production of the viral core protein. This protein is a major component of the viral nucleocapsid and a multifunctional protein involved in viral pathogenesis and hepatocarcinogenesis. They found that this protein is degraded through the ubiquitin-proteasome pathway and that the

ubiquitin ligase E6AP mediates ubiquitination and degradation of the HCV core protein via this pathway. They proposed that the E6AP-mediated ubiquitin-proteasome pathway may affect the production of HCV particles through controlling the amounts of viral nucleocapsid protein (Shirakura *et al.*, 2006). They also found in other studies done that other HCV proteins such as the nonstructural proteins NS5B (Gao *et al.*, 2003) and NS2 (Franck *et al.*, 2005) are also degraded through the ubiquitin-proteasome pathway.

In a study done on the rotavirus NSP1 protein, it was found that this protein can act as an E3-ubiquitin ligase, but also can auto regulate its expression by binding ubiquitin that targets the protein for degradation via a proteasome-dependent pathway. NSP1 is a down-regulator of the interferon response, since it binds to the interferon regulatory factor 3 (IRF3) and induces its degradation. This interferon response is initiated by the host cell when infected by the rotavirus. The study showed that NSP1 can act as an ubiquitin ligase by recruiting the IRF3, allowing ubiquitination of the IRF3 that targets the protein for degradation. NSP1 also allows self ubiquitination, regulating its own expression levels in the infected cells. It was found that a RING finger motif (7 conserved cysteines and one histidine coordinating two zinc atoms in a cross-braced structure) in NSP1 can explain its proteasome susceptibility as well as its ability to induce IRF3 degradation via a proteasome-dependent pathway (Pina-Vazquez *et al.*, 2007).

The other protein that showed interaction with our bait, NS3 N-terminal 20 – 274, was the heat shock protein 70 Ab (Hsp70). Hsp70 is quite a common protein involved in protein folding reactions. It has also been shown to be important for protein translocation across membranes of organelles and is thought to catalyze protein assembly. Hsp70 also has the ability to bind to many proteins of different structures during their translation (Pratt, 1993). Recent literature shows the relevance of the Hsp70 family members in virus entry and virus replication in rotavirus, another member of the *Reoviridae* family. The heat shock cognate protein 70 (Hsc70) has been proposed to be involved during rotavirus entry at a post-binding step, probably during penetration (Lopez & Arias, 2004, Perez-Vargas *et al.*, 2006). It has been shown that heat-stress facilitates the replication of rotaviruses in baby hamster kidney (BHK) cells during cell entry, as well as at a post-entry stage (Lopez *et al.*, 2006).

Another study showed that Hsp70 is rapidly, specifically and transiently induced upon rotavirus infection of intestinal cells. Hsp70 was specifically identified in lipid rafts that were obtained from intestinal epithelial Caco-2 cells. This is a cell line for which the well-polarized and enterocyte-like phenotype closely corresponds to the natural in vivo target of rotavirus. This Hsp70 induction was not a general response to viral infection, but instead shown to be a highly specific response both with regard to the infecting virus, and the host cell. In these Caco-2 cells, Hsp70 silencing was associated

with an increased virus protein level and an enhanced progeny production. Upon Hsp70 silencing, they also observed that the ubiquitination of the main rotavirus structural proteins was strongly reduced. When they used proteasome inhibitors, this induced an accumulation of bioavailability of viral proteins within the cells for virus morphogenesis (Broquet *et al.*, 2006).

The significance of the last few paragraphs can be pointed out in the observation that in two different viruses (rotavirus and HCV), both the ubiquitin and the Hsp70 proteins play a role in regulating the bioavailability of viral proteins in an infected host cell. NS3 seems to be differentially regulated in different cell types, with low expression in mammalian cells (French *et al.*, 1989) when compared to insect cells (Guirakhoo *et al.*, 1995). Up to date, no explanation could be given except for the assumption that the increased NS3 expression in insect cells could be linked to the virus preferring NS3 mediated budding over lytic release in these cells resulting in the low CPE observed (Homan & Yunker, 1988, Wechsler & McHolland, 1988). Therefore it could be that ubiquitin together with the Hsp70 regulate the availability of the NS3 protein, explaining the differences seen the viral exit between mammalian and insect cells.

To conclude, by using the proteins expressed from a *Drosophila melanogaster* cDNA library and the AHSV2 NS3 N-terminal domain (amino acids 1 - 118) as bait we wanted to investigate possible viral-cellular protein-protein interactions that could take place in the vector (*Culicoides*) relating to virus exit. We hoped to find cellular proteins potentially involved in regulating or mediating aspects of virus trafficking or release. We identified two cDNA library clones (Ubiquitin and Hsp70) that specifically interacted with our bait and not with any other domains in the NS3 protein. It seems that the ubiquitin protein could play a role in AHSV release, but further functional analysis would be needed to shed more light on the relevancy of ubiquitin. The other scenario including both ubiquitin and the Hsp70 in possibly regulating the bioavailability of the NS3 protein is a hypothesis to investigate. It would explain the different levels of NS3 present in mammalian versus insect cells, and therefore have an effect in controlling budding versus lytic release. By using the yeast two-hybrid assay, it allowed us to quickly and efficiently scan a cDNA library for protein-protein interactions of significance. This was the first step in unravelling the secrets of viral release in AHSV; many more studies will be needed to sufficiently comprehend the questions and answers gained to produce a picture of this virus's lifecycle.

Concluding remarks

We have set out to investigate viral and cellular protein-protein interaction in AHSV. Our study was based on results obtained for BTV, the prototype virus of the *Orbivirus* genus. Here it was shown that a membrane protein NS3, presumably forms a bridging molecule across the plasma membrane and associates with the outer capsid protein, VP2 present on newly formed BTV virions, with its cytosolic C-terminal domain and with a host cellular protein, p11 (part of exocytosis pathway) with its cytosolic N-terminal domain. With this NS3-mediated mechanism, the BTV would then literally hi-jack the host exocytosis pathway and allow the newly formed BTV virions to exit the host cell, presumably via budding. We wanted to see whether these same mechanisms could be at work in AHSV. We decided to use the yeast two-hybrid system to investigate VP2 – NS3 interaction as well as NS3 – insect cell protein interaction. To ensure consistency, we also used the GST pull-down and membrane flotation assay to investigate NS3 – VP2 protein-protein interaction. As the BTV study utilised a mammalian (human) cDNA library to identify the p11 protein, we wanted to investigate whether any other significant proteins from an insect (*Drosophila melanogaster*) cDNA library could be detected. We expected to find evidence supporting the hypothesis that the virus would use budding to exit *Culicoides* cells (vector of AHSV) as no severe CPE is seen in infected cells.

For the investigation of AHSV NS3 – VP2 interaction, no conclusive results were obtained. The yeast two-hybrid system and GST pull-down assay failed to show any interaction, although the positive control provided with the yeast two-hybrid system worked. The GST pulldown results portrayed results that showed that NS3 and VP2 did not interact under the conditions used. But these results are also inconclusive as we did not have a positive control for this assay. The only preliminary evidence of interaction was observed with the membrane flotation assay. Here the VP2 protein had an effect on the position of NS3 in the gradient. But individually expressed VP2 was also present in the upper fractions of the gradient, where the protein was not expected – making this experiment unconvincing. As most of the problems arose due to NS3 or VP2 not being expressed in their native environment, leading to improper protein folding and aggregation, the next step should be to test these proteins in their native form as they are expressed in insect cells. The way to do this would be to use confocal microscopy and monoclonal antibodies specific to NS3 and VP2. Co-localization of NS3 and VP2 would suggest protein-protein interaction.

Positive results were obtained for the NS3 – *Drosophila* cDNA library screening study. Ubiquitin and a heat shock 70 protein were retrieved as potential role players in the questions posed relating to viral cell exiting. The Gag protein (nuclear capsid protein) of retroviruses contains late domains that recognize and associate with cellular proteins such as Tsg101 and ubiquitin ligases. It has been

shown that these associations are needed for the retrovirus to successfully bud from infected host cells. These retroviruses also bind to cellular ubiquitin that plays a role in the pinching off of budding vesicles from the plasma membrane. Only recently evidence was found for the presence of these late domains in the NS3 protein of BTV and AHSV. Interaction between Tsg101 and BTV/AHSV NS3 were shown, as well as interaction between ubiquitin ligases and BTV NS3. The role ubiquitin could play in the release of BTV or AHSV is unknown although budding seems to be a method of virus release for AHSV, it makes sense that NS3 could recruit ubiquitin to enable the newly assembled virus particles to bud from the cellular membrane explaining the non cytotoxic release seen in insect cells

The latest information shows that ubiquitin and Hsp70 could influence the bioavailability of viral proteins as seen in studies done by Broquet *et al.* (2007) and Shirakura *et al.* (2007). Our study showed that the NS3 N-terminal (amino acids 1 - 118) specifically interacted with ubiquitin and Hsp70. It could be that the difference in NS3 levels seen between mammalian cells and insect cells could be explained by ubiquitin/Hsp70 association. Furthermore, this regulation of NS3 could shed even more light on how increased levels of NS3 results in budding and reduced levels of NS3 results in lytic release.

With the positive results of the discovery of ubiquitin and Hsp70 as cellular binding partners to NS3, a novel discovery has been made. For AHSV, variation seen in NS3 between the different serotypes pose interesting questions, as this variation is not present in other orbiviruses. It could be interesting to investigate whether the different AHSV serotypes differs in their association with ubiquitin and Hsp70. Also a knockout experiment using siRNAs to inhibit ubiquitin and Hsp70 production could enlighten us in the effect these protein have on viral release or even other aspects in the virus morphogenesis. It should also be investigated whether the *Culicoides* protein homologues to Hsp70 and ubiquitin interact with the NS3 N-terminal as been shown by the *Drosophila* homologues in this study. With the knowledge gained from these studies, one would hope to better understand the morphogenesis and lifecycle of the virus, which in the end would lead to better control of the virus.

Scientific publications

Some results of this study were presented in the form of poster presentations at national and international meetings:

Beyleveld M, Van Staden V and Huismans H (2006) Investigating viral and cellular protein-protein interaction in African horsesickness virus, South African Genetics Society 19th conference, Bloemfontein, South Africa, 3 - 5 April 2006.

Beyleveld M, Van Staden V and Huismans H (2006) Screening of a *Drosophila* cDNA library for protein-protein interaction with African horsesickness virus membrane protein NS3, 9th International symposium on double stranded RNA viruses, Cape town, South Africa, 22 – 27 October 2006.

Appendix

LIST OF FIGURES AND TABLES

List of figures and tables in chapter 1

List of figures and tables in chapter 2

List of figures and tables in chapter 3

LIST OF ABBREVIATIONS

3-AT	3-amino-1,2,4-triazol
a.a.	amino acid
AD	Activation domain
Ade	Adenine
Ado Met	S-adenosyl -L-methionine
AHSV	African horsesickness virus
BHK	Baby hamster kidney cells
bp	Base pairs
BTV	Bluetongue virus
cDNA	Complimentary deoxyribonucleic acid
CPE	Cytopathic effect
DDO	Double dropout
DNA-BD	DNA binding domain
dNTP	Deoxyribonucleotide triphosphate
dsRNA	Double stranded RNA
E. coli	*Escherichia coli*
EDTA	Ethylenediaminetetra-acetic acid
ER	Endoplasmic reticulum
ESCRT	Escort
FRET	Fluorescence resonance energy transfer
Fwd	Forward
GAL	Galactosidase
GFP	Green fluorescent protein
GST	Gluthione-S-transferase
His	Histidine
HIV	Human immunodeficiency syndrome
Hsc	Heat-shock cognate
Hsp	Heat-shock protein
IPTG	Isopropyl-β-D-thiogalactopyranoside
ISVP	Intermediate subviral particles
Kb	kilobase
L(number)	Large segment
LB-broth	Luria Bertani broth
L-domain	Late domain
Leu	Leucine
LiAc	Lithium acetate
M(number)	Medium segment
MOI	Multiplicity of infection
NS(number)	Nonstructural
NSP(number)	Nonstructural protein
ORF	Open reading frame
PAGE	Polyacrylamide gel electrophoresis
PBS	Phosphate buffered saline
PCR	Polymerase chain reaction
pfu	plaque forming units
p.i.	post infection
PSB	Protein solvent buffer
QDO	Quadruple dropout
Rev	Reverse
S(number)	Small segment
SD medium	Standard deficient medium

SDS	Sodium dodecyl sulphate
Sf9	*Spodoptera frugiperda* insect cells
ssRNA	Single stranded RNA
TDO	Triple dropout
TGN	Trans-Golgi network
Trp	Tryptophan
UAS	Upstream activation site
UHQ	Ultra high quality
VIB	Viral inclusion body
VP(number)	Viral protein
YPD	Yeast extract, Peptone and Dextrose

METRICAL UNITS

U	Units
kD or KDa	kilo dalton
M	Molar
mM	milli molar
nm	nanometre
rpm	revolution per minute
w/v	weight/volume
µg	micrograms
µl	micro litre

PLASMID MAPS

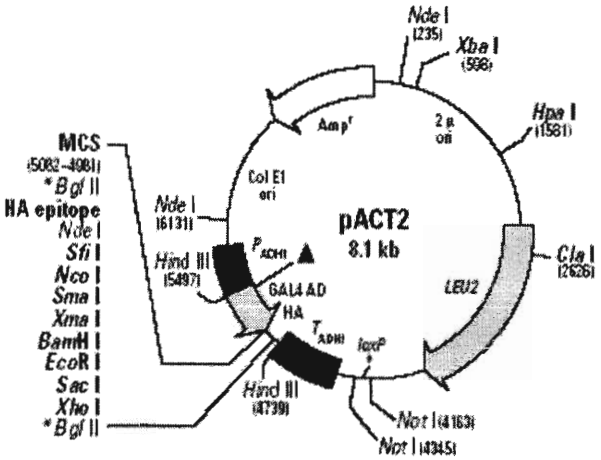

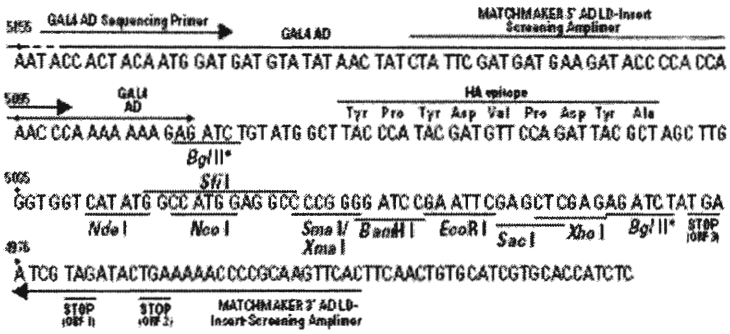

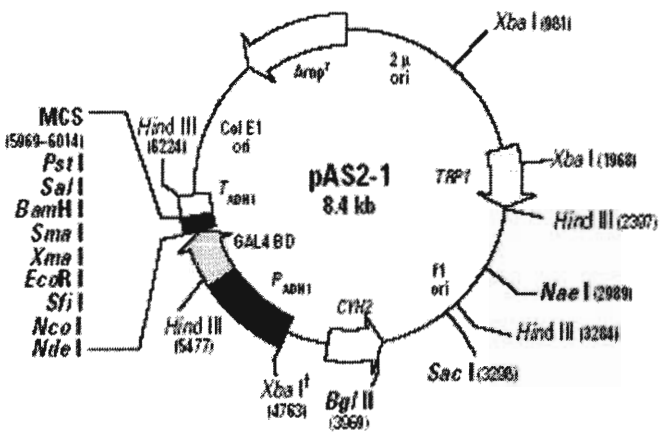

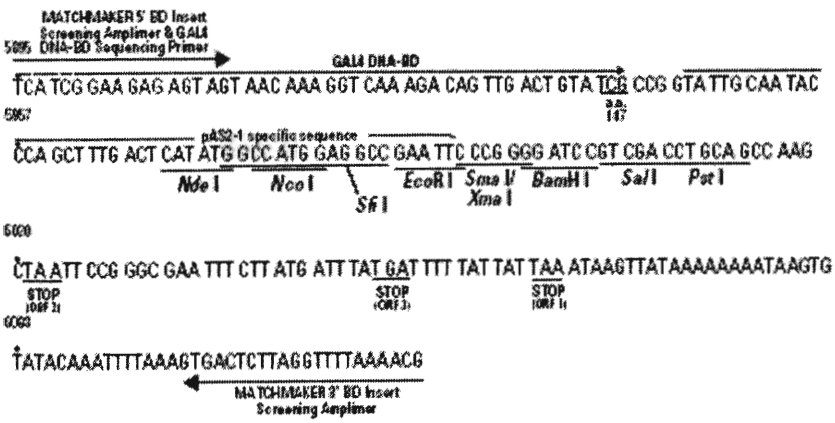

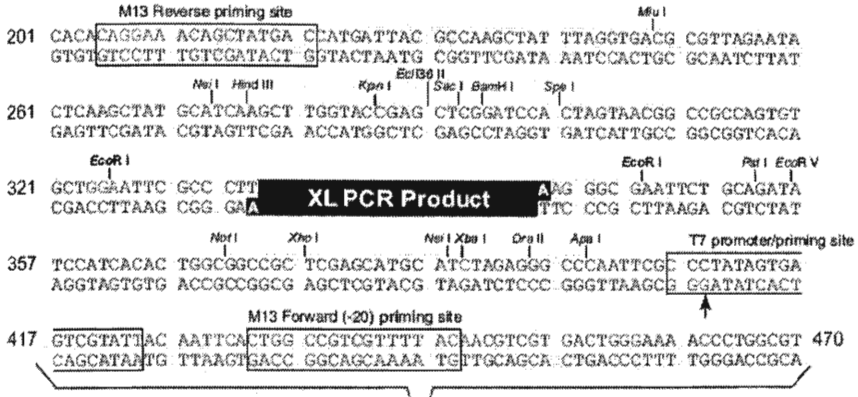
M13 Reverse priming site
Mlu I
201 CACACAGGAA ACAGCTATGA CCATGATTAC GCCAAGCTAT TTAGGTGACG CGTTAGAATA
GTGTGTCCTT TGTCGATACT GGTACTAATG CGGTTCGATA AATCCACTGC GCAATCTTAT
Nsi I Hind III Kpn I EcI136 II Sac I BamH I Spe I
261 CTCAAGCTAT GCATCAAGCT TGGTACCGAG CTCGGATCCA CTAGTAACGG CCGCCAGTGT
GAGTTCGATA CGTAGTTCGA ACCATGGCTC GAGCCTAGGT GATCATTGCC GGCGGTCACA
EcoR I
EcoR I Pst I EcoR V
321 GCTGGAATTC GCC CTT XL PCR Product AAG GGC GAATTCT GCAGATA
CGACCTTAAG CGG GAA TTC CCG CTTAAGA CGTCTAT
Not I Xho I Nsi I Xba I Dra II Apa I
T7 promoter/priming site
357 TCCATCACAC TGGCGGCCGC TCGAGCATGC ATCTAGAGGG CCCAATTCGC CCTATAGTGA
AGGTAGTGTG ACCGCCGGCG AGCTCGTACG TAGATCTCCC GGGTTAAGCG GGATATCACT
M13 Forward (-20) priming site
417 GTCGTATTAC AATTCACTGG CCGTCGTTTT ACAACGTCGT GACTGGGAAA ACCCTGGCGT 470
CAGCATAATG TTAAGTGACC GGCAGCAAAA TGTTGCAGCA CTGACCCTTT TGGGACCGCA

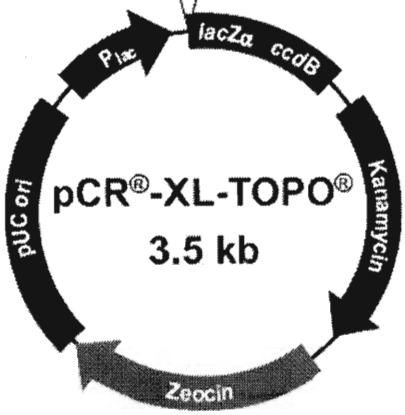
pCR®-XL-TOPO®
3.5 kb
P lac
lacZα ccdB
Kanamycin
Zeocin
pUC ori

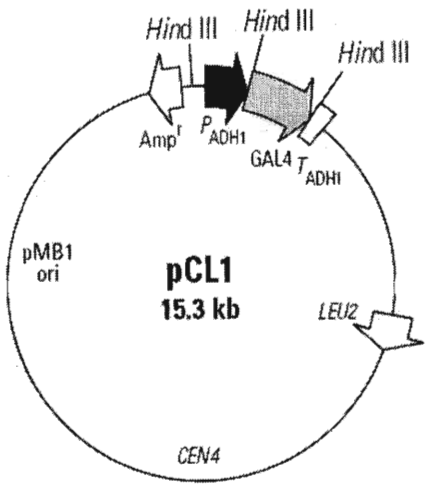
Hind III
Hind III
Hind III
Amp r
P ADH1
GAL4
T ADH1
pMB1
ori
pCL1
15.3 kb
LEU2
CEN4

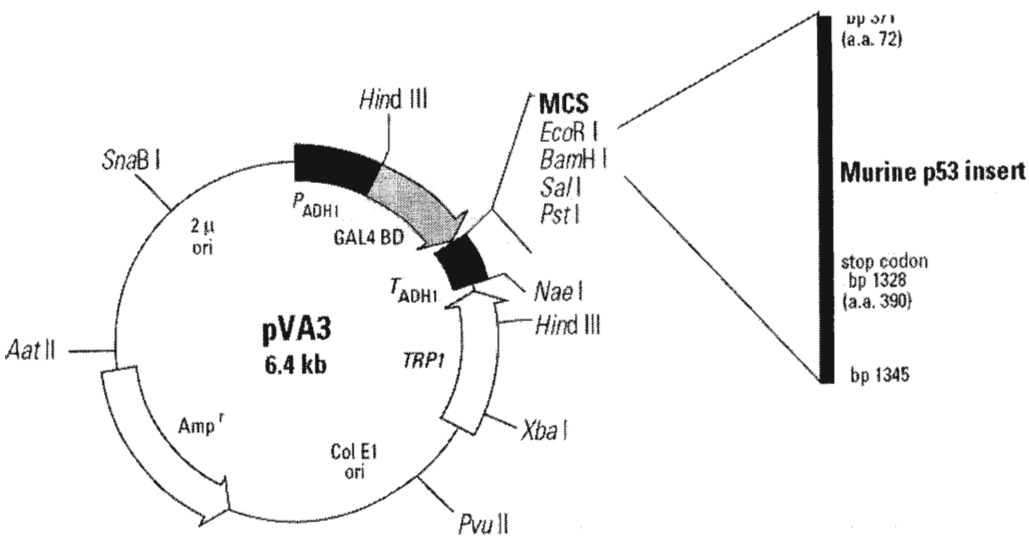
Hind III
MCS
EcoR I
BamH I
Sal I
Pst I
SnaB I
P ADH1
GAL4 BD
2 µ
ori
T ADH1
Nae I
Hind III
Aat II
pVA3
6.4 kb
TRP1
Amp r
Col E1
ori
Xba I
Pvu II
bp 371
(a.a. 72)
Murine p53 insert
stop codon
bp 1328
(a.a. 390)
bp 1345

References

Arias, C. F., Dector, M. A., Segovia, L., Lopez, T., Camacho, M., Isa, P., Espinosa, R. & Lopez, S. (2004). RNA silencing of rotavirus gene expression. *Virus Res* **102**, 43-51.

Arias, C. F., Isa, P., Guerrero, C. A., Mendez, E., Zarate, S., Lopez, T., Espinosa, R., Romero, P. & Lopez, S. (2002). Molecular biology of rotavirus cell entry. *Arch Med Res* **33**, 356-61.

Babst, M. (2005). A protein's final ESCRT. *Traffic* **6**, 2-9.

Babst, M., Katzmann, D. J., Estepa-Sabal, E. J., Meerloo, T. & Emr, S. D. (2002a). Escrt-III: an endosome-associated heterooligomeric protein complex required for mvb sorting. *Dev Cell* **3**, 271-82.

Babst, M., Katzmann, D. J., Snyder, W. B., Wendland, B. & Emr, S. D. (2002b). Endosome-associated complex, ESCRT-II, recruits transport machinery for protein sorting at the multivesicular body. *Dev Cell* **3**, 283-9.

Babst, M., Odorizzi, G., Estepa, E. J. & Emr, S. D. (2000). Mammalian tumor susceptibility gene 101 (TSG101) and the yeast homologue, Vps23p, both function in late endosomal trafficking. *Traffic* **1**, 248-58.

Barton, E. S., Forrest, J. C., Connolly, J. L., Chappell, J. D., Liu, Y., Schnell, F. J., Nusrat, A., Parkos, C. A. & Dermody, T. S. (2001). Junction adhesion molecule is a receptor for reovirus. *Cell* **104**, 441-51.

Basak, A. K., Gouet, P., Grimes, J., Roy, P. & Stuart, D. (1996). Crystal structure of the top domain of African horse sickness virus VP7: comparisons with bluetongue virus VP7. *J Virol* **70**, 3797-806.

Basak, A. K., Grimes, J. M., Gouet, P., Roy, P. & Stuart, D. I. (1997). Structures of orbivirus VP7: implications for the role of this protein in the viral life cycle. *Structure* **5**, 871-83.

Beaton, A. R., Rodriguez, J., Reddy, Y. K. & Roy, P. (2002). The membrane trafficking protein calpactin forms a complex with bluetongue virus protein NS3 and mediates virus release. *Proc Natl Acad Sci U S A* **99**, 13154-9.

Becker, M. M., Peters, T. R. & Dermody, T. S. (2003). Reovirus sigma NS and mu NS proteins form cytoplasmic inclusion structures in the absence of viral infection. *J Virol* **77**, 5948-63.

Bhattacharya, P. & Roy, P. (2006). Interaction of BTV VP2 with celular factors during virus maturation. In *9th dsRNA virus symposium*, pp. 52. Capetown, Bantry bay.

Blot, V., Perugi, F., Gay, B., Prevost, M. C., Briant, L., Tangy, F., Abriel, H., Staub, O., Dokhelar, M. C. & Pique, C. (2004). Nedd4.1-mediated ubiquitination and subsequent recruitment of Tsg101 ensure HTLV-1 Gag trafficking towards the multivesicular body pathway prior to virus budding. *J Cell Sci* **117**, 2357-67.

Borsa, J., Morash, B. D., Sargent, M. D., Copps, T. P., Lievaart, P. A. & Szekely, J. G. (1979). Two modes of entry of reovirus particles into L cells. *J Gen Virol* **45**, 161-70.

Bouamr, F., Melillo, J. A., Wang, M. Q., Nagashima, K., de Los Santos, M., Rein, A. & Goff, S. P. (2003). PPPYVEPTAP motif is the late domain of human T-cell leukemia virus type 1 Gag and mediates its functional interaction with cellular proteins Nedd4 and Tsg101 [corrected]. *J Virol* **77**, 11882-95.

Boyce, M., Wehrfritz, J., Noad, R. & Roy, P. (2004). Purified recombinant bluetongue virus VP1 exhibits RNA replicase activity. *J Virol* **78**, 3994-4002.

Bremer, C. W. (1976). A gel electrophoretic study of the protein and nucleic acid components of African horsesickness virus. *Onderstepoort J Vet Res* **43**, 193-9.

Briggs, J. A., Wilk, T. & Fuller, S. D. (2003). Do lipid rafts mediate virus assembly and pseudotyping? *J Gen Virol* **84**, 757-68.

Brignati, M. J., Loomis, J. S., Wills, J. W. & Courtney, R. J. (2003). Membrane association of VP22, a herpes simplex virus type 1 tegument protein. *J Virol* **77**, 4888-98.

Brookes, S. M., Hyatt, A. D. & Eaton, B. T. (1993). Characterization of virus inclusion bodies in bluetongue virus-infected cells. *J Gen Virol* **74**, 525-30.

Broquet, A. H., Lenoir, C., Gardet, A., Sapin, C., Chwetzoff, S., Jouniaux, A. M., Lopez, S., Trugnan, G., Bachelet, M. & Thomas, G. (2006). Hsp70 Negatively Controls Rotavirus Protein Bioavailability in Caco-2 Cells Infected by the Rotavirus Rf Strain. *J Virol*.

Campbell, M. K. (1999). Biochemistry. In *Saunders Golden Sunburst Series*, Third edn, pp. 725: Harcourt College Publishers.

Castro, A. E., Montague, S. R., Dotson, J. F., Jessup, D. A. & DeForge, J. R. (1989). Susceptibility of a fetal tongue cell line derived from bighorn sheep to five serotypes of bluetongue virus and its potential for the isolation of viruses. *J Vet Diagn Invest* **1**, 247-53.

Chazal, N. & Gerlier, D. (2003). Virus entry, assembly, budding, and membrane rafts. *Microbiol Mol Biol Rev* **67**, 226-37, table of contents.

Chevalier, C., Galloux, M., Pous, J., Henry, C., Denis, J., Da Costa, B., Navaza, J., Lepault, J. & Delmas, B. (2005). Structural peptides of a nonenveloped virus are involved in assembly and membrane translocation. *J Virol* **79**, 12253-63.

Chuma, T., Le Blois, H., Sanchez-Vizcaino, J. M., Diaz-Laviada, M. & Roy, P. (1992). Expression of the major core antigen VP7 of African horsesickness virus by a recombinant baculovirus and its use as a group-specific diagnostic reagent. *J Gen Virol* **73 (Pt 4)**, 925-31.

Cowley, J. A. & Gorman, B. M. (1987). Genetic reassortants for identification of the genome segment coding for the bluetongue virus hemagglutinin. *J Virol* **61**, 2304-6.

Craven, R. C., Harty, R. N., Paragas, J., Palese, P. & Wills, J. W. (1999). Late domain function identified in the vesicular stomatitis virus M protein by use of rhabdovirus-retrovirus chimeras. *J Virol* **73**, 3359-65.

Creighton, T. E. (1984). Proteins-Structures and Molecular Properties, pp. 498: W.H. Freeman and Company.

Cuadras, M. A., Bordier, B. B., Zambrano, J. L., Ludert, J. E. & Greenberg, H. B. (2006). Dissecting rotavirus particle-raft interaction with small interfering RNAs: insights into rotavirus transit through the secretory pathway. *J Virol* **80**, 3935-46.

De Sa, R. O., Zellner, M. & Grubman, M. J. (1994). Phylogenetic analysis of segment 10 from African horsesickness virus and cognate genes from other orbiviruses. *Virus Res* **33**, 157-65.

Demirov, D. G. & Freed, E. O. (2004). Retrovirus budding. *Virus Res* **106**, 87-102.

Devaney, M. A., Kendall, J. & Grubman, M. J. (1988). Characterization of a nonstructural phosphoprotein of two orbiviruses. *Virus Res* **11**, 151-64.

Dimitrova, M., Imbert, I., Kieny, M. P. & Schuster, C. (2003). Protein-protein interactions between hepatitis C virus nonstructural proteins. *J Virol* **77**, 5401-14.

Drewes, G. & Bouwmeester, T. (2003). Global approaches to protein-protein interactions. *Curr Opin Cell Biol* **15**, 199-205.

Driscoll, J. & Goldberg, A. L. (1990). The proteasome (multicatalytic protease) is a component of the 1500-kDa proteolytic complex which degrades ubiquitin-conjugated proteins. *J Biol Chem* **265**, 4789-92.

du Plessis, M., Cloete, M., Aitchison, H. & Van Dijk, A. A. (1998). Protein aggregation complicates the development of baculovirus-expressed African horsesickness virus serotype 5 VP2 subunit vaccines. *Onderstepoort J Vet Res* **65**, 321-9.

Eaton, B. T. & Crameri, G. S. (1989). The site of bluetongue virus attachment to glycophorins from a number of animal erythrocytes. *J Gen Virol* **70**, 3347-53.

Eaton, B. T., Hyatt, A. D. & White, J. R. (1988). Localization of the nonstructural protein NS1 in bluetongue virus-infected cells and its presence in virus particles. *Virology* **163**, 527-37.

Eichwald, C., Rodriguez, J. F. & Burrone, O. R. (2004). Characterization of rotavirus NSP2/NSP5 interactions and the dynamics of viroplasm formation. *J Gen Virol* **85**, 625-34.

Fields, S. & Bartel, P. L. (2001). The two-hybrid system: A personal view. In *Two hybrid systems - Methods and Protocols*, pp. 3 - 8. Edited by P. N. MacDonald. Totowa, New Jersey: Humana Press.

Fields, S. & Song, O. (1989). A novel genetic system to detect protein-protein interactions. *Nature* **340**, 245-6.

Fillmore, G. C., Lin, H. & Li, J. K. (2002). Localization of the single-stranded RNA-binding domains of bluetongue virus nonstructural protein NS2. *J Virol* **76**, 499-506.

Filter, R. D. (2000). Characterisation and co-expression of the two outer capsid proteins of African Horsesickness virus serotype 3. In *Msc thesis*.

Franck, N., Le Seyec, J., Guguen-Guillouzo, C. & Erdtmann, L. (2005). Hepatitis C virus NS2 protein is phosphorylated by the protein kinase CK2 and targeted for degradation to the proteasome. *J Virol* **79**, 2700-8.

Freed, E. O. (2002). Viral late domains. *J Virol* **76**, 4679-87.

Freed, E. O. (2004). Mechanisms of enveloped virus release. *Virus Res* **106**, 85-6.

French, T. J., Inumaru, S. & Roy, P. (1989). Expression of two related nonstructural proteins of bluetongue virus (BTV) type 10 in insect cells by a recombinant baculovirus: production of polyclonal ascitic fluid and characterization of the gene product in BTV-infected BHK cells. *J Virol* **63**, 3270-8.

French, T. J., Marshall, J. J. & Roy, P. (1990). Assembly of double-shelled, viruslike particles of bluetongue virus by the simultaneous expression of four structural proteins. *J Virol* **64**, 5695-700.

Gao, L., Tu, H., Shi, S. T., Lee, K. J., Asanaka, M., Hwang, S. B. & Lai, M. M. (2003). Interaction with a ubiquitin-like protein enhances the ubiquitination and degradation of hepatitis C virus RNA-dependent RNA polymerase. *J Virol* **77**, 4149-59.

Garrus, J. E., von Schwedler, U. K., Pornillos, O. W., Morham, S. G., Zavitz, K. H., Wang, H. E., Wettstein, D. A., Stray, K. M., Cote, M., Rich, R. L., Myszka, D. G. & Sundquist, W. I. (2001). Tsg101 and the vacuolar protein sorting pathway are essential for HIV-1 budding. *Cell* **107**, 55-65.

Gosselin-Grenet, A. S., Mottet-Osman, G. & Roux, L. (2006). From assembly to virus particle budding: pertinence of the detergent resistant membranes. *Virology* **344**, 296-303.

Gottwein, E., Jager, S., Habermann, A. & Krausslich, H. G. (2006). Cumulative mutations of ubiquitin acceptor sites in human immunodeficiency virus type 1 gag cause a late budding defect. *J Virol* **80**, 6267-75.

Gouet, P., Diprose, J. M., Grimes, J. M., Malby, R., Burroughs, J. N., Zientara, S., Stuart, D. I. & Mertens, P. P. (1999). The highly ordered double-stranded RNA genome of bluetongue virus revealed by crystallography. *Cell* **97**, 481-90.

Grimes, J. M., Burroughs, J. N., Gouet, P., Diprose, J. M., Malby, R., Zientara, S., Mertens, P. P. & Stuart, D. I. (1998). The atomic structure of the bluetongue virus core. *Nature* **395**, 470-8.

Grimes, J. M., Jakana, J., Ghosh, M., Basak, A. K., Roy, P., Chiu, W., Stuart, D. I. & Prasad, B. V. (1997). An atomic model of the outer layer of the bluetongue virus core derived from X-ray crystallography and electron cryomicroscopy. *Structure* **5**, 885-93.

Grubman, M. J. & Lewis, S. A. (1992). Identification and characterization of the structural and nonstructural proteins of African horsesickness virus and determination of the genome coding assignments. *Virology* **186**, 444-51.

Guirakhoo, F., Catalan, J. A. & Monath, T. P. (1995). Adaptation of bluetongue virus in mosquito cells results in overexpression of NS3 proteins and release of virus particles. *Arch Virol* **140**, 967-74.

Haglund, K. & Dikic, I. (2005). Ubiquitylation and cell signaling. *Embo J* **24**, 3353-9.

Han, Z. & Harty, R. N. (2004). The NS3 protein of bluetongue virus exhibits viroporin-like properties. *J Biol Chem* **279**, 43092-7.

Harder, T., Kellner, R., Parton, R. G. & Gruenberg, J. (1997). Specific release of membrane-bound annexin II and cortical cytoskeletal elements by sequestration of membrane cholesterol. *Mol Biol Cell* **8**, 533-45.

Harty, R. N., Brown, M. E., Wang, G., Huibregtse, J. & Hayes, F. P. (2000). A PPxY motif within the VP40 protein of Ebola virus interacts physically and functionally with a ubiquitin ligase: implications for filovirus budding. *Proc Natl Acad Sci U S A* **97**, 13871-6.

Hassan, S. H., Wirblich, C., Forzan, M. & Roy, P. (2001). Expression and functional characterization of bluetongue virus VP5 protein: role in cellular permeabilization. *J Virol* **75**, 8356-67.

Hassan, S. S. & Roy, P. (1999). Expression and functional characterization of bluetongue virus VP2 protein: role in cell entry. *J Virol* **73**, 9832-42.

Herman, B., Krishnan, R. V. & Centonze, V. E. (2004). Microscopic analysis of fluorescence resonance energy transfer (FRET). In *Protein-Protein interactions - Methods and Applications*, pp. 351-370. Edited by H. Fu: Humana press, Totowa, New Jersey.

Hershko, A. & Ciechanover, A. (1998). The ubiquitin system. *Annu Rev Biochem* **67**, 425-79.

Hewat, E. A., Booth, T. F., Loudon, P. T. & Roy, P. (1992a). Three-dimensional reconstruction of baculovirus expressed bluetongue virus core-like particles by cryo-electron microscopy. *Virology* **189**, 10-20.

Hewat, E. A., Booth, T. F. & Roy, P. (1992b). Structure of bluetongue virus particles by cryoelectron microscopy. *J Struct Biol* **109**, 61-9.

Hicke, L. & Riezman, H. (1996). Ubiquitination of a yeast plasma membrane receptor signals its ligand-stimulated endocytosis. *Cell* **84**, 277-87.

Hoeller, D., Crosetto, N., Blagoev, B., Raiborg, C., Tikkanen, R., Wagner, S., Kowanetz, K., Breitling, R., Mann, M., Stenmark, H. & Dikic, I. (2006). Regulation of ubiquitin-binding proteins by monoubiquitination. *Nat Cell Biol* **8**, 163-9.

Homan, E. J. & Yunker, C. E. (1988). Growth of bluetongue and epizootic hemorrhagic disease of deer viruses in poikilothermic cell systems. *Vet Microbiol* **16**, 15-24.

Huismans, H. & Els, H. J. (1979). Characterization of the tubules associated with the replication of three different orbiviruses. *Virology* **92**, 397-406.

Huismans, H. & Erasmus, B. J. (1981). Identification of the serotype-specific and group-specific antigens of bluetongue virus. *Onderstepoort J Vet Res* **48**, 51-8.

Huismans, H., van Dijk, A. A. & Els, H. J. (1987). Uncoating of parental bluetongue virus to core and subcore particles in infected L cells. *Virology* **157**, 180-8.

Huismans, H. & Verwoerd, D. W. (1973). Control of transcription during the expression of the bluetongue virus genome. *Virology* **52**, 81-8.

Hwang, G., Yang, Y., Chiou, J. & Li, J. K. (1992). Sequence conservation among the cognate nonstructural NS3/3A protein genes of six bluetongue viruses. *Virus Res* **23**, 151-161.

Hyatt, A. D., Eaton, B. T. & Brookes, S. M. (1989). The release of bluetongue virus from infected cells and their superinfection by progeny virus. *Virology* **173**, 21-34.

Hyatt, A. D., Gould, A. R., Coupar, B. & Eaton, B. T. (1991). Localization of the non-structural protein NS3 in bluetongue virus- infected cells. *J Gen Virol* **72**, 2263-7.

Hyatt, A. D., Zhao, Y. & Roy, P. (1993). Release of bluetongue virus-like particles from insect cells is mediated by BTV nonstructural protein NS3/NS3A. *Virology* **193**, 592-603.

Inumaru, S. & Roy, P. (1987). Production and characterization of the neutralization antigen VP2 of bluetongue virus serotype 10 using a baculovirus expression vector. *Virology* **157**, 472-9.

Jensen, M. J., Cheney, I. W., Thompson, L. H., Mecham, J. O., Wilson, W. C., Yamakawa, M., Roy, P. & Gorman, B. M. (1994). The smallest gene of the orbivirus, epizootic hemorrhagic disease, is expressed in virus-infected cells as two proteins and the expression differs from that of the cognate gene of bluetongue virus. *Virus Res* **32**, 353-64.

Kar, A. K., Ghosh, M. & Roy, P. (2004). Mapping the assembly pathway of Bluetongue virus scaffolding protein VP3. *Virology* **324**, 387-99.

Katzmann, D. J., Babst, M. & Emr, S. D. (2001). Ubiquitin-dependent sorting into the multivesicular body pathway requires the function of a conserved endosomal protein sorting complex, ESCRT-I. *Cell* **106**, 145-55.

Khu, Y. L., Tan, Y. J., Lim, S. G., Hong, W. & Goh, P. Y. (2004). Hepatitis C virus non-structural protein NS3 interacts with LMP7, a component of the immunoproteasome, and affects its proteasome activity. *Biochem J* **384**, 401-9.

Kikonyogo, A., Bouamr, F., Vana, M. L., Xiang, Y., Aiyar, A., Carter, C. & Leis, J. (2001). Proteins related to the Nedd4 family of ubiquitin protein ligases interact with the L domain of Rous sarcoma virus and are required for gag budding from cells. *Proc Natl Acad Sci U S A* **98**, 11199-204.

Le Blois, H., French, T., Mertens, P. P. C., Burroughs, J. N. & Roy, P. (1992). The expressed VP4 protein of bluetongue virus binds GTP and is the candidate guanylyl transferase of the virus. *Virology* **189**, 757-761.

Le Blois, H. & Roy, P. (1993). A single point mutation in the VP7 Majore Core Protein of Bluetongue Virus prevents the formation of core-like particles. *Virology* **67**, 353-359.

Lee, J. W. & Roy, P. (1986). Nucleotide sequence of a cDNA clone of RNA segment 10 of bluetongue virus (serotype 10). *J Gen Virol* **67**, 2833-7.

Liu, H. M., Booth, T. F. & Roy, P. (1992). Interactions between bluetongue virus core like capsid protein translated in vitro. *General Virology* **73**, 2577-2584.

Lopez, S. & Arias, C. F. (2004). Multistep entry of rotavirus into cells: a Versaillesque dance. *Trends Microbiol* **12**, 271-8.

Lopez, T., Lopez, S. & Arias, C. F. (2006). Heat shock enhances the susceptibility of BHK cells to rotavirus infection through the facilitation of entry and post-entry virus replication steps. *Virus Res* **121**, 74-83.

Luker, G. D., Sharma, V. & Piwnica-Worms, D. (2003). Visualizing protein-protein interactions in living animals. *Methods* **29**, 110-22.

Lymperopoulos, K., Noad, R., Tosi, S., Nethisinghe, S., Brierley, I. & Roy, P. (2006). Specific binding of Bluetongue virus NS2 to different viral plus-strand RNAs. *Virology* **353**, 17-26.

Maree, F. F. & Huismans, H. (1997). Characterization of tubular structures composed of nonstructural protein NS1 of African horsesickness virus expressed in insect cells. *J Gen Virol* **78**, 1077-82.

Maree, S., Durbach, S. & Huismans, H. (1998). Intracellular production of African horsesickness virus core-like particles by expression of the two major core proteins, VP3 and VP7, in insect cells. *J Gen Virol* **79**, 333-7.

Martin-Serrano, J., Perez-Caballero, D. & Bieniasz, P. D. (2004). Context-dependent effects of L domains and ubiquitination on viral budding. *J Virol* **78**, 5554-63.

Martin-Serrano, J., Yarovoy, A., Perez-Caballero, D. & Bieniasz, P. D. (2003a). Divergent retroviral late-budding domains recruit vacuolar protein sorting factors by using alternative adaptor proteins. *Proc Natl Acad Sci U S A* **100**, 12414-9.

Martin-Serrano, J., Zang, T. & Bieniasz, P. D. (2001). HIV-1 and Ebola virus encode small peptide motifs that recruit Tsg101 to sites of particle assembly to facilitate egress. *Nat Med* **7**, 1313-9.

Martin-Serrano, J., Zang, T. & Bieniasz, P. D. (2003b). Role of ESCRT-I in retroviral budding. *J Virol* **77**, 4794-804.

Martin, L. A., Meyer, A. J., O'Hara, R. S., Fu, H., Mellor, P. S., Knowles, N. J. & Mertens, P. P. (1998). Phylogenetic analysis of African horse sickness virus segment 10: sequence variation, virulence characteristics and cell exit. *Arch Virol Suppl* **14**, 281-93.

Martinez-Torrecuadrada, J. L., Diaz-Laviada, M., Roy, P., Sanchez, C., Vela, C., Sanchez-Vizcaino, J. M. & Casal, J. I. (1996). Full protection against African horsesickness (AHS) in horses induced by baculovirus-derived AHS virus serotype 4 VP2, VP5 and VP7. *J Gen Virol* **77 (Pt 6)**, 1211-21.

Martinez-Torrecuadrada, J. L., Iwata, H., Venteo, A., Casal, I. & Roy, P. (1994). Expression and characterization of the two outer capsid proteins of African horsesickness virus: the role of VP2 in virus neutralization. *Virology* **202**, 348-59.

Martinez-Torrecuadrada, J. L., Langeveld, J. P., Meloen, R. H. & Casal, J. I. (2001). Definition of neutralizing sites on African horse sickness virus serotype 4 VP2 at the level of peptides. *J Gen Virol* **82**, 2415-24.

McGuire, M. J., Croall, D. E. & DeMartino, G. N. (1988). ATP-stimulated proteolysis in soluble extracts of BHK 21/C13 cells. Evidence for multiple pathways and a role for an enzyme related to the high-molecular-weight protease, macropain. *Arch Biochem Biophys* **262**, 273-85.

Meiswinkel, R., Baylis, M. & Labuschagne, K. (2000). Stabling and the protection of horses from Culicoides bolitinos (Diptera: Ceratopogonidae), a recently identified vector of African horse sickness. *Bull Entomol Res* **90**, 509-15.

Meiswinkel, R. & Paweska, J. T. (2003). Evidence for a new field Culicoides vector of African horse sickness in South Africa. *Prev Vet Med* **60**, 243-53.

Mellor, P. S. (1990). The replication of bluetongue virus in Culicoides vectors. *Curr Top Microbiol Immunol* **162**, 143-61.

Mertens, P. P., Burroughs, J. N. & Anderson, J. (1987). Purification and properties of virus particles, infectious subviral particles, and cores of bluetongue virus serotypes 1 and 4. *Virology* **157**, 375-86.

Mertens, P. P. & Diprose, J. (2004). The bluetongue virus core: a nano-scale transcription machine. *Virus Res* **101**, 29-43.

Modrof, J., Lymperopoulos, K. & Roy, P. (2005). Phosphorylation of bluetongue virus nonstructural protein 2 is essential for formation of viral inclusion bodies. *J Virol* **79**, 10023-31.

Mortola, E., Noad, R. & Roy, P. (2004). Bluetongue virus outer capsid proteins are sufficient to trigger apoptosis in mammalian cells. *J Virol* **78**, 2875-83.

Moss, S. R., Jones, L. D. & Nuttall, P. A. (1992). Comparison of the nonstructural protein, NS3, of tick-borne and insect-borne orbiviruses. *Virology* **187**, 841-844.

Nakata, T., Sobue, K. & Hirokawa, N. (1990). Conformational change and localization of calpactin I complex involved in exocytosis as revealed by quick-freeze, deep-etch electron microscopy and immunocytochemistry. *J Cell Biol* **110**, 13-25.

Nason, E. L., Rothagel, R., Mukherjee, S. K., Kar, A. K., Forzan, M., Prasad, B. V. & Roy, P. (2004). Interactions between the inner and outer capsids of bluetongue virus. *J Virol* **78**, 8059-67.

Nichols, B. J. & Lippincott-Schwartz, J. (2001). Endocytosis without clathrin coats. *Trends Cell Biol* **11**, 406-12.

Nooren, I. M. & Thornton, J. M. (2003). Diversity of protein-protein interactions. *Embo J* **22**, 3486-92.

O'Hara, R. S., Meyer, A. J., Burroughs, J. N., Pullen, L., Martin, L. A. & Mertens, P. P. (1998). Development of a mouse model system, coding assignments and identification of the genome segments controlling virulence of African horse sickness virus serotypes 3 and 8. *Arch Virol Suppl* **14**, 259-79.

Ono, A. & Freed, E. O. (2001). Plasma membrane rafts play a critical role in HIV-1 assembly and release. *Proc Natl Acad Sci U S A* **98**, 13925-30.

Owens, R. J., Limn, C. & Roy, P. (2004). Role of an arbovirus nonstructural protein in cellular pathogenesis and virus release. *J Virol* **78**, 6649-56.

Patnaik, A., Chau, V. & Wills, J. W. (2000). Ubiquitin is part of the retrovirus budding machinery. *Proc Natl Acad Sci U S A* **97**, 13069-74.

Patton, J. T., Silvestri, L. S., Tortorici, M. A., Vasquez-Del Carpio, R. & Taraporewala, Z. F. (2006). Rotavirus genome replication and morphogenesis: role of the viroplasm. *Curr Top Microbiol Immunol* **309**, 169-87.

Perez-Vargas, J., Romero, P., Lopez, S. & Arias, C. F. (2006). The peptide-binding and ATPase domains of recombinant hsc70 are required to interact with rotavirus and reduce its infectivity. *J Virol* **80**, 3322-31.

Perez, M., Craven, R. C. & de la Torre, J. C. (2003). The small RING finger protein Z drives arenavirus budding: implications for antiviral strategies. *Proc Natl Acad Sci U S A* **100**, 12978-83.

Pesavento, J. B., Crawford, S. E., Estes, M. K. & Prasad, B. V. (2006). Rotavirus proteins: structure and assembly. *Curr Top Microbiol Immunol* **309**, 189-219.

Pesavento, J. B., Lawton, J. A., Estes, M. E. & Venkataram Prasad, B. V. (2001). The reversible condensation and expansion of the rotavirus genome. *Proc Natl Acad Sci U S A* **98**, 1381-6.

Phizicky, E. M. & Fields, S. (1995). Protein-protein interactions: methods for detection and analysis. *Microbiol Rev* **59**, 94-123.

Pierce, C. M., Balasuriya, U. B. & MacLachlan, N. J. (1998). Phylogenetic analysis of the S10 gene of field and laboratory strains of bluetongue virus from the United States. *Virus Res* **55**, 15-27.

Pina-Vazquez, C., De Nova-Ocampo, M., Guzman-Leon, S. & Padilla-Noriega, L. (2007). Post-translational regulation of rotavirus protein NSP1 expression in mammalian cells. *Arch Virol* **152**, 345-68.

Pornillos, O., Garrus, J. E. & Sundquist, W. I. (2002). Mechanisms of enveloped RNA virus budding. *Trends Cell Biol* **12**, 569-79.

Potgieter, A. C., Cloete, M., Pretorius, P. J. & van Dijk, A. A. (2003). A first full outer capsid protein sequence data-set in the Orbivirus genus (family Reoviridae): cloning, sequencing, expression and analysis of a complete set of full-length outer capsid VP2 genes of the nine African horsesickness virus serotypes. *J Gen Virol* **84**, 1317-26.

Prasad, B. V., Yamaguchi, S. & Roy, P. (1992). Three-dimensional structure of single-shelled bluetongue virus. *J Virol* **66**, 2135-42.

Pratt, W. B. (1993). The role of heat shock proteins in regulating the function, folding, and trafficking of the glucocorticoid receptor. *J Biol Chem* **268**, 21455-8.

Putterman, D., Pepinsky, R. B. & Vogt, V. M. (1990). Ubiquitin in avian leukosis virus particles. *Virology* **176**, 633-7.

Raiborg, C., Rusten, T. E. & Stenmark, H. (2003). Protein sorting into multivesicular endosomes. *Curr Opin Cell Biol* **15**, 446-55.

Ramadevi, N., Burroughs, N. J., Mertens, P. P., Jones, I. M. & Roy, P. (1998). Capping and methylation of mRNA by purified recombinant VP4 protein of bluetongue virus. *Proc Natl Acad Sci U S A* **95**, 13537-42.

Roy, P., Adachi, A., Urakawa, T., Booth, T. F. & Thomas, C. P. (1990). Identification of bluetongue virus VP6 in virus-infected vertebrate cells. *J Virol* **64**, 1-8.

Roy, P. & Noad, R. (2006). Bluetongue virus assembly and morphogenesis. *Curr Top Microbiol Immunol* **309**, 87-116.

Salghetti, S. E., Caudy, A. A., Chenoweth, J. G. & Tansey, W. P. (2001). Regulation of transcriptional activation domain function by ubiquitin. *Science* **293**, 1651-3.

Sambrook, J. & Russel, D. W. (2001). Molecular cloning - a Laboratory manual, 3 rd Edition. edn: Cold Spring Harbor Laboratory Press, Cold Spring Harbor, New York.

Sarafian, T., Pradel, L. A., Henry, J. P., Aunis, D. & Bader, M. F. (1991). The participation of annexin II (calpactin I) in calcium-evoked exocytosis requires protein kinase C. *J Cell Biol* **114**, 1135-47.

Scianimanico, S., Schoehn, G., Timmins, J., Ruigrok, R. H., Klenk, H. D. & Weissenhorn, W. (2000). Membrane association induces a conformational change in the Ebola virus matrix protein. *Embo J* **19**, 6732-41.

Shirakura, M., Murakami, K., Ichimura, T., Suzuki, R., Shimoji, T., Fukuda, K., Abe, K., Sato, S., Fukasawa, M., Yamakawa, Y., Nishijima, M., Moriishi, K., Matsuura, Y., Wakita, T., Suzuki, T., Howley, P. M., Miyamura, T. & Shoji, I. (2006). The E6AP ubiquitin ligase mediates ubiquitylation and degradation of hepatitis C virus core protein. *J Virol*.

Simons, K. & Ehehalt, R. (2002). Cholesterol, lipid rafts, and disease. *J Clin Invest* **110**, 597-603.

Simons, K. & Ikonen, E. (1997). Functional rafts in cell membranes. *Nature* **387**, 569-72.

Snippe, M., Borst, J. W., Goldbach, R. & Kormelink, R. (2005). The use of fluorescence microscopy to visualise homotypic interactions of tomato spotted wilt virus nucleocapsid protein in living cells. *J Virol Methods* **125**, 15-22.

Stoltz, M. A., van der Merwe, C. F., Coetzee, J. & Huismans, H. (1996). Subcellular localization of the nonstructural protein NS3 of African horsesickness virus. *Onderstepoort Journal of Veterinary Research* **63**, 57-61.

Strack, B., Calistri, A., Accola, M. A., Palu, G. & Gottlinger, H. G. (2000). A role for ubiquitin ligase recruitment in retrovirus release. *Proc Natl Acad Sci U S A* **97**, 13063-8.

Strack, B., Calistri, A., Craig, S., Popova, E. & Gottlinger, H. G. (2003). AIP1/ALIX is a binding partner for HIV-1 p6 and EIAV p9 functioning in virus budding. *Cell* **114**, 689-99.

Stuart, D. I., Gouet, P., Grimes, J., Malby, R., Diprose, J., Zientara, S., Burroughs, J. N. & Mertens, P. P. (1998). Structural studies of orbivirus particles. *Arch Virol Suppl* **14**, 235-50.

Surjit, M., Liu, B., Kumar, P., Chow, V. T. & Lal, S. K. (2004). The nucleocapsid protein of the SARS coronavirus is capable of self-association through a C-terminal 209 amino acid interaction domain. *Biochem Biophys Res Commun* **317**, 1030-6.

Tan, B. H., Nason, E., Staeuber, N., Jiang, W., Monastryrskaya, K. & Roy, P. (2001). RGD tripeptide of bluetongue virus VP7 protein is responsible for core attachment to Culicoides cells. *J Virol* **75**, 3937-47.

Theron, J. & Nel, L. H. (1997). Stable protein-RNA interaction involves the terminal domains of bluetongue virus mRNA, but not the terminally conserved sequences. *Virology* **229**, 134-42.

Thomas, C. P., Booth, T. F. & Roy, P. (1990). Synthesis of bluetongue virus-encoded phosphoprotein and formation of inclusion bodies by recombinant baculovirus in insect cells: it binds the single-stranded RNA species. *J Gen Virol* **71**, 2073-83.

Uetz, P. & Hughes, R. E. (2000). Systematic and large-scale two-hybrid screens. *Curr Opin Microbiol* **3**, 303-8.

Urakawa, T., Ritter, D. G. & Roy, P. (1989). Expression of largest RNA segment and synthesis of VP1 protein of bluetongue virus in insect cells by recombinant baculovirus: association of VP1 protein with RNA polymerase activity. *Nucleic Acids Res* **17**, 7395-401.

Uyeda, S., Masuta, C. & Uyeda, I. (1999). The C-terminal region of the P3 structural protein of rice dwarf phytoreovirus is important for P3-P3 interaction. *Arch Virol* **144**, 1653-7.

Van Criekinge, W. & Beyaert, R. (1999). Yeast Two-Hybrid: State of the Art. *Biol Proced Online* **2**, 1-38.

Van Dijk, A. A. & Huismans, H. (1980). The in vitro activation and further characterization of the bluetongue virus-associated transcriptase. *Virology* **104**, 347-56.

Van Dijk, A. A. & Huismans, H. (1982). The effect of temperature on the in vitro transcriptase reaction of bluetongue virus, epizootic haemorrhagic disease virus and African horsesickness virus. *Onderstepoort J Vet Res* **49**, 227-32.

Van Niekerk, M., Smit, C. C., Fick, W. C., van Staden, V. & Huismans, H. (2001). Membrane association of African horsesickness virus nonstructural protein NS3 determines its cytotoxicity. *Virology* **279**, 499-508.

Van Staden, V. & Huismans, H. (1991). A comparison of the genes which encode non-structural protein NS3 of different orbiviruses. *J Gen Virol* **72 (Pt 5)**, 1073-9.

Van Staden, V., Smit, C. C., Stoltz, M. A., Maree, F. F. & Huismans, H. (1998). Characterization of two African horse sickness virus nonstructural proteins, NS1 and NS3. *Arch Virol Suppl* **14**, 251-8.

Van Staden, V., Stoltz, M. A. & Huismans, H. (1995). Expression of nonstructural protein NS3 of African horsesickness virus (AHSV): evidence for a cytotoxic effect of NS3 in insect cells, and characterization of the gene products in AHSV infected Vero cells. *Arch Virol* **140**, 289-306.

Venter, M., Napier, G. & Huismans, H. (2000). Cloning, sequencing and expression of the gene that encodes the major neutralisation-specific antigen of African horsesickness virus serotype 9. *J Virol Methods* **86**, 41-53.

Vikis, H. G. & Guan, K. (2004). Glutathione-S-Transferase-fusion based assays for studying protein-protein interactions. In *Protein-Protein interactions - Methods and Applications*, pp. 175-186. Edited by H. Fu: Humana Press, Totowa, New Jersey.

Vollert, C. & Uetz, P. (2003). The Two-Hybrid System. *Encyclopedic Reference of Genomics and Proteomics in Molecular Medicine*, 1 - 7.

von Schwedler, U. K., Stuchell, M., Muller, B., Ward, D. M., Chung, H. Y., Morita, E., Wang, H. E., Davis, T., He, G. P., Cimbora, D. M., Scott, A., Krausslich, H. G., Kaplan, J., Morham, S. G. & Sundquist, W. I. (2003). The protein network of HIV budding. *Cell* **114**, 701-13.

Wechsler, S. J. & McHolland, L. E. (1988). Susceptibilities of 14 cell lines to bluetongue virus infection. *J Clin Microbiol* **26**, 2324-7.

Wirblich, C., Bhattacharya, B. & Roy, P. (2006). Nonstructural protein 3 of bluetongue virus assists virus release by recruiting ESCRT-I protein Tsg101. *J Virol* **80**, 460-73.

Xu, A., Bellamy, A. R. & Taylor, J. A. (2000). Immobilization of the early secretory pathway by a virus glycoprotein that binds to microtubules. *Embo J* **19**, 6465-74.

Xu, G., Wilson, W., Mecham, J., Murphy, K., Zhou, E. M. & Tabachnick, W. (1997). VP7: an attachment protein of bluetongue virus for cellular receptors in Culicoides variipennis. *J Gen Virol* **78 (Pt 7)**, 1617-23.

Zientara, S., Sailleau, C., Moulay, S. & Cruciere, C. (1995). Differentiation of African horse sickness viruses by polymerase chain reaction and segments 10 restriction patterns. *Vet Microbiol* **47**, 365-75.

Zientara, S., Sailleau, C., Plateau, E., Moulay, S., Mertens, P. P. & Cruciere, C. (1998). Molecular epidemiology of African horse sickness virus based on analyses and comparisons of genome segments 7 and 10. *Arch Virol Suppl* **14**, 221-34.

N-terminal and not the truncated version could hint to the importance of the last 26 amino acids of the N-terminal domain for these interactions. The other proteins interacted with either the truncated version of NS3 N-terminal (clone 539 encoding Hsp68) or with the NS3 C-terminal (clone 409 encoding Yolk 1 protein). The interaction of clone 539 with both the N-terminal proteins assayed for indicates that the interacting domain could be outside of or overlapping with the 26 amino acid region unique to the NS3 N-terminal 20 – 296 bait. For clone 409 that encodes the yolk-1 protein it could be that this protein interacts with more than one domain present in the NS3 protein, although it would be highly unlikely. In unpublished data obtained from Rencia Appelgryn (Department of Genetics, University of Pretoria), it was found by using the PRATT analysis program that AHSV NS3 contains two patterns, one present in the N-terminal region and the other one present in the C-terminal region, that are similar. This could explain why the yolk-1 protein interacts with both the N- and C-terminal domain of NS3. The PRATT program was designed to find flexible patterns in a set of unaligned protein sequences. The program finds common sequence patterns or motifs in a group of functionally related proteins, often indicating important conserved residues in functionally important parts of the protein.

In the β-galactosidase assay done, the blue intensity of the ubiquitin protein was relatively low, with a rating of 2 as it was in the case of the Hsp70 protein. This should reflect the strength of the interaction, which in this case is not very strong. But the fact that these proteins showed specific interaction with our bait, and grew on SD/-Leu/-Trp/-His/-Ade medium repeatedly should underline the accuracy of these interactions. It seems that both the Hsp68 and yolk 1 protein performed better, having a higher blue intensity when compared to the Hsp70 and ubiquitin.

The clones that do not encode functional protein products seemed to circumvent the specificity of the yeast two-hybrid system. Most of these clones still grew on SD/-Leu/-Trp/-His/-Ade medium when re-screened with NS3 N-terminal 20 – 374. The only clone that fell out was clone 753. This clone contains *Drosophila melanogaster* DNA sequence although in the wrong orientation with respect to the orientation of the pACT2 plasmid reading frame. Therefore no functional product is possible from such an insert. It was therefore reassuring that this clone was eliminated.

3.3.9 Alignment and description of important clones identified

The four proteins that showed interaction with our bait, NS3 N-terminal amino acids 1 – 118, after being re-screened for true interactions were ubiquitin, Hsp70, Hsp68 and the yolk-1 protein. The pBlast or psiBlast alignment data will be given for these four clones together with a short description of their functions. Information on these four proteins was also obtained from www.expasy.org. The

```
>gi|21428336|gb|AAM49828.1|  GH17513p [Drosophila melanogaster]
Length=306

 Score =  283 bits (724),  Expect = 1e-75
 Identities = 145/147 (98%), Positives = 145/147 (98%), Gaps = 0/147 (0%)

Query  7    LTGXXITLEVEPSDTIENVKAKIQDKEGIPPDQQRLIFAGKQLEDGRTLSDYNIQKESTL  66
            LTG  ITLEVEPSDTIENVKAKIQDKEGIPPDQQRLIFAGKQLEDGRTLSDYNIQKESTL
Sbjct  160  LTGKTITLEVEPSDTIENVKAKIQDKEGIPPDQQRLIFAGKQLEDGRTLSDYNIQKESTL  219

Query  67   HLVLRLRGGMQIFVKTLTGKTITLEVEPSDTIENVKAKIQDKEGIPPDQQRLIFAGKQLE  126
            HLVLRLRGGMQIFVKTLTGKTITLEVEPSDTIENVKAKIQDKEGIPPDQQRLIFAGKQLE
Sbjct  220  HLVLRLRGGMQIFVKTLTGKTITLEVEPSDTIENVKAKIQDKEGIPPDQQRLIFAGKQLE  279

Query  127  DGRTLSDYNIQKESTLHLVLRLRGGAI  153
            DGRTLSDYNIQKESTLHLVLRLRGGAI
Sbjct  280  DGRTLSDYNIQKESTLHLVLRLRGGAI  306
```

Figure 3.9: Using pBlast from NCBI, clone 2 (query) was found to encode the GH17513p protein (Sbjct) from *Drosophila melanogaster*. This is a multiubiquitin fusion protein with a total length of 305 amino acids.

ExPASy (**Ex**pert **P**rotein **A**nalysis **Sy**stem) is a proteomics server of the Swiss Institute of Bioinformatics (SIB) that is dedicated to the analysis of protein sequences and structures as well as 2-D PAGE. Therefore the primary accession number for each protein searched on this database is given in brackets. In Figure 3.9 the alignment between the subject (multiubiquitin fusion protein) and the query (clone 2) is seen with a 98% similarity. The 2% discrepancy is due to a sequencing error present in the sequence of clone 2. The multiubiquitin fusion protein consists of 305 amino acids. The insert of clone 2 encodes 153 amino acids; this aligns with the last 153 amino acids of the full length multiubiquitin fusion protein. This fusion protein consists of 3 tandem copies of the ubiquitin protein. The protein expressed from the cDNA library clone 2 aligns to almost two complete copies of ubiquitin (first ubiquitin protein lacks 7 amino acids at the 5' end). An interesting finding was that the full length copy of the ubiquitin protein present in our insert also matches 98% to the ubiquitin protein of *Culicoides sonorensis* (AAV84266.1), the insect vector for BTV and AHSV. Ubiquitin binds target proteins to modify them post-translationally to function in particular cellular responses (UniProtKB/TrEMBL entry Q8MT02).

In Figure 3.10 the pBlast alignment data is seen for clone 539 that encodes Hsp68. Hsp68 is a 635 amino acid protein of which 75 amino acids (431 – 506) are represented in clone 539. This protein belongs to the heat shock 70 family and mutant studies have shown it to play a role in determining the lifespan of an adult fly (UniProtKB/Swiss-Prot entry O97125). As a very small portion of Hsp68 is represented in clone 539, interaction with NS3 most probably will occur via a linear protein structure.

```
>gb|AAM11231.1| RE48592p [Drosophila melanogaster]
 ref|NP_524474.1| Heat shock protein 68 CG5436-PA [Drosophila melanogaster]
 gb|AAD16140.1| heat shock protein 68 [Drosophila melanogaster]
 gb|AAF56230.1| CG5436-PA [Drosophila melanogaster]
 sp|O97125|HSP68_DROME Heat shock protein 68
Length=635

 Score =  143 bits (360),  Expect = 2e-33
 Identities = 71/78 (91%), Positives = 71/78 (91%), Gaps = 0/78 (0%)

Query  9    DNQXXXTIQVFEGERALTKDNNVLGTFDLTGVPPAPRGXPKIDVTFDLDANGILNVTAKE  68
            DNQ   TIQVFEGERALTKDNNVLGTFDLTGVPPAPRG PKIDVTFDLDANGILNVTAKE
Sbjct  431  DNQPAVTIQVFEGERALTKDNNVLGTFDLTGVPPAPRGVPKIDVTFDLDANGILNVTAKE  490

Query  69   QGXGNAXNITIKNDKGDL  86
            QG GNA NITIKNDKG L
Sbjct  491  QGTGNAKNITIKNDKGRL  508
```

Figure 3.10: Using pBlast from NCBI, clone 539 (query) was found to encode the heat shock protein 68 (Sbjct) from *Drosophila melanogaster*. The total length of this protein is 635 amino acids.

In Figure 3.11 the pBlast alignment data is seen for clone 635. This clone encodes amino acids 429 – 601 (172 in total) of the 642 amino acid major Hsp70 protein Ab. This protein also belongs to the heat shock 70 family and plays a role in protein binding and has a response to heat and unfolded protein (UniProtKB/Swiss-Prot entry P02825). Once again the full length Hsp70 is not represented by the

```
 gb|AAN13535.1| CG31366-PA [Drosophila melanogaster]
 sp|P02825|HSP71_DROME Major heat shock 70 kDa protein Ab (Heat shock protein 70Ab)
(HSP70-87A7)
Length=642

 Score =  337 bits (864),  Expect = 1e-91
 Identities = 168/175 (96%), Positives = 169/175 (96%), Gaps = 0/175 (0%)

Query  8    YADNQPGVSIQVYEGERAMTKDNNALGTFDLSGIPPAPRGVPXIEVTFDLDANGILNVSA  67
            YADNQPGVSIQVYEGERAMTKDNNALGTFDLSGIPPAPRGVP IEVTFDLDANGILNVSA
Sbjct  429  YADNQPGVSIQVYEGERAMTKDNNALGTFDLSGIPPAPRGVPQIEVTFDLDANGILNVSA  488

Query  68   KEMSTGKAKNITIKNDKGRLSQAEIDRMVNEAEKYAXXDXKHRQRITSRNAXESYVFNVK  127
            KEMSTGKAKNITIKNDKGRLSQAEIDRMVNEAEKYA  D KHRQRITSRNA ESYVFNVK
Sbjct  489  KEMSTGKAKNITIKNDKGRLSQAEIDRMVNEAEKYADEDEKHRQRITSRNALESYVFNVK  548

Query  128  QAVEQAPAGKLDEADKNSVLDKCNDTIRWLDSNTTAEKEEFDHKLEELTRHCSQL  182
            QAVEQAPAGKLDEADKNSVLDKCNDTIRWLDSNTTAEKEEFDHKLEELTRHCS +
Sbjct  549  QAVEQAPAGKLDEADKNSVLDKCNDTIRWLDSNTTAEKEEFDHKLEELTRHCSPI  603
```

Figure 3.11: Using pBlast from NCBI, clone 635 (query) was found to encode the major heat shock protein 70 Ab (Sbjct) from *Drosophila melanogaster*. The total length of this protein is 642 amino acids.

library clone, and interaction would probably not be dependent on correct protein folding.

In Figure 3.12 the psiBlast alignment data is seen for clone 409 that encodes the Vitellogin-1 precursor or yolk-1 protein. Vitellogenin is the major yolk protein of eggs where it is used as a food source during embryogenesis. It is only expressed in female flies and is synthesized in the fat body and ovarian follicle cells and accumulates in the oocyte. The protein belongs to the lipase family in the AB hydrolase superfamily (UniProtKB/Swiss-Prot entry P02843). Clone 409 encodes amino acids 215 – 439 (224 in total) of the 439 amino acid yolk-1 protein.

```
>ref|NP_511103.1| Yolk protein 1 CG2985-PA [Drosophila melanogaster]
 gb|AAF46548.1| CG2985-PA [Drosophila melanogaster]
 sp|P02843|VIT1_DROME Vitellogenin-1 precursor (Vitellogenin I) (Yolk protein 1)
 emb|CAA23502.1| unnamed protein product [Drosophila melanogaster]
Length=439

 Score =  447 bits (1150),  Expect = 2e-124
 Identities = 219/225 (97%), Positives = 219/225 (97%), Gaps = 0/225 (0%)

Query  8    TYERYAMLDIEKTGAKIGKWIVQMVNELDMPFDTIHLIGQNXGAHVAGAAAQEFXRLTGH  67
            TYERYAMLDIEKTGAKIGKWIVQMVNELDMPFDTIHLIGQN GAHVAGAAAQEF RLTGH
Sbjct  215  TYERYAMLDIEKTGAKIGKWIVQMVNELDMPFDTIHLIGQNVGAHVAGAAAQEFTRLTGH  274

Query  68   KLRRVTGLDPSKIVAXSKNTLTGLARGDAEFVDAIHTSVYGMGTPIRSGDVDFYPNGPAA  127
            KLRRVTGLDPSKIVA SKNTLTGLARGDAEFVDAIHTSVYGMGTPIRSGDVDFYPNGPAA
Sbjct  275  KLRRVTGLDPSKIVAKSKNTLTGLARGDAEFVDAIHTSVYGMGTPIRSGDVDFYPNGPAA  334

Query  128  GVPGASNVVEAAMRATRYFAXSVRPXNERSFPAVPANSLQQYKQNDGFGKRAYMGIDTAH  187
            GVPGASNVVEAAMRATRYFA SVRP NERSFPAVPANSLQQYKQNDGFGKRAYMGIDTAH
Sbjct  335  GVPGASNVVEAAMRATRYFAESVRPGNERSFPAVPANSLQQYKQNDGFGKRAYMGIDTAH  394

Query  188  DLEGDYFLQVNPKSPFGRNAPAQKQSSYHGVHQAWNTNQDSKDYQ  232
            DLEGDY LQVNPKSPFGRNAPAQKQSSYHGVHQAWNTNQDSKDYQ
Sbjct  395  DLEGDYILQVNPKSPFGRNAPAQKQSSYHGVHQAWNTNQDSKDYQ  439
```

Figure 3.12: Using psiBlast from NCBI, clone 409 (query) was found to encode the Yolk-1 protein (Sbjct) from *Drosophila melanogaster*. The total length of this protein is 439 amino acids. Clone 409 consists of 224 amino acids and aligns with amino acids 215 - 439 of the full length Yolk-1 protein.

3.4 Discussion

The aim of this part of the study was to identify putative binding partners encoded from a *Drosophila melanogaster* cDNA library that interact with AHSV2 NS3 N-terminal amino acids 1 - 118. This study was undertaken based on the lack of knowledge in cellular-viral interactions present in assisting the AHSV to exit insect cells. Both BTV and AHSV are vectored by a small biting midge of the genus *Culicoides* and replicate in both insect and mammalian cells. We know from cell culture studies done that BTV is released from insect cells with no cytopathic effect (CPE) (Homan & Yunker, 1988) while release from mammalian cells is highly cytopathic (Castro *et al*., 1989). BTV and AHSV are released

from infected mammalian cells mainly by cell lysis (Wechsler & McHolland, 1988). BTV release from vector cells (*Culicoides*) is nonlytic and it is postulated that this might be the result of viral budding being used by the virus to escape from the infected insect cells (Hyatt *et al.*, 1989, Hyatt *et al.*, 1993).

We know from studies done on BTV using proteins expressed from mammalian cDNA libraries that NS3 interacts with the p11 protein, part of the Annexin II complex (Beaton *et al.*, 2002) as well as with Tsg101 and Nedd4-like ubiquitin ligases (Wirblich *et al.*, 2006). It has also been shown that AHSV NS3 binds Tsg101 and that both BTV and AHSV NS3 bind to the *Drosophila* homologue of Tsg101. It is thought that the virus buds from an infected cell as follow: Newly assembled viral cores are released from NS2 inclusion bodies and associate with outer capsid proteins VP5 and VP2. NS3 associates with the intracellular trafficking protein p11 and forms a bridge between this protein and newly assembled virus particles by secondary interaction with VP2. This leads to trafficking of the virus particle to the cell membrane where interaction between the PSAP motif in NS3 and the cellular release factor Tsg101 results in the pinching off of vesicles containing virus particles followed by release of mature virion particles from these vesicles (Roy & Noad, 2006).

With this knowledge we set out to identify other insect specific cellular binding partners that could assist the AHSV via its NS3 protein to exit insect cells. We hoped it would shed some light on how the virus might employ different strategies that would enable one to understand why the virus is released lytically from mammalian cells but nonlytically from insect cells. A *Drosophila melanogaster* cDNA library was purchased from Clontech Laboratories, Inc. The library's inserts were cloned as activation domain fusions to be used in the yeast two-hybrid system. The AHSV2 NS3 N-terminal 20 – 274 was used as bait and cloned as a DNA-binding domain fusion. After 850 SD/-Leu/-Trp/-His colonies were screened on SD/-Leu/-Trp/-His/-Ade plates, 19 of the clones that survived were prepared for sequencing. Twelve of the inserts encoded known *Drosophila* protein sequences; these included a ubiquitin protein (matches the *Culicoides* (vector) ubiquitin sequence), 5 proteins from the heat shock 70 family, and the yolk 1 protein. Seven of the 19 clones did not encode any known protein sequences.

The clones that encoded functional protein products were re-screened with NS3 N-terminal 20 - 374 to verify whether they indeed were true interactions. We also included a truncated version of NS3 N-terminal that lacked the coiled-coiled domain at the end of the NS3 N-terminal domain as well as the C-terminal domain of NS3. This was done to investigate the specificity of the interaction. More conclusive results could have been obtained if the *Drosophila* proteins were also tested for interaction with the GAL4 DNA-binding domain (empty pAS2-1 vector) as this could have eliminated false positives such as the yolk protein that showed interaction with both the NS3 N-term (20-374) and NS3

C-term (544-764). Only two clones showed interaction specific to the NS3 N-terminal (amino acids 1 - 118) and not to the truncated NS3 N-terminal of C-terminal domains, namely ubiquitin and Hsp70. The yolk-1 protein showed interaction to both NS3 N-terminal (amino acids 1 - 118) and NS3 C-terminal domains. The Hsp68 protein showed interaction with NS3 N-terminal (amino acids 1 - 118) and to a lesser extent to NS3 N-terminal (amino acids 1 - 92). According to the website (http://www.fccc.edu/research/labs/golemis/Table2.html), heat shock proteins and ubiquitin are commonly found as false positives in cDNA library screens. We decided to continue to investigate the Hsp70 and ubiquitin proteins as literature showed possible roles for these proteins in virus lifecycles.

The clones that did not encode functional protein products were also re-screened with only NS3 N-terminal 20 – 374 to determine the specificity of the yeast two-hybrid system. Only one clone fell out, with 5 others that showed interaction although it must be observed that for some only 1 out of the 4 colonies screened grew most probably indicating non-specific interactions or mutations that took place in those colonies.

The fact that only two positive protein-protein interactions were detected could be explained by the lack of an exhaustive screen. Replica plating yeast colonies from TDO to QDO to β-galactosidase plates would have allowed the screening of all colonies present and not only the colonies picked manually as described. This would definitely have allowed a better representation of the proteins available from the library, and we might therefore still have missed relevant interactors.

As indicated previously, late domains have been found in BTV and AHSV NS3 (Strack *et al.*, 2000, Wirblich *et al.*, 2006). Two of the three classes of late-domain motifs have been identified namely P(T/S)AP and PPXY. The PSAP motif recruits the cellular protein Tsg101. This protein forms part of the ESCRT-I complex (Garrus *et al.*, 2001, Martin-Serrano *et al.*, 2001, Martin-Serrano *et al.*, 2003b). The PPXY motif plays a role in recruiting host ubiquitin ligases (Blot et al., 2004, Bouamr et al., 2003, Kikonyogo et al., 2001, von Schwedler et al., 2003). The identification of a Drosophila ubiquitin protein that interacts specifically with the N-terminal of AHSV was very interesting. The PPXY motif, which has been shown in retroviruses to recruit host ubiquitin ligases, is present in the N-terminal of BTV and AHSV NS3, although not highly conserved throughout the different AHSV serotypes. In AHSV2 NS3 the motif is present as PPPY between amino acids 25 – 28. Wirblich *et al.,* (2006) showed that BTV NS3 (PPRY) showed interaction with GST-tagged WW domains of NEDD4.1, WWP1, and Itch. These are three different ubiquitin ligases shown to be recruited by retroviruses needed for the budding process. It has been shown that the Gag protein (nuclear capsid protein) of HIV-1, human T-cell leukemia virus type 1 and Rous sarcoma virus bind via their PPXY motif to various ubiquitin

ligases (Bouamr et al., 2003, Kikonyogo et al., 2001, Martin-Serrano et al., 2004, Strack et al., 2000, von Schwedler et al., 2003).

Not only ubiquitin ligases, but also ubiquitin was found to interact with the Gag protein. Ubiquitin is a small, highly abundant protein that can be covalently attached to certain Lys residues in target proteins (Hershko & Ciechanover, 1998). AHSV NS3 serotype 2 contains 8 Lysine residues (spaced out in protein) in the N-terminal situated more to the end of the N-terminal domain (amino acids 65 – 114). Four of these lysines are present in the 26 amino acids that are truncated from NS3 N-terminal amino acids 1 – 92 protein. It could be that the four lysines present in the last 26 amino acids of the NS3 N-terminal domain could play a significant role in binding ubiquitin. Ubiquitin binds target proteins to modify them post-translationally to function in particular cellular responses that include degradation (Driscoll & Goldberg, 1990, McGuire *et al.*, 1988), protein trafficking and transcription activation (Babst *et al.*, 2000, Hicke & Riezman, 1996, Salghetti *et al.*, 2001). It has been shown that ubiquitination in itself also has an effect on viral release. Several retroviruses contain free, virion-associated ubiquitin (Putterman *et al.*, 1990) and a small amount of mono-ubiquitylated Gag. It has been found that poly-ubiquitylated proteins are known to be associated with their degradation through the proteasome (Haglund & Dikic, 2005). More recently is has been proposed that the mono-ubiquitination of proteins may result in their targeting to the endosomal/lysosomal compartment where either degradation or further processing may occur (Hoeller *et al.*, 2006). It is also thought that mono-ubiquitination tags membrane-associated proteins for internalization and/or sorting into the endosomal pathway (Demirov & Freed, 2004).

It has been postulated that by depleting the intracellular pools of free ubiquitin, proteasome inhibitors limit the extent to which Gag is ubiquitylated, therefore resulting in a disruption in viral budding (Demirov & Freed, 2004). The importance of ubiquitin associated Gag was supported by a study that showed that virus like particles generated with Gag-Ubiquitin fusion proteins were partially resistant to proteasome inhibitors (Patnaik *et al.*, 2000). Another study also showed that cumulative mutations of ubiquitin acceptor sites in HIV-1 Gag caused a late budding defect. These results indicated that ubiquitination of lysine residues in Gag in the vicinity of the viral late domain is important for HIV-1 budding (Gottwein *et al.*, 2006).

The role that ubiquitination and association of the ubiquitin ligases have on viral budding can be summarized as seen in Figure 3.13 (Putterman et al., 1990). After the newly assembled virus has reached the host plasma membrane and prepared for exiting by forming a spherical particle ready to pinch off, some ubiquitin molecules both free and conjugated to Gag, are present in the virus. A ubiquitin ligase is recruited to the site of budding by the PXXY late domain present in the Gag protein.

This ligase forms a bridge, binding ubiquitin to some of the Gag molecules and perhaps to cellular proteins. These ubiquitin conjugates may interact with other cellular proteins that will set up the machinery to pinch off the virus bud (Putterman et al., 1990). The machinery that catalyzes Gag ubiquitination has not been identified and ongoing research is focusing on this aspect.

The role the ubiquitin protein could play in orbivirus release is another study on itself – one difference being that orbiviruses do not contain a lipid envelope that in itself allows viruses such as HIV to bud. Also, enveloped viruses such as HIV contain a nuclear capsid protein, Gag that allows interaction with the multivesicular body machinery via the presence of late domains. For orbiviruses such as BTV and AHSV, the nonstructural protein NS3 contains similar late domains that could possibly help these viruses to bud from host cells. A functional study possibly including cells lacking ubiquitin could shed some light on whether this cellular protein indeed has any real effect on the virus exit. Also, whether the late domains present in AHSV NS3 interact with ubiquitin or ubiquitin ligase. Another factor would also be how NS3 is ubiquitylated, whether mono-ubiquitylated or poly-ubiquitylated NS3 is needed.

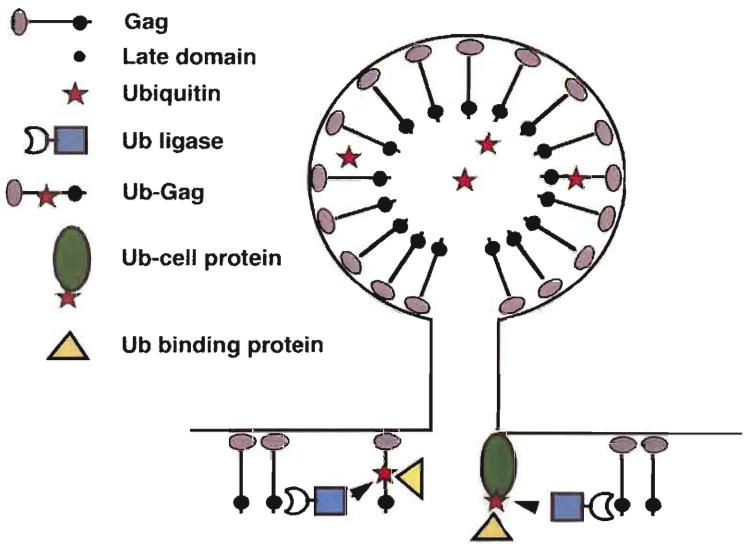

Figure 3.13: Speculative representation of late stage in retroviral budding. The Gag molecules have formed a spherical particle ready to pinch off from the plasma membrane. Some ubiquitin molecules (red star), both free and conjugated to Gag, are present in the nascent virus. A ubiquitin ligase (blue rectangle) is recruited to the site of budding by the Gag late domain, and it conjugates ubiquitin to some of the Gag molecules and perhaps to cellular proteins (green oval). Other cellular proteins (yellow triangle) may bind to these ubiquitin conjugates, setting up the machinery to pinch off the virus bud (Image and description taken from Vogt, 2000).

In a very recent study done in hepatitis C virus (HCV), the authors investigated the role of ubiquitination in the production of the viral core protein. This protein is a major component of the viral nucleocapsid and a multifunctional protein involved in viral pathogenesis and hepatocarcinogenesis. They found that this protein is degraded through the ubiquitin-proteasome pathway and that the

ubiquitin ligase E6AP mediates ubiquitination and degradation of the HCV core protein via this pathway. They proposed that the E6AP-mediated ubiquitin-proteasome pathway may affect the production of HCV particles through controlling the amounts of viral nucleocapsid protein (Shirakura *et al.*, 2006). They also found in other studies done that other HCV proteins such as the nonstructural proteins NS5B (Gao *et al.*, 2003) and NS2 (Franck *et al.*, 2005) are also degraded through the ubiquitin-proteasome pathway.

In a study done on the rotavirus NSP1 protein, it was found that this protein can act as an E3-ubiquitin ligase, but also can auto regulate its expression by binding ubiquitin that targets the protein for degradation via a proteasome-dependent pathway. NSP1 is a down-regulator of the interferon response, since it binds to the interferon regulatory factor 3 (IRF3) and induces its degradation. This interferon response is initiated by the host cell when infected by the rotavirus. The study showed that NSP1 can act as an ubiquitin ligase by recruiting the IRF3, allowing ubiquitination of the IRF3 that targets the protein for degradation. NSP1 also allows self ubiquitination, regulating its own expression levels in the infected cells. It was found that a RING finger motif (7 conserved cysteines and one histidine coordinating two zinc atoms in a cross-braced structure) in NSP1 can explain its proteasome susceptibility as well as its ability to induce IRF3 degradation via a proteasome-dependent pathway (Pina-Vazquez *et al.*, 2007).

The other protein that showed interaction with our bait, NS3 N-terminal 20 – 274, was the heat shock protein 70 Ab (Hsp70). Hsp70 is quite a common protein involved in protein folding reactions. It has also been shown to be important for protein translocation across membranes of organelles and is thought to catalyze protein assembly. Hsp70 also has the ability to bind to many proteins of different structures during their translation (Pratt, 1993). Recent literature shows the relevance of the Hsp70 family members in virus entry and virus replication in rotavirus, another member of the *Reoviridae* family. The heat shock cognate protein 70 (Hsc70) has been proposed to be involved during rotavirus entry at a post-binding step, probably during penetration (Lopez & Arias, 2004, Perez-Vargas *et al.*, 2006). It has been shown that heat-stress facilitates the replication of rotaviruses in baby hamster kidney (BHK) cells during cell entry, as well as at a post-entry stage (Lopez *et al.*, 2006).

Another study showed that Hsp70 is rapidly, specifically and transiently induced upon rotavirus infection of intestinal cells. Hsp70 was specifically identified in lipid rafts that were obtained from intestinal epithelial Caco-2 cells. This is a cell line for which the well-polarized and enterocyte-like phenotype closely corresponds to the natural in vivo target of rotavirus. This Hsp70 induction was not a general response to viral infection, but instead shown to be a highly specific response both with regard to the infecting virus, and the host cell. In these Caco-2 cells, Hsp70 silencing was associated

with an increased virus protein level and an enhanced progeny production. Upon Hsp70 silencing, they also observed that the ubiquitination of the main rotavirus structural proteins was strongly reduced. When they used proteasome inhibitors, this induced an accumulation of bioavailability of viral proteins within the cells for virus morphogenesis (Broquet *et al.*, 2006).

The significance of the last few paragraphs can be pointed out in the observation that in two different viruses (rotavirus and HCV), both the ubiquitin and the Hsp70 proteins play a role in regulating the bioavailability of viral proteins in an infected host cell. NS3 seems to be differentially regulated in different cell types, with low expression in mammalian cells (French *et al.*, 1989) when compared to insect cells (Guirakhoo *et al.*, 1995). Up to date, no explanation could be given except for the assumption that the increased NS3 expression in insect cells could be linked to the virus preferring NS3 mediated budding over lytic release in these cells resulting in the low CPE observed (Homan & Yunker, 1988, Wechsler & McHolland, 1988). Therefore it could be that ubiquitin together with the Hsp70 regulate the availability of the NS3 protein, explaining the differences seen the viral exit between mammalian and insect cells.

To conclude, by using the proteins expressed from a *Drosophila melanogaster* cDNA library and the AHSV2 NS3 N-terminal domain (amino acids 1 - 118) as bait we wanted to investigate possible viral-cellular protein-protein interactions that could take place in the vector (*Culicoides*) relating to virus exit. We hoped to find cellular proteins potentially involved in regulating or mediating aspects of virus trafficking or release. We identified two cDNA library clones (Ubiquitin and Hsp70) that specifically interacted with our bait and not with any other domains in the NS3 protein. It seems that the ubiquitin protein could play a role in AHSV release, but further functional analysis would be needed to shed more light on the relevancy of ubiquitin. The other scenario including both ubiquitin and the Hsp70 in possibly regulating the bioavailability of the NS3 protein is a hypothesis to investigate. It would explain the different levels of NS3 present in mammalian versus insect cells, and therefore have an effect in controlling budding versus lytic release. By using the yeast two-hybrid assay, it allowed us to quickly and efficiently scan a cDNA library for protein-protein interactions of significance. This was the first step in unravelling the secrets of viral release in AHSV; many more studies will be needed to sufficiently comprehend the questions and answers gained to produce a picture of this virus's lifecycle.

Concluding remarks

We have set out to investigate viral and cellular protein-protein interaction in AHSV. Our study was based on results obtained for BTV, the prototype virus of the *Orbivirus* genus. Here it was shown that a membrane protein NS3, presumably forms a bridging molecule across the plasma membrane and associates with the outer capsid protein, VP2 present on newly formed BTV virions, with its cytosolic C-terminal domain and with a host cellular protein, p11 (part of exocytosis pathway) with its cytosolic N-terminal domain. With this NS3-mediated mechanism, the BTV would then literally hi-jack the host exocytosis pathway and allow the newly formed BTV virions to exit the host cell, presumably via budding. We wanted to see whether these same mechanisms could be at work in AHSV. We decided to use the yeast two-hybrid system to investigate VP2 – NS3 interaction as well as NS3 – insect cell protein interaction. To ensure consistency, we also used the GST pull-down and membrane flotation assay to investigate NS3 – VP2 protein-protein interaction. As the BTV study utilised a mammalian (human) cDNA library to identify the p11 protein, we wanted to investigate whether any other significant proteins from an insect (*Drosophila melanogaster*) cDNA library could be detected. We expected to find evidence supporting the hypothesis that the virus would use budding to exit *Culicoides* cells (vector of AHSV) as no severe CPE is seen in infected cells.

For the investigation of AHSV NS3 – VP2 interaction, no conclusive results were obtained. The yeast two-hybrid system and GST pull-down assay failed to show any interaction, although the positive control provided with the yeast two-hybrid system worked. The GST pulldown results portrayed results that showed that NS3 and VP2 did not interact under the conditions used. But these results are also inconclusive as we did not have a positive control for this assay. The only preliminary evidence of interaction was observed with the membrane flotation assay. Here the VP2 protein had an effect on the position of NS3 in the gradient. But individually expressed VP2 was also present in the upper fractions of the gradient, where the protein was not expected – making this experiment unconvincing. As most of the problems arose due to NS3 or VP2 not being expressed in their native environment, leading to improper protein folding and aggregation, the next step should be to test these proteins in their native form as they are expressed in insect cells. The way to do this would be to use confocal microscopy and monoclonal antibodies specific to NS3 and VP2. Co-localization of NS3 and VP2 would suggest protein-protein interaction.

Positive results were obtained for the NS3 – *Drosophila* cDNA library screening study. Ubiquitin and a heat shock 70 protein were retrieved as potential role players in the questions posed relating to viral cell exiting. The Gag protein (nuclear capsid protein) of retroviruses contains late domains that recognize and associate with cellular proteins such as Tsg101 and ubiquitin ligases. It has been

shown that these associations are needed for the retrovirus to successfully bud from infected host cells. These retroviruses also bind to cellular ubiquitin that plays a role in the pinching off of budding vesicles from the plasma membrane. Only recently evidence was found for the presence of these late domains in the NS3 protein of BTV and AHSV. Interaction between Tsg101 and BTV/AHSV NS3 were shown, as well as interaction between ubiquitin ligases and BTV NS3. The role ubiquitin could play in the release of BTV or AHSV is unknown although budding seems to be a method of virus release for AHSV, it makes sense that NS3 could recruit ubiquitin to enable the newly assembled virus particles to bud from the cellular membrane explaining the non cytotoxic release seen in insect cells

The latest information shows that ubiquitin and Hsp70 could influence the bioavailability of viral proteins as seen in studies done by Broquet *et al.* (2007) and Shirakura *et al.* (2007). Our study showed that the NS3 N-terminal (amino acids 1 - 118) specifically interacted with ubiquitin and Hsp70. It could be that the difference in NS3 levels seen between mammalian cells and insect cells could be explained by ubiquitin/Hsp70 association. Furthermore, this regulation of NS3 could shed even more light on how increased levels of NS3 results in budding and reduced levels of NS3 results in lytic release.

With the positive results of the discovery of ubiquitin and Hsp70 as cellular binding partners to NS3, a novel discovery has been made. For AHSV, variation seen in NS3 between the different serotypes pose interesting questions, as this variation is not present in other orbiviruses. It could be interesting to investigate whether the different AHSV serotypes differs in their association with ubiquitin and Hsp70. Also a knockout experiment using siRNAs to inhibit ubiquitin and Hsp70 production could enlighten us in the effect these protein have on viral release or even other aspects in the virus morphogenesis. It should also be investigated whether the *Culicoides* protein homologues to Hsp70 and ubiquitin interact with the NS3 N-terminal as been shown by the *Drosophila* homologues in this study. With the knowledge gained from these studies, one would hope to better understand the morphogenesis and lifecycle of the virus, which in the end would lead to better control of the virus.

Scientific publications

Some results of this study were presented in the form of poster presentations at national and international meetings:

Beyleveld M, Van Staden V and Huismans H (2006) Investigating viral and cellular protein-protein interaction in African horsesickness virus, South African Genetics Society 19th conference, Bloemfontein, South Africa, 3 - 5 April 2006.

Beyleveld M, Van Staden V and Huismans H (2006) Screening of a *Drosophila* cDNA library for protein-protein interaction with African horsesickness virus membrane protein NS3, 9th International symposium on double stranded RNA viruses, Cape town, South Africa, 22 – 27 October 2006.

Appendix

LIST OF FIGURES AND TABLES

List of figures and tables in chapter 1

List of figures and tables in chapter 2

List of figures and tables in chapter 3

LIST OF ABBREVIATIONS

3-AT	3-amino-1,2,4-triazol
a.a.	amino acid
AD	Activation domain
Ade	Adenine
Ado Met	S-adenosyl -L-methionine
AHSV	African horsesickness virus
BHK	Baby hamster kidney cells
bp	Base pairs
BTV	Bluetongue virus
cDNA	Complimentary deoxyribonucleic acid
CPE	Cytopathic effect
DDO	Double dropout
DNA-BD	DNA binding domain
dNTP	Deoxyribonucleotide triphosphate
dsRNA	Double stranded RNA
E. coli	*Escherichia coli*
EDTA	Ethylenediaminetetra-acetic acid
ER	Endoplasmic reticulum
ESCRT	Escort
FRET	Fluorescence resonance energy transfer
Fwd	Forward
GAL	Galactosidase
GFP	Green fluorescent protein
GST	Gluthione-S-transferase
His	Histidine
HIV	Human immunodeficiency syndrome
Hsc	Heat-shock cognate
Hsp	Heat-shock protein
IPTG	Isopropyl-β-D-thiogalactopyranoside
ISVP	Intermediate subviral particles
Kb	kilobase
L(number)	Large segment
LB-broth	Luria Bertani broth
L-domain	Late domain
Leu	Leucine
LiAc	Lithium acetate
M(number)	Medium segment
MOI	Multiplicity of infection
NS(number)	Nonstructural
NSP(number)	Nonstructural protein
ORF	Open reading frame
PAGE	Polyacrylamide gel electrophoresis
PBS	Phosphate buffered saline
PCR	Polymerase chain reaction
pfu	plaque forming units
p.i.	post infection
PSB	Protein solvent buffer
QDO	Quadruple dropout
Rev	Reverse
S(number)	Small segment
SD medium	Standard deficient medium

SDS	Sodium dodecyl sulphate
Sf9	*Spodoptera frugiperda* insect cells
ssRNA	Single stranded RNA
TDO	Triple dropout
TGN	Trans-Golgi network
Trp	Tryptophan
UAS	Upstream activation site
UHQ	Ultra high quality
VIB	Viral inclusion body
VP(number)	Viral protein
YPD	Yeast extract, Peptone and Dextrose

METRICAL UNITS

U	Units
kD or KDa	kilo dalton
M	Molar
mM	milli molar
nm	nanometre
rpm	revolution per minute
w/v	weight/volume
µg	micrograms
µl	micro litre

PLASMID MAPS

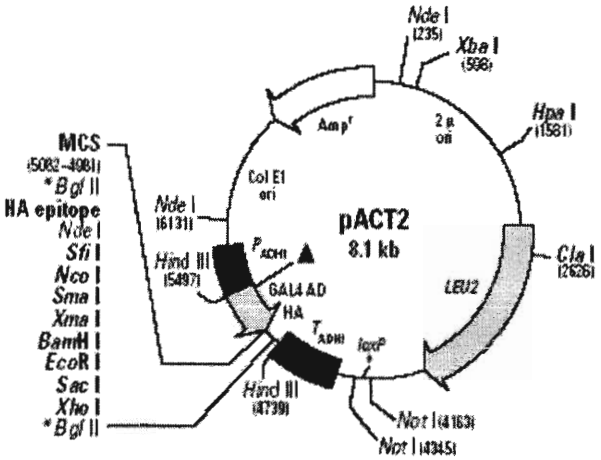

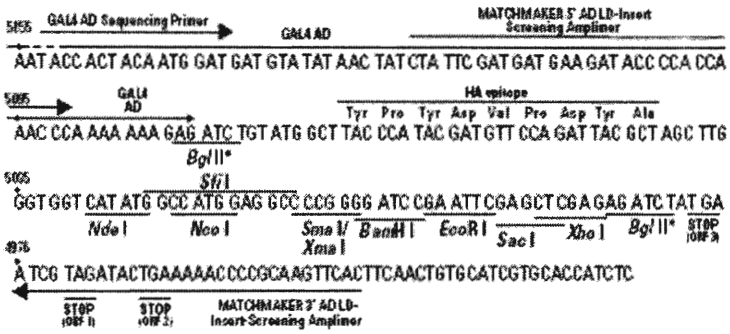

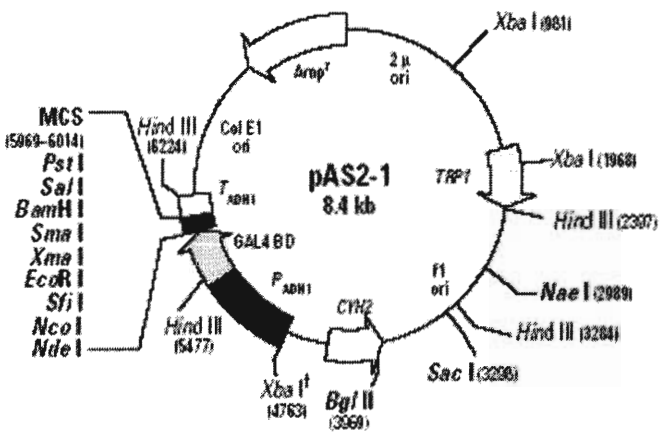

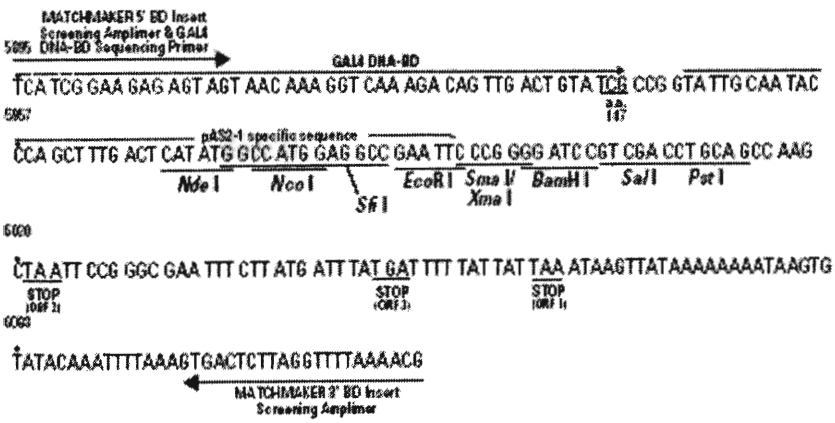

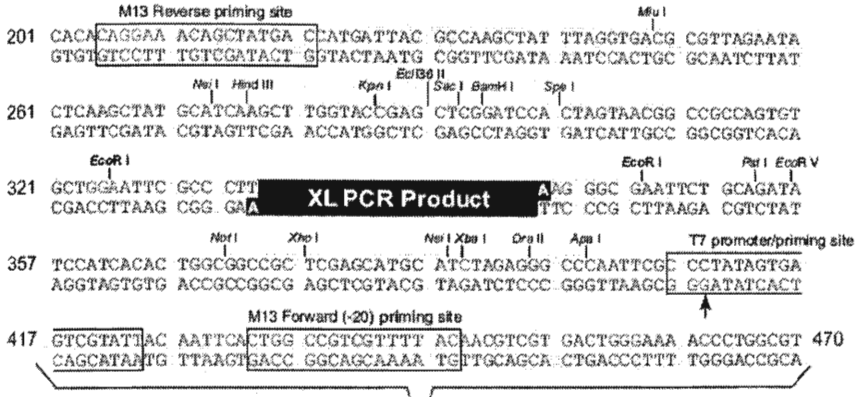
M13 Reverse priming site
Mlu I
201 CACACAGGAA ACAGCTATGA CCATGATTAC GCCAAGCTAT TTAGGTGACG CGTTAGAATA
GTGTGTCCTT TGTCGATACT GGTACTAATG CGGTTCGATA AATCCACTGC GCAATCTTAT
Nsi I Hind III Kpn I EcI136 II Sac I BamH I Spe I
261 CTCAAGCTAT GCATCAAGCT TGGTACCGAG CTCGGATCCA CTAGTAACGG CCGCCAGTGT
GAGTTCGATA CGTAGTTCGA ACCATGGCTC GAGCCTAGGT GATCATTGCC GGCGGTCACA
EcoR I
EcoR I Pst I EcoR V
321 GCTGGAATTC GCC CTT XL PCR Product AAG GGC GAATTCT GCAGATA
CGACCTTAAG CGG GAA TTC CCG CTTAAGA CGTCTAT
Not I Xho I Nsi I Xba I Dra II Apa I
T7 promoter/priming site
357 TCCATCACAC TGGCGGCCGC TCGAGCATGC ATCTAGAGGG CCCAATTCGC CCTATAGTGA
AGGTAGTGTG ACCGCCGGCG AGCTCGTACG TAGATCTCCC GGGTTAAGCG GGATATCACT
M13 Forward (-20) priming site
417 GTCGTATTAC AATTCACTGG CCGTCGTTTT ACAACGTCGT GACTGGGAAA ACCCTGGCGT 470
CAGCATAATG TTAAGTGACC GGCAGCAAAA TGTTGCAGCA CTGACCCTTT TGGGACCGCA

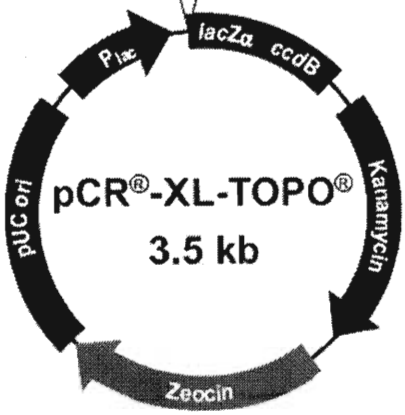
pCR®-XL-TOPO®
3.5 kb
P lac
lacZα ccdB
Kanamycin
Zeocin
pUC ori

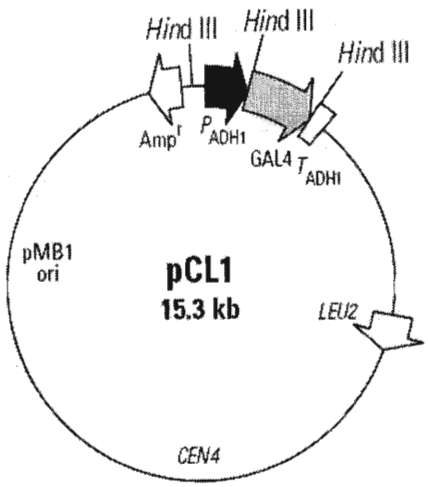
Hind III
Hind III
Hind III
Amp r
P ADH1
GAL4
T ADH1
pMB1
ori
pCL1
15.3 kb
LEU2
CEN4

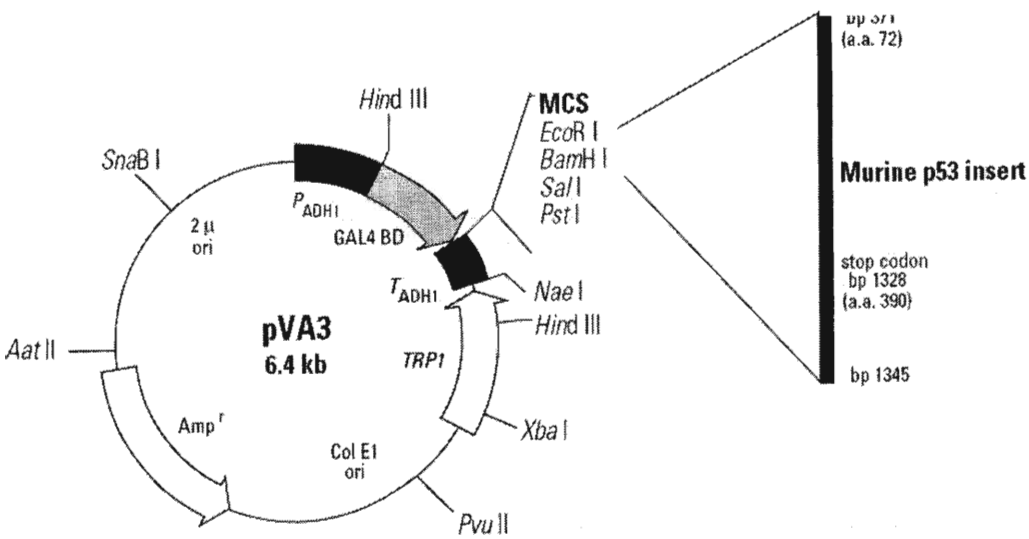
Hind III
MCS
EcoR I
BamH I
Sal I
Pst I
SnaB I
P ADH1
GAL4 BD
2 µ
ori
T ADH1
Nae I
Hind III
Aat II
pVA3
6.4 kb
TRP1
Amp r
Col E1
ori
Xba I
Pvu II
bp 371
(a.a. 72)
Murine p53 insert
stop codon
bp 1328
(a.a. 390)
bp 1345

References

Arias, C. F., Dector, M. A., Segovia, L., Lopez, T., Camacho, M., Isa, P., Espinosa, R. & Lopez, S. (2004). RNA silencing of rotavirus gene expression. *Virus Res* **102**, 43-51.

Arias, C. F., Isa, P., Guerrero, C. A., Mendez, E., Zarate, S., Lopez, T., Espinosa, R., Romero, P. & Lopez, S. (2002). Molecular biology of rotavirus cell entry. *Arch Med Res* **33**, 356-61.

Babst, M. (2005). A protein's final ESCRT. *Traffic* **6**, 2-9.

Babst, M., Katzmann, D. J., Estepa-Sabal, E. J., Meerloo, T. & Emr, S. D. (2002a). Escrt-III: an endosome-associated heterooligomeric protein complex required for mvb sorting. *Dev Cell* **3**, 271-82.

Babst, M., Katzmann, D. J., Snyder, W. B., Wendland, B. & Emr, S. D. (2002b). Endosome-associated complex, ESCRT-II, recruits transport machinery for protein sorting at the multivesicular body. *Dev Cell* **3**, 283-9.

Babst, M., Odorizzi, G., Estepa, E. J. & Emr, S. D. (2000). Mammalian tumor susceptibility gene 101 (TSG101) and the yeast homologue, Vps23p, both function in late endosomal trafficking. *Traffic* **1**, 248-58.

Barton, E. S., Forrest, J. C., Connolly, J. L., Chappell, J. D., Liu, Y., Schnell, F. J., Nusrat, A., Parkos, C. A. & Dermody, T. S. (2001). Junction adhesion molecule is a receptor for reovirus. *Cell* **104**, 441-51.

Basak, A. K., Gouet, P., Grimes, J., Roy, P. & Stuart, D. (1996). Crystal structure of the top domain of African horse sickness virus VP7: comparisons with bluetongue virus VP7. *J Virol* **70**, 3797-806.

Basak, A. K., Grimes, J. M., Gouet, P., Roy, P. & Stuart, D. I. (1997). Structures of orbivirus VP7: implications for the role of this protein in the viral life cycle. *Structure* **5**, 871-83.

Beaton, A. R., Rodriguez, J., Reddy, Y. K. & Roy, P. (2002). The membrane trafficking protein calpactin forms a complex with bluetongue virus protein NS3 and mediates virus release. *Proc Natl Acad Sci U S A* **99**, 13154-9.

Becker, M. M., Peters, T. R. & Dermody, T. S. (2003). Reovirus sigma NS and mu NS proteins form cytoplasmic inclusion structures in the absence of viral infection. *J Virol* **77**, 5948-63.

Bhattacharya, P. & Roy, P. (2006). Interaction of BTV VP2 with celular factors during virus maturation. In *9th dsRNA virus symposium*, pp. 52. Capetown, Bantry bay.

Blot, V., Perugi, F., Gay, B., Prevost, M. C., Briant, L., Tangy, F., Abriel, H., Staub, O., Dokhelar, M. C. & Pique, C. (2004). Nedd4.1-mediated ubiquitination and subsequent recruitment of Tsg101 ensure HTLV-1 Gag trafficking towards the multivesicular body pathway prior to virus budding. *J Cell Sci* **117**, 2357-67.

Borsa, J., Morash, B. D., Sargent, M. D., Copps, T. P., Lievaart, P. A. & Szekely, J. G. (1979). Two modes of entry of reovirus particles into L cells. *J Gen Virol* **45**, 161-70.

Bouamr, F., Melillo, J. A., Wang, M. Q., Nagashima, K., de Los Santos, M., Rein, A. & Goff, S. P. (2003). PPPYVEPTAP motif is the late domain of human T-cell leukemia virus type 1 Gag and mediates its functional interaction with cellular proteins Nedd4 and Tsg101 [corrected]. *J Virol* **77**, 11882-95.

Boyce, M., Wehrfritz, J., Noad, R. & Roy, P. (2004). Purified recombinant bluetongue virus VP1 exhibits RNA replicase activity. *J Virol* **78**, 3994-4002.

Bremer, C. W. (1976). A gel electrophoretic study of the protein and nucleic acid components of African horsesickness virus. *Onderstepoort J Vet Res* **43**, 193-9.

Briggs, J. A., Wilk, T. & Fuller, S. D. (2003). Do lipid rafts mediate virus assembly and pseudotyping? *J Gen Virol* **84**, 757-68.

Brignati, M. J., Loomis, J. S., Wills, J. W. & Courtney, R. J. (2003). Membrane association of VP22, a herpes simplex virus type 1 tegument protein. *J Virol* **77**, 4888-98.

Brookes, S. M., Hyatt, A. D. & Eaton, B. T. (1993). Characterization of virus inclusion bodies in bluetongue virus-infected cells. *J Gen Virol* **74**, 525-30.

Broquet, A. H., Lenoir, C., Gardet, A., Sapin, C., Chwetzoff, S., Jouniaux, A. M., Lopez, S., Trugnan, G., Bachelet, M. & Thomas, G. (2006). Hsp70 Negatively Controls Rotavirus Protein Bioavailability in Caco-2 Cells Infected by the Rotavirus Rf Strain. *J Virol*.

Campbell, M. K. (1999). Biochemistry. In *Saunders Golden Sunburst Series*, Third edn, pp. 725: Harcourt College Publishers.

Castro, A. E., Montague, S. R., Dotson, J. F., Jessup, D. A. & DeForge, J. R. (1989). Susceptibility of a fetal tongue cell line derived from bighorn sheep to five serotypes of bluetongue virus and its potential for the isolation of viruses. *J Vet Diagn Invest* **1**, 247-53.

Chazal, N. & Gerlier, D. (2003). Virus entry, assembly, budding, and membrane rafts. *Microbiol Mol Biol Rev* **67**, 226-37, table of contents.

Chevalier, C., Galloux, M., Pous, J., Henry, C., Denis, J., Da Costa, B., Navaza, J., Lepault, J. & Delmas, B. (2005). Structural peptides of a nonenveloped virus are involved in assembly and membrane translocation. *J Virol* **79**, 12253-63.

Chuma, T., Le Blois, H., Sanchez-Vizcaino, J. M., Diaz-Laviada, M. & Roy, P. (1992). Expression of the major core antigen VP7 of African horsesickness virus by a recombinant baculovirus and its use as a group-specific diagnostic reagent. *J Gen Virol* **73 (Pt 4)**, 925-31.

Cowley, J. A. & Gorman, B. M. (1987). Genetic reassortants for identification of the genome segment coding for the bluetongue virus hemagglutinin. *J Virol* **61**, 2304-6.

Craven, R. C., Harty, R. N., Paragas, J., Palese, P. & Wills, J. W. (1999). Late domain function identified in the vesicular stomatitis virus M protein by use of rhabdovirus-retrovirus chimeras. *J Virol* **73**, 3359-65.

Creighton, T. E. (1984). Proteins-Structures and Molecular Properties, pp. 498: W.H. Freeman and Company.

Cuadras, M. A., Bordier, B. B., Zambrano, J. L., Ludert, J. E. & Greenberg, H. B. (2006). Dissecting rotavirus particle-raft interaction with small interfering RNAs: insights into rotavirus transit through the secretory pathway. *J Virol* **80**, 3935-46.

De Sa, R. O., Zellner, M. & Grubman, M. J. (1994). Phylogenetic analysis of segment 10 from African horsesickness virus and cognate genes from other orbiviruses. *Virus Res* **33**, 157-65.

Demirov, D. G. & Freed, E. O. (2004). Retrovirus budding. *Virus Res* **106**, 87-102.

Devaney, M. A., Kendall, J. & Grubman, M. J. (1988). Characterization of a nonstructural phosphoprotein of two orbiviruses. *Virus Res* **11**, 151-64.

Dimitrova, M., Imbert, I., Kieny, M. P. & Schuster, C. (2003). Protein-protein interactions between hepatitis C virus nonstructural proteins. *J Virol* **77**, 5401-14.

Drewes, G. & Bouwmeester, T. (2003). Global approaches to protein-protein interactions. *Curr Opin Cell Biol* **15**, 199-205.

Driscoll, J. & Goldberg, A. L. (1990). The proteasome (multicatalytic protease) is a component of the 1500-kDa proteolytic complex which degrades ubiquitin-conjugated proteins. *J Biol Chem* **265**, 4789-92.

du Plessis, M., Cloete, M., Aitchison, H. & Van Dijk, A. A. (1998). Protein aggregation complicates the development of baculovirus-expressed African horsesickness virus serotype 5 VP2 subunit vaccines. *Onderstepoort J Vet Res* **65**, 321-9.

Eaton, B. T. & Crameri, G. S. (1989). The site of bluetongue virus attachment to glycophorins from a number of animal erythrocytes. *J Gen Virol* **70**, 3347-53.

Eaton, B. T., Hyatt, A. D. & White, J. R. (1988). Localization of the nonstructural protein NS1 in bluetongue virus-infected cells and its presence in virus particles. *Virology* **163**, 527-37.

Eichwald, C., Rodriguez, J. F. & Burrone, O. R. (2004). Characterization of rotavirus NSP2/NSP5 interactions and the dynamics of viroplasm formation. *J Gen Virol* **85**, 625-34.

Fields, S. & Bartel, P. L. (2001). The two-hybrid system: A personal view. In *Two hybrid systems - Methods and Protocols*, pp. 3 - 8. Edited by P. N. MacDonald. Totowa, New Jersey: Humana Press.

Fields, S. & Song, O. (1989). A novel genetic system to detect protein-protein interactions. *Nature* **340**, 245-6.

Fillmore, G. C., Lin, H. & Li, J. K. (2002). Localization of the single-stranded RNA-binding domains of bluetongue virus nonstructural protein NS2. *J Virol* **76**, 499-506.

Filter, R. D. (2000). Characterisation and co-expression of the two outer capsid proteins of African Horsesickness virus serotype 3. In *Msc thesis*.

Franck, N., Le Seyec, J., Guguen-Guillouzo, C. & Erdtmann, L. (2005). Hepatitis C virus NS2 protein is phosphorylated by the protein kinase CK2 and targeted for degradation to the proteasome. *J Virol* **79**, 2700-8.

Freed, E. O. (2002). Viral late domains. *J Virol* **76**, 4679-87.

Freed, E. O. (2004). Mechanisms of enveloped virus release. *Virus Res* **106**, 85-6.

French, T. J., Inumaru, S. & Roy, P. (1989). Expression of two related nonstructural proteins of bluetongue virus (BTV) type 10 in insect cells by a recombinant baculovirus: production of polyclonal ascitic fluid and characterization of the gene product in BTV-infected BHK cells. *J Virol* **63**, 3270-8.

French, T. J., Marshall, J. J. & Roy, P. (1990). Assembly of double-shelled, viruslike particles of bluetongue virus by the simultaneous expression of four structural proteins. *J Virol* **64**, 5695-700.

Gao, L., Tu, H., Shi, S. T., Lee, K. J., Asanaka, M., Hwang, S. B. & Lai, M. M. (2003). Interaction with a ubiquitin-like protein enhances the ubiquitination and degradation of hepatitis C virus RNA-dependent RNA polymerase. *J Virol* **77**, 4149-59.

Garrus, J. E., von Schwedler, U. K., Pornillos, O. W., Morham, S. G., Zavitz, K. H., Wang, H. E., Wettstein, D. A., Stray, K. M., Cote, M., Rich, R. L., Myszka, D. G. & Sundquist, W. I. (2001). Tsg101 and the vacuolar protein sorting pathway are essential for HIV-1 budding. *Cell* **107**, 55-65.

Gosselin-Grenet, A. S., Mottet-Osman, G. & Roux, L. (2006). From assembly to virus particle budding: pertinence of the detergent resistant membranes. *Virology* **344**, 296-303.

Gottwein, E., Jager, S., Habermann, A. & Krausslich, H. G. (2006). Cumulative mutations of ubiquitin acceptor sites in human immunodeficiency virus type 1 gag cause a late budding defect. *J Virol* **80**, 6267-75.

Gouet, P., Diprose, J. M., Grimes, J. M., Malby, R., Burroughs, J. N., Zientara, S., Stuart, D. I. & Mertens, P. P. (1999). The highly ordered double-stranded RNA genome of bluetongue virus revealed by crystallography. *Cell* **97**, 481-90.

Grimes, J. M., Burroughs, J. N., Gouet, P., Diprose, J. M., Malby, R., Zientara, S., Mertens, P. P. & Stuart, D. I. (1998). The atomic structure of the bluetongue virus core. *Nature* **395**, 470-8.

Grimes, J. M., Jakana, J., Ghosh, M., Basak, A. K., Roy, P., Chiu, W., Stuart, D. I. & Prasad, B. V. (1997). An atomic model of the outer layer of the bluetongue virus core derived from X-ray crystallography and electron cryomicroscopy. *Structure* **5**, 885-93.

Grubman, M. J. & Lewis, S. A. (1992). Identification and characterization of the structural and nonstructural proteins of African horsesickness virus and determination of the genome coding assignments. *Virology* **186**, 444-51.

Guirakhoo, F., Catalan, J. A. & Monath, T. P. (1995). Adaptation of bluetongue virus in mosquito cells results in overexpression of NS3 proteins and release of virus particles. *Arch Virol* **140**, 967-74.

Haglund, K. & Dikic, I. (2005). Ubiquitylation and cell signaling. *Embo J* **24**, 3353-9.

Han, Z. & Harty, R. N. (2004). The NS3 protein of bluetongue virus exhibits viroporin-like properties. *J Biol Chem* **279**, 43092-7.

Harder, T., Kellner, R., Parton, R. G. & Gruenberg, J. (1997). Specific release of membrane-bound annexin II and cortical cytoskeletal elements by sequestration of membrane cholesterol. *Mol Biol Cell* **8**, 533-45.

Harty, R. N., Brown, M. E., Wang, G., Huibregtse, J. & Hayes, F. P. (2000). A PPxY motif within the VP40 protein of Ebola virus interacts physically and functionally with a ubiquitin ligase: implications for filovirus budding. *Proc Natl Acad Sci U S A* **97**, 13871-6.

Hassan, S. H., Wirblich, C., Forzan, M. & Roy, P. (2001). Expression and functional characterization of bluetongue virus VP5 protein: role in cellular permeabilization. *J Virol* **75**, 8356-67.

Hassan, S. S. & Roy, P. (1999). Expression and functional characterization of bluetongue virus VP2 protein: role in cell entry. *J Virol* **73**, 9832-42.

Herman, B., Krishnan, R. V. & Centonze, V. E. (2004). Microscopic analysis of fluorescence resonance energy transfer (FRET). In *Protein-Protein interactions - Methods and Applications*, pp. 351-370. Edited by H. Fu: Humana press, Totowa, New Jersey.

Hershko, A. & Ciechanover, A. (1998). The ubiquitin system. *Annu Rev Biochem* **67**, 425-79.

Hewat, E. A., Booth, T. F., Loudon, P. T. & Roy, P. (1992a). Three-dimensional reconstruction of baculovirus expressed bluetongue virus core-like particles by cryo-electron microscopy. *Virology* **189**, 10-20.

Hewat, E. A., Booth, T. F. & Roy, P. (1992b). Structure of bluetongue virus particles by cryoelectron microscopy. *J Struct Biol* **109**, 61-9.

Hicke, L. & Riezman, H. (1996). Ubiquitination of a yeast plasma membrane receptor signals its ligand-stimulated endocytosis. *Cell* **84**, 277-87.

Hoeller, D., Crosetto, N., Blagoev, B., Raiborg, C., Tikkanen, R., Wagner, S., Kowanetz, K., Breitling, R., Mann, M., Stenmark, H. & Dikic, I. (2006). Regulation of ubiquitin-binding proteins by monoubiquitination. *Nat Cell Biol* **8**, 163-9.

Homan, E. J. & Yunker, C. E. (1988). Growth of bluetongue and epizootic hemorrhagic disease of deer viruses in poikilothermic cell systems. *Vet Microbiol* **16**, 15-24.

Huismans, H. & Els, H. J. (1979). Characterization of the tubules associated with the replication of three different orbiviruses. *Virology* **92**, 397-406.

Huismans, H. & Erasmus, B. J. (1981). Identification of the serotype-specific and group-specific antigens of bluetongue virus. *Onderstepoort J Vet Res* **48**, 51-8.

Huismans, H., van Dijk, A. A. & Els, H. J. (1987). Uncoating of parental bluetongue virus to core and subcore particles in infected L cells. *Virology* **157**, 180-8.

Huismans, H. & Verwoerd, D. W. (1973). Control of transcription during the expression of the bluetongue virus genome. *Virology* **52**, 81-8.

Hwang, G., Yang, Y., Chiou, J. & Li, J. K. (1992). Sequence conservation among the cognate nonstructural NS3/3A protein genes of six bluetongue viruses. *Virus Res* **23**, 151-161.

Hyatt, A. D., Eaton, B. T. & Brookes, S. M. (1989). The release of bluetongue virus from infected cells and their superinfection by progeny virus. *Virology* **173**, 21-34.

Hyatt, A. D., Gould, A. R., Coupar, B. & Eaton, B. T. (1991). Localization of the non-structural protein NS3 in bluetongue virus- infected cells. *J Gen Virol* **72**, 2263-7.

Hyatt, A. D., Zhao, Y. & Roy, P. (1993). Release of bluetongue virus-like particles from insect cells is mediated by BTV nonstructural protein NS3/NS3A. *Virology* **193**, 592-603.

Inumaru, S. & Roy, P. (1987). Production and characterization of the neutralization antigen VP2 of bluetongue virus serotype 10 using a baculovirus expression vector. *Virology* **157**, 472-9.

Jensen, M. J., Cheney, I. W., Thompson, L. H., Mecham, J. O., Wilson, W. C., Yamakawa, M., Roy, P. & Gorman, B. M. (1994). The smallest gene of the orbivirus, epizootic hemorrhagic disease, is expressed in virus-infected cells as two proteins and the expression differs from that of the cognate gene of bluetongue virus. *Virus Res* **32**, 353-64.

Kar, A. K., Ghosh, M. & Roy, P. (2004). Mapping the assembly pathway of Bluetongue virus scaffolding protein VP3. *Virology* **324**, 387-99.

Katzmann, D. J., Babst, M. & Emr, S. D. (2001). Ubiquitin-dependent sorting into the multivesicular body pathway requires the function of a conserved endosomal protein sorting complex, ESCRT-I. *Cell* **106**, 145-55.

Khu, Y. L., Tan, Y. J., Lim, S. G., Hong, W. & Goh, P. Y. (2004). Hepatitis C virus non-structural protein NS3 interacts with LMP7, a component of the immunoproteasome, and affects its proteasome activity. *Biochem J* **384**, 401-9.

Kikonyogo, A., Bouamr, F., Vana, M. L., Xiang, Y., Aiyar, A., Carter, C. & Leis, J. (2001). Proteins related to the Nedd4 family of ubiquitin protein ligases interact with the L domain of Rous sarcoma virus and are required for gag budding from cells. *Proc Natl Acad Sci U S A* **98**, 11199-204.

Le Blois, H., French, T., Mertens, P. P. C., Burroughs, J. N. & Roy, P. (1992). The expressed VP4 protein of bluetongue virus binds GTP and is the candidate guanylyl transferase of the virus. *Virology* **189**, 757-761.

Le Blois, H. & Roy, P. (1993). A single point mutation in the VP7 Majore Core Protein of Bluetongue Virus prevents the formation of core-like particles. *Virology* **67**, 353-359.

Lee, J. W. & Roy, P. (1986). Nucleotide sequence of a cDNA clone of RNA segment 10 of bluetongue virus (serotype 10). *J Gen Virol* **67**, 2833-7.

Liu, H. M., Booth, T. F. & Roy, P. (1992). Interactions between bluetongue virus core like capsid protein translated in vitro. *General Virology* **73**, 2577-2584.

Lopez, S. & Arias, C. F. (2004). Multistep entry of rotavirus into cells: a Versaillesque dance. *Trends Microbiol* **12**, 271-8.

Lopez, T., Lopez, S. & Arias, C. F. (2006). Heat shock enhances the susceptibility of BHK cells to rotavirus infection through the facilitation of entry and post-entry virus replication steps. *Virus Res* **121**, 74-83.

Luker, G. D., Sharma, V. & Piwnica-Worms, D. (2003). Visualizing protein-protein interactions in living animals. *Methods* **29**, 110-22.

Lymperopoulos, K., Noad, R., Tosi, S., Nethisinghe, S., Brierley, I. & Roy, P. (2006). Specific binding of Bluetongue virus NS2 to different viral plus-strand RNAs. *Virology* **353**, 17-26.

Maree, F. F. & Huismans, H. (1997). Characterization of tubular structures composed of nonstructural protein NS1 of African horsesickness virus expressed in insect cells. *J Gen Virol* **78**, 1077-82.

Maree, S., Durbach, S. & Huismans, H. (1998). Intracellular production of African horsesickness virus core-like particles by expression of the two major core proteins, VP3 and VP7, in insect cells. *J Gen Virol* **79**, 333-7.

Martin-Serrano, J., Perez-Caballero, D. & Bieniasz, P. D. (2004). Context-dependent effects of L domains and ubiquitination on viral budding. *J Virol* **78**, 5554-63.

Martin-Serrano, J., Yarovoy, A., Perez-Caballero, D. & Bieniasz, P. D. (2003a). Divergent retroviral late-budding domains recruit vacuolar protein sorting factors by using alternative adaptor proteins. *Proc Natl Acad Sci U S A* **100**, 12414-9.

Martin-Serrano, J., Zang, T. & Bieniasz, P. D. (2001). HIV-1 and Ebola virus encode small peptide motifs that recruit Tsg101 to sites of particle assembly to facilitate egress. *Nat Med* **7**, 1313-9.

Martin-Serrano, J., Zang, T. & Bieniasz, P. D. (2003b). Role of ESCRT-I in retroviral budding. *J Virol* **77**, 4794-804.

Martin, L. A., Meyer, A. J., O'Hara, R. S., Fu, H., Mellor, P. S., Knowles, N. J. & Mertens, P. P. (1998). Phylogenetic analysis of African horse sickness virus segment 10: sequence variation, virulence characteristics and cell exit. *Arch Virol Suppl* **14**, 281-93.

Martinez-Torrecuadrada, J. L., Diaz-Laviada, M., Roy, P., Sanchez, C., Vela, C., Sanchez-Vizcaino, J. M. & Casal, J. I. (1996). Full protection against African horsesickness (AHS) in horses induced by baculovirus-derived AHS virus serotype 4 VP2, VP5 and VP7. *J Gen Virol* **77 (Pt 6)**, 1211-21.

Martinez-Torrecuadrada, J. L., Iwata, H., Venteo, A., Casal, I. & Roy, P. (1994). Expression and characterization of the two outer capsid proteins of African horsesickness virus: the role of VP2 in virus neutralization. *Virology* **202**, 348-59.

Martinez-Torrecuadrada, J. L., Langeveld, J. P., Meloen, R. H. & Casal, J. I. (2001). Definition of neutralizing sites on African horse sickness virus serotype 4 VP2 at the level of peptides. *J Gen Virol* **82**, 2415-24.

McGuire, M. J., Croall, D. E. & DeMartino, G. N. (1988). ATP-stimulated proteolysis in soluble extracts of BHK 21/C13 cells. Evidence for multiple pathways and a role for an enzyme related to the high-molecular-weight protease, macropain. *Arch Biochem Biophys* **262**, 273-85.

Meiswinkel, R., Baylis, M. & Labuschagne, K. (2000). Stabling and the protection of horses from Culicoides bolitinos (Diptera: Ceratopogonidae), a recently identified vector of African horse sickness. *Bull Entomol Res* **90**, 509-15.

Meiswinkel, R. & Paweska, J. T. (2003). Evidence for a new field Culicoides vector of African horse sickness in South Africa. *Prev Vet Med* **60**, 243-53.

Mellor, P. S. (1990). The replication of bluetongue virus in Culicoides vectors. *Curr Top Microbiol Immunol* **162**, 143-61.

Mertens, P. P., Burroughs, J. N. & Anderson, J. (1987). Purification and properties of virus particles, infectious subviral particles, and cores of bluetongue virus serotypes 1 and 4. *Virology* **157**, 375-86.

Mertens, P. P. & Diprose, J. (2004). The bluetongue virus core: a nano-scale transcription machine. *Virus Res* **101**, 29-43.

Modrof, J., Lymperopoulos, K. & Roy, P. (2005). Phosphorylation of bluetongue virus nonstructural protein 2 is essential for formation of viral inclusion bodies. *J Virol* **79**, 10023-31.

Mortola, E., Noad, R. & Roy, P. (2004). Bluetongue virus outer capsid proteins are sufficient to trigger apoptosis in mammalian cells. *J Virol* **78**, 2875-83.

Moss, S. R., Jones, L. D. & Nuttall, P. A. (1992). Comparison of the nonstructural protein, NS3, of tick-borne and insect-borne orbiviruses. *Virology* **187**, 841-844.

Nakata, T., Sobue, K. & Hirokawa, N. (1990). Conformational change and localization of calpactin I complex involved in exocytosis as revealed by quick-freeze, deep-etch electron microscopy and immunocytochemistry. *J Cell Biol* **110**, 13-25.

Nason, E. L., Rothagel, R., Mukherjee, S. K., Kar, A. K., Forzan, M., Prasad, B. V. & Roy, P. (2004). Interactions between the inner and outer capsids of bluetongue virus. *J Virol* **78**, 8059-67.

Nichols, B. J. & Lippincott-Schwartz, J. (2001). Endocytosis without clathrin coats. *Trends Cell Biol* **11**, 406-12.

Nooren, I. M. & Thornton, J. M. (2003). Diversity of protein-protein interactions. *Embo J* **22**, 3486-92.

O'Hara, R. S., Meyer, A. J., Burroughs, J. N., Pullen, L., Martin, L. A. & Mertens, P. P. (1998). Development of a mouse model system, coding assignments and identification of the genome segments controlling virulence of African horse sickness virus serotypes 3 and 8. *Arch Virol Suppl* **14**, 259-79.

Ono, A. & Freed, E. O. (2001). Plasma membrane rafts play a critical role in HIV-1 assembly and release. *Proc Natl Acad Sci U S A* **98**, 13925-30.

Owens, R. J., Limn, C. & Roy, P. (2004). Role of an arbovirus nonstructural protein in cellular pathogenesis and virus release. *J Virol* **78**, 6649-56.

Patnaik, A., Chau, V. & Wills, J. W. (2000). Ubiquitin is part of the retrovirus budding machinery. *Proc Natl Acad Sci U S A* **97**, 13069-74.

Patton, J. T., Silvestri, L. S., Tortorici, M. A., Vasquez-Del Carpio, R. & Taraporewala, Z. F. (2006). Rotavirus genome replication and morphogenesis: role of the viroplasm. *Curr Top Microbiol Immunol* **309**, 169-87.

Perez-Vargas, J., Romero, P., Lopez, S. & Arias, C. F. (2006). The peptide-binding and ATPase domains of recombinant hsc70 are required to interact with rotavirus and reduce its infectivity. *J Virol* **80**, 3322-31.

Perez, M., Craven, R. C. & de la Torre, J. C. (2003). The small RING finger protein Z drives arenavirus budding: implications for antiviral strategies. *Proc Natl Acad Sci U S A* **100**, 12978-83.

Pesavento, J. B., Crawford, S. E., Estes, M. K. & Prasad, B. V. (2006). Rotavirus proteins: structure and assembly. *Curr Top Microbiol Immunol* **309**, 189-219.

Pesavento, J. B., Lawton, J. A., Estes, M. E. & Venkataram Prasad, B. V. (2001). The reversible condensation and expansion of the rotavirus genome. *Proc Natl Acad Sci U S A* **98**, 1381-6.

Phizicky, E. M. & Fields, S. (1995). Protein-protein interactions: methods for detection and analysis. *Microbiol Rev* **59**, 94-123.

Pierce, C. M., Balasuriya, U. B. & MacLachlan, N. J. (1998). Phylogenetic analysis of the S10 gene of field and laboratory strains of bluetongue virus from the United States. *Virus Res* **55**, 15-27.

Pina-Vazquez, C., De Nova-Ocampo, M., Guzman-Leon, S. & Padilla-Noriega, L. (2007). Post-translational regulation of rotavirus protein NSP1 expression in mammalian cells. *Arch Virol* **152**, 345-68.

Pornillos, O., Garrus, J. E. & Sundquist, W. I. (2002). Mechanisms of enveloped RNA virus budding. *Trends Cell Biol* **12**, 569-79.

Potgieter, A. C., Cloete, M., Pretorius, P. J. & van Dijk, A. A. (2003). A first full outer capsid protein sequence data-set in the Orbivirus genus (family Reoviridae): cloning, sequencing, expression and analysis of a complete set of full-length outer capsid VP2 genes of the nine African horsesickness virus serotypes. *J Gen Virol* **84**, 1317-26.

Prasad, B. V., Yamaguchi, S. & Roy, P. (1992). Three-dimensional structure of single-shelled bluetongue virus. *J Virol* **66**, 2135-42.

Pratt, W. B. (1993). The role of heat shock proteins in regulating the function, folding, and trafficking of the glucocorticoid receptor. *J Biol Chem* **268**, 21455-8.

Putterman, D., Pepinsky, R. B. & Vogt, V. M. (1990). Ubiquitin in avian leukosis virus particles. *Virology* **176**, 633-7.

Raiborg, C., Rusten, T. E. & Stenmark, H. (2003). Protein sorting into multivesicular endosomes. *Curr Opin Cell Biol* **15**, 446-55.

Ramadevi, N., Burroughs, N. J., Mertens, P. P., Jones, I. M. & Roy, P. (1998). Capping and methylation of mRNA by purified recombinant VP4 protein of bluetongue virus. *Proc Natl Acad Sci U S A* **95**, 13537-42.

Roy, P., Adachi, A., Urakawa, T., Booth, T. F. & Thomas, C. P. (1990). Identification of bluetongue virus VP6 in virus-infected vertebrate cells. *J Virol* **64**, 1-8.

Roy, P. & Noad, R. (2006). Bluetongue virus assembly and morphogenesis. *Curr Top Microbiol Immunol* **309**, 87-116.

Salghetti, S. E., Caudy, A. A., Chenoweth, J. G. & Tansey, W. P. (2001). Regulation of transcriptional activation domain function by ubiquitin. *Science* **293**, 1651-3.

Sambrook, J. & Russel, D. W. (2001). Molecular cloning - a Laboratory manual, 3 rd Edition. edn: Cold Spring Harbor Laboratory Press, Cold Spring Harbor, New York.

Sarafian, T., Pradel, L. A., Henry, J. P., Aunis, D. & Bader, M. F. (1991). The participation of annexin II (calpactin I) in calcium-evoked exocytosis requires protein kinase C. *J Cell Biol* **114**, 1135-47.

Scianimanico, S., Schoehn, G., Timmins, J., Ruigrok, R. H., Klenk, H. D. & Weissenhorn, W. (2000). Membrane association induces a conformational change in the Ebola virus matrix protein. *Embo J* **19**, 6732-41.

Shirakura, M., Murakami, K., Ichimura, T., Suzuki, R., Shimoji, T., Fukuda, K., Abe, K., Sato, S., Fukasawa, M., Yamakawa, Y., Nishijima, M., Moriishi, K., Matsuura, Y., Wakita, T., Suzuki, T., Howley, P. M., Miyamura, T. & Shoji, I. (2006). The E6AP ubiquitin ligase mediates ubiquitylation and degradation of hepatitis C virus core protein. *J Virol*.

Simons, K. & Ehehalt, R. (2002). Cholesterol, lipid rafts, and disease. *J Clin Invest* **110**, 597-603.

Simons, K. & Ikonen, E. (1997). Functional rafts in cell membranes. *Nature* **387**, 569-72.

Snippe, M., Borst, J. W., Goldbach, R. & Kormelink, R. (2005). The use of fluorescence microscopy to visualise homotypic interactions of tomato spotted wilt virus nucleocapsid protein in living cells. *J Virol Methods* **125**, 15-22.

Stoltz, M. A., van der Merwe, C. F., Coetzee, J. & Huismans, H. (1996). Subcellular localization of the nonstructural protein NS3 of African horsesickness virus. *Onderstepoort Journal of Veterinary Research* **63**, 57-61.

Strack, B., Calistri, A., Accola, M. A., Palu, G. & Gottlinger, H. G. (2000). A role for ubiquitin ligase recruitment in retrovirus release. *Proc Natl Acad Sci U S A* **97**, 13063-8.

Strack, B., Calistri, A., Craig, S., Popova, E. & Gottlinger, H. G. (2003). AIP1/ALIX is a binding partner for HIV-1 p6 and EIAV p9 functioning in virus budding. *Cell* **114**, 689-99.

Stuart, D. I., Gouet, P., Grimes, J., Malby, R., Diprose, J., Zientara, S., Burroughs, J. N. & Mertens, P. P. (1998). Structural studies of orbivirus particles. *Arch Virol Suppl* **14**, 235-50.

Surjit, M., Liu, B., Kumar, P., Chow, V. T. & Lal, S. K. (2004). The nucleocapsid protein of the SARS coronavirus is capable of self-association through a C-terminal 209 amino acid interaction domain. *Biochem Biophys Res Commun* **317**, 1030-6.

Tan, B. H., Nason, E., Staeuber, N., Jiang, W., Monastryrskaya, K. & Roy, P. (2001). RGD tripeptide of bluetongue virus VP7 protein is responsible for core attachment to Culicoides cells. *J Virol* **75**, 3937-47.

Theron, J. & Nel, L. H. (1997). Stable protein-RNA interaction involves the terminal domains of bluetongue virus mRNA, but not the terminally conserved sequences. *Virology* **229**, 134-42.

Thomas, C. P., Booth, T. F. & Roy, P. (1990). Synthesis of bluetongue virus-encoded phosphoprotein and formation of inclusion bodies by recombinant baculovirus in insect cells: it binds the single-stranded RNA species. *J Gen Virol* **71**, 2073-83.

Uetz, P. & Hughes, R. E. (2000). Systematic and large-scale two-hybrid screens. *Curr Opin Microbiol* **3**, 303-8.

Urakawa, T., Ritter, D. G. & Roy, P. (1989). Expression of largest RNA segment and synthesis of VP1 protein of bluetongue virus in insect cells by recombinant baculovirus: association of VP1 protein with RNA polymerase activity. *Nucleic Acids Res* **17**, 7395-401.

Uyeda, S., Masuta, C. & Uyeda, I. (1999). The C-terminal region of the P3 structural protein of rice dwarf phytoreovirus is important for P3-P3 interaction. *Arch Virol* **144**, 1653-7.

Van Criekinge, W. & Beyaert, R. (1999). Yeast Two-Hybrid: State of the Art. *Biol Proced Online* **2**, 1-38.

Van Dijk, A. A. & Huismans, H. (1980). The in vitro activation and further characterization of the bluetongue virus-associated transcriptase. *Virology* **104**, 347-56.

Van Dijk, A. A. & Huismans, H. (1982). The effect of temperature on the in vitro transcriptase reaction of bluetongue virus, epizootic haemorrhagic disease virus and African horsesickness virus. *Onderstepoort J Vet Res* **49**, 227-32.

Van Niekerk, M., Smit, C. C., Fick, W. C., van Staden, V. & Huismans, H. (2001). Membrane association of African horsesickness virus nonstructural protein NS3 determines its cytotoxicity. *Virology* **279**, 499-508.

Van Staden, V. & Huismans, H. (1991). A comparison of the genes which encode non-structural protein NS3 of different orbiviruses. *J Gen Virol* **72 (Pt 5)**, 1073-9.

Van Staden, V., Smit, C. C., Stoltz, M. A., Maree, F. F. & Huismans, H. (1998). Characterization of two African horse sickness virus nonstructural proteins, NS1 and NS3. *Arch Virol Suppl* **14**, 251-8.

Van Staden, V., Stoltz, M. A. & Huismans, H. (1995). Expression of nonstructural protein NS3 of African horsesickness virus (AHSV): evidence for a cytotoxic effect of NS3 in insect cells, and characterization of the gene products in AHSV infected Vero cells. *Arch Virol* **140**, 289-306.

Venter, M., Napier, G. & Huismans, H. (2000). Cloning, sequencing and expression of the gene that encodes the major neutralisation-specific antigen of African horsesickness virus serotype 9. *J Virol Methods* **86**, 41-53.

Vikis, H. G. & Guan, K. (2004). Glutathione-S-Transferase-fusion based assays for studying protein-protein interactions. In *Protein-Protein interactions - Methods and Applications*, pp. 175-186. Edited by H. Fu: Humana Press, Totowa, New Jersey.

Vollert, C. & Uetz, P. (2003). The Two-Hybrid System. *Encyclopedic Reference of Genomics and Proteomics in Molecular Medicine*, 1 - 7.

von Schwedler, U. K., Stuchell, M., Muller, B., Ward, D. M., Chung, H. Y., Morita, E., Wang, H. E., Davis, T., He, G. P., Cimbora, D. M., Scott, A., Krausslich, H. G., Kaplan, J., Morham, S. G. & Sundquist, W. I. (2003). The protein network of HIV budding. *Cell* **114**, 701-13.

Wechsler, S. J. & McHolland, L. E. (1988). Susceptibilities of 14 cell lines to bluetongue virus infection. *J Clin Microbiol* **26**, 2324-7.

Wirblich, C., Bhattacharya, B. & Roy, P. (2006). Nonstructural protein 3 of bluetongue virus assists virus release by recruiting ESCRT-I protein Tsg101. *J Virol* **80**, 460-73.

Xu, A., Bellamy, A. R. & Taylor, J. A. (2000). Immobilization of the early secretory pathway by a virus glycoprotein that binds to microtubules. *Embo J* **19**, 6465-74.

Xu, G., Wilson, W., Mecham, J., Murphy, K., Zhou, E. M. & Tabachnick, W. (1997). VP7: an attachment protein of bluetongue virus for cellular receptors in Culicoides variipennis. *J Gen Virol* **78 (Pt 7)**, 1617-23.

Zientara, S., Sailleau, C., Moulay, S. & Cruciere, C. (1995). Differentiation of African horse sickness viruses by polymerase chain reaction and segments 10 restriction patterns. *Vet Microbiol* **47**, 365-75.

Zientara, S., Sailleau, C., Plateau, E., Moulay, S., Mertens, P. P. & Cruciere, C. (1998). Molecular epidemiology of African horse sickness virus based on analyses and comparisons of genome segments 7 and 10. *Arch Virol Suppl* **14**, 221-34.